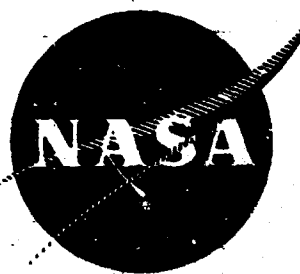


CR# 134920

NASA CI
R75AEC



**QUIET CLEAN SHORT-HAUL EXPERIMENTAL ENGINE
(QCSEE)**

**Under-the-Wing Engine
Digital Control System Design Report**

JANUARY 1978

by

**Advanced Engineering and Technology Programs Department
GENERAL ELECTRIC COMPANY**

(NASA-CR-134920) QUIET CLEAN SHORT-HAUL
EXPERIMENTAL ENGINE (QCSEE) UNDER-THE-WING
ENGINE DIGITAL CONTROL SYSTEM DESIGN REPORT
(General Electric Co.) 321 p HC A14/MF A01

N80-15090

Unclas
CSCL 21E G3/07 33467

68
JUL 19
CEIVE
711 FIGHT
232425

National Aeronautics and Space Administration

NASA Lewis Research Center

Contract NAS3-18021

TABLE OF CONTENTS

<u>Section</u>		<u>Page</u>
1.0	SUMMARY	1
2.0	INTRODUCTION	3
3.0	ENGINE CONTROL SYSTEM	5
3.1	Design Requirements and Criteria	5
3.2	General System Description	10
3.3	System Operation	16
3.3.1	Automatic Control	16
3.3.2	Manual Control	32
3.3.3	Failure Detection and Correction	33
4.0	CONTROL SYSTEM ANALYSIS	36
4.1	Analysis Background	36
4.2	Control Mode Analysis	37
4.2.1	Definition of Potential Thrust Parameter	38
4.2.2	Definition of Tolerances	40
4.2.3	Mode Analysis Runs and Results	44
4.3	Parameter Interrelationships	54
4.4	Scheduleability	60
4.5	Transient Response Capability	63
4.6	Stability Analysis	81
4.6.1	Stability of Primary Automatic Control Mode	81
4.6.2	Steady-State Hunting Investigation with GE Variable-Pitch Actuation System	95
4.6.3	Stability of Alternate Automatic Control Mode	101
4.7	Failure Analysis	107
4.8	Pressure Sensor Location Studies	110
4.9	Starting Studies	111
5.0	DIGITAL CONTROL SUBSYSTEM	118
5.1	General Description	118
5.2	Digital Control Description	123
5.2.1	Program Memory	126
5.2.2	Central Processor	126
5.2.3	Instructions	128
5.2.4	Input-Output Section	141
5.2.5	Other Circuits	142
5.3	Electrical Circuit Construction	149
5.4	Digital Control Product Design	153
5.5	Software Design	161
5.6	Variations for Flight Design	168
5.7	Off-Engine Digital Control Elements	168

TABLE OF CONTENTS (Continued)

<u>Section</u>		<u>Page</u>
6.0	HYDROMECHANICAL CONTROL	176
6.1	Purpose	176
6.2	Description	176
6.3	Operation	177
6.4	Installation	183
6.5	Variation for Flight Design	183
7.0	FUEL DELIVERY SYSTEM	185
7.1	Purpose	185
7.2	Description	185
7.3	Operation	185
7.4	Variations for Flight Design	187
7.5	Fuel Metering Section	187
7.6	Main Fuel Pump	188
7.7	Fuel Filter	188
7.8	Fuel-Oil Heat Exchanger	190
7.9	Drain Eductor	191
8.0	VARIABLE GEOMETRY ACTUATION SYSTEMS	194
8.1	Hydraulic Supply System	194
8.2	Hydraulic Pump	196
8.3	Relief Valve	199
8.4	Filters	199
8.5	Chip Detector	200
8.6	Flow Control Valves	201
8.7	Fan Nozzle (A18) Actuation	201
8.8	Variable-Pitch Actuation	206
8.9	Core Stator Actuation and Feedback	209
9.0	SENSORS	212
9.1	Low Pressure Turbine (LPT) Speed Sensor	212
9.2	Fan Inlet Temperature (T12) Sensor	214
9.3	Core Inlet Temperature Sensor	217
9.4	Compressor Discharge Temperature Sensor (T3)	217
9.5	Absolute and Differential Pressure Transducers	217
9.6	Compressor Discharge Pressure Sensing	221
10.0	MISCELLANEOUS	222
10.1	Control Alternator	222
10.2	Electrical Interconnections	224
10.3	Weight	224

TABLE OF CONTENTS (Concluded)

<u>Section</u>	<u>Page</u>
APPENDICES	
A - Nomenclature	228
B - Control System Failure Analysis	230
C - Computer Simulation of Control System Failures	244
D - Digital Control Processor Instruction Set and Program	278
REFERENCES	309

LIST OF ILLUSTRATIONS

<u>Figure</u>		<u>Page</u>
1.	UTW Experimental Propulsion System.	6
2.	QCSEE UTW Operating Envelope.	7
3.	System Interconnection Schematic.	11
4.	Control Room Elements of QCSEE Digital Control.	13
5.	Sensed Engine and Control Variables.	14
6.	Rated PS3/PTO Schedule.	18
7.	T12 Reference in Digital Control.	19
8.	PS3/PTO Power Demand Schedule.	20
9.	Digital Electronic Fuel Flow Control Block Diagram.	22
10.	Detail Block Diagrams for Lag-Rate Feedbacks with Rate Limits in Fuel Flow Control Loop.	23
11.	Digital Electronic Fan Exhaust Area Control Block Diagram.	26
12.	Detail Block Diagram for Lag-Rate Feedback with Rate Limits in Fan Exhaust Area Control Loop.	27
13.	Digital Electronic Fan Pitch Control Block Diagram.	29
14.	Detail Block Diagrams for Lag-Rate Feedbacks with Rate Limits in Fan Pitch Control Loop.	31
15.	Takeoff Power Mode Throttle/Thrust Characteristics for PS3/PTO.	58
16.	Takeoff Power Mode Throttle/Thrust Characteristics for TP5.	59
17.	Method for Reducing Thrust Parameter Interdependence.	61
18.	T12 Reference.	62
19.	Free-Stream Total Pressure Versus Aircraft Mach Number.	64
20.	Takeoff Engine Pressure Ratio Schedule.	65
21.	Takeoff Percent Corrected Fan rpm Schedule.	66

LIST OF ILLUSTRATIONS (Continued)

<u>Figure</u>		<u>Page</u>
22.	M0 Correction for Takeoff Power Schedules, UTW Experimental Engine.	67
23.	Power Schedule Integration for UTW Flight Design.	68
24.	Throttle Burst from 62% to 100% Thrust at Sea Level Static, Standard Day, Zero Bleed.	70
25.	Effect of WF/PS3 Acceleration Fuel Scheduling Tolerance on Acceleration Time from 62% to 95% Net Thrust.	72
26.	Transient from Takeoff to Maximum Reverse Through Stall at Sea Level Static, Standard Day.	74
27.	Fan Horsepower Transient Versus Fan Pitch Angle During Transition from Takeoff to Maximum Reverse Thrust Through Stall.	76
28.	Transient from Takeoff to Reverse Through Flat Pitch at Sea Level Static, Standard Day.	78
29.	Transient from 60% Power Setting to Reverse Through Flat Pitch at Sea Level Static, Standard Day.	80
30.	Magnitude of Engine Frequency Response from βF to NIK at Maximum Thrust.	86
31.	Phase-Magnitude Ratio Diagram PS3/PTO-WF Inner Loop Analysis.	88
32.	Phase-Magnitude Ratio Diagram Final NIK- βF Outer Loop.	89
33.	Phase-Magnitude Ratio Diagram Final NIK- βF Inner Loop.	90
34.	Phase-Magnitude Ratio Diagram Final PS3/PTO-WF Outer Loop.	91
35.	Phase-Magnitude Ratio Diagram Final PS3/PTO-WF Inner Loop.	92
36.	Phase-Magnitude Ratio Diagram, Final XM11-A18 Inner Loop.	93
37.	Phase-Magnitude Ratio Diagram, Final XM11-A18 Inner Loop.	94
38.	UTW Engine and Control System Hunting at Normal Design Conditions, Sea Level Static, Standard Day.	97

LIST OF ILLUSTRATIONS (Continued)

<u>Figure</u>		<u>Page</u>
39.	Hunting Due to Hysteresis in Feedback Sensing of Fan Pitch Hydraulic Motor Position at Takeoff, Sea Level Static, Standard Day.	99
40.	Hunting Due to Hysteresis in Feedback Sensing of Fuel Metering Valve Position at Takeoff, Sea Level Static, Standard Day.	100
41.	Phase-Magnitude Ratio Diagram TP5-WF Outer Loop.	102
42.	Phase-Magnitude Ratio Diagram TP5-WF Outer Loop.	103
43.	QCSEE UTW Engine Control System with TP5-WF Control Design.	104
44.	QCSEE UTW Engine Control System with TP5-WF Control Design.	105
45.	Inlet Pressure Sensing Data.	112
46.	Inlet Mach Number Correlation Data.	113
47.	Estimated QCSEE Engine Torques.	115
48.	Expected Starter Torque for QCSEE Development Engine.	116
49.	QCSEE Start Time Study of March 1975.	117
50.	A Block Diagram of Digital Control System.	120
51.	Digital Control Block Diagram.	125
52.	QCSEE Digital Control Arithmetic Elements.	127
53.	Typical Analog Circuit.	143
54.	Digital Driver Amplifier for Fail-Fixed Servovalve.	144
55.	Typical Analog Module.	151
56.	Typical Digital Module.	152
57.	Digital Control Installation.	154
58.	Vibration Testing.	156
59.	Module Arrangement Digital control.	158

LIST OF ILLUSTRATIONS (Continued)

<u>Figure</u>		<u>Page</u>
60.	Cooling Air Flowpath.	159
61.	Flow Chart of Positive Limit Check in Fuel Flow Channel.	163
62.	Flow Chart of Negative Limit Check in Fuel Flow Channel.	164
63.	Flow Chart of Forward Mode Reverse Interlock Activation Logic.	167
64.	Operator Control Panel.	170
65.	Engineering Control Panel.	171
66.	Off-Engine Block Diagram.	173
67.	Hydromechanical Control Schematic.	178
68.	Fail-Fixed Servovalve.	182
69.	Hydromechanical Control and Pump.	184
70.	Fuel Delivery System.	186
71.	Drain Eductor Cross Section.	192
72.	Hydraulic Supply System Schematic.	195
73.	Hydraulic Pump.	197
74.	Electrohydraulic Servovalve.	202
75.	A18 Actuation.	203
76.	A18 Actuator Cross Section.	205
77.	Hamilton Standard Variable-Pitch System.	207
78.	General Electric Ball Spline Actuator System.	208
79.	Core Stator Actuator.	211
80.	Low Pressure Turbine Speed Sensor.	213
81.	Fan Inlet Temperature (T12) Sensor.	216

LIST OF ILLUSTRATIONS (Continued)

<u>Figure</u>		<u>Page</u>
82.	Compressor Discharge Temperature (T3) Sensor.	218
83.	Pressure Transducer.	220
84.	Control Alternator.	223
85.	Electrical Interconnections.	225
86.	UTW Experimental Engine Transient When WF Metering Valve Position Feedback Signal Fails (Takeoff, SLS, Std. Day).	251
87.	UTW Experimental Engine Transient When A18 Feedback Signal Fails (Takeoff, SLS, Std. Day).	253
88.	UTW Experimental Engine Transient When T12 Sensor Element Short Circuits (Takeoff, SLS, Std. Day).	255
89.	UTW Experimental Engine Transient When PTO Sensor Opens or Shorts and Indicates Minimum PTO (Takeoff, SLS, Std. Day).	257
90.	UTW Experimental Engine Transient When PTO Sensor Opens or Shorts and Indicates Maximum PTO (Takeoff, SLS, Std. Day).	259
91.	UTW Experimental Engine Transient When PS3 Sensing Line Leaks (Takeoff, SLS, Std. Day).	261
92.	UTW Experimental Engine Transient When PS3 Sensor Opens or Shorts and Indicates Minimum PS3 (Takeoff, SLS, Std. Day).	263
93.	UTW Experimental Engine Transient When PS3 Sensor Opens or Shorts and Indicates Maximum PS3 (Takeoff, SLS, Std. Day).	265
94.	UTW Experimental Engine Transient When Digital Control WF Output Circuit Fails to Maximum Increase (Takeoff, SLS, Std. Day).	267
95.	UTW Experimental Engine Transient When Digital Control WF Output Circuit Fails to Maximum Decrease (Takeoff, SLS, Std. Day).	269

LIST OF ILLUSTRATIONS (Concluded)

<u>Figure</u>		<u>Page</u>
96.	UTW Experimental Engine Transient When Digital Control Fan Pitch Output Circuit Fails to Maximum Open (Takeoff, SLS, Std. Day).	271
97.	UTW Experimental Engine Transient When Digital Control Fan Pitch Output Circuit Fails to Maximum Close (Takeoff, SLS, Std. Day).	272
98.	UTW Experimental Engine Transient When Digital Control A18 Output Circuit Fails to Maximum Open (Takeoff, SLS, Std. Day).	274
99.	UTW Experimental Engine Transient When Digital Control A18 Output Circuit Fails to Maximum Closed (Takeoff, SLS, Std. Day).	276

LIST OF TABLES

<u>Table</u>		<u>Page</u>
I.	Mode Analysis Controlled Variable Tolerances.	41
II.	Mode Analysis Sensing Tolerances.	43
III.	Mode Analysis Engine Component Variations.	45
IV.	Mode Analysis Thrust Accuracy Results (Complete).	46
V.	Mode Analysis Results (Summary), SLS.	51
VI.	Mode Analysis Results (Summary), 0.7/25K.	52
VII.	Controls Coupling Derivatives.	56
VIII.	Effect of Control Variables on System Hunting.	98
IX.	Control and Engine Monitor Data.	120
X.	Fault Indication.	121
XI.	Digital Control Inputs and Outputs.	124
XII.	Arithmetic Logic Unit (ALU) Operations.	129
XIII.	54/74 Family Typical Performance Characteristics (TTL).	146
XIV.	Fuel Pump Characteristics (F101).	189
XV.	Control System Weight.	227

1.0 SUMMARY

The QCSEE Program was established under NASA sponsorship to develop and demonstrate the technology required for propulsion systems for quiet, clean, economically viable, commercial short-haul aircraft. One element of the program has been to develop a digital electronic control system which provides a propulsion engine control in a manner which offers improvements in noise, pollution, thrust response, operational monitoring, and pilot workload relative to current engines. This report describes the design of the control system for one of the two engines in the QCSEE Program, the Under-the-Wing (UTW) engine.

The QCSEE UTW engine requires control of four variables; fuel flow, fan pitch, fan nozzle area, and core compressor stator angle. The system designed to accomplish this task incorporates two basic control components, a modified hydromechanical fuel control from a current engine (F101) and an engine-mounted digital electronic control designed specifically for the QCSEE.

The system includes both automatic and manual operating modes. The automatic mode provides integrated control of engine variables to allow exploration of steady-state and transient characteristics of the engine when automatically controlled. Several different automatic mode options will be explored. The manual mode and several partial-automatic, partial-manual modes are provided to allow independent manipulation of controlled variables so that engine characteristics can be completely mapped. In addition, a remote mode is provided in which the system is integrated with a remote digital computer simulating a STOL transport aircraft computer, thus allowing STOL propulsion system investigations to be performed.

The definition of the automatic control mode was made primarily on the basis of a control mode analysis using a computer program which evaluated many potential modes relative to the accuracy with which they maintain key engine variables when subjected to typical control and engine manufacturing tolerances, sensing tolerances, and hardware deterioration. Scheduling practicality, stability, response, and failure considerations were also

factors in choosing the control mode. The primary mode which has been chosen is one in which the fuel flow controls engine pressure ratio (compressor discharge pressure/inlet total pressure - variables closely related to thrust), the fan pitch controls fan rpm, and the fan nozzle area controls inlet Mach number (a key inlet noise parameter).

The system contains provisions for monitoring and displaying forty-eight engine and control variables, for detecting certain malfunctions, and for taking corrective action in the event of some critical malfunctions such as fan drive gear failure, high vibration, loss of fan speed signal, and certain digital computation faults.

An F101 fuel pump is utilized in the system for supplying fuel for engine operation, for operating servomechanisms in the hydromechanical control, and for providing a source of high-pressure fuel for operation of the actuators which position the core compressor stator vanes.

A variable displacement, constant pressure hydraulic pump supplies fluid for operation of the actuators which position the fan nozzle and the hydraulic motor which drives the variable-pitch actuation mechanisms.

2.0 INTRODUCTION

The QCSEE Program is a program established by NASA to develop and demonstrate propulsion system technology for an advanced, short-haul, commercial aircraft having short-takeoff-or-landing (STOL) capability and producing less noise and atmospheric pollution than current aircraft. A number of specific technological objectives were established at the beginning of the program. One of these was to provide the digital electronic control technology required to accommodate certain specific QCSEE features which are not included in current commercial aircraft propulsion systems.

Control systems for current commercial aircraft turbine engines, most of which have only one or two controlled variables, use primarily hydraulic and mechanical computing elements. This has proven generally adequate although recently there has been a move toward the addition of limited-authority electronic trim of the hydromechanical controls to provide more automatic control of thrust and thus reduce pilot workload.

The QCSEE Program definitely requires engine control system capability beyond that provided on current commercial engines; even those incorporating limited electronic trims. The main reasons are:

- More variables must be controlled.
- Automatic responsive engine and aircraft control coordination is required for STOL operation near the ground where the engines provide lift-assist as well as thrust.
- Automatic thrust control throughout the flight envelop is desired to reduce pilot workload.
- Engine and control data transmittal to the aircraft are desired for operational and engine health monitoring.
- Automatic failure detection and corrective action are desired for certain key control system elements.

Consideration of these new functional requirements, in conjunction with the recognition of the trend toward use of digital computation in aircraft control and indication systems, led to the QCSEE Program objective stated above; namely that digital electronic technology be developed for incorpora-

tion into the QCSEE control system. This report describes in detail how this is being done and how the digital electronic elements are mated with the more traditional engine control elements to make up the QCSEE UTW control system.

The following section outlines basic system design requirements and gives an overall description of the design. Analytical background material follows this. The remainder of the report gives design details of individual system components.

3.0 ENGINE CONTROL SYSTEM

3.1 DESIGN REQUIREMENTS AND CRITERIA

The QCSEE UTW control system design is based on requirements and design criteria established by the QCSEE Program contract and by the nature of the UTW engine, a cross section of which is shown in Figure 1. The major requirements are outlined below.

General System Design

Design a digital control system for controlling the UTW engine utilizing existing controls and accessories (where applicable) supplemented by digital electronics to perform functions not now provided by hydromechanical controls; and provide a flexible interface with a powered lift aircraft. The functions provided shall include reverse control, variable nozzle control, failure monitoring, engine supervisory control, and variable-pitch control.

Operating Regime

Design for ground static, wind tunnel, and altitude chamber operation. Flight envelope to be as shown on Figure 2.

Flight Design

Design for flight operation (i.e., flight weight, performance) except for designated exceptions made for cost purposes. Control system related exceptions include accessories and accessory gearbox, heat exchangers, auxiliary power supply, piping, wiring, drains, and vents. Analyses shall be performed on all nonflight hardware to provide flight weight and performance predictions considering flight design life requirements.

Variables To Be Controlled

The QCSEE UTW requires control of four variables; fuel flow, compressor stator angle, fan pitch angle, and fan exhaust area.

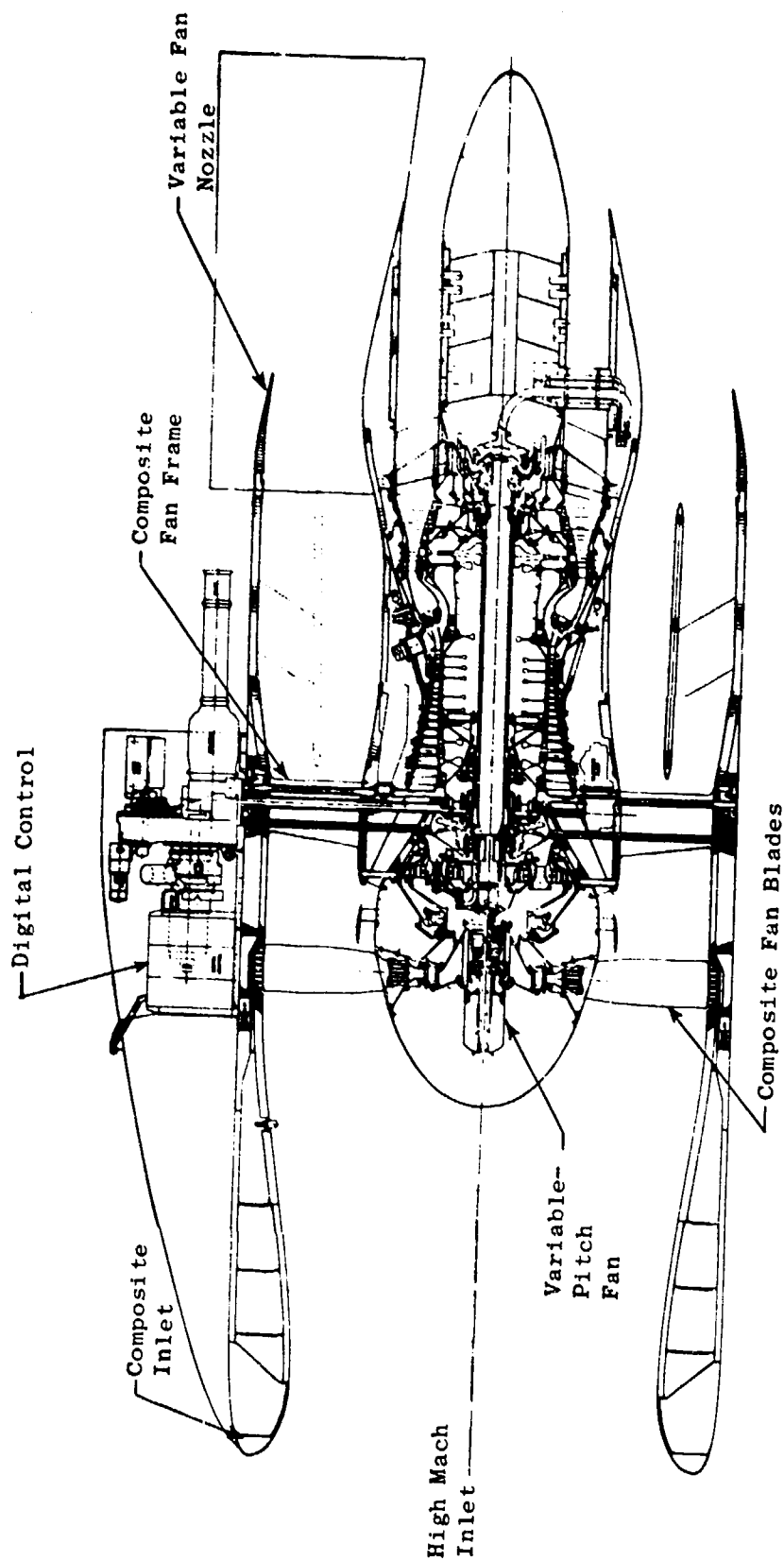


Figure 1. UTW Experimental Propulsion System.

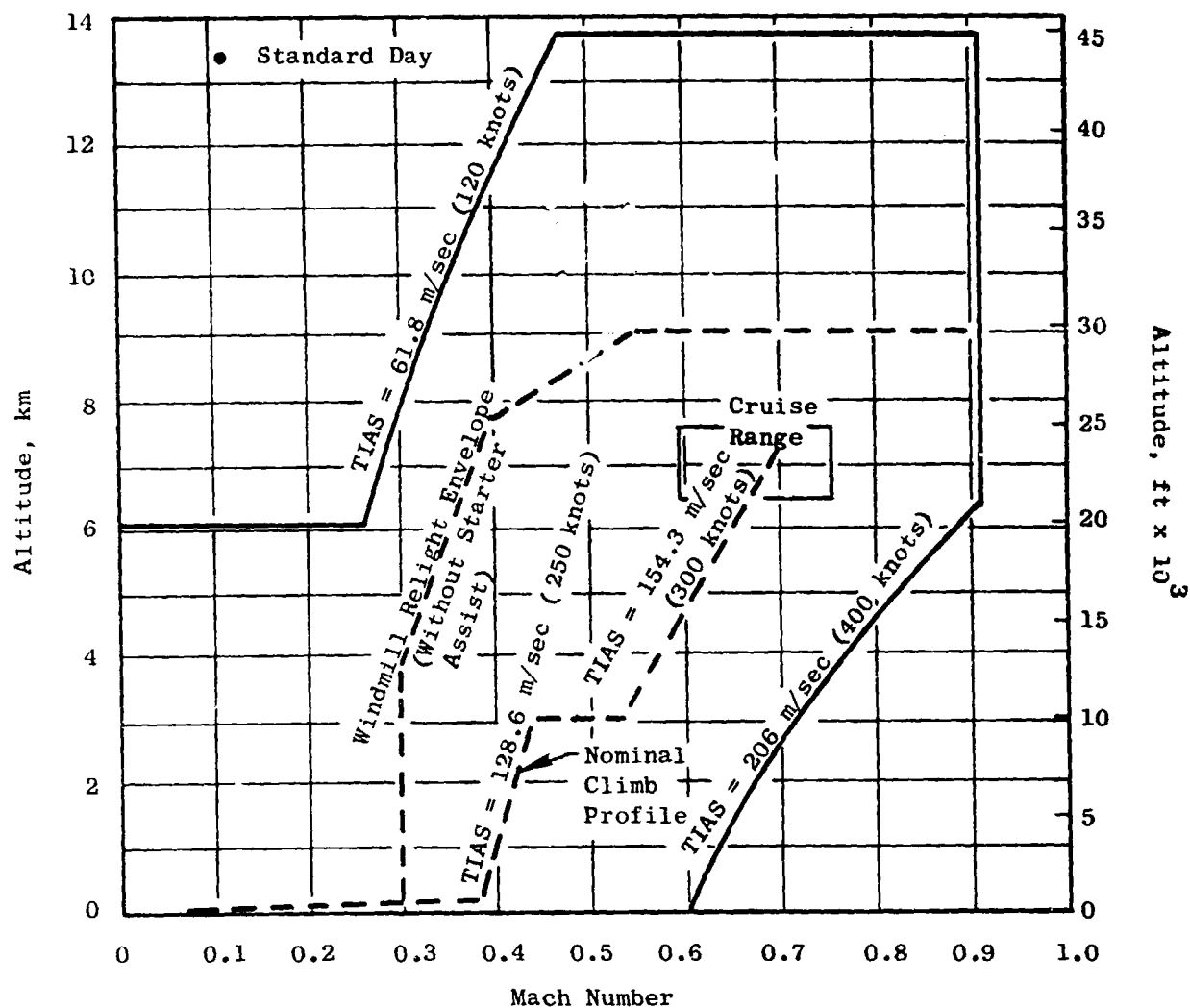


Figure 2. QCSEE UTW Operating Envelope.

Experimental Engine Flexibility

The system shall be capable of independently manipulating variables so that engine characteristics can be completely explored.

Automatic Control Capability

The system shall be capable of coordinated control of variables so that simulated STOL aircraft propulsion investigations can be performed with the intent of achieving:

- Thrust control with minimum pilot workload in all flight segments
- Fast thrust response
 - 1.0 second 62% to 95% thrust, sea level to 1.83 km (6000 ft.)
 - 1.5 seconds Takeoff to maximum reverse
- Specified noise and pollution goals for the engine

Engine Protection

The system shall protect the engine from rotor overspeeds, turbine overtemperature, and excessive fan or compressor back pressures.

Bleed and Power Extraction

The system shall be compatible with air bleed and power extraction for aircraft use up to 13% core airflow and up to 2.2 hp per 450 Kg (1000 lb.) installed thrust, respectively. Neither will be demonstrated in the initial QCSEE Program.

Starter

Design for use of a typical, current, commercial transport starter.

Altitude Starts

Capability the same as present commercial transports as shown on Figure 2.

Overboard Drainage

There shall be no overboard fluid leakage during normal operation.

Maintainability

The system shall be compatible with the following engine maintainability goals.

- The engine shall be easily removable from the nacelle without requiring removal of the fan exhaust duct once it is installed.
- The engine shall be capable of being trimmed on a test stand with no additional trimming required if installed on an aircraft.
- Accessories shall be located for easy inspection.
- Access to borescope ports shall be provided without requiring removal of any engine component.
- Any propulsion system accessory shall be replaceable in 45 minutes.
- Modular construction is desired to facilitate maintenance.

Supplementing the requirements and design criteria outlined above, a set of aircraft-oriented general principles for automatic control of the UTW engine was established early in the program based on coordination with NASA, McDonnell Douglas, and Boeing. These are:

1. A separate power lever link is assumed from the aircraft to the engine to be used as an enable and for backup fuel control only.
2. A digital electrical signal is assumed from the aircraft computer to the engine digital control demanding percent of available thrust.
3. A digital electrical mode signal is assumed from the aircraft computer to the engine digital control to select between available operating modes such as takeoff, climb, cruise, etc.
4. The engine digital control shall compute maximum rated thrust at all flight conditions and shall be capable of setting this thrust, or any portion of it, as a function of a single aircraft thrust demand signal (unless some safety limit such as rotor speed or gas temperature prevents attainment of full thrust).

5. The engine control system shall provide selected engine safety limits that protect against rotor overspeeds, fan or compressor stall, turbine overtemperature, and compressor discharge overpressure.
6. Manual control of thrust via the throttle shall be maintainable within safe limits if the engine digital control and/or aircraft digital control fails.
7. It is desirable that no throttle or thrust demand changes be required during takeoff except in the event of an abort.
8. It shall be an objective that fan pitch shall not change if the engine digital control fails.
9. It shall be an objective that fan nozzle area shall go to the takeoff position in the event of a failure.

3.2 GENERAL SYSTEM DESCRIPTION

A schematic diagram of the QCSEE UTW Control System is shown in Figure 3. The digital electronic control is the heart of the system and controls the manipulated variables in response to commands representing those which would be received from an aircraft propulsion system computer. The system includes an existing (F101) hydromechanical control as called for in the program requirements. This control includes an electrohydraulic torque motor servovalve (TM) through which the digital control maintains primary control of fuel flow. The fuel-operated servomechanisms in the hydromechanical control serve primarily as backup controlling elements and limits, although they are the primary controlling elements for the core compressor stator actuators.

The hydromechanical control is mounted on an F101 fuel pump which is a centrifugally boosted, positive displacement, vane pump. Pump discharge flow is delivered to the control through the mounting interface and the control returns excess fuel to the vane element inlet through a similar channel.

The fuel system includes an eductor to evacuate interstage seal cavities within fuel-handling components and thus reduce the possibility of external fuel leakage.

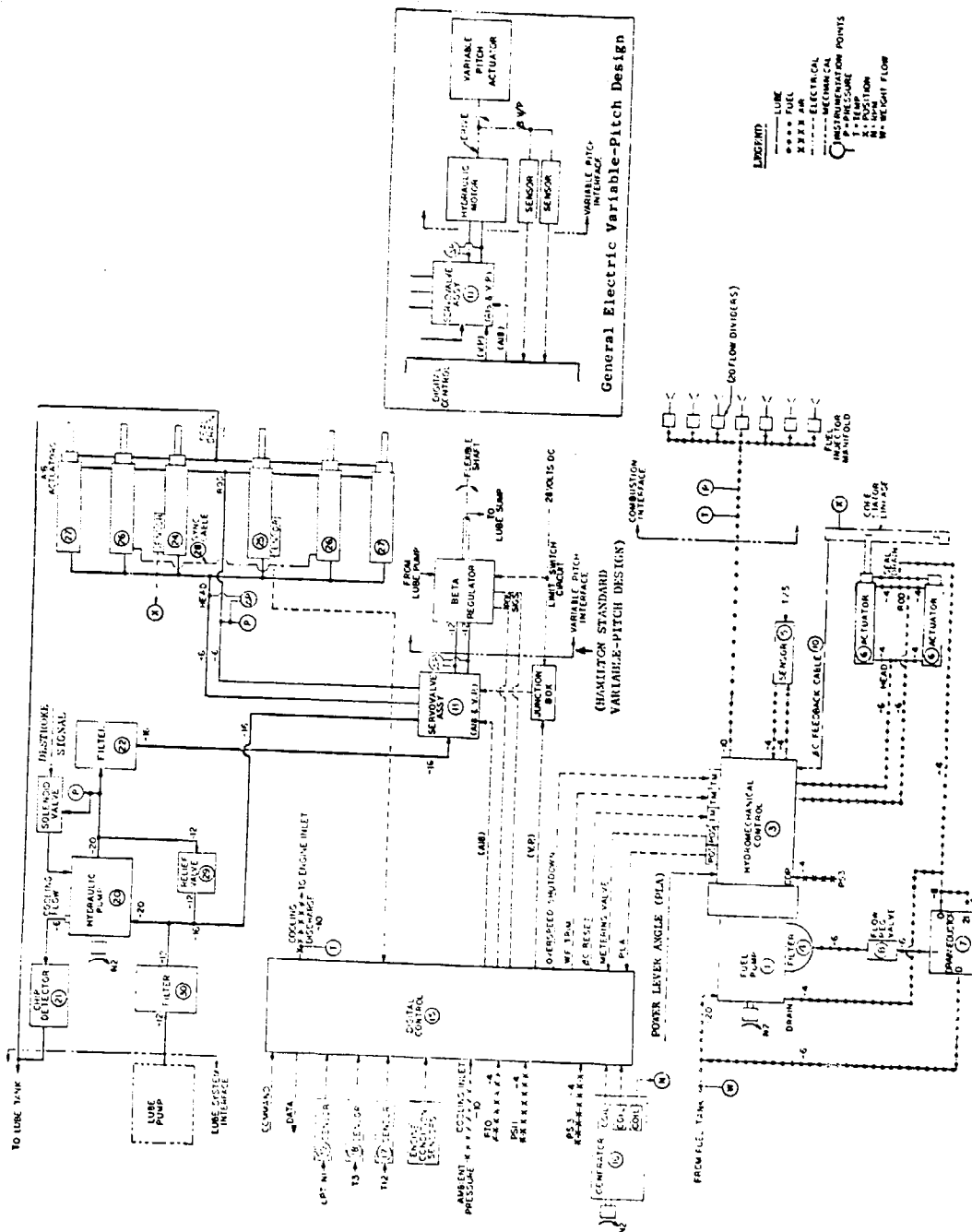


Figure 3. System Interconnection Schematic.

ORIGINAL PAGE IS
OF POOR QUALITY

Fan pitch angle and fan exhaust nozzle area are both controlled solely by the digital electronic control which furnishes electrical signals to electrohydraulic servovalves in the servovalve assembly. These servovalves direct hydraulic fluid to the hydraulic motor which positions the fan pitch mechanism and to the six hydraulic rams which position the variable fan exhaust nozzle in response to the signals from the digital control. As shown on Figure 3, the control system is designed to accommodate either of two fan pitch actuation systems which are being designed for the QCSEE UTW.

The hydraulic system which supplies the pitch and nozzle servovalve assembly consists of an engine-driven, variable displacement, constant pressure piston pump, a filter, and the servovalves. The system is essentially a closed circuit with only a small fluid interchange with the engine lubrication system for cooling and to transiently account for differential actuation areas.

In order to achieve the operational flexibility required by the QCSEE Program, the commands to the digital electronic control are being introduced through the control room elements shown on Figure 4. The interconnect unit, operator panel, and engineering panel are actually peripheral elements of the digital control. They provide the means for the engine operators to introduce commands, to switch between available operating modes, to adjust various control constants, and to monitor control and engine data. The remote computer is a separate digital computer system supplied by NASA to represent a typical aircraft computer. The engine digital control is designed to accommodate the digital input-output language of this remote computer.

In addition to these digital commands from the control room, the system also receives a mechanical input in the form of a power lever angle (PLA) transmitted to the hydromechanical control. This serves as an input to the backup governor and operates a positive fuel shutoff valve in the control.

A number of control and engine variables are sensed by the control system. These are shown schematically in Figure 5 and discussed briefly below.

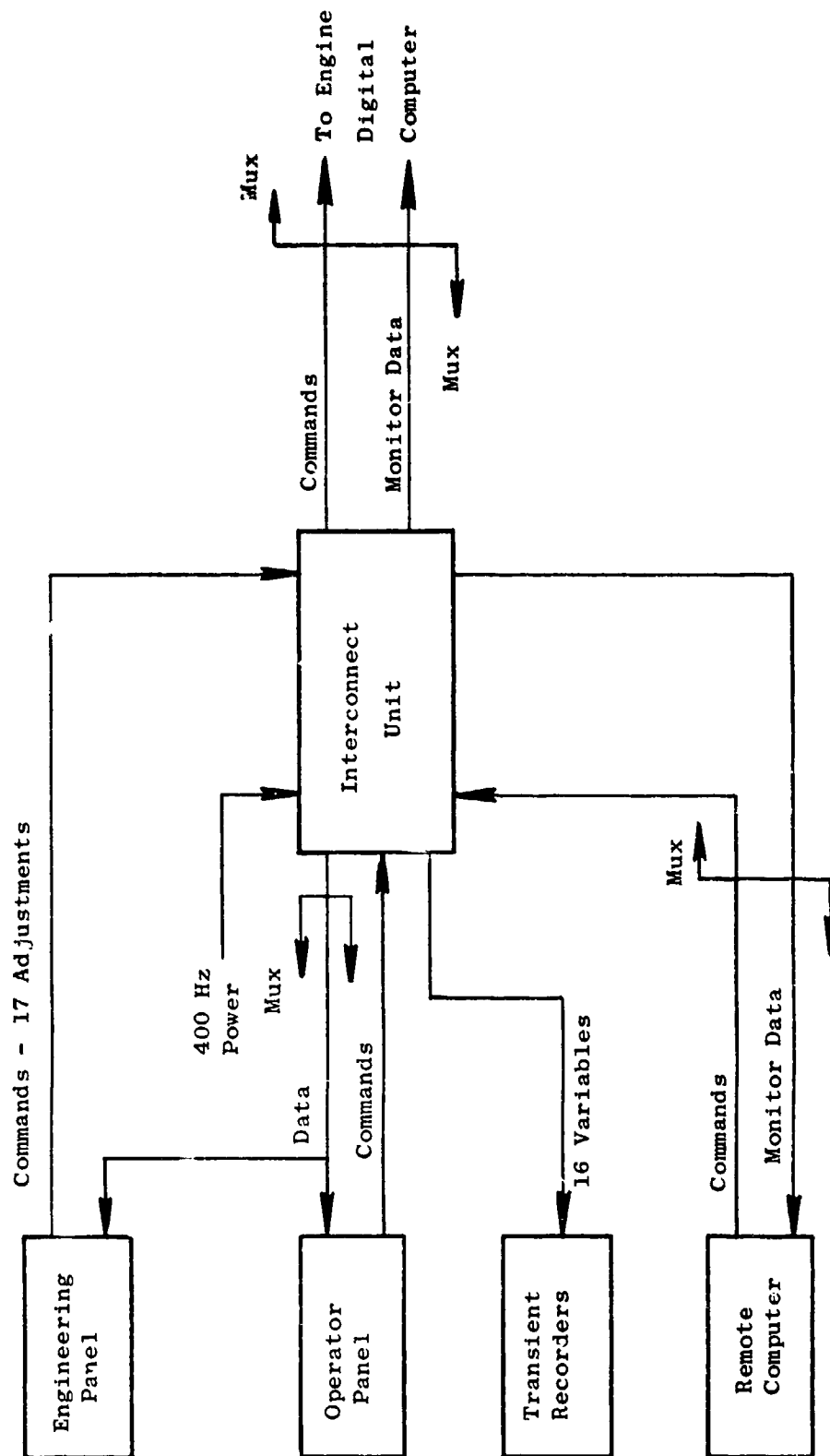


Figure 4. Control Room Elements of QCSEE Digital Control.

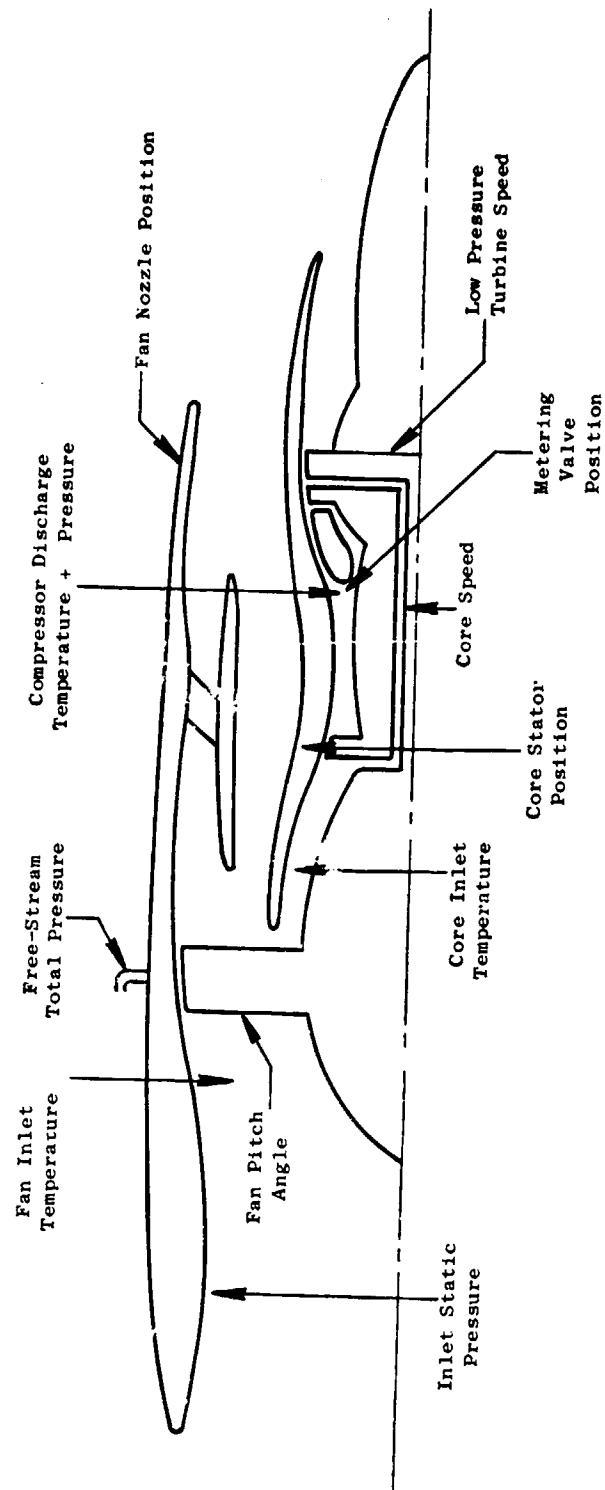


Figure 5. Sensed Engine and Control Variables.

Core Speed - This speed is sensed electrically by measuring the output frequency of the generator which supplies digital control computer power and is sensed mechanically by a rotational input from the accessory gearbox to the hydromechanical control.

Low Pressure Turbine Speed - This speed, which is proportional to fan speed, is sensed by a stationary magnetic pickup located near a multitoothed disk which rotates with the turbine shaft. A turbine speed signal is preferred to a fan speed signal because it is mechanically simpler to acquire, and it remains available to initiate correction of a turbine overspeed which might result from a fan or fan gearing failure.

Core Inlet Temperature - Sensed (as on the F101) by means of a gas-filled coil in the core compressor inlet which operates a hydromechanical fuel-sensing servomechanism.

Core Stator Position - Sensed mechanically by means of a push-pull cable between the stator actuation linkage and the hydromechanical control.

Compressor Discharge Pressure - Sensed through a static pressure tap in the entrance to the engine combustor and piped to a pressure-to-electrical transducer in the digital control and to a fuel-sensing servomechanism in the hydromechanical control.

Compressor Discharge Temperature - Sensed by a chromel-alumel thermocouple at the entrance to the core combustor.

Metering Valve Position - This is used as a measure of fuel flow in the digital control and is sensed with a transducer (rotary differential transformer) in the hydromechanical control.

Engine Inlet Static Pressure - Sensed through two static taps in the inlet duct wall and piped to one side of a differential pressure transducer in the digital control. The taps are on the inlet horizontal centerline and diametrically opposed to minimize angle-of-attack and crosswind effects. They are located in a position near the inlet throat - a position which NASA model data indicates will give the most consistent pressure reading.

Fan Inlet Temperature - Sensed by an electrical resistance temperature detector protruding through the inlet wall into the airstream.

Free-Stream Total Pressure - Sensed by means of a total pressure probe on the bottom centerline of the nacelle extending into the external air-stream. This pressure is actually used as a measure of engine inlet total pressure but is sensed outside where the probe will not be affected by the aerodynamic distortions which can exist inside the inlet and thus will give a more consistent indication of average inlet total pressure.

Fan Pitch Angle - Sensed by means of electrical position transducers (linear differential transformers) in the fan pitch actuation system. Because fan pitch angle is critical to satisfactory engine operation, two sensors are used. They are averaged by the digital control and protection is provided against failures of one unit as described in Section 3.3.3.

Fan Nozzle Position - Sensed by means of an electrical position transducer (linear differential transformer) in one of the nozzle actuators.

3.3 SYSTEM OPERATION

The system has several different modes of operation. The automatic mode provides integrated control of engine variables to allow exploration of steady-state and transient characteristics of the engine when automatically controlled. The manual mode and several partial-automatic, partial-manual modes are provided to allow independent manipulation of controlled variables so that engine characteristics can be completely mapped. Operation in the various modes is described below with the analyses and studies which led to the choice of these modes discussed later in the report.

3.3.1 Automatic Control

In the automatic control mode, the system basically manipulates fuel flow to control thrust, exhaust area to control inlet throat air velocity, and fan pitch to control fan rpm. Overrides are applied to each of the manipulated variables under certain conditions for safety or operational reasons.

The system uses the ratio of compressor discharge pressure to free-stream total pressure ($PS3/PT0$) as a measure of engine thrust. At any operating condition the digital control computes a value of maximum available thrust ($PS3/PT0$) as a function of engine inlet conditions as shown in Figure 6 with an inlet temperature reference ($T12$ reference) as shown in Figure 7. Fuel flow is manipulated as required to provide the percentage of this maximum available thrust called for by the power setting. This power setting is a digital electronic input supplied from the control room or, in an aircraft application, from the pilot or aircraft flight control computer. The power setting schedule is shown in Figure 8. The system includes a number of limits which can override the thrust control and limit fuel flow to prevent engine damage or unsatisfactory operation. These are listed below.

T41 Limit - Turbine inlet gas temperature ($T41$) is calculated in the digital control from compressor discharge temperature ($T3$), fuel flow, and compressor discharge pressure. Fuel flow is limited to prevent this calculated $T41$ from exceeding a predetermined limit.

Acceleration Limit - An acceleration fuel schedule which is a function of core rpm, core compressor inlet temperature, and core compressor discharge pressure is incorporated in the hydromechanical control; fuel flow is prevented from exceeding this schedule. The schedule is designed to provide satisfactory starts and rapid acceleration without core compressor stall or excessive turbine temperature transients.

Deceleration Limit - To prevent loss of combustion during rapid thrust reductions, the hydromechanical control prevents $WF/PS3$ from dropping below a prescribed minimum limit.

Fan Speed Limit (Normal) - The digital control limits fuel flow to prevent exceeding a predetermined normal fan speed (LP turbine) limit.

Maximum Core Speed Limit - The digital control and hydromechanical control both include functions for limiting fuel flow to prevent core overspeed.

Backup Governor - This governor in the hydromechanical control can reduce fuel flow and speed in response to the mechanical power lever input in the event of an electrical malfunction.

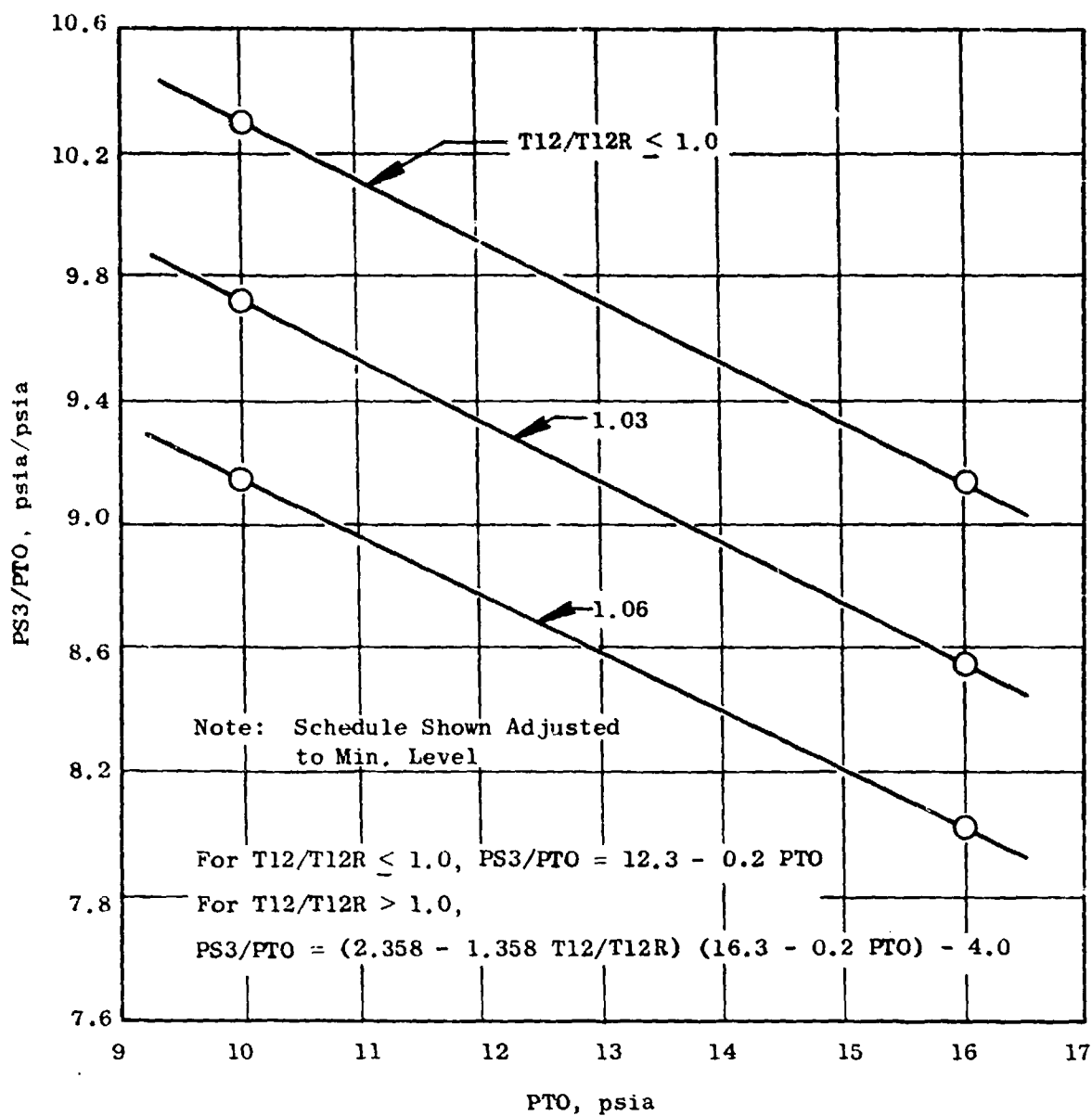


Figure 6. Rated PS3/PTO Schedule.

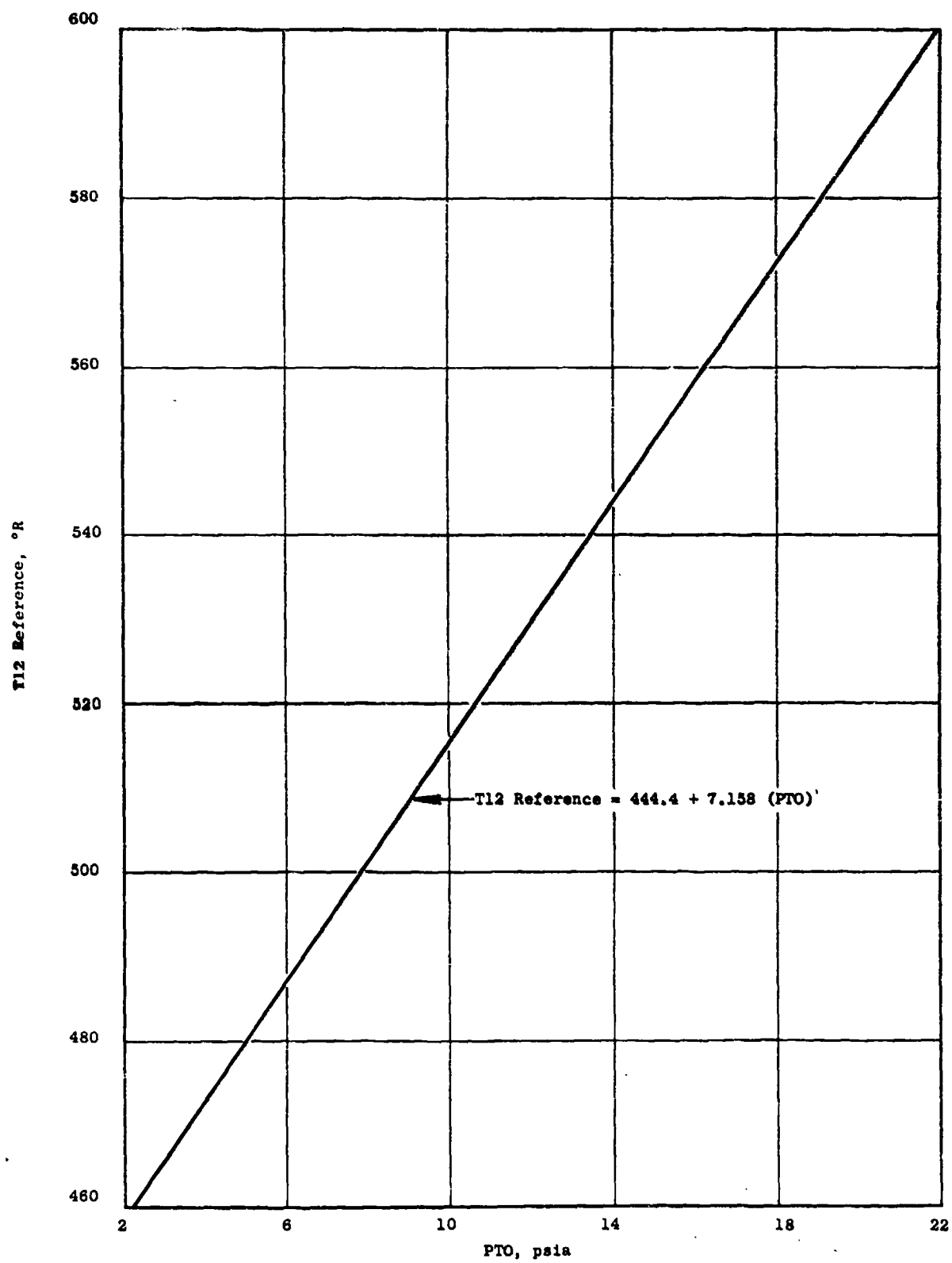


Figure 7. T12 Reference in Digital Control.

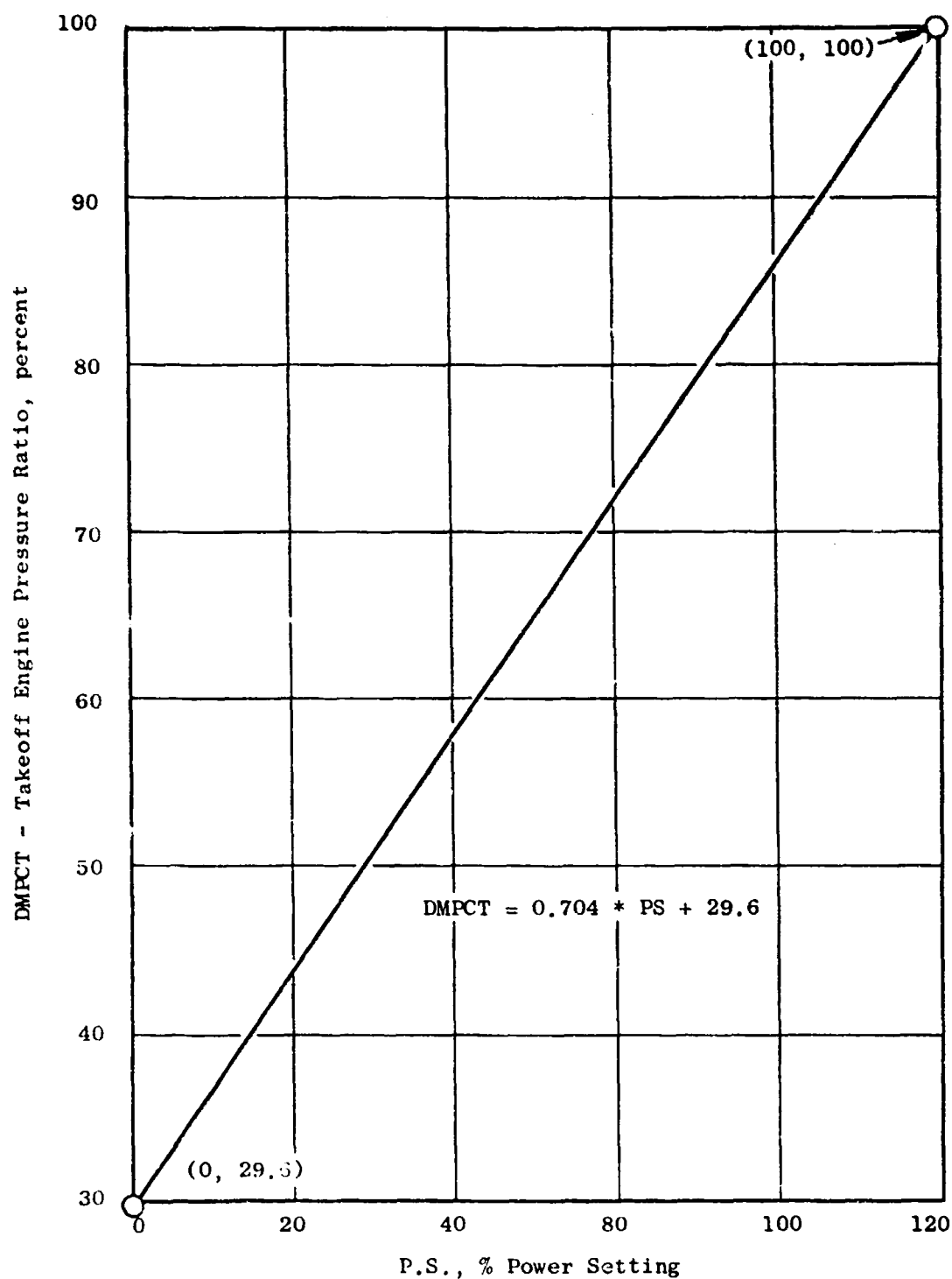


Figure 8. PS3/PTO Power Demand Schedule.

Minimum Idle Speed - The digital control limits fuel flow in the downward direction to prevent idle speed from dropping below an allowable minimum (an experimental engine limit only - related to lube sump pressurization).

Reverse Interlock - The digital control reduces fuel flow if the fan blades are in reverse region with forward thrust selected or in the forward region with reverse selected. This feature unloads the core engine to assist in normal transients into and out of reverse and limits the amount of mis-directed thrust if the fan pitch inadvertently moves into the wrong region.

Fault Correction - Fuel flow is also limited by several fault detection and correction features in the system which are described in Section 3.3.3.

The PS3/PTO control function and the limits on fuel flow are shown in block diagram form on Figure 9. The PS3/PTO schedule and error calculation are shown at the upper left. The error signal proceeds through a network which includes a lagged-rate feedback for stability and transient anticipation (detailed in Figure 10), logic for switching to other control modes, selectors through which the limits are applied, and elements which generate an output signal. This output signal operates a torque motor servovalve in the hydromechanical control to control fuel flow within the bounds of hydromechanical acceleration, deceleration, and core speed schedules.

The T41, maximum fan speed, maximum core speed, minimum idle speed, and fault limits are all generated in the right portion of the block diagram and applied to the main channel through the maximum and minimum selectors in the upper-right corner. The vertical array of four blocks at the left center is the logic for the reverse interlock. This logic reduces the maximum core speed limit to idle whenever the fan pitch is in transition in either direction between forward and reverse or when the pitch is not in the correct region for the mode selected.

Figure 9 also includes the manual fuel control mode and logic for switching into this mode which is discussed in Section 3.3.2.

Fan exhaust area in the automatic control mode is varied to maintain the inlet throat Mach number at an intermediate level between the high level desired for inlet noise reduction and the low level desired for best inlet

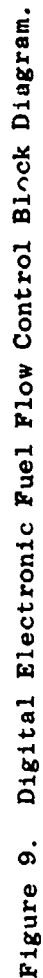


Figure 9. Digital Electronic Fuel Flow Control Diagram.

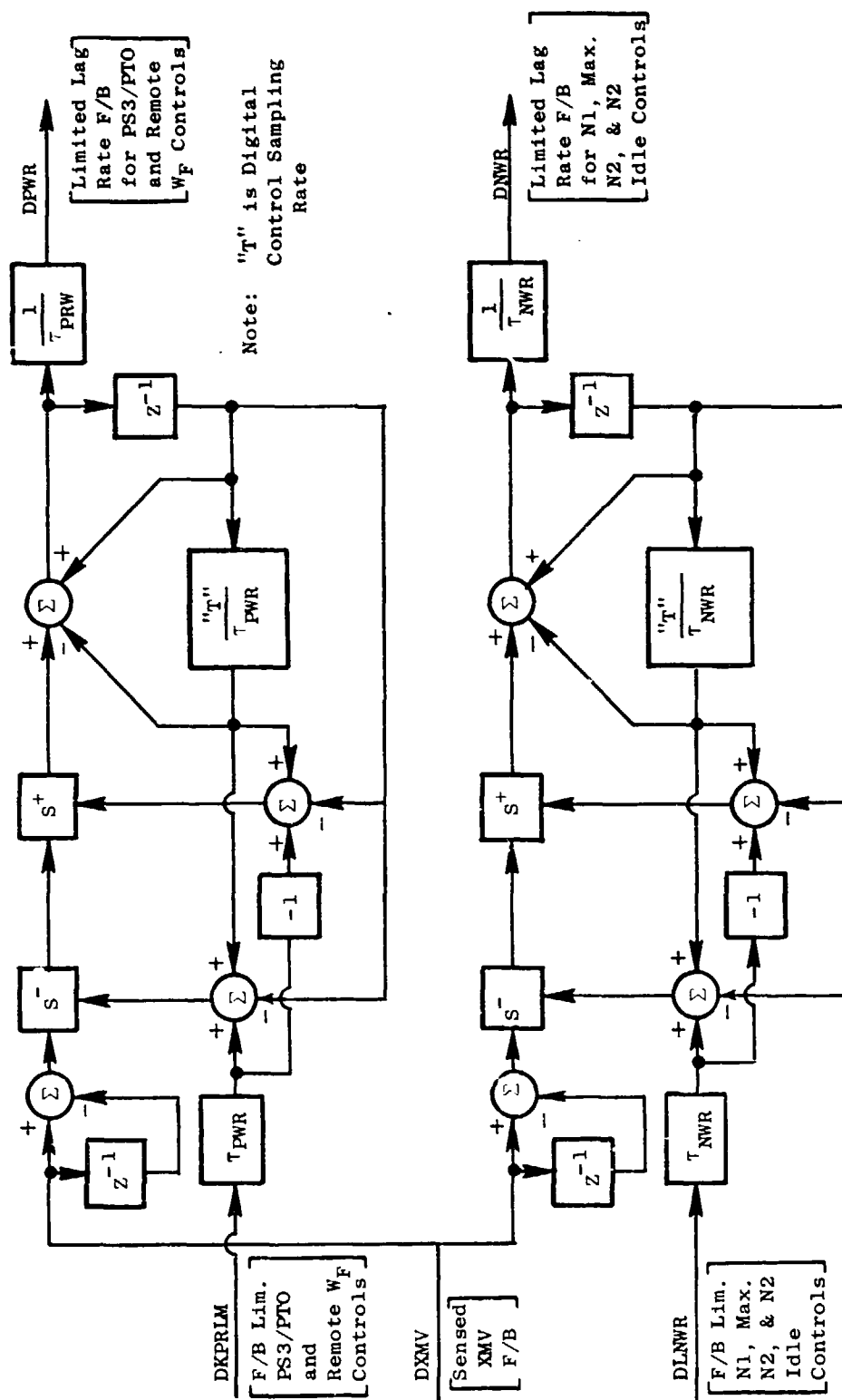


Figure 10. Detail Block Diagrams for Lag-Rate Feedbacks with Rate Limits in Fuel Flow Control Loop.

performance. Maintaining the inlet Mach in this manner also provides reduced exhaust velocity and lower exhaust noise at a given thrust level. The operation of this function is limited by a power-setting-generated roof schedule which improves transient response and prevents excessive area in the event of certain failures. Absolute maximum and minimum area limits are also provided.

A block diagram of the area control loops is shown in Figure 11 with the basic inlet Mach number control channel along the top and limit functions below which are introduced into the main channel through maximum and minimum selectors. The control uses free-stream total pressure and a static pressure near the inlet throat (PS11) to calculate a pressure function, $(PTO-PS11)/PTO$, which is a measure of inlet Mach number. This is shown at the upper left in the diagram. Any difference in the pressure function from the desired value creates an error signal which proceeds to the right through other elements in the main channel. This includes a lagged-rate feedback for stability compensation and transient anticipation (detailed on Figure 12); selectors through which limits are applied; logic for switching to other control modes; and elements for generating an output signal. The output signal operates a torque motor servovalve which controls the flow of hydraulic fluid to actuators which vary exhaust area.

Shown below the main channel in successive layers are the roof schedule channel, a transient roof reset, the minimum area limit channel, and a manual control channel. These all operate through logic blocks shown in the main channel to produce their effect on area control.

Automatic control of fan pitch involves maintaining constant fan speed at most operating conditions. This is done primarily to provide rapid thrust response from low to high thrust by eliminating the need to accelerate the fan rotor. The governing action is limited to maximum and minimum blade angles beyond which fan operation may be unsatisfactory. A limit in the flat pitch direction is also imposed by the power-setting-generated floor schedule which is included to aid in transient response investigation on the experimental engine. This schedule is adjustable and will make it possible to evaluate accelerations with different fan pitch settings. Fan pitch is

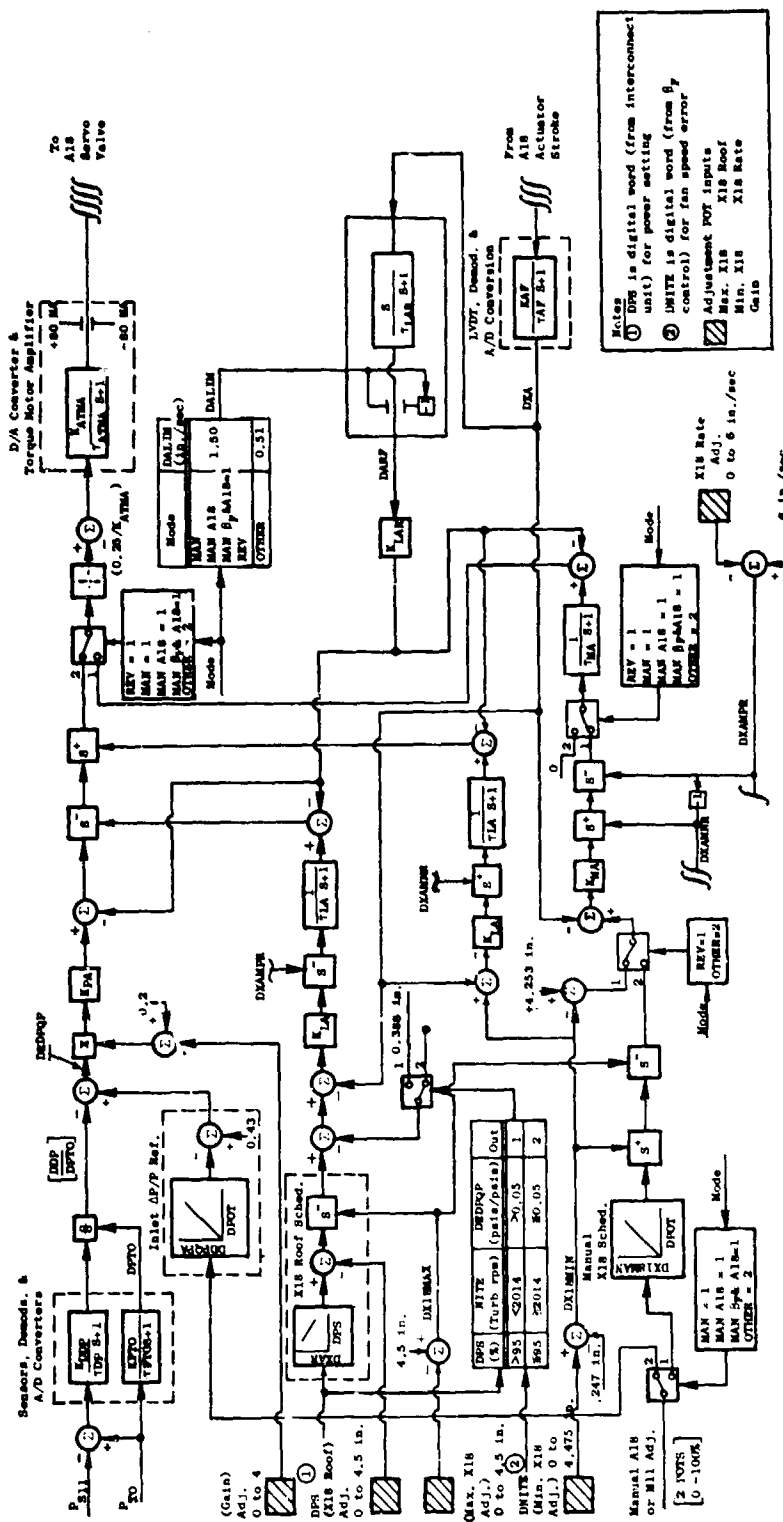


Figure 11. Digital Electronic Fan Exhaust Area Control Block Diagram.

ORIGINAL PAGE IS
OF POOR QUALITY

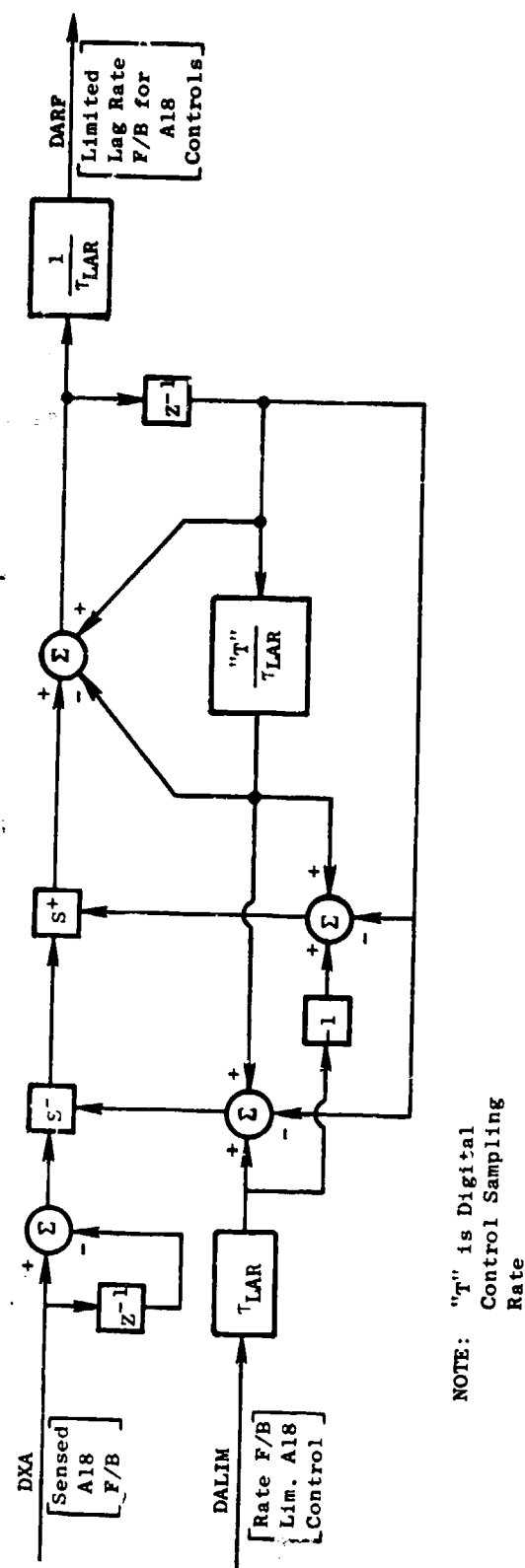


Figure 12. Detail Block Diagram for Lag-Rate Feedback with Rate Limits in Fan Exhaust Area Control Loop.

reversed to provide engine thrust reversal. This is done by changing operating modes within the control system to a mode which positions the blades in their reverse position. In this automatic reverse mode the variable-area exhaust is set at its maximum open position (actually serving as inlet in this mode), and fuel flow is manipulated to control fan speed as demanded by the power demand signal. The fuel flow interlock noted above in the fuel control loop description aids in performing transitions into and out of reverse.

Figure 13 is a block diagram of the fan pitch control loop. The main channel is shown along the top with the basic fan speed scheduling and error calculation performed at the left. As in the other control loops described above, the error signal passes through a network which includes a lagged-rate feedback for stability compensation and transient anticipation (detailed on Figure 14), maximum and minimum selectors for applying limits, mode switching logic, and elements which generate an output signal. The output signal operates an electrohydraulic valve which controls flow to a hydraulic motor which, in turn, drives the pitch actuation mechanism.

Shown in successive layers below the main channel on Figure 13 are the floor (maximum closed pitch) schedule limit channel with an associated transient reset, the roof (maximum open pitch) limit channel, the reverse pitch channel, and the manual control channel. The ganged switching logic shown to the left in these channels is provided to accommodate the two fan pitch mechanization options on the QCSEE UTW demonstrator, one of which goes to reverse-through-stall pitch and the other through flat pitch.

Position feedback from the fan pitch actuation device is provided by two electrical LVDT position transducers. These signals are shown entering at the right center in Figure 13. The control averages these signals under normal conditions but chooses the larger signal if the two signals disagree by the equivalent of three degrees pitch or more. This latter feature provides protection against the most likely LVDT failure mode which is complete loss of signal due to open or short circuits.

The core compressor variable stators in the automatic mode and in all other modes are controlled hydromechanically as they are on the F101 engine.

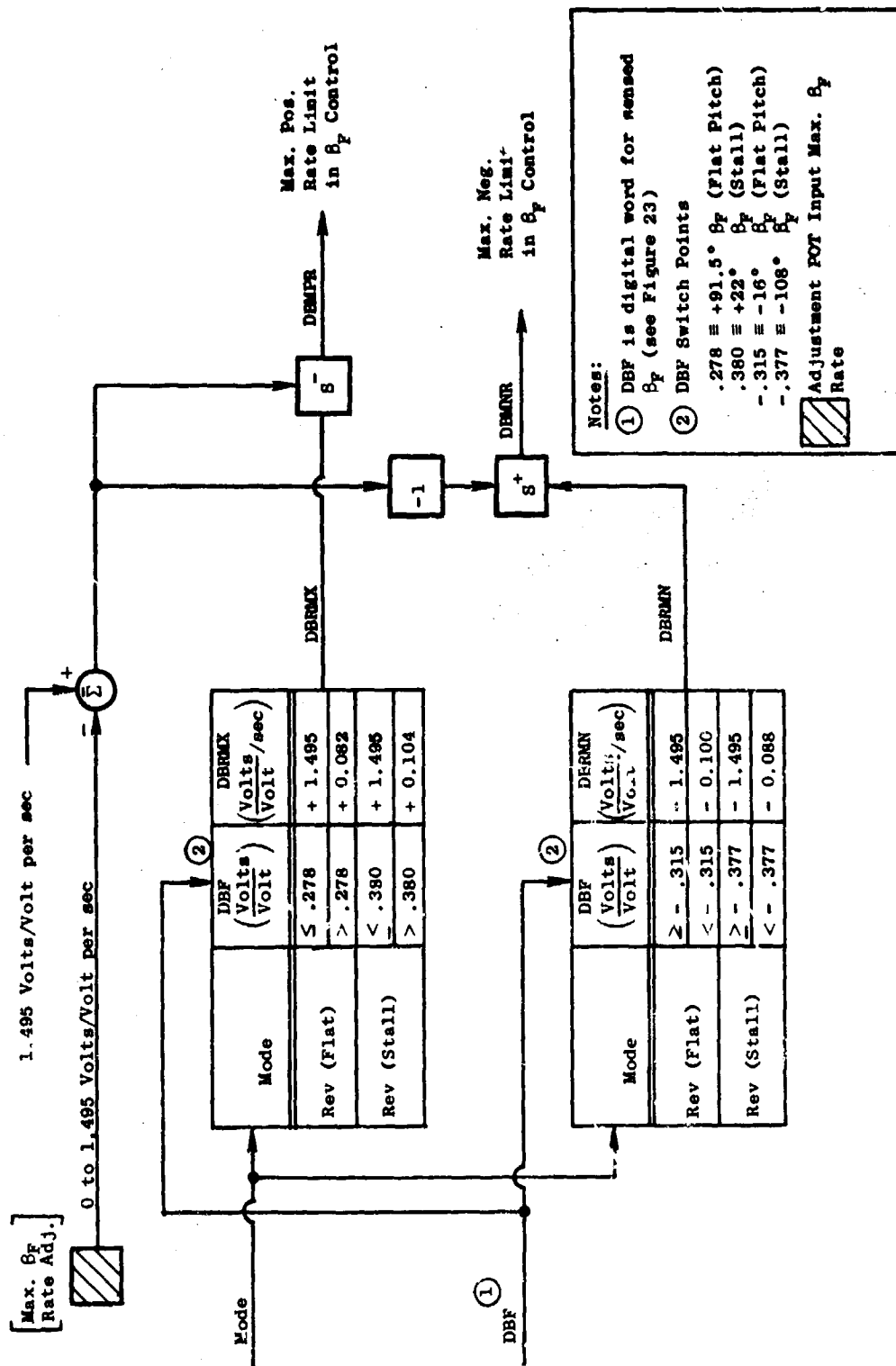


Figure 13. Digital Electronic Fan Pitch Control Block Diagram (Concluded).

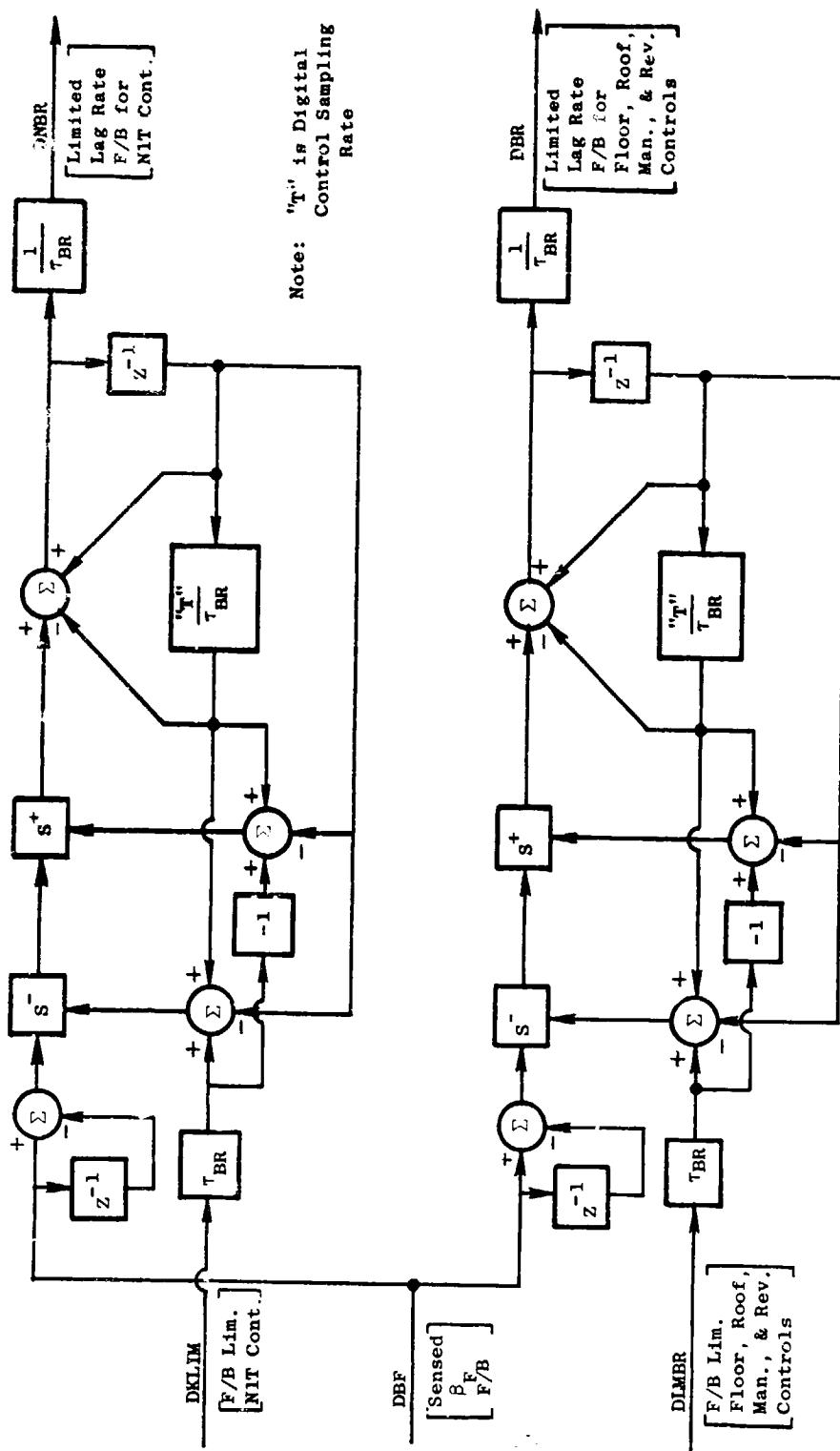


Figure 14. Detail Block Diagrams for Lag-Rate Feedbacks with Rate Limits in Fan Pitch Control Loop

Stator position is set as a function of core speed and core inlet temperature. A reset is included (in response to an electrical signal from the digital control) which translates the entire schedule by a small amount toward the closed direction in order to provide additional core compressor stall margin under certain conditions.

3.3.2 Manual Control

The system includes a manual control mode and several partially-manual modes in which all or some of the manipulated variables can be controlled independently from the control room. The manual modes are provided so that the characteristics of the engine with its variable geometry can be thoroughly explored.

In the all-manual mode, the system operates in response to four basic inputs from the control room, three potentiometer inputs to the digital control computer, and the manual power lever input to the hydromechanical control.

One of the potentiometer inputs serves as a fan speed demand causing fuel flow to be manipulated to set and maintain the fan speed desired. All of the fuel control loop limits described in Section 3.3.1 (except the reverse interlock) remain in effect to protect the engine and provide manual PLA control of core speed if desired (or necessary due to an electrical malfunction).

The other two potentiometers serve as inputs to the digital control for operation of independent position control loops for fan pitch and fan exhaust area. Thus, in the all-manual mode, fan speed (or core speed), fan pitch, and fan exhaust area can each be controlled independently. The three manual control loops are shown on the block diagram in Figures 9, 11, and 13.

Three partially-manual modes are provided. In one, fan pitch is under manual control while fuel flow and fan exhaust area are automatically controlled as described in Section 3.3.1. In the second, fan exhaust area is under manual control while fuel flow and fan pitch are in the automatic mode. In the third, both pitch and area are manually controlled and only fuel is operating in the automatic mode.

In all of the manual modes, control of the core variable stators is the same as in the automatic mode.

3.3.3 Failure Detection and Correction

One objective of the QCSEE Program digital control technology development is to utilize the inherent abilities of a digital computer to record and compare large amounts of data for engine condition monitoring and fault correction.

The UTW control system incorporates several active fault detection and correction features which are listed below. A fault light on the operator panel indicates when one or more of the faults has occurred and a digital indicator on the engineering panel identifies the fault or faults. A switch is available on the engineering panel to deactivate each of the features except the fan overspeed emergency shutdown.

Engine Vibration - Engine horizontal and vertical vibrations are sensed: if either exceeds 40 mils, fuel flow is reduced to set idle core speed.

Loss of Command Data Link - A test word is among the set of digital commands that are transmitted respectively in series from the control room to the engine-mounted digital control computer. An error in this word at any time causes the control to revert to the last set of commands received and to continue operating at this condition until the fault is corrected.

Computer Fault - The program memory in the digital control computer includes test elements which, if found to be incorrect for two successive iterations through the program, will interrupt the control outputs and cause fuel flow to drift downward, fan exhaust area to drift open, and fan pitch angle to drift open (increased pitch).

Fan Overspeed Emergency Shutdown - If the LP turbine (fan) speed signal exceeds an absolute maximum limit, or if it increases at a rate indicating loss in turbine load (as would occur with fan or fan gearbox failure), an electrical signal from the digital control to the hydromechanical control causes fuel flow to be shutoff immediately. All elements of this feature are electrically isolated from the remainder of the system so that it also

protects against control system faults which might cause overspeed. If power should be lost for this function so that it is unavailable at the operator panel, a fault light will alert the operator.

LP Turbine Speed Sensing Fault - Loss of the LP turbine (fan) speed signal can result in overspeed to the emergency shutdown level under certain conditions when operating on the automatic mode. To prevent this, the digital control reduces fuel flow to set idle core speed if the LP turbine speed signal is lost. This function is ineffective below 45% core speed so that it will not interfere with starts.

Fan Pitch Transducer Failure - The signals from the two fan pitch position transducers are normally averaged by the digital control. However, if the signals differ by three degrees or more the control uses the signal with the largest voltage level, discarding the other on the premise that the transducer producing the lower voltage may well have failed because the predominant failure mode for such transducers is loss of signal.

Lube Supply Temperature - If this temperature exceeds 180° F, the engineering panel fault light illuminates, but there is no automatic corrective action.

Gearbox Bearing Temperature - If this temperature exceeds 250° F, the engineering panel fault light illuminates, but there is no automatic corrective action.

Hydraulic Pump Pressure - If this pressure falls below 2500 psia with core speed above 45%, the engineering panel fault light illuminates but no automatic corrective action is taken.

Computer Timing Failure - The digital control includes redundant oscillators for timing in both the engine-mounted computer and in the control room portion of the control. An oscillator failure in the former will illuminate the fault light on the engineering panel, and a fault in the latter will illuminate a light on the interconnect unit in the control room.

The digital control system also includes provisions for monitoring control and engine variables. Some variables are displayed continuously on the operator panel, some are provided for continuous recording on transient data

recorders, and some are available for display (one at a time) on a selectable digital display on the engineering panel. A detailed list of monitored information is given with the digital control description in Section 5.0 of this report.

4.0 CONTROL SYSTEM ANALYSIS

4.1 ANALYSIS BACKGROUND

One fundamental task to be performed in designing an automatic control system is to define the control mode or modes; that is, define which engine variables (speeds, pressures, temperatures, etc.) should be controlled by the available manipulated variables to achieve the desired operating conditions. This involves analyses comparing potential modes on the bases of accuracy, stability, response, and other similar performance considerations.

On most previous transport aircraft engines, control mode definition has been relatively simple because only one manipulated variable, fuel flow, was a significant factor in controlling the primary engine characteristics which require control, namely thrust and thrust response. To define the control mode it was necessary only to determine a variable that can be sensed practically, provides a good indication of thrust, and will provide a responsive, stable fuel control loop.

The QCSEE UTW analysis necessary to define control modes was more difficult because of the additional manipulated variables, the need to consider noise control as well as thrust, and the desire to provide more automatic control of thrust than on previous engines. At the outset it was decided that one of the manipulated variables, core stator position, is clearly best controlled by scheduling position as a function of core corrected speed as on the F101 engine. Still, there remained three manipulated variables (fuel flow, fan pitch, and fan exhaust area) each of which could be used to control a variety of engine variables or sets of variables.

Key operational objectives at various conditions were established prior to beginning the automatic control mode analytical process. These were:

- Takeoff - Set guaranteed maximum static thrust or percent thereof.

Set inlet throat Mach number (XM11) for optimum noise and performance trade off.

- Climb - Set guaranteed maximum installed thrust or percent thereof.

Control inlet Mach number for optimum installed performance.

- Cruise - Attain minimum installed sfc at required thrust level.
- Descent - Maintain sufficient core speed for air conditioning and power extraction.
- Approach - Fast thrust response at readily controlled level up to guaranteed maximum.

Control inlet Mach number and airflow for low noise.

- Ground Idle - Low thrust.

Low exhaust pollution.

Low noise.

RPM sufficient for centrifugal anti-icing.

The sections which follow describe the analytical studies performed to translate these requirements in the choice of control modes.

4.2 CONTROL MODE ANALYSIS

One of the first steps taken in control mode definition was to perform a control mode analysis. This is a computer-aided process in which the effect of typical engine and control component tolerances on important engine characteristics (such as thrust, sfc, turbine temperature, stall margin, etc.) are determined for all potential control modes.

The starting point for the mode analysis was a computer deck representing the UTW engine cycle under steady-state, installed conditions. A special computer program was used with this deck to generate matrices of partial differentials of certain dependent variables with respect to certain other independent variables. Among the independent variables were potential control variables, air bleeds, power extraction, and engine component performance variables which contribute significantly to overall propulsion system performance. The dependent variables included such key cycle variables as thrust, sfc, temperatures, stall margins, rotor speeds, and inlet throat Mach number.

The mode analysis consisted of a series of computer runs using the matrices of partial differentials just described. For each run, a different set of potential control variables equal in number to the number of manipulated variables (3 for the UTW engine) was designated and the matrix used was that which had these as independent variables. Predicted tolerances for sensors, controls, and engine components were multiplied by the partial differentials. The computer tallied the accumulation of these effects on key dependent variables in several ways including (1) the arithmetic sum, (2) the square root of the sum of the squares (RSS), and (3) RSS with zero control tolerances. Deterioration factors based on actual field experience were applied to the partials and the RSS accumulation of these factors was also calculated.

Runs were made at SLS takeoff conditions and at Mach 0.7, 7.62 km (25,000 ft.) climb conditions.

Details relative to the potential modes subjected to this type of analysis, the tolerances used, and typical results, are given in the sections which follow.

4.2.1 Definition of Potential Thrust Parameter

One important task in defining potential control modes for analysis was to establish potential thrust parameters which would indicate net thrust at any flight condition as a percentage of the maximum rated thrust at that condition. Ideally, the thrust parameter should be such that it could be used for cockpit indication and correlate with percent-net-available thrust independent of customer air bleed, control errors, engine component variations, and flight conditions. The ideal thrust parameter also would have negligible thrust-correlation errors during engine stalls or control failures (failures which for this engine might result in large deviations in fan pitch or exhaust area from normal settings).

The potential thrust parameters used in the mode analysis are listed below and discussed in succeeding paragraphs (symbols defined in Appendix A).

TP1 = P49/PTO

TP2 = PS3/PTO

$TP3 = f(P18/PAMB) \times (A18)$
 $TP4 = f(P14/PTO) \times (A18)$
 $TP5 = f(M11)/(A18)$
 $TP6 = f(P14/PTO) \times f_2(M11)$
 $TP7 = K1 + K2(\Delta A18) + K3(\Delta \beta F) + f(PCNLR)$
 $TP8 = T41C/T1$
 $TP9 = PCNHR$
 $TP10 = PS3/PS8$
 $TP11 = T8/T1$
 $TP12 = [(T14-T1)/T14] \times f(M11)$
 $TP13 = WFM/PTO$

TP1 is a good traditional parameter which would be applicable to a variable-pitch fan system. P49/PTO is a good indicator of core extracted power and correlates well with net thrust, but the mechanical design for QCSEE does not permit the insertion of total pressure rakes between the turbines. Static pressure measurement was considered as a substitute for P49, but the close-coupled turbine configuration prevents acquisition of a consistently representative static pressure. TP2 provides much better accuracy than could be obtained using PS49 (but not as good as using PT49); therefore, the mode studies include P49/PTO to provide a standard of comparison and PS3/PTO as a practical alternative for the experimental program. Core engine temperatures were bypassed in the initial listing of alternatives because the best choice, T49, had the same installation problem as P49, and all of the core temperatures are particularly sensitive to component deterioration.

The expression for TP3 was developed from the equation which states that gross thrust is equal to the product of mass airflow times velocity. With the full exhaust expansion present in the UTW cycle over the range of practical consideration and with the engine's high-bypass ratio, it is only a minor approximation to assume that the total thrust is a constant times the thrust of the bypass stream. Using this consideration and applying fundamental compressible-flow equations resulted in the transformation of the basic gross-thrust equation into an equation for TP3 as a function of fan exhaust pressure ratio and area as shown above.

Additional mathematical manipulation translated the P14/PAMB function into a P14/PTO (fan pressure ratio) function resulting in the TP4 expression.

TP5 and TP6 were also derived from the basic gross-thrust equation with manipulations performed so that the mass airflow is expressed in terms of an inlet airflow indicator, inlet Mach number, a variable which is sensed by the control system for noise control purposes.

TP7 is a semilinearized equation including one of the conventional fan engine thrust parameters (fan corrected speed) with factors accounting for deviations in fan pitch and exhaust area.

The remaining thrust parameters, except for TP12, are corrected engine variables which are indicative of core engine power (core engine power being fundamentally a more comprehensive indicator of net thrust than any simple fan system parameter). TP12 is a corrected fan power parameter.

4.2.2 Definition of Tolerances

A vital factor in setting up the control mode analysis was the definition of tolerances for the independent variables - that is, for the controlled variables in each mode being studied and for basic engine component characteristics.

A total of 19 controlled variables were considered to have potential for the UTW; 12 of the 13 thrust parameters described previously plus 7 others. These are listed in Table I with tolerances which were estimated in the manner described below.

Controlled variable tolerance estimates were begun by estimating sensing tolerances. Current state-of-the-art sensors were assumed with full-scale ranges set based on the UTW cycle and flight envelope. Tolerance distributions were optimized, when possible, for certain scale ranges based on engine needs.

The tolerance assignments also included analog-to-digital conversion errors and estimated sampling errors based on the uncontrolled effects of local flow distortions. Scheduling errors were also estimated where secondary

Table I. Mode Analysis Controlled Variable Tolerances.

Controlled Variables	SLS Takeoff Max. Climb	
	Error	Error (0.7/25K)
PCNLR - Corrected Fan Speed	±0.38%	±0.67%
A18 - Duct Nozzle Area	1.20	1.63
β_F - Fan Blade Pitch Angle	0.50	0.50
M11 - Inlet Duct Mach No.	1.68	2.40
P49QOT - LP Turbine EPR (P49/PTO)	1.20	2.29
PS3QOT - HP Turbine EPR (PS3/PTO)	1.03	2.22
TP3 - Thrust Parameter from A18 & (P18/PO)	7.03	2.76
TP4 - Thrust Parameter from A18 & (P14/PTO)	3.94	4.68
TP5 - Thrust Parameter from A18 & M11	1.80	2.29
TP6 - Thrust Parameter from M11 & P14/PTO	2.16	4.47
TP7 - Thrust Parameter from NL, A18, β_F	2.65	2.78
T41CT2 - T41C/T2	1.23	1.61
T49QT2 - T49/T2	1.09	1.10
T8QT2 - T8/T2	0.95	1.22
PCNHR - Corrected Core Speed	0.31	0.33
TP12 - $f(M11)$ (T14-T12)/T12	2.41	2.49
WFQPTO - WFM/PTO	1.34	2.13
M14 - Fan Duct Mach No. Parameter	3.86	5.46
P14QOT - P14/PTO	0.81	2.33

or trim parameters were used to define operating values for the control variables. Errors calculated for each of the sensed variables are listed in Table II. Errors due to sampling, sensors, signal conditions, and A-to-D conversion were combined by the root-sum-square method.

The sensing errors from Table II were used to calculate control parameter errors based on derivatives of the control parameter equations. As an example, the error synthesis for T41C (computed T41) is described as follows:

1. At the time of the mode studies, T41C was defined by the equation:

$$T41C = T3 + k_2 \frac{WF}{PS3} \sqrt{T41C}$$

2. The log differential equation for the parameter equation was derived:

$$\frac{\Delta T41C}{T41C} = \frac{2T41C}{T41C + T3} \left[\frac{T3}{T41C} \left(\frac{\Delta T3}{T3} \right) + \frac{T41C - T3}{T41C} \left(\frac{\Delta WF}{WF} - \frac{\Delta PS3}{PS3} \right) \right]$$

3. The three terms in this equation were root-sum-squared to obtain the overall error for T41C.
4. For the parameter T41C/T2, the errors for T41C and T2 were root-sum-squared. The error computed for T41C/T2 using this method and the data in Table II is $\pm 1.23\%$. The final result in terms of T41 was evaluated by the computer mode study and the final results include effects of engine component variations.

The equation for T41C was changed subsequent to the mode studies. The new equation defined below was chosen to avoid iteration in the digital engine control. The new equation was:

$$T41C = k_1 + k_2 T3 + k_3 \left(\frac{WF}{PS3} \right)^{1.245}$$

The resulting differential equation for errors was:

$$\frac{\Delta T41C}{T41C} = 0.476 \left(\frac{\Delta T3}{T3} \right) + 0.6585 \left(\frac{\Delta WF}{WF} \right) - 0.6585 \left(\frac{\Delta PS3}{PS3} \right)$$

Table II. Mode Analysis Sensing Tolerances.

(Includes profile, sensors, signal conditioning, and A-to-D conversion.)

Sensed Variable	Max. Value	Min. Value	Sampling at Takeoff	Sampling at Climb	Overall Takeoff Errors	Overall Climb Errors
Percent of point unless noted otherwise						
PTO(PSIA)	19.0	3.78	0.25	0.25	0.74	1.71
PTO-PS11	7.8	1.30	2.08	2.08	2.43	3.26
P14	23.2	5.17	0.50	0.50	0.86	1.58
P14-PS14	8.2	0.76	3.94	3.94	4.37	5.82
P14-PTO	4.2	1.40	3.54	3.54	3.93	4.22
PS3	257.0	56.40	0.25	0.25	0.72	1.41
P49	70.0	16.20	0.50	0.50	0.87	1.52
PO(PS8)	17.7	2.72	1.00	1.00	1.22	2.79
T12	600	387	0	0	0.36	0.36
T14-T12	55	34	0.75	0.75	1.37	1.40
T3(°R)	1350	900	0.75	0.75	0.98	1.00
T49(°R)	2240	1660	0.75	0.75	1.02	1.04
T8(°R)	1710	1190	0.75	0.75	0.87	1.16
NL(RPM)	3400	2500	---	---	0.25	0.25
NH(RPM)	14500	11000	---	---	0.25	0.27
WFM(PPH)	6200	1530	*0.44	0.44	1.09	1.15
A18(in. ²)	3300	1600	---	---	1.20	1.63
BF Degrees	-2	+90	---	---	0.54°	0.54°

*Heating Value Variations.

The new error-stacking result was:

$$\frac{\Delta T_{41C}}{T_{41C}} = \sqrt{\left(0.476 \frac{\Delta T_3}{T_3}\right)^2 + \left(0.6585 \frac{\Delta W_F}{W_F}\right)^2 + \left(0.6585 \frac{\Delta P_{S3}}{P_{S3}}\right)^2}$$

The new parameter error for T41C/I2 became $\pm 1.05\%$.

The other control parameters had errors evaluated using the same techniques described above for T41C; Table I has the tabulated results.

There are noncontrol factors which influence engine performance to a varying degree depending on the mode of control. These include the engine component variation due to manufacturing tolerances and service wear; they also include engine bleed and power extraction as required for anti-icing and aircraft accessories. Table III lists the values used in the calculation of control errors as defined in Table I.

4.2.3 Mode Analysis Runs and Results

As noted previously, the control mode analysis itself consisted of a series of computer runs with various combinations of three of the 19 potential control variables. The theoretical total of such combinations is 969 but some obviously have no prospective interest. For example, any combination including two or three thrust parameters is not reasonable.

The primary strategy used to identify prospective candidate modes was to pair up the likely parameters for nozzle and pitch control and then use each of these pairs with every thrust parameter. Thrust parameters were thereby tentatively assigned a fuel-controlling role. Some modes were considered which did not qualify under the primary strategy, and some modes used two parameters which could be considered thrust parameters: the cost of the computerized analysis was so low that every interesting combination could be tried.

The parameter groups which were evaluated are listed in Table IV along with the results for thrust control errors and thrust "deterioration" as determined from the Table III deterioration factors. Note that engine deterioration may result in thrust increases depending on the control mode. In every case where thrust deterioration is positive, the turbine temperature

Table III. Mode Analysis Engine Component Variations (% of Point).

Variable	Variation	Deterioration
Fan Corrected Flow	$\pm 1.5\%$	-0.5%
Fan Efficiency	1.5	-0.5
Core Compressor Corrected Flow	1.0	-0.7
Core Compressor Efficiency	1.0	-0.5
Burner Pressure Loss (P4/P3)	0.5	0
Burner Efficiency	0.3	0
HP Turbine Area Corrected Flow	1.0	0
HP Turbine Efficiency	1.0	-1.5
LP Turbine Area Corrected Flow	1.0	0
LP Turbine Efficiency	1.0	-1.0
Fan Duct Pressure Loss	0.2	0
Postturbine Core Pressure Loss	0.1	0
Compressor Interstage Bleed (% of W25)	1.0	0
Compressor Discharge Bleed (% of W25)	1.0	0
Shaft Power Extraction (Horsepower)	25.0	0
Inlet Duct Area Variation	0.1	0
Core Engine Jet Nozzle Area	0.5	0
Turbine Cooling Flow (WC/W25)	0.55	0

Table IV. Mode Analysis Thrust Accuracy Results (Complete).

(Shown as Percent of Point)

Mode No.	Mode Parameter			SLS Takeoff		Climb 0.7/25K	
				RSS FN	FN Det	RSS FN	FN Det
1 (Base)	PCNL	A18	BF	±2.34	-0.12	±10.52	-1.31
2*	PCNL	SM12	FNIN	---	---	---	---
3	M11	A18	BF	1.91	+0.41	7.40	+2.01
4	M11	P49QOT	BF	2.84	-0.21	7.40	-1.79
5	M11	PS3QOT	BF	3.53	+0.33	7.18	-0.52
6	M11	TP3	BF	7.41	+0.14	14.83	-0.57
7	M11	TP4	BF	4.52	+0.12	24.16	-0.28
8	M11	TP5	BF	1.84	+0.38	7.39	+1.46
9	M11	TP6	BF	2.31	+0.26	17.17	+0.78
10	M11	TP7	BF	3.45	-0.28	22.16	-3.99
11	M11	T41CT2	BF	7.12	-5.15	12.62	-8.03
12	M11	T49CT2	BF	7.66	-7.34	13.00	-10.52
13	M11	M14	BF	7.10	+0.06	14.36	+2.10
14	M11	T8QT2	BF	9.64	-10.52	12.20	-12.02
15	M11	P14QOT	BF	3.09	+0.27	8.15	+1.13
16**	M11	P14QOT	BF	2.32	+0.27	---	---
17	M11	PCNHR	BF	8.81	+4.28	12.93	+3.51
18	M11	TP12	BF	3.20	-0.30	9.34	-2.22
19	M11	TP7	A18	2.90	+0.63	32.29	-6.41
20	M11	TP12	A18	1.35	+0.28	4.74	+1.02
21	M11	A18	PCNL	1.97	+0.35	6.17	+1.33
22	M11	P49QOT	PCNL	2.62	-0.03	4.60	+0.23
23	M11	PS3QOT	PCNL	3.38	+0.51	5.21	+0.77
24	M11	TP3	PCNL	7.37	+0.09	15.01	-0.83
25	M11	TP4	PCNL	4.51	+0.07	24.23	-0.52
26	M11	TP5	PCNL	1.96	+0.31	7.28	+0.69
27	M11	TP6	PCNL	2.45	+0.20	17.24	+0.22
28	M11	TP7	PCNL	3.88	-0.51	22.61	-4.19
29	M11	T41CT2	PCNL	6.91	-4.93	7.81	-5.21
30	M11	T49QT2	PCNL	7.47	-7.17	7.73	-7.61
31	M11	M14	PCNL	6.97	+0.51	13.72	+1.40
32	M11	T8QT2	PCNL	9.59	10.45	8.92	-9.56
33	M11	P14QOT	PCNL	3.02	+0.21	7.84	+0.62
34**	M11	P14QOT	PCNL	2.34	+0.21	---	---
35	M11	PCNHR	PCNL	8.80	+4.71	10.67	+6.28
36	M11	TP12	PCNL	2.79	-0.03	3.46	+0.03
37	M11	TP5	TP12	1.46	+0.24	5.49	+0.53
38	M11	TP6	TP12	1.92	+0.16	13.81	+0.18
39	M11	TP7	TP12	2.43	-0.29	20.78	-3.85
40	M14	P49QOT	PCNL	2.59	+0.13	4.45	+0.28
41	M14	PS3QOT	PCNL	3.02	+0.51	5.04	+0.79
42	M14	TP3	PCNL	7.54	+0.07	10.05	+0.15

Table IV. Mode Analysis Thrust Accuracy Results (Complete), (Continued).

(Shown as Percent of Point)

Mode No.	Mode Parameter			SLS Takeoff		Climb 0.7/25K	
				RSS FN	FN Det	RSS FN	FN Det
43	M14	TP4	PCNL	4.42	+0.07	14.24	+0.37
44	M14	TP5	PCNL	2.16	+0.029	6.33	+0.88
45	M14	TP6	PCNL	2.43	+0.18	11.98	+0.64
46	M14	TP7	PCNL	3.31	-0.19	12.55	-1.34
47	M14	T41CT2	PCNL	4.59	-2.08	6.95	-4.27
48	M14	T49QT2	PCNL	4.76	-3.15	6.87	-6.35
49	M14	P14QOT	PCNL	5.06	+0.07	11.08	+0.37
50**	M14	P14QOT	PCNL	4.13	+0.07	---	---
51	M14	T8QT2	PCNL	5.40	-4.30	7.80	-7.89
52	M14	PCNHR	PCNL	5.28	2.37	8.88	+5.19
53	M14	TP12	PCNL	2.81	+0.16	3.34	+0.10
54	M14	PS3QOR	BF	3.17	+0.42	5.78	+0.23
55	M14	TP3	BF	8.18	+0.10	10.50	+0.38
56	M14	TP4	BF	4.72	+0.10	15.65	+0.64
57	M14	TP5	BF	2.61	+0.34	7.04	+1.50
58	M14	TP6	BF	2.72	+0.22	13.73	+1.07
59	M14	TP7	BF	3.09	-0.16	12.86	-1.34
60	M14	T41CT2	BF	4.61	-1.86	8.09	-3.11
61	M14	T8QT2	BF	5.27	-3.90	8.06	-5.53
62	M14	P14QOT	BF	4.70	4.10	13.64	+0.63
63**	M14	P14QOT	BF	5.65	+0.10	---	---
64	M14	PCHNR	BF	5.18	+2.09	8.58	+2.79
65	M14	TP12	BF	3.20	+0.09	6.68	-0.45
66	P14QOT	PS3QOT	BF	1.78	+0.29	4.92	+0.37
67	P14QOT	TP4	BF	10.13	+0.10	9.93	+0.64
68	P14QOT	TP5	BF	5.12	+0.10	6.41	+1.40
69	P14QOT	TP6	BF	4.44	+0.51	10.11	+0.94
70	P14QOT	TP7	BF	3.58	+0.26	8.16	-0.44
71	P14QOT	T41CT2	BF	2.40	-0.11	6.16	-1.30
72	P14QOT	TP12	BF	2.11	-0.83	5.51	+0.03
73	P14QOT	A18	BF	1.61	+0.06	12.43	+0.65
74	PS3QOT	A18	BF	1.73	+0.36	4.55	+0.23
75	TP3	A18	BF	8.77	+0.10	9.47	+0.37
76	TP4	A18	BF	4.86	+0.10	14.69	+0.63
77	TP5	A18	BF	2.59	+0.38	6.98	+1.49
78	TP6	A18	BF	2.88	+0.23	13.34	+1.06
79	TP7	A18	BF	2.70	-0.13	11.52	-1.31
80	T41CT2	A18	BF	2.02	-1.29	5.43	-3.04
81	P14QOT	A18	BF	5.35	+0.08	12.43	+0.65
82	TP12	A18	BF	1.27	+0.10	4.40	-0.44
83	PS3QOT	A18	PCNL	2.00	+0.44	5.00	+0.79
84	TP3	A18	PCNL	7.84	+0.07	3.39	+0.14

Table IV. Mode Analysis Thrust Accuracy Results (Complete), (Continued).

(Shown as Percent of Point)

Mode No.	Mode Parameter			SLS Takeoff		Climb 0.7/25K	
				RSS FN	FN Det	RSS FN	FN Det
85	TP4	A18	PCNL	4.36	+0.08	12.78	+0.36
86	TP5	A18	PCNL	2.36	4.31	5.40	+0.87
87	TP6	A18	PCNL	2.50	+0.18	10.97	+0.63
88	TP7	A18	PCNL	2.22	-0.13	10.69	-1.31
89	T41CT2	A18	PCNL	2.32	-1.48	6.68	-4.24
90	P14QOT	A18	PCNL	4.59	+0.05	10.57	+0.38
91	TP12	A18	PCNL	1.43	+0.15	3.26	+0.10
92	PS3QOT	M14	PCNL	3.02	+0.51	5.04	+0.79
93	TP3	M14	PCNL	7.64	+0.07	10.05	+0.15
94	TP4	M14	PCNL	4.42	+0.07	14.24	+0.37
95	TP5	M14	PCNL	2.16	+0.29	6.33	+0.88
96	TP6	M14	PCNL	2.43	+18.00	11.98	+0.64
97	TP7	M14	PCNL	3.31	-0.19	12.55	-1.34
98	T41CT2	M14	PCNL	4.59	-2.08	6.95	-4.27
99	P14QOT	M14	PCNL	4.13	+0.07	11.08	+0.37
100	TP12	M14	PCNL	2.81	+0.16	3.34	+0.10
101	PS3QOT	P14QOT	PCNL	1.84	+0.34	4.59	+0.75
102	TP3	P14QOT	PCNL	8.34	+0.07	6.91	+0.28
103	TP4	P14QOT	PCNL	4.24	+0.07	8.06	+0.37
104	TP5	P14QOT	PCNL	3.12	+0.38	5.50	+0.65
105	TP6	P14QOT	PCNL	2.77	+0.20	7.54	+0.50
106	TP7	P14QOT	PCNL	1.98	-0.08	7.61	-0.29
107	T41CT2	P14QOT	PCNL	2.15	-0.90	5.59	-2.84
108	TP12	P14QOT	PCNL	1.64	+0.12	3.14	+0.14
109	TP4	PS3QOT	BF	4.22	+0.13	47.28	-0.95
110	TP5	PS3QOT	BF	1.54	+0.37	9.22	+1.85
111	TP6	PS3QOT	BF	1.96	+0.27	61.07	+3.89
112	TP12	PS3QOT	BF	12.38	+1.98	12.94	+1.82
113	TP4	PS3QOT	PCNL	4.72	+0.04	5.60	+0.83
114	TP5	PS3QOT	PCNL	1.55	+0.36	5.92	+0.78
115	TP6	PS3QOT	PCNL	2.05	+0.24	5.77	+0.81
116	TP12	PS3QOT	PCNL	14.34	+2.22	18.46	+2.47
117	PS3QOT	PCNL	BF	3.76	+0.86	5.23	+0.87
118	TP3	PCNL	BF	7.35	+0.06	15.61	+1.34
119	TP4	PCNL	BF	4.51	+0.08	25.10	+1.89
120	TP5	PCNL	BF	1.95	+0.22	7.66	+1.69
121	TP6	PCNL	BF	2.44	+0.16	17.69	+1.76
122	TP7	PCNL	BF	3.37	-0.14	18.37	-1.31
123	TP12	PCNL	BF	3.46	+0.41	3.52	+0.19
124	WFQPTO	A18	BF	1.27	-0.85	3.92	-1.89
125	WFQPTO	A18	PCNL	1.43	-0.96	3.44	-2.18
126	M11	WFQPTO	PCNL	3.18	-2.44	3.77	-2.52

Table IV. Mode Analysis Thrust Accuracy Results (Complete), (Concluded).

(Shown as Percent of Point)

Mode No.	Mode Parameter			SLS Takeoff		Climb 0.7/25K	
				RSS FN	FN Det	RSS FN	FN Det
127	WFQPTO	PCNL	βF	4.08	-1.99	3.99	-2.26
128	WFQPTO	M14	PCNL	3.10	-1.27	3.61	-2.19
129	M11	TP5	TP12	1.46	+0.24	5.49	+0.53
130	M14	PCNL	βF	---	---	16.15	-1.37
131	M14	T49QT2	βF	---	---	8.17	-4.31
132	P14QOT	TP3	βF	---	---	7.41	+0.48

*This case was not a control mode case; it was run for derivatives only.

**Mode as repeated for SLS takeoff using a second and more optimistic estimate for the P14QOT statistical error (i.e., a sensing system was assumed that would use fan ΔP and PT0 - the P14QOT error was reduced from ±1.14% to ±0.81% by this means).

Note: The results for the climb condition include the effects of a ±0.01 variation in flight Mach Number.

"deterioration" exceeds that required to maintain constant thrust. Thrust results are all in terms of percent-of-point of installed net thrust.

The results for the climb condition include the effects of a ± 0.01 variation in the flight Mach number. This variation can be viewed as a real error in M_0 or as an error in the M_0 data provided to the engine control.

The initial list of modes was reduced to those remaining in Tables V and VI using as criteria thrust stackup, deterioration magnitude, fan stall margin stackup, inlet Mach stackup (where "floating"), turbine inlet temperature stackup, and fan speed stackup (where "floating"). The process of elimination was continued as follows:

1. Modes using TP12 were eliminated from experimental engine candidates primarily for (1) uncertainty regarding water ingestion effects on fan temperature rise measurement and (2) because of the slow response inherent in temperature measurement devices. More data are needed on the correlation of TP12 with thrust under unusual atmospheric condition; more data are also needed for temperature profile variation which affects the choice of location and the number of sensors.
2. Modes using P49/PTO were eliminated from the experimental program because the applicable F101 engine hardware did not allow adequate instrumentation. Analysis results do not show a decisive superiority of P49/PTO over PS3/PTO considering the added cost, weight, and reliability factors associated with engine design (close-coupled turbine and multiple-probe acquisition system needed to get an accurate P49 signal).
3. The control modes using T41C were not seriously considered in the elimination process leading to the primary control, basically because a turbine temperature parameter had already been chosen to provide a safety override function. Therefore, a redundancy advantage would be lost if the temperature were also used as the thrust parameter. T49 was eliminated for the same reasons given above for P49.
4. The control modes which included WF/PTO were eliminated for a combination of factors. The deterioration effects were relatively large (but not so large as to be definitive without other factors); fuel flow measurement is used in the computed temperature parameter T41C; the estimated fuel flow measuring accuracy needs more experimental verification; and perhaps more development may be needed for assurance reasons.

Table V. Mode Analysis Results (Summary) SLS.

Rank	Mode No.	Mode Identification			* Thrust		RSS Stack up (\pm)			Det.
		1	2	3	P.I.	FN	T41	SM12	M11	
1	82	TP12	A18	β F	1.32	1.27	2.0	9.2	1.5	+0.1
2	91	TP12	A18	PCNL	1.42	1.43	2.0	5.5	2.0	+0.1
3	125	WF/PTO	A18	PCNL	1.93	1.43	1.1	5.6	2.0	-1.0
4	120	TP5	PCNL	β F	2.05	1.95	2.6	7.9	2.6	+0.2
5	26	TP5	M11	PCNL	2.11	1.96	2.2	7.2	1.7	+0.3
6	21	A18	M11	PCNL	2.12	1.97	2.3	7.4	1.7	+0.3
7	83	PS3/PTO	A18	PCNL	2.20	2.00	2.8	7.7	2.7	+0.4
8	88	TP7	A18	PCNL	2.27	2.22	2.9	10.3	2.8	-0.1
9	1	PCNL	A18	β F	2.39	2.34	2.9	10.4	2.5	-0.1
10	34	P14/PTO	M11	PCNL	2.44	2.34	2.3	8.1	1.7	+0.2
11	86	TP5	A18	PCNL	2.51	2.36	3.0	9.2	3.3	+0.3
12	121	TP6	PCNL	β F	2.54	2.44	2.5	8.6	2.6	+0.2
13	27	TP6	M11	PCNL	2.55	2.45	2.2	8.2	1.7	+0.2
14	23	PS3/PTO	M11	PCNL	3.63	3.38	2.4	10.6	1.7	+0.5

*Root Sum Square of FNIN Plus 1/2 Deterioration.

Table VI. Mode Analysis Results (Summary) 0.7/7.62 km (25K ft).

Rank	Mode No.	Mode Identification			* Thrust P.I.	RSS Stack up (\pm)			PCNL	FN Det.
		1	2	3		T41	SM12	M11		
1	91	TP12	A18	PCNL	3.35	3.3	2.0	10	4.2	+0.1
2	100	TP12	M14	PCNL	3.35	3.3	2.0	16	8.7	+0.1
3	36	TP12	M11	PCNL	3.5	3.5	1.9	13	2.4	0
4	123	TP12	PCNL	β F	3.6	3.5	2.0	16	6.8	+0.2
5	125	WFM/PTO	A18	PCNL	4.5	3.4	1.3	11	2.7	-2.2
6	22	P49/PTO	M11	PCNL	4.7	4.6	2.3	15	2.4	+0.2
7	124	WFM/PTO	A18	β F	4.8	3.9	1.4	21	3.9	-1.9
8	126	WFM/PTO	M11	PCNL	5.0	3.8	1.3	14	2.4	-2.5
9	83	PS3/PTO	A18	PCNL	5.4	5.0	2.7	14	5.0	+0.8
10	23	PS3/PTO	M11	PCNL	5.6	5.2	2.6	19	2.4	+0.8
11	86	TP5	A18	PCNL	5.8	5.4	2.6	15	4.5	+0.9
12	21	M11	A18	PCNL	6.8	6.2	2.6	19	2.4	+1.3
13	26	TP5	M11	PCNL	7.6	7.3	2.9	25	2.4	+0.7

*Root Sum Square of FNIN Plus 1/2 Deterioration.

5. Modes using P14/PTO and TP6 (which includes P14/PTO) had poor thrust control performance at the cruise condition unless used in combination with TP12 or PS3/PTO. These exceptions, where they looked competitive for thrust control (modes 66, 71, 101, 104, 107, 108, and 115), were spoiled by other considerations. Fan speed "floated" in mode 66 and the stackup was $\pm 3.6\%$ at takeoff and over 8% for the climb case. Mode 71 was rejected for the same reason. Modes 101, 104, 107, 108, and 115 all had excessive stackups for inlet duct Mach number for operation at climb power setting at altitude. These modes would be good candidates for an engine with a conservatively-sized inlet duct but they are not good candidates for control at takeoff.
6. For a low-pressure cycle engine with variable geometry, the power control schedules make large memory demands for multivariable functions. An important advantage was recognized for a common power control mode for both takeoff and climb. Using this criterion, the remaining takeoff modes (Table V) which wouldn't perform well at altitude were eliminated. The dividing line was chosen as 5.5% stackup in installed thrust at the climb condition. The arbitrary appearance of the 5.5% value resulted from the fact that there was a tight group of three that gave better performance and a fairly large gap separated these from the next best mode (i.e., M11-A18-PCNL).
7. The only modes remaining at this stage were numbers 23, 83, and 26. Only two of the thrust parameters survived to this stage - PS3/PTO and TP5. TP5 was later eliminated for experimental engine consideration based on a controls stability problem as discussed in Section 4.6.3. Modes 23 and 83 will be tested on the experimental engine.

The relatively large thrust stackups at takeoff for the selected modes ($\pm 2\%$ for 83 and $\pm 3.38\%$ for 23) are cause for discussion. Thrust tolerance for the CF6-50 at rated fan speed is stated to be less than $\pm 1\%$ (excluding deterioration which is about -0.5%). The stipulation "at rated fan speed" is very important for it means zero tolerance on the thrust setting parameter. When a tolerance on corrected fan speed is included equal to the 0.38% used in the QCSEE analysis, the thrust spread becomes $\pm 1.45\%$. The UTW engine has variable geometry not used on the CF6 which introduces additional variation. For example, the analysis of QCSEE mode 83 reflects the variable A18 and βF by including tolerances of $\pm 1.2\%$ A18, $\pm 1.5\%$ fan airflow, and $\pm 1.5\%$ fan efficiency. These tolerances are $\pm 0.5\%$, $\pm 1.2\%$, and $\pm 0.65\%$, respectively, in a comparable CF6 analysis reflecting only the estimated manufacturing tolerances of a fixed A18 and a fixed geometry fan.

Mode 83 thrust tolerance could be improved somewhat by making a control adjustment on the engine based on the measured turbine diaphragm area, or trimming diaphragms in production as a result of the flow checks which are a routine production procedure. This has the potential of reducing the thrust stackup approximately 0.3 percentage points. Other opportunities for improvement would have little effect except for the PS3/PTO instrument itself. As an example of the potential improvement, a reduction of the PS3/PTO tolerance to $\pm 0.5\%$ would reduce the $\pm 2.0\%$ FN to $\pm 1.8\%$ FN.

Mode 23 includes direct control of the primary inlet-radiated noise parameter and has a slight advantage in this respect, but a price must be paid for this feature. As with mode 83, there are potential improvements. Effects of turbine diaphragm-area variation if eliminated would reduce the $\pm 3.83\%$ to 2.89% . A reduction of the PS3/PTO tolerance to $\pm 0.5\%$ would further reduce this to $\pm 2.57\%$ FN. Other error sources are fairly evenly distributed among customer bleed, A49, turbine cooling, and component efficiencies.

One of the goals of the experimental engine test program is to obtain data which can be utilized to define a better thrust setting parameter (or parameters) than PS3/PTO. Particular attention will be given to data pertinent to TP5, or parameters closely related to it, evaluating the potential of using such a parameter for controlling thrust at high power settings and using a more traditional parameter at low power settings if the stability of TP5 proves inadequate as predicted by analysis (reference Section 4.6.3).

4.3 PARAMETER INTERRELATIONSHIPS

The control mode analysis just described does not identify the inter-relationship between manipulated and controlled variables. That is, it does not identify which of the three manipulated variables (WF, βF , or A18) should be used to control each of the controlled variables in any given control mode. Further analysis is required to accomplish this.

Ideally, each manipulated variable would have an effect on its control variable and no other, and this ideal would hold throughout the flight map and required power ranges. With the QCSEE cycle we were very far from an

ideal coupling situation, and the first problem was to link variables to produce the least amount of cross-coupling and gain changes in the operating ranges. With the selected thrust parameter, PS3/PTO, the choice for engine variable was clearly defined as WF (shown by comparison of derivatives):

	<u>SLS Takeoff</u>	<u>Max. Climb</u>
$\frac{\% \Delta PS3QOT}{\% \Delta WF}$ (with A18 and βF constant)	0.547	0.580
$\frac{\% \Delta PS3QOT}{\% \Delta A18}$ (with WF and βF constant)	-0.126	-0.233
$\frac{\% \Delta PS3QOT}{\% \Delta \beta F}$ (with WF and A18 constant)	0.004	-0.577

The choices for A18 and βF are less clear. Table VII shows the derivative matrices at takeoff and maximum climb for control mode 23. With the choice of WF to control PS3/PTO, the first row and first column of these matrices are eliminated. Examination of the remaining matrices shows that, for the SLS case, the effect of A18 on M11 is identical to the effect of A18 on PCNL, but the effect of βF is much greater on PCNL than it is on M11. Choosing βF to control PCNL therefore minimizes the undesired coupling of βF to M11. For the maximum climb case, cross-coupling is also minimized but not to the same degree as for the SLS case.

Thus, the UTW control variable interrelationships were established with the manipulation of WF to control the thrust parameter (PS3/PTO), βF to control fan rpm, and A18 to control inlet throat Mach number (XM11).

Table VII. Controls Coupling Derivatives.

SLS Takeoff

<u>Engine Variables (Independent)</u>	<u>Control Parameters (Dependent)</u>		
	<u>% PS3/PTO</u>	<u>% M11</u>	<u>% PCNL</u>
% WF	0.547	0.458	0.503
% A18	-0.126	0.441	0.441
% β F	0.004	-0.812	2.907

Maximum Climb 0.7/7.62 km (25K ft)

<u>Engine Variables (Independent)</u>	<u>Control Parameters (Dependent)</u>		
	<u>% PS3/PTO</u>	<u>% M11</u>	<u>% PCNL</u>
% WF	0.58	0.404	0.500
% A18	-0.233	1.036	1.281
% β F	-0.577	-3.61	5.031

At this point it would be well to point out that a limitation exists with most all thrust parameters which is related to interrelationships between variables. A major objective of the QCSEE design studies was to establish as the thrust parameter a variable which was uniquely related to net thrust. This uniqueness was to hold even for large changes in flight Mach number, compressor bleed, and off-design variable geometry (βF , βC , A_{18}). The objective was also to avoid use of a flight Mach number signal in the engine control; the reason being that it is unlikely that the variables needed to compute Mach number could be measured with desired accuracy on the powerplant, and airframe supplied signals were to be avoided if at all possible to avoid placing aircraft dispatch reliability at the mercy of any off-engine device.

The objective of avoiding Mach number (M_0) signal dependence was not met. The pressure ratio of the cycle being much lower than conventional cycles was the primary factor, the variable geometry fan and duct nozzle were major contributing factors, and the inability to measure total pressure between the turbines was the coup-de-gras. The thrust parameter which comes the closest to being independent of M_0 is PS_3/PT_0 . Therefore, the magnitude of the control errors due to loss of M_0 signal is less than for TP_5 (the only other survivor of the error studies as applicable to the demonstrator program). Figures 15 and 16 show the lesser sensitivity of PS_3/PT_0 to M_0 ; it also shows a greater sensitivity to bleed and ambient temperature effects.

The problem of finding a unique thrust parameter was not satisfactorily resolved for the demonstrator program, but approaches that promise a satisfactory solution for a flight engine have been identified. Two of these approaches that may be mentioned here await only the larger capacity digital computer which is anticipated for a flight engine design. The first applies to TP_5 which already has a high degree of uniqueness for variables other than M_0 . The approach is to convert TP_5 to a net thrust parameter defined as follows:

$$\frac{FN}{PT_0} = \frac{FG}{PT_0} - \frac{FD}{PT_0} = \frac{k_1}{A_{18}} \left[f_1(M_{11}) \right] f_2(M_0) - k_2 \sqrt{f_1(M_{11})} \left[f_3(M_0) \right]$$

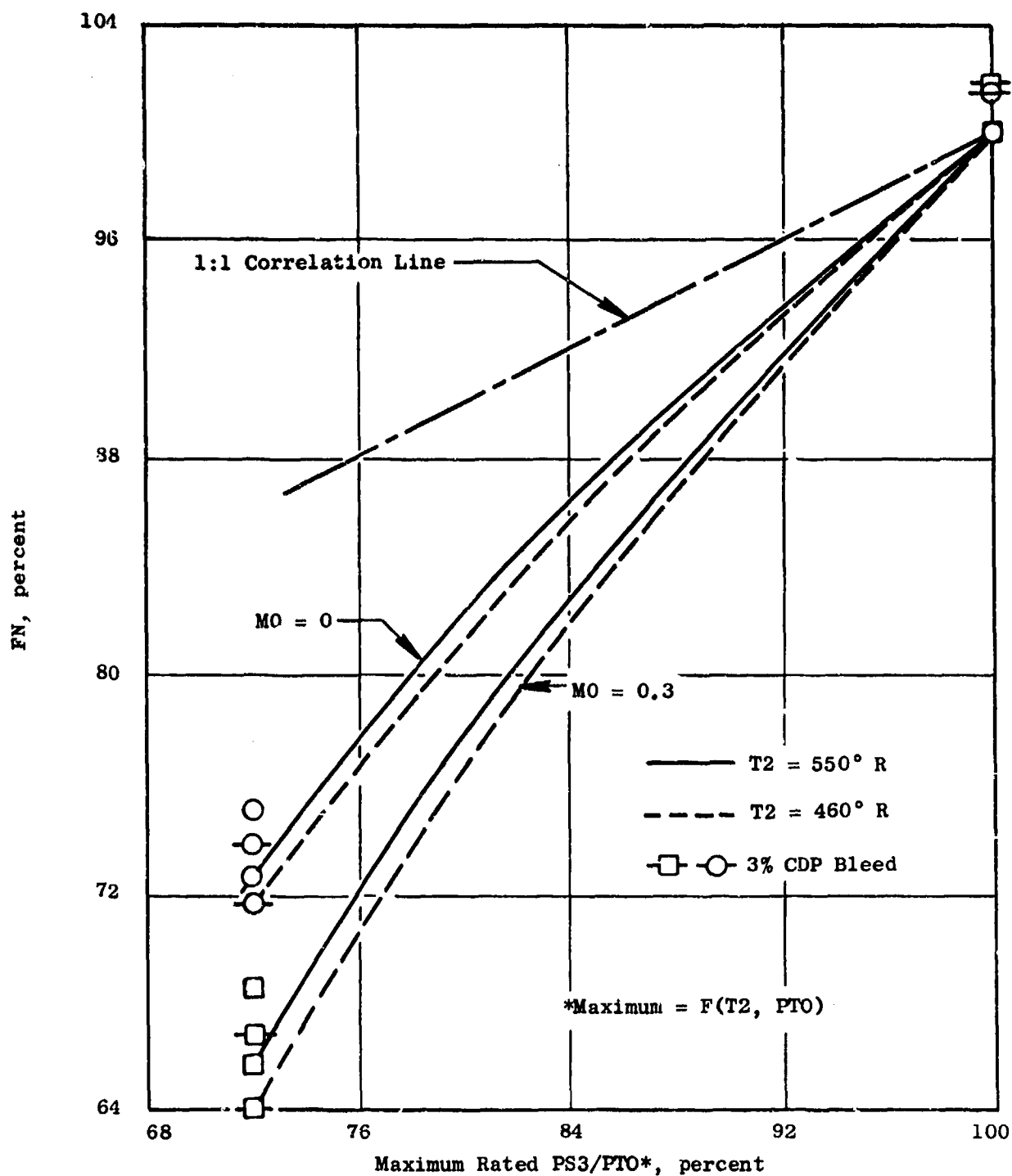


Figure 15. Takeoff Power Mode Throttle/Thrust Characteristics for PS3/PTO.

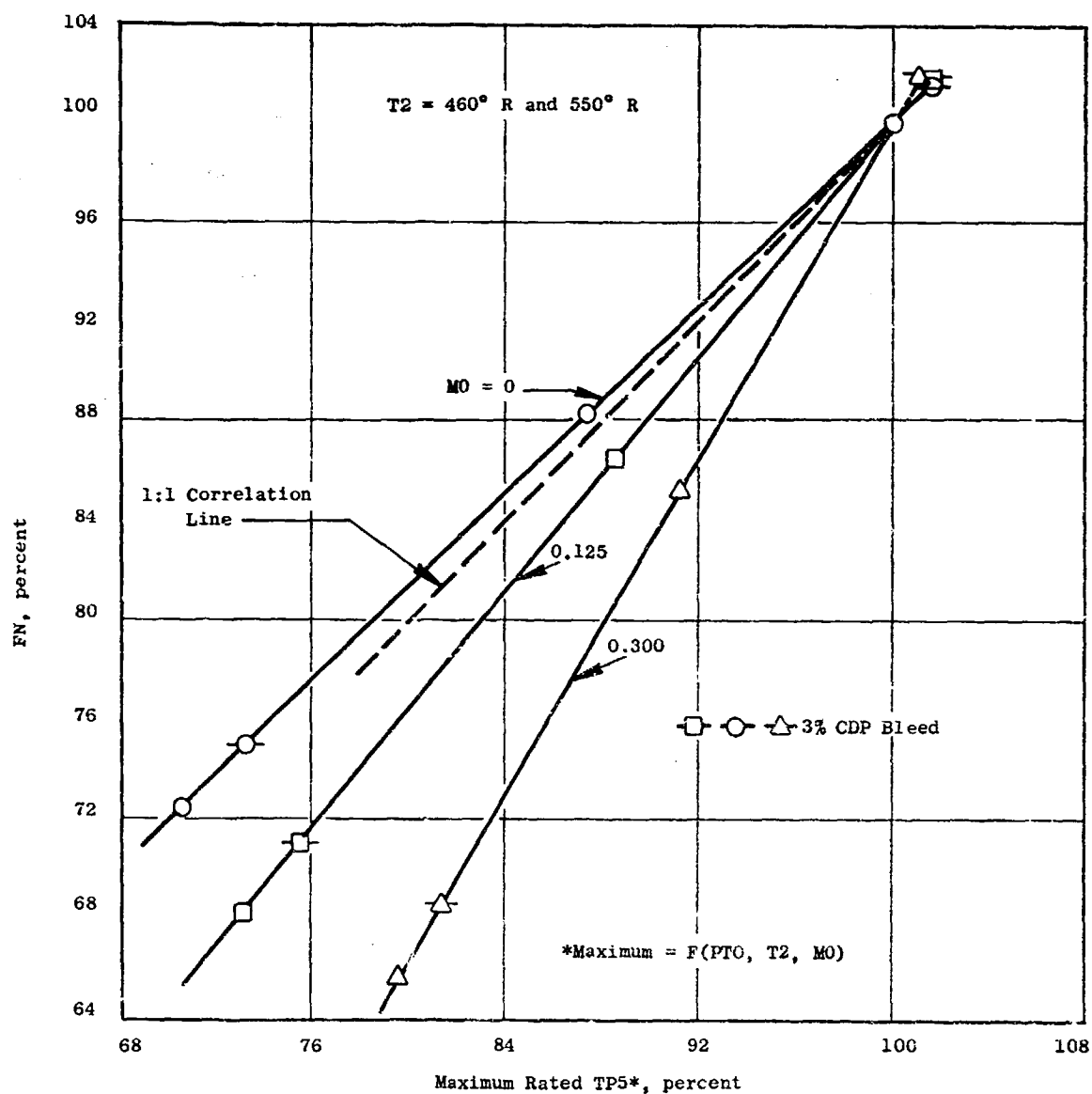


Figure 16. Takeoff Power Mode Throttle/Thrust Characteristics for TP5.

The second approach is particularly applicable to PS3/PTO, but the technique can also be used to further improve on a net-thrust version of TP5. The second approach, as defined in block diagram form in Figure 17, makes the power lever the basis for a thrust parameter indication synthesized from PLA, control errors (such as resulting from limits or actuator malfunction), and a bleed signal.

4.4 SCHEDULEABILITY

Another study performed in conjunction with the control mode analysis was one involving scheduleability. Power control scheduling requirements were considered for alternative modes using PS3/PTO, TP5, TP6, and P14/PTO as thrust parameters. Flight-type schedules were considered in order that mode selection criteria would be comprehensive. Cycle data were run as required to define ideal schedules for both takeoff and climb conditions. The operating conditions covered by the cycle data were as follows:

Takeoff: $0 < M_0 < 0.378$, $10.1 < PTO < 16.22$, $0.74 < T_{12}/T \text{ Ref.} < 1.06$

Climb: $0.378 < M_0 < 0.80$, $7.57 < PTO < 16.22$, $0.82 < T_{12}/T \text{ Ref.} < 1.10$

Matrices of cycle points were run for five levels of the T_{12} parameter, four levels of M_0 , and four levels of PTO. A minimum of 80 points for take-off and 80 points for climb was considered necessary to evaluate characteristic trends; much more data would be run for final design schedules. The rationale for organizing data requirements is as follows:

1. The matrix is defined in terms of the schedule parameters which would be used for scheduling the mode controlled variables.
2. $T_{12}/T \text{ Ref.}$ was chosen over T_{12} in order that the control schedules data arrays would use the minimum number of points for accuracy. And also accommodate the engine rating plan which leads to a sharp dichotomy between the temperature range on which thrust is flat-rated and the range in which it decreases to prevent turbine over-temperature. This dichotomy is established on the basis of a differential above standard day temperature and, thus, the temperature at which the thrust rating changes from flat to decreasing varies with altitude.
3. $T \text{ Ref.}$ is defined as a function of PTO (Figure 18) which is a measured parameter rather than P_0 which probably will not be available on the typical aircraft installation. To accommodate this

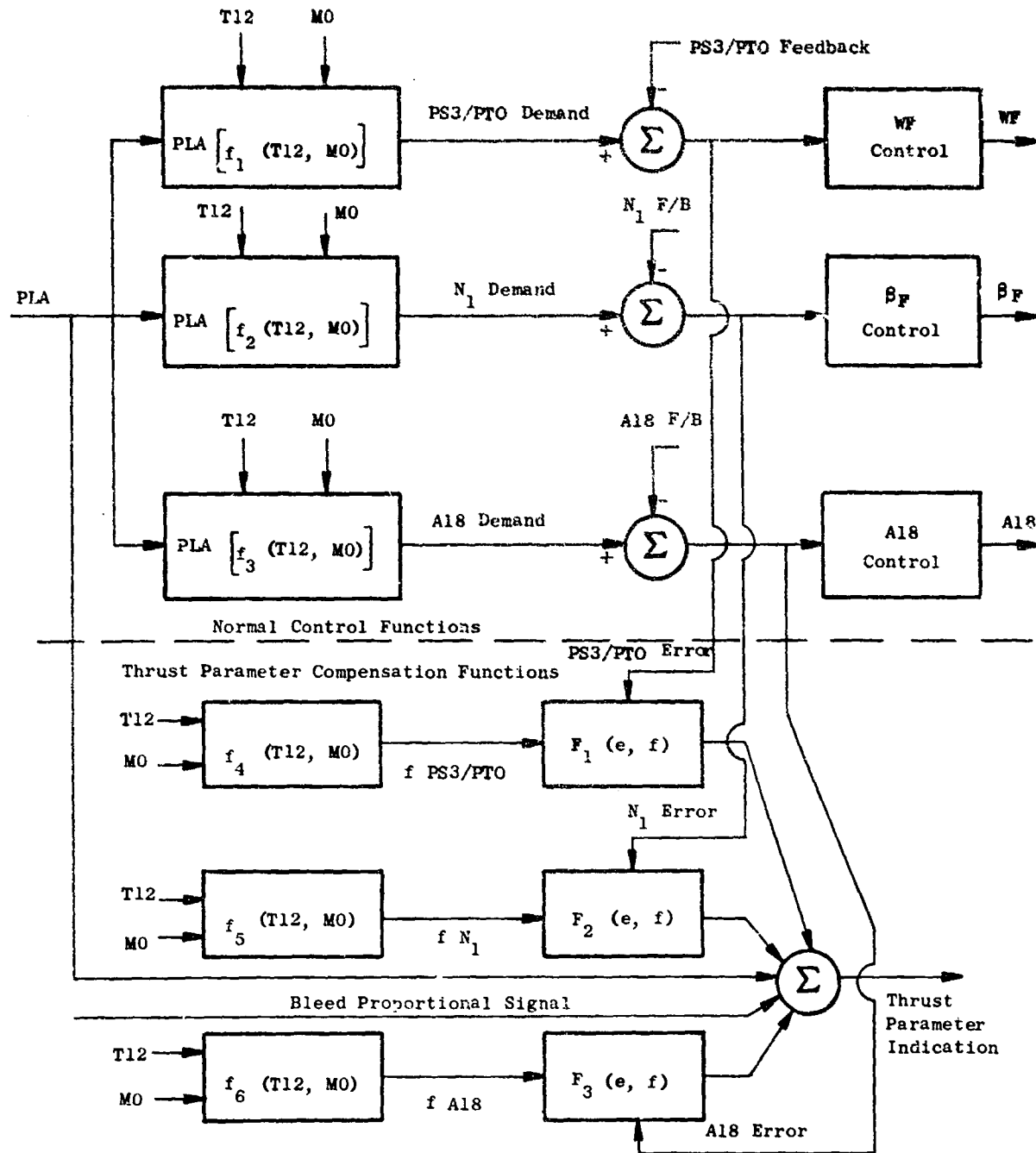


Figure 17. Method for Reducing Thrust Parameter Interdependence.

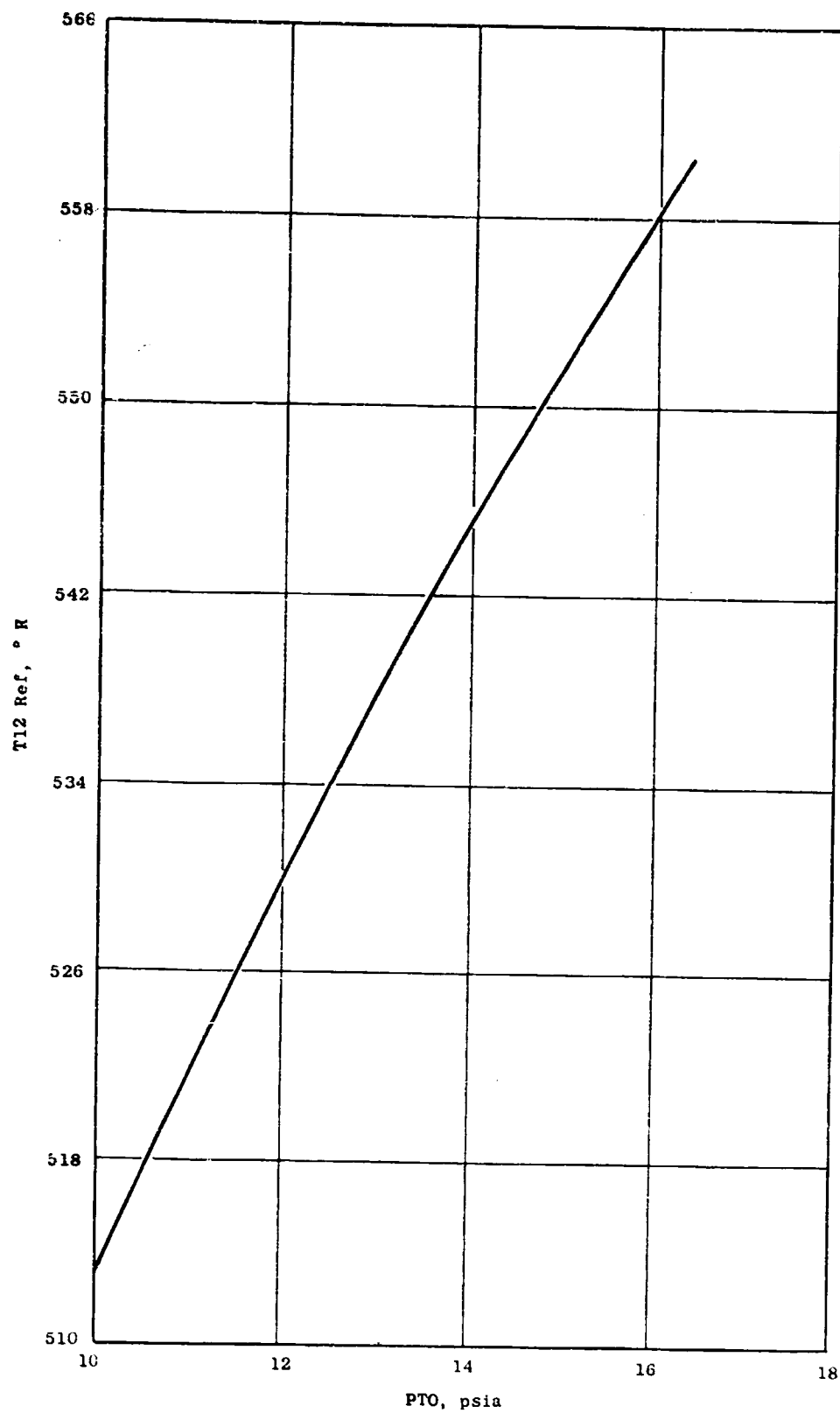


Figure 18. T12 Reference.

approximation a climb profile appropriate to the aircraft is defined (M0 vs. P0, see Figure 19) which is nominal and M0 is treated as a plus and minus trim from the nominal M0 profile. The situation is analogous to the T12 reference scheme, but an explicit M0-reference schedule is not as important as for T12 because no sharp discontinuities are required for M0 effects on the control parameters.

The cycle deck was set up to run the "rated" power data using the following procedure:

1. Data cases for the "corner point" day ($T_0 = 31^\circ \text{ F}$ above standard for takeoff and 18° F above standard for climb) where $T_{12}/T_{\text{Ref.}} = 1.0$ were run first. T_{41} was an input demand at the rated temperature (2914° R for takeoff and 2850° R for maximum climb). Fan stall margin was also a power control demand and was selected as a function of PTO based on the basic engine design objectives. Throat Mach number (M11) was also input at its "requirements" value for takeoff. There were no M11 requirements for the maximum climb, but cycle data based on performance optimization showed that a constant value for M11 would be an appropriate criterion.
2. After data points were checked for the "corner point" day, the data cases were run for all of the "hot" day cases using the same power control criterion defined in item (1).
3. Different power control criteria were used for the "cold" day cases. The same M11 values were used but to maintain flat-rated thrust the other two input parameters were βF and A_{18} . The values for these parameters were lifted from the "corner point" cycle data to keep the same A_{18} and βF as defined for each M0 and PTO.

Control schedules were defined from plots of cycle data value for the control parameters. Figures 20 and 21 present the primary schedules for PS3/PTO and PCNLR. Trim schedules as functions of M0 are given in Figure 22. Figure 23 shows a possible means of implementing schedules for a UTW flight-type design.

4.5 TRANSIENT RESPONSE CAPABILITY

Another factor considered during the control system analysis process was transient response. This was done primarily through the use of a hybrid-computer simulation of the engine and control system which was developed as the control mode analysis and parameter interrelationship

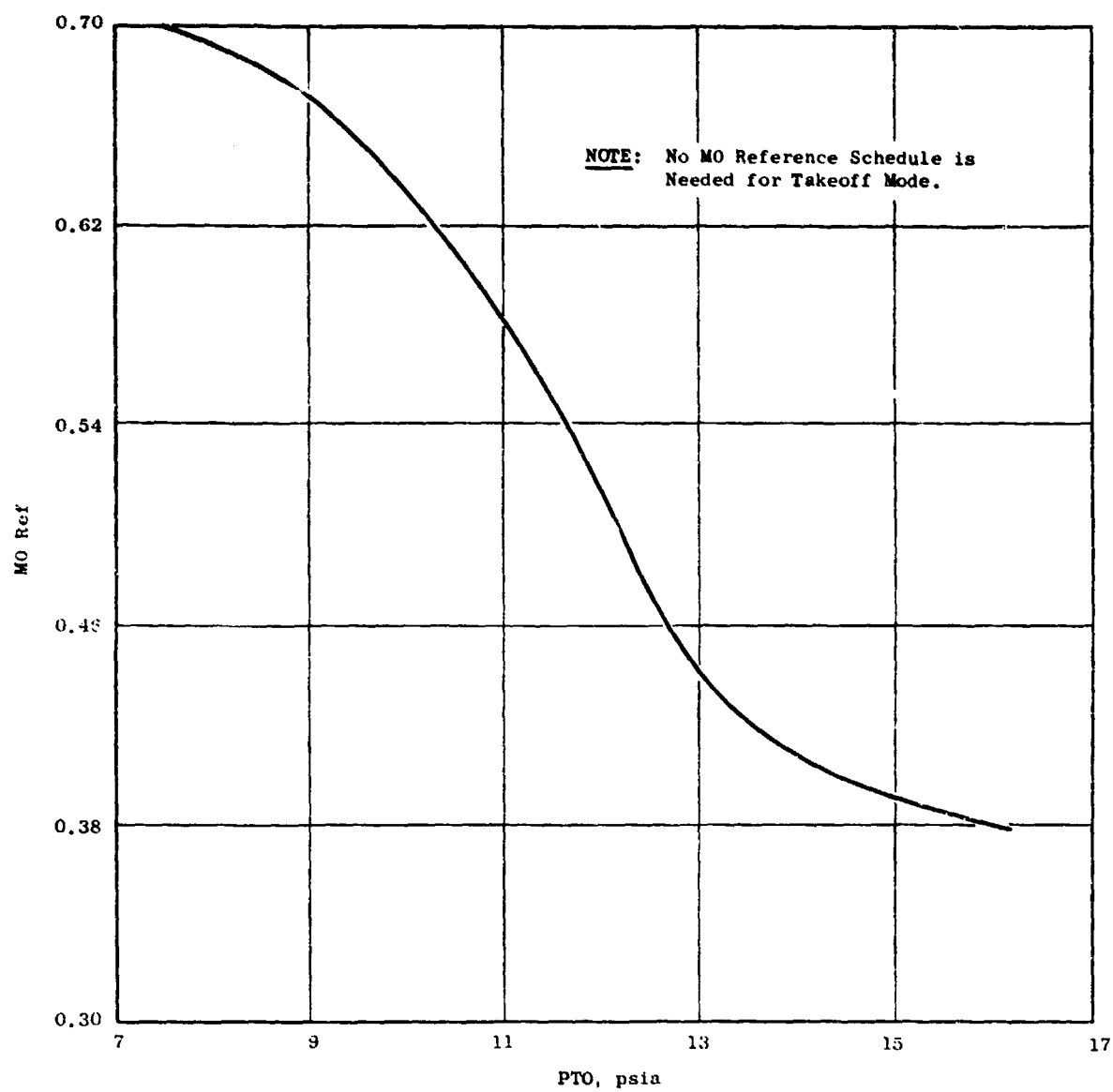


Figure 19. Free-Stream Total Pressure Versus Aircraft Mach Number.

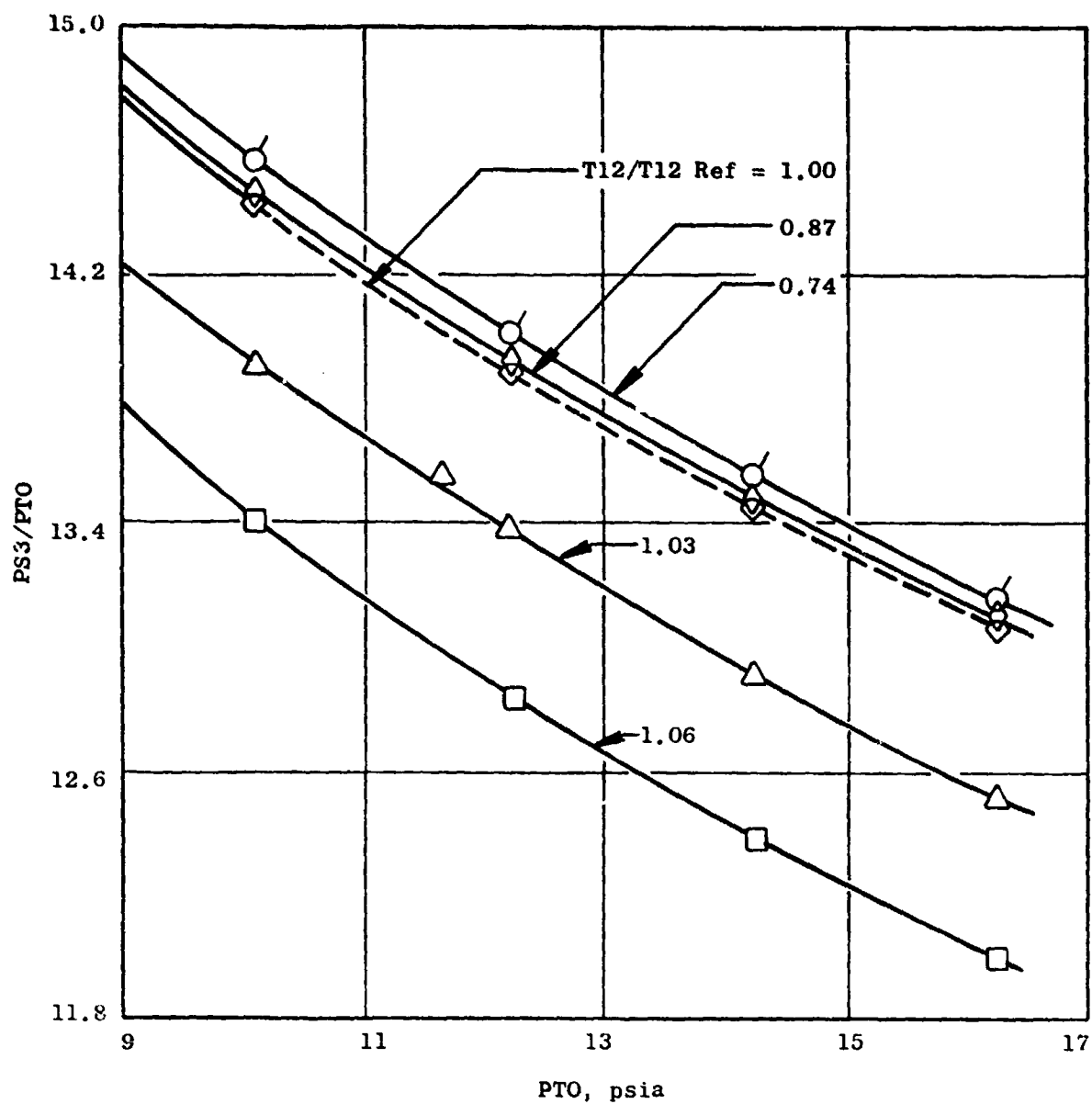


Figure 20. Takeoff Engine Pressure Ratio Schedule.

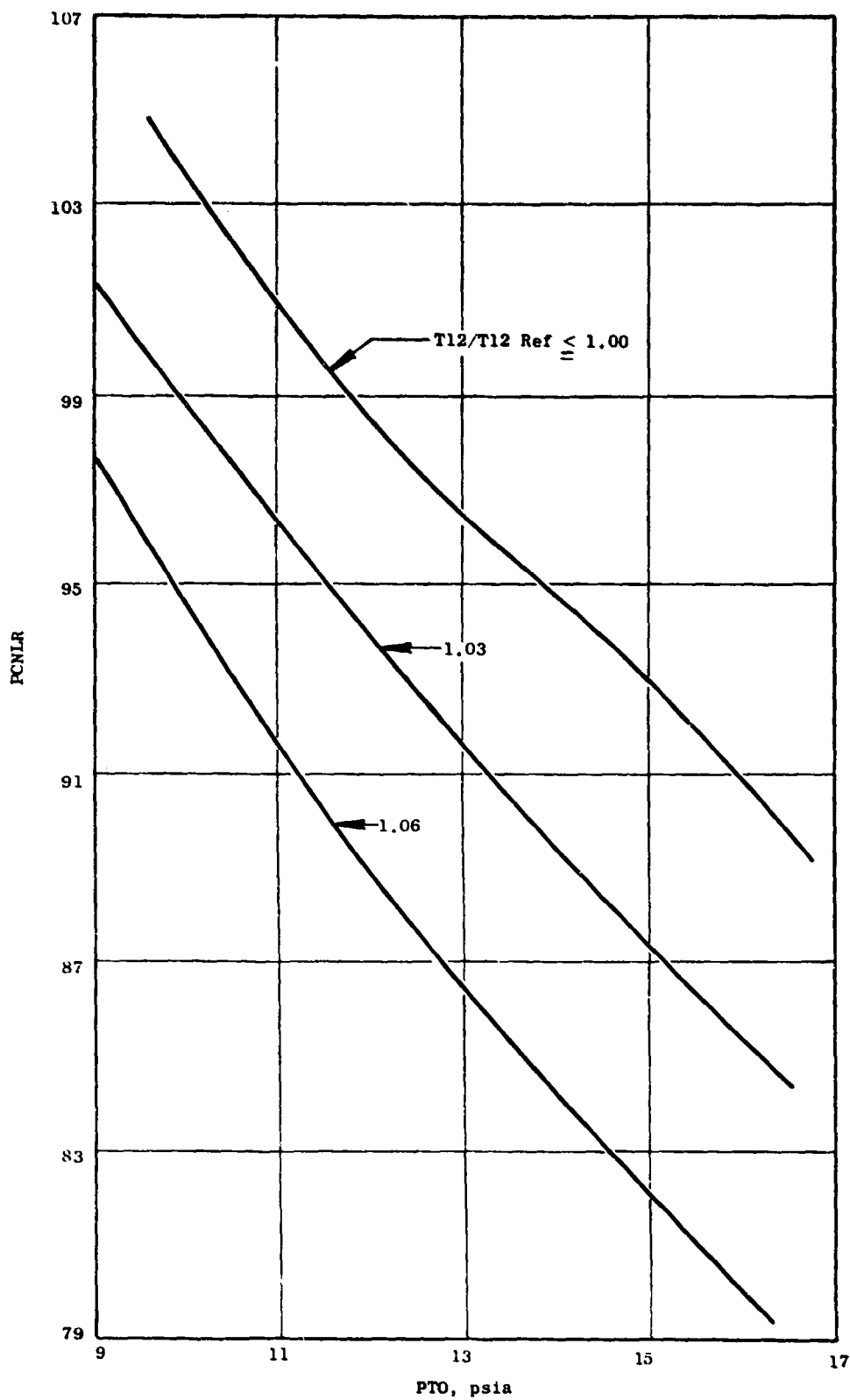


Figure 21. Takeoff Percent Corrected Fan rpm Schedule.

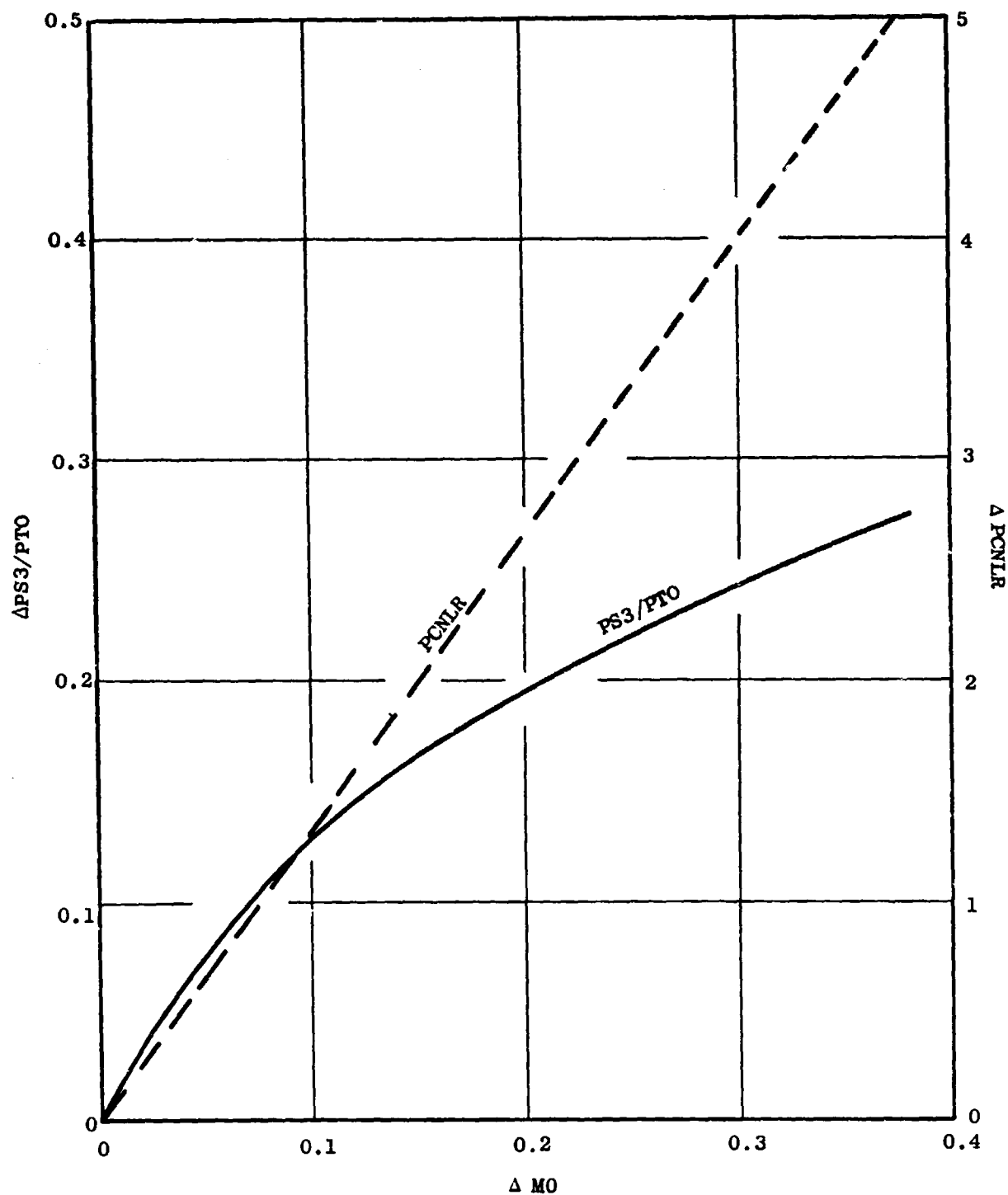


Figure 22. MO Correction for Takeoff Power Schedules, UTW Experimental Engine.

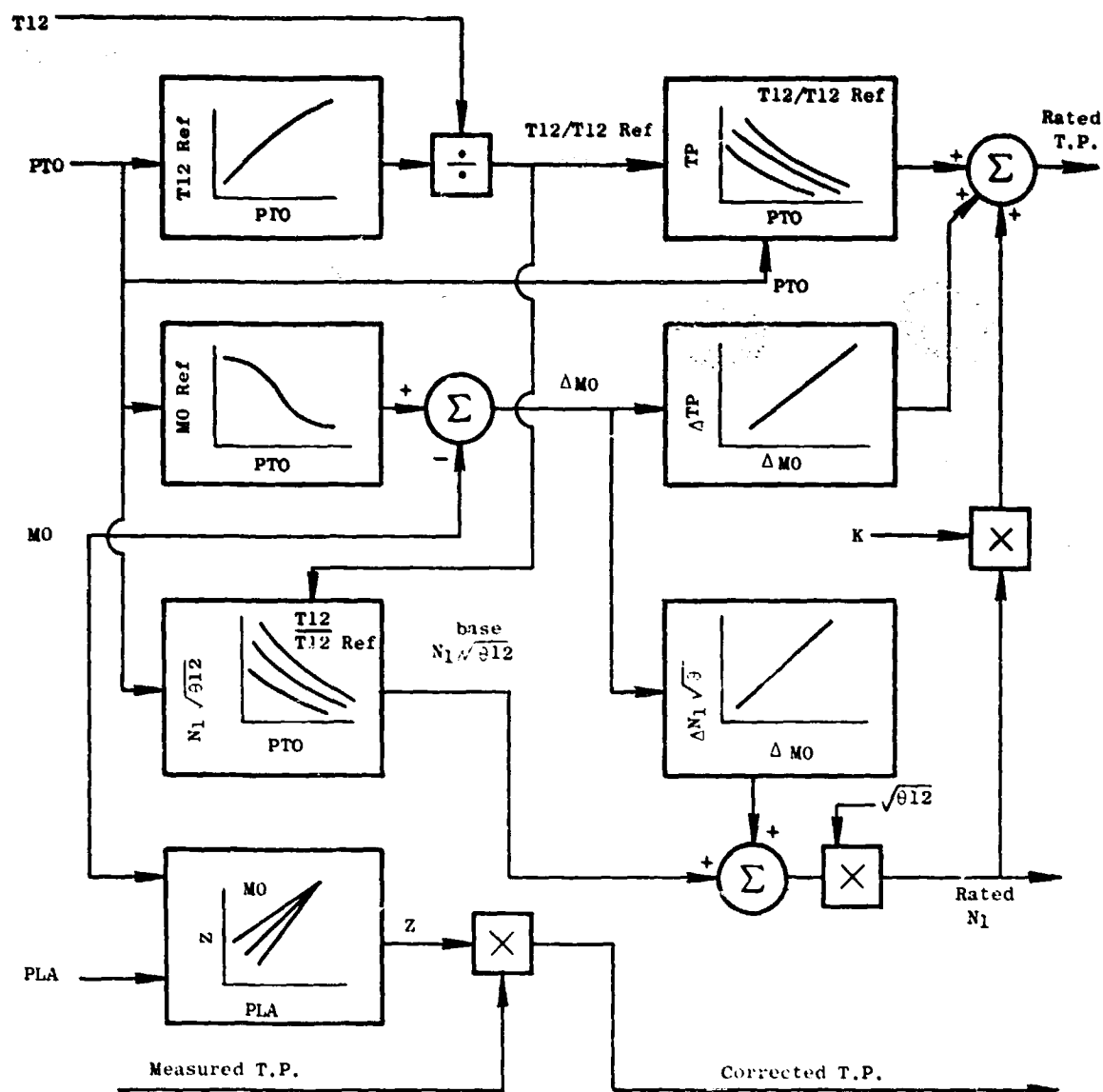


Figure 23. Power Schedule Integration for UTW Flight Design.

studies progressed. This computer simulation was used to explore the various potential control modes from a stability and transient response point of view.

The two basic QCSEE UTW response time requirements are 1.0 second maximum from 62% to 95% net forward thrust (sea level to 1.83 km [6000 ft] elevation) and 1.5 seconds maximum from maximum installed net forward thrust to maximum reverse thrust.

The forward thrust response requirements are aimed primarily at the landing approach conditions in which rapid thrust recovery is sometimes required. Using the preferred control modes established by the mode and variable interrelationship analyses, the hybrid-computer simulation was used to determine that the best transient response from the 62% thrust approach condition is to schedule variables as follows:

- Fuel flow manipulated to maintain the scheduled PS3/PTO for 62% thrust.
- Fan exhaust area open to a roof limit (attempting to maintain high M11).
- Fan pitch angle closes to maintain high fan rpm.

Transient data traces from an acceleration made on the hybrid-computer simulation with this type scheduling are shown in Figure 24 and described below:

- The left-hand end of the traces show conditions existing at 62% thrust.
- The transient thrust response time from power setting change to achievement of 95% thrust is 0.65 seconds.
- The fuel flow is increased but limited by the acceleration fuel schedule to prevent compressor stall and excessive turbine over-temperature. Minimum compressor stall margin is 17.0% and turbine temperature peaks at +70 degrees above the final temperature.
- The fan exhaust nozzle is moved rapidly to a position slightly less than takeoff area. This action provides a rapid increase in thrust (62% to 73% in 0.35 seconds) and limits the inlet Mach number overshoot to 0.01 above the final steady-state value of 0.78.

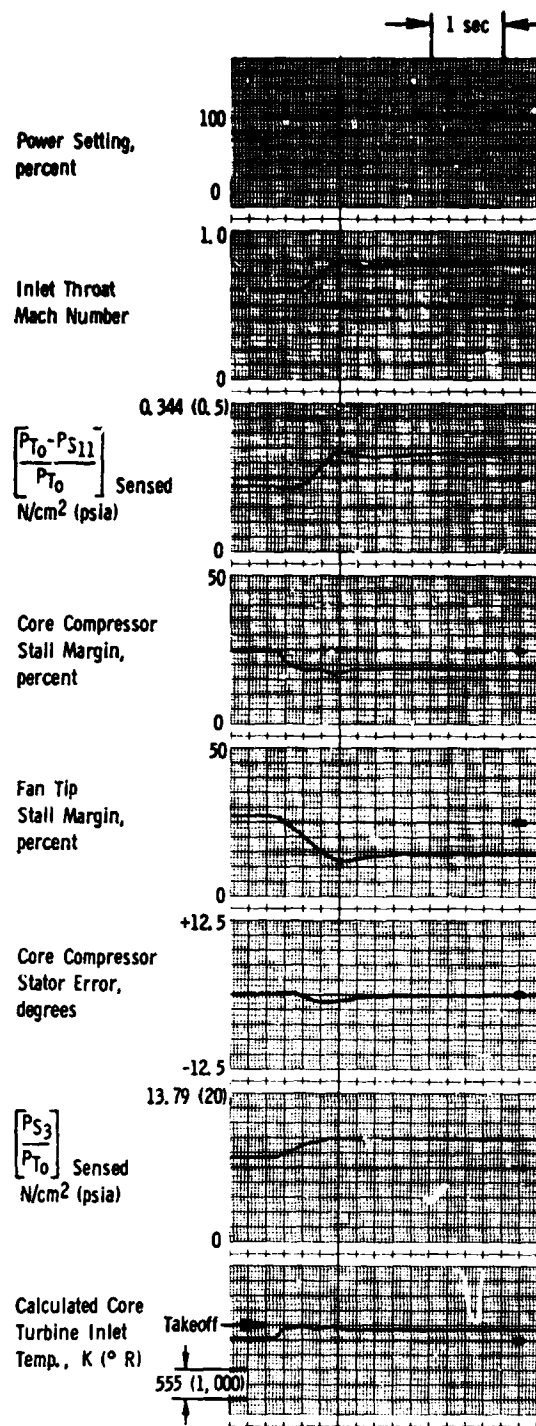
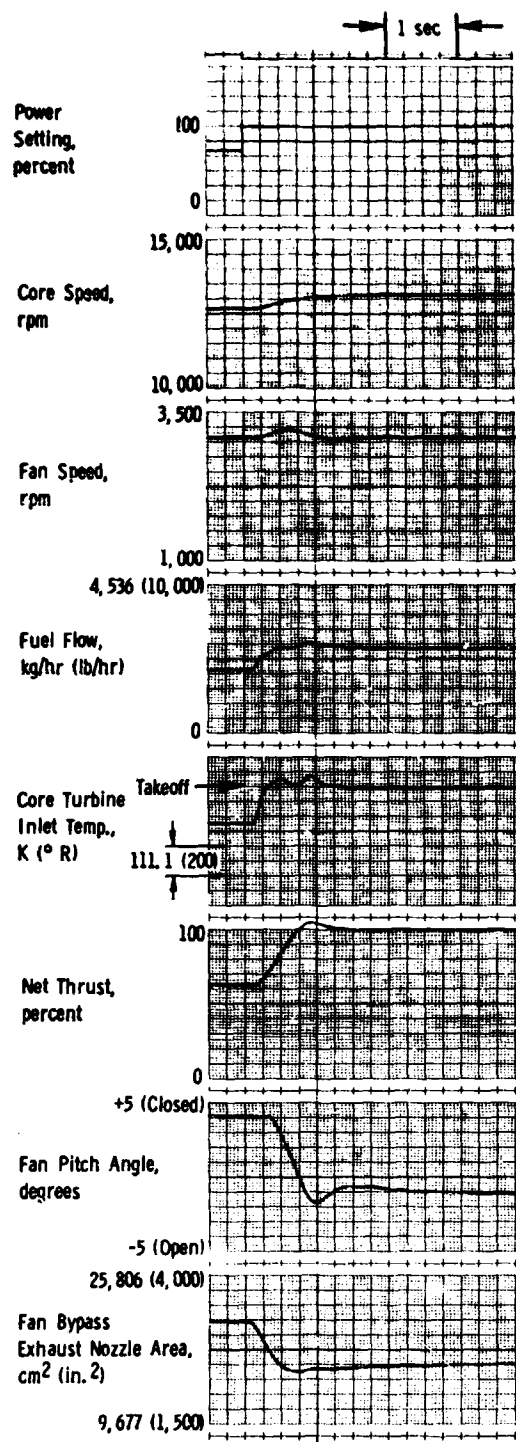


Figure 24. Throttle Burst from 62% to 100% Thrust at Sea Level Static, Standard Day, Zero Bleed.

- The fan pitch starts to open rapidly at approximately 0.35 seconds after the step increase in power setting. It is opened because the fan speed-pitch control senses the acceleration of the fan above the scheduled takeoff speed. Opening fan pitch increases fan airflow and thus maintains the rapid thrust increase in the time interval from 0.35 to 0.9 seconds. At approximately 1.0 second, the fan decelerates back to the scheduled takeoff speed. The fan pitch then closes and opens slightly while settling to the steady-state takeoff fan speed.

The specified tolerance for the WF/PS3 acceleration fuel schedule in the hydromechanical control affects the core engine acceleration time, which in turn, affects the time to achieve 95% net thrust during a throttle burst from 62% to 100% net thrust. In this engine operating range, the specified tolerance for the acceleration fuel schedule is $\pm 4\%$ from nominal. The effect of this $\pm 4\%$ tolerance on transient response was investigated on the simulation. The results in Figure 25 show the response-time trend as a function of the acceleration fuel schedule tolerance. In this figure, the time-scale multiplier indicates the time to accelerate from 62% to 95% thrust as compared to the baseline case of zero acceleration fuel schedule tolerance. For example, this figure shows that the nominal response time from 62% to 95% net thrust should be multiplied by approximately 1.3 when the acceleration schedule operates at the -4% tolerance limit and by approximately 0.85 for the $+4\%$ tolerance limit. These results indicate that the 1.0 second acceleration time goal can be met because the acceleration schedule, if it falls in the low side of the tolerance band, can be adjusted upward using the specific gravity adjustment on the hydromechanical fuel control.

The hybrid-computer simulation was also used to investigate transients between forward and reverse thrust conditions. Reverse thrust is achieved on the UTW engine by reversing the pitch of the fan blades so that flow through the fan reverses. The fan exhaust flaps are actuated to a divergent position (relative to the forward airflow direction) in which they serve as an inlet for the reverse fan flow. The control system must perform the pitch and nozzle actuation rapidly while maintaining safe engine operation.

The UTW engine is designed for fan-pitch actuation into reverse in two directions; one is the forward-to-reverse-pitch angle changes thru stall

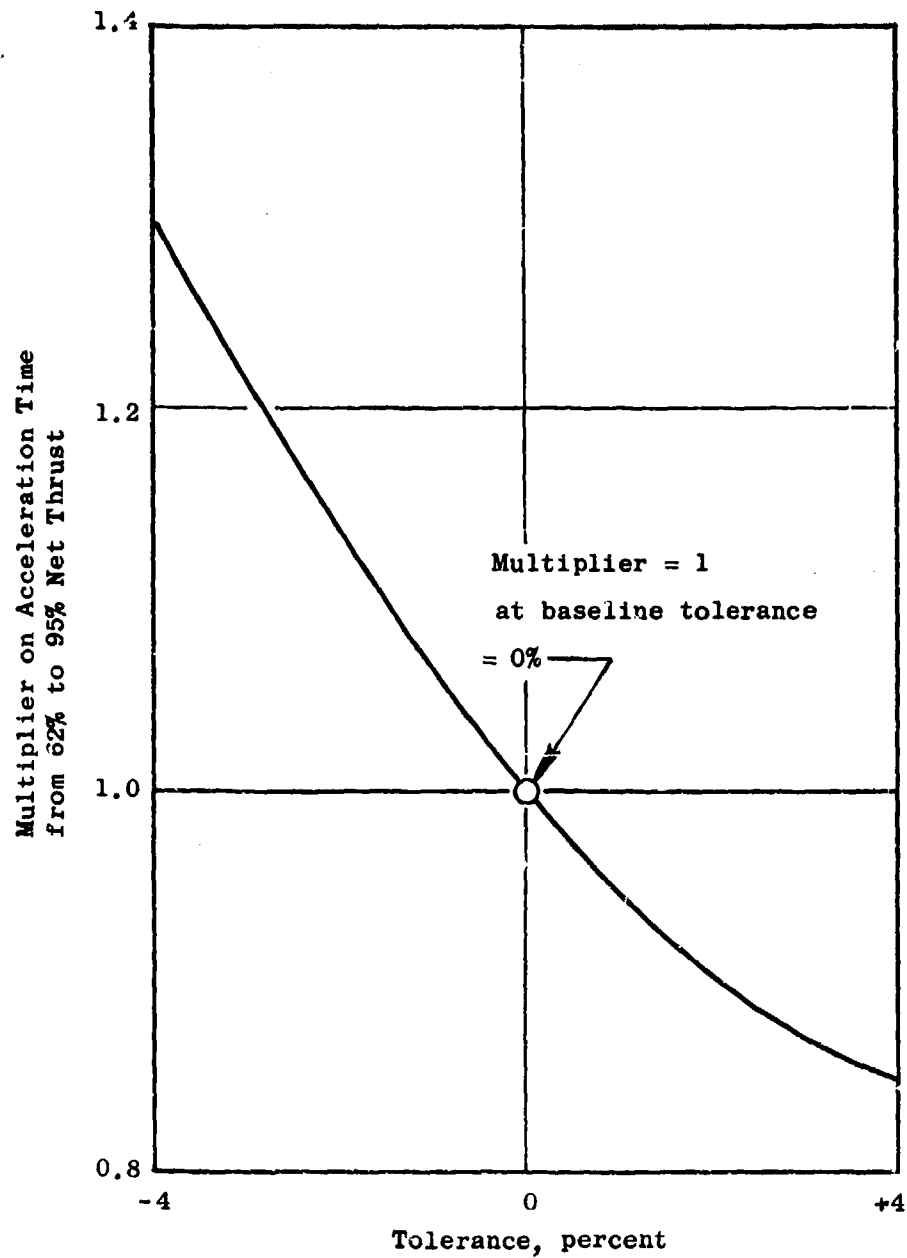


Figure 25. Effect of WF/PS3 Acceleration Fuel Scheduling Tolerance on Acceleration Time from 62% to 95% Net Thrust.

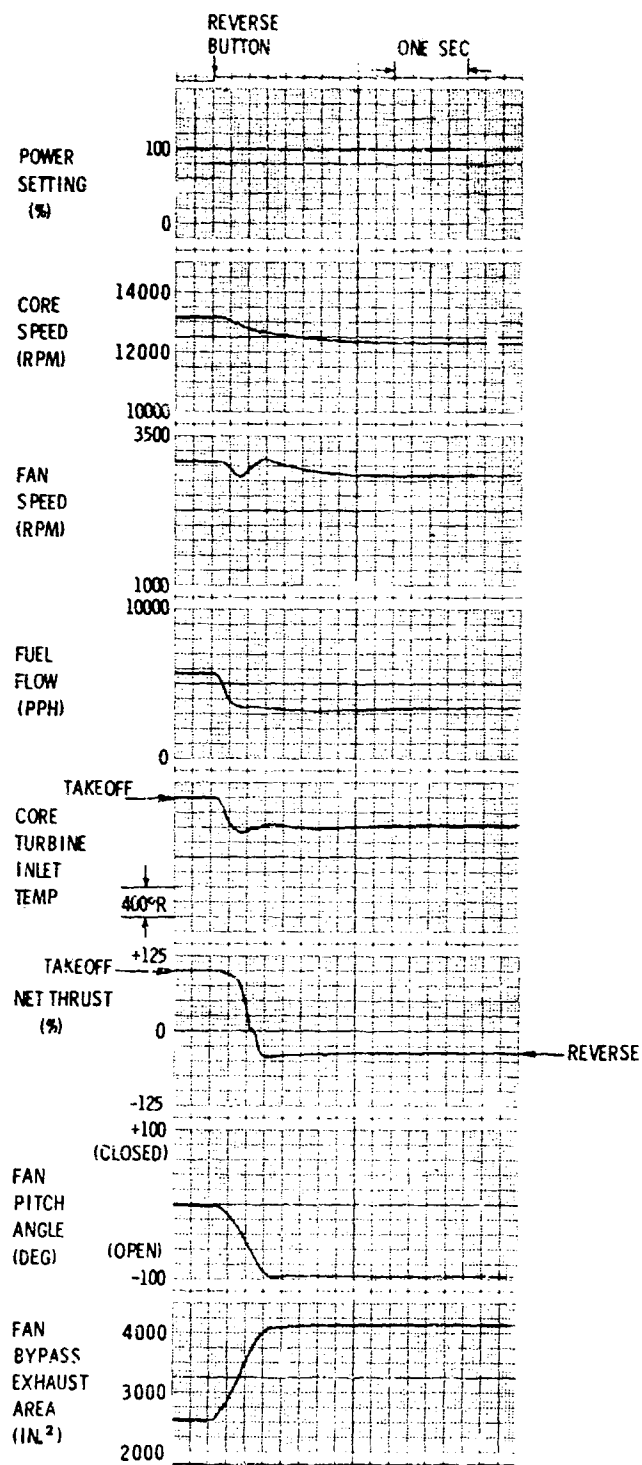
(i.e., feather); the second is angle changes thru flat pitch. During transition between the forward and reverse thrust fan-pitch angle positions, the fan shaft power absorption decreases and thus causes a tendency for the fan to accelerate. Quantitative information on fan horsepower during transition does not exist at this point in the UTW experimental engine development program and will not be known until the fan is tested on the engine. It is expected, however, that transitions through flat pitch will have less fan shaft power absorption and thus more tendency to overspeed when compared to reverse transients through stall.

Because of the unknown fan shaft power absorption level, the computer simulation has been used to investigate a range of minimum fan horsepower during the transients to reverse. The objective has been to determine the range of control adjustments needed to prevent excessive fan speeds and yet achieve the required transient time of 1.5 seconds during experimental engine testing. This study on reverse thrust transients was performed at sea level static (SLS) standard day condition.

Reverse Transients Through Stall - A transient from takeoff power to maximum reverse through stall is shown in Figure 26. The left-hand portion of this figure shows the specific values of selected engine and control variables at the takeoff power condition. The transient to reverse is initiated by the reverse command. Upon receipt of this signal the control system operates as follows.

- Power control of the engine is switched from the pressure ratio-fuel control mode to a core speed fuel control mode. The core speed demand is set at a flight idle position which causes the fuel to decrease.
- The fan pitch angle is opened to a predetermined reverse position.
- When fan pitch angle passes a predetermined interlock position, the power control of the engine is switched from the flight idle core speed-fuel flow control mode to the fan speed-fuel flow control mode.

As shown in Figure 26, the nozzle area and fan pitch are moved rapidly from the takeoff to the reverse position. Fuel flow is reduced and produces a corresponding reduction in turbine inlet temperature and core speed. Fan



ORIGINAL PAGE
OF POOR QUALITY

Figure 26. Transient from Takeoff to Maximum Reverse Through Stall at Sea Level Static, Standard Day.

speed decreases and then increases due to the expected reduction in fan horsepower during transition through stall. For the transient in Figure 26, the pitch angle, fuel flow interlock position is set at -80 degrees. (Note: Reverse transients through stall were performed for interlock positions over a range from -20 degrees through -80 degrees. The digital control system includes an adjustment on the interlock position so that the best setting can be established experimentally during engine test.) When pitch angle passes through the -80 degrees interlock point, the power control is switched to the fan speed-fuel flow control mode. Since fan speed is above the final value, fuel flow continues to decrease and eliminate the fan speed error to achieve the final steady-state speed. Reverse thrust is achieved in approximately 0.7 seconds after initiation of the reverse command.

Time from forward-to-reverse thrust is affected by many variables. Some of these are:

- Core speed-idle speed setting - a setting too low will cause excessive reversal times and a setting too high will cause the fan to accelerate.
- Minimum fan horsepower absorption in stall - the absolute level and its variations are not predictable. Horsepower absorption will affect times to reverse since it will affect the transient fan speed characteristics, which must be controlled to provide engine protection. Figure 27 shows the range of minimum fan horsepower considered in this simulation study.
- The pitch angle-fuel flow interlock point - early releases should reduce time to reverse but may cause a temporary undesirable fan acceleration.
- Fan-pitch rate of change
- Fan exhaust nozzle rate of change
- Dynamics associated with airflow reversal in the fan and its duct
- Fan stall recovery point of the fan during the reverse transient

The first three of the above mentioned variables were jointly investigated on the simulation. The purpose was to determine the variation in engine transient characteristics with several levels of minimum fan horse-

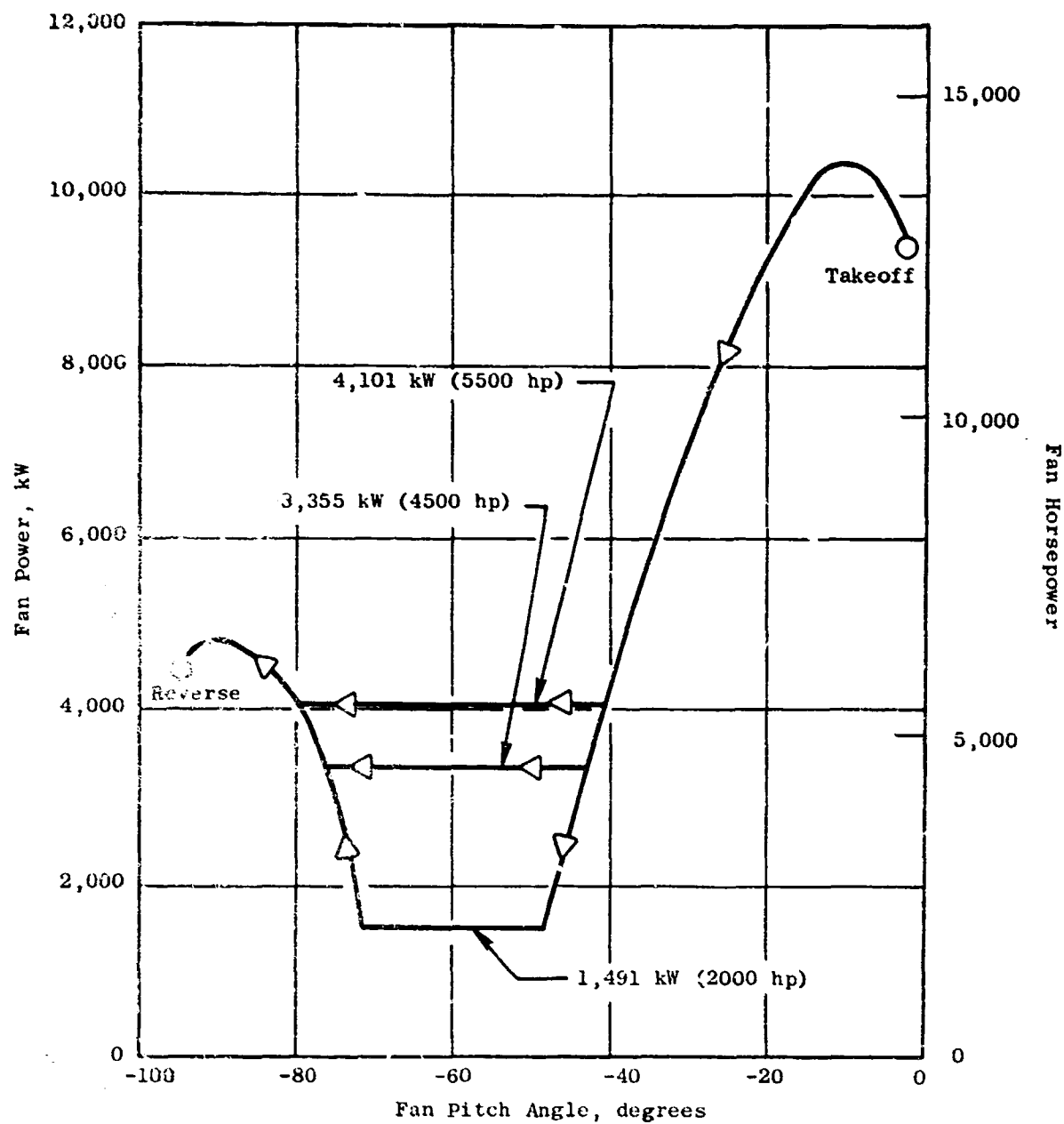


Figure 27. Fan Horsepower Transient Versus Fan Pitch Angle During Transition from Takeoff to Maximum Reverse Thrust Through Stall.

power absorption, core idle speed settings, and pitch angle interlock points. For the conditions investigated, the results indicate that the core idle speed adjustment should be set between 11,700 rpm to 12,500 rpm. With this core idle speed adjustment range and the capability to adjust the pitch angle interlock release point, the simulation predicts that the experimental engine will achieve reverse thrust in less than 1.5 seconds without excessive fan speeds.

The last four items of the variables noted above were not investigated on the engine simulation. Sufficient data were not available to model and investigate the fan stall recovery point and the dynamics associated with airflow reversal. The fan exhaust nozzle rate of change was not investigated because the system is designed for rapid nozzle opening to reduce forward thrust. However, the experimental control system is designed with an adjustable nozzle rate limit so that this parameter may be investigated during experimental engine testing. The fan-pitch angle rate of change was not investigated because it is expected that a rapid rate of blade angle change is required to reduce the fan stresses. However, the experimental control system is designed with an adjustable fan-pitch rate limit so that this parameter may be investigated during experimental engine testing.

Reverse Transients Through Flat Pitch - A transient from takeoff power to reverse through flat pitch is shown in Figure 28. The left-hand portion of this figure shows the specific values of selected engine and control variables at the takeoff power condition. The transient to reverse is initiated by the reverse command. Upon receipt of this signal, the control logic causes the fuel flow to decrease, the fan nozzle to open to its reverse position, and the fan pitch to close to its reverse position. For this transient, power control of the engine is switched from the pressure ratio-fuel flow mode, to the core speed-fuel flow control mode, and finally to the fan speed-fuel flow control mode - in the same manner as for the reverse transients through stall.

As shown in Figure 28, the nozzle area and fan pitch are rapidly moved from the takeoff to their reverse positions. Fuel flow is reduced and produces a corresponding reduction in turbine inlet temperature and core speed. Fan speed increases due to the low level assumed for fan shaft

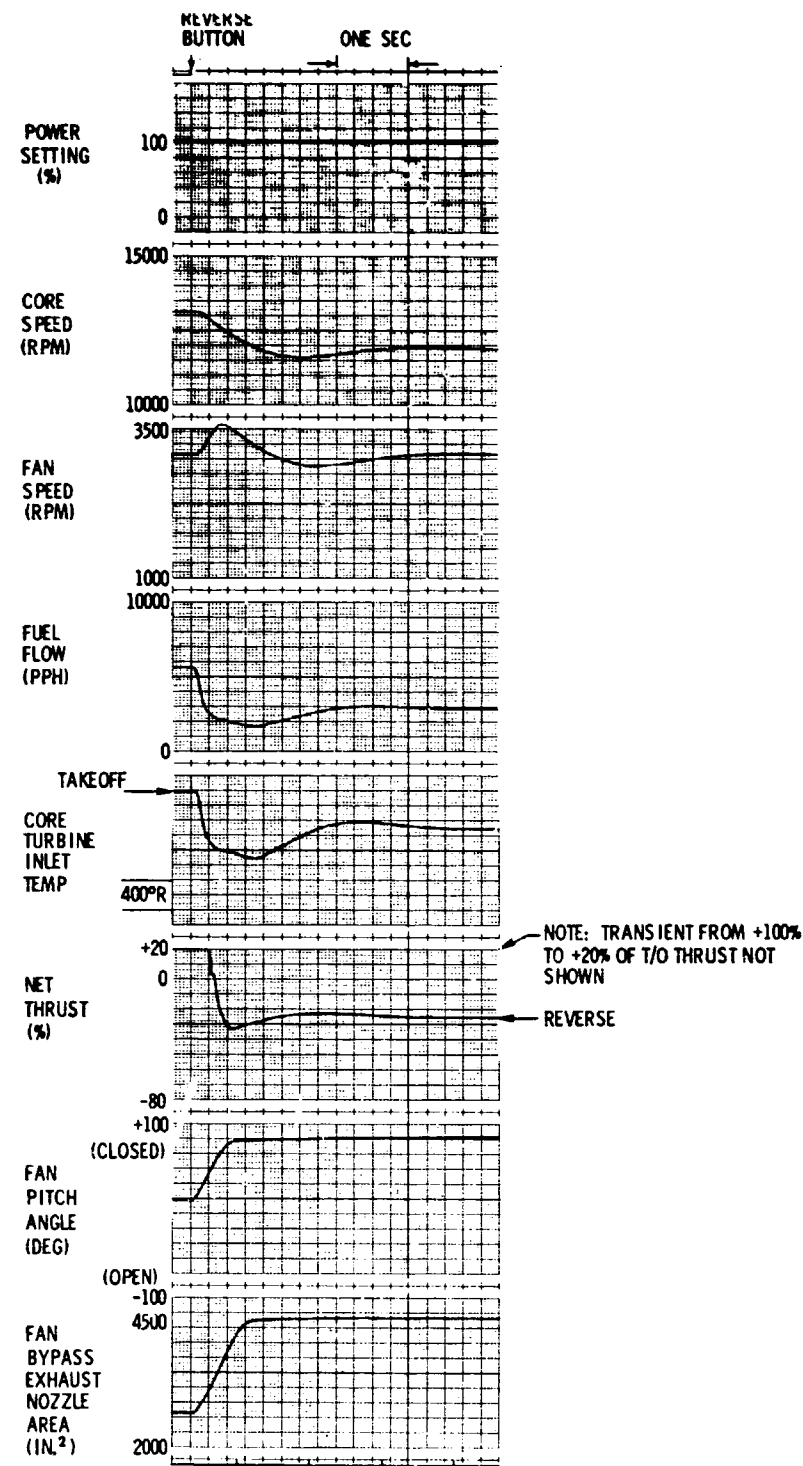


Figure 28. Transient from Takeoff to Reverse Through Flat Pitch at Sea Level Static, Standard Day.

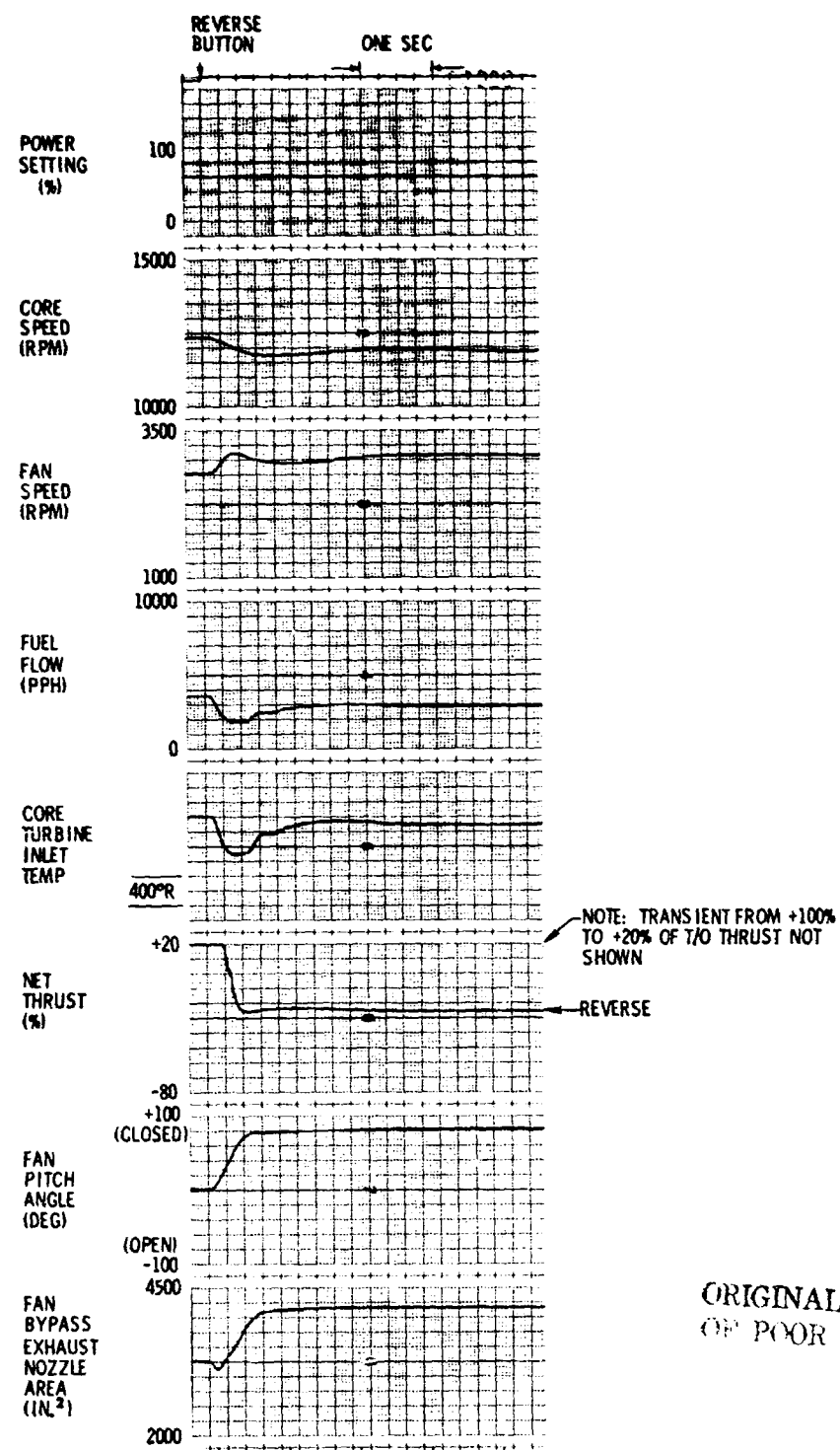
horsepower absorption (minimum = 2000 hp). For the transient in Figure 29 the pitch angle - fuel flow interlock position is set at +70 degrees.

(Note: Reverse transients through flat pitch were performed for interlock positions over the range from +30 degrees to +70 degrees. The digital control system includes an adjustment on the interlock position so that the best setting can be established experimentally during engine test.) At the +70 degrees interlock point, the deceleration schedule continues to control fuel flow because the fan speed is above the final value. As the fan decelerates, fuel flow increases in order to control the fan at the final speed level.

The takeoff-to-reverse transient in Figure 28 predicts that fan speed will exceed the maximum reverse thrust speed limit of 3408 rpm (i.e., fan turbine speed = 8400 rpm) when the fan shaft power absorption reduces to the 2000 hp minimum during the transition.

A potential design change to reduce the above peak fan speed is to delay closing the fan pitch to its reverse position. This involves adding more logic to the control design for the experimental engine and thereby having different logic for reverse transients through stall pitch and through flat pitch. The decision has been to continue with the original control logic design until quantitative information on fan shaft power absorption has been determined from the fan evaluation portion of the engine test program. This decision was based on the following considerations:

- Delay in closing fan pitch to reverse position could cause unacceptable transient times to reverse thrust.
- Reverse thrust transients through stall pitch had been selected as the primary mode.
- As shown by simulation results in Figure 29, the original control design can be used for reverse transients which start from power settings in the approach thrust range (i.e., 60% power setting).



ORIGINAL PAGE IS
OF POOR QUALITY

Figure 29. Transient from 60% Power Setting to Reverse through Flat Pitch at Sea Level Static, Standard Day.

4.6 STABILITY ANALYSIS

The stability analysis has been the basis for specifying the dynamics of the digital electronic control to be used on the first build of the QCSEE UTW experimental engine. The objective of the analysis has been to develop an accurate, stable, fast-response, closed-loop, engine control system. Both linear-servo analysis procedures and the hybrid-computer simulation of the engine and controls have been used to accomplish this objective.

The control mode analysis, reported in Section 4.2, indicated two potential automatic control modes for the first engine build. A stability analysis was performed on each. Results from the stability analysis indicated that the control dynamics for the mode of PS3/PTO-WF, N1K- β F, and XM11-A18 could be designed to meet the objectives cited above. But problems were encountered in developing a stable dynamic design for the automatic control mode of TP5-WF, N1K- β F, and XM11-A18. As a consequence, the control mode of PS3/PTO-WF, N1K- β F, and XM11-A18 was selected as the primary mode for the first engine build. The stability analysis on this primary control mode is discussed in the paragraphs which follow. Next, hybrid simulation results on steady-state hunting of the engine and control system are presented. Results for the primary control mode predict that peak-to-peak magnitudes of thrust hunting will be maintained within 0.1% limits. The final portion of this section discusses the stability problem associated with the alternate control mode of TP5-WF, N1K- β F, and XM11-A18.

4.6.1 STABILITY OF PRIMARY AUTOMATIC CONTROL MODE

The analysis for the primary control mode started with linear stability studies at the takeoff, sea level static, standard day condition. The QCSEE UTW cycle deck was used to generate engine partial derivatives at this steady-state operating condition. These engine partial derivatives along with linear transfer functions for the hydromechanical portions of the control system were used to determine the required dynamics for the digital electronic portion of the control system. The linear transfer functions for the hydromechanical fuel power piston and metering valve assembly, the β F hydraulic motor and gear train assembly, and the A18 hydromechanical actuation system

were developed from information provided by the respective component engineers. The dynamics for the digital electronic control were determined based on the following criteria for adequate stability margin:

- Magnitude of the closed-loop frequency response less than or equal to 1.5
- At least 2 to 1 (i.e., 6 decibels) gain margin when the open-loop transfer function phase margin is zero

Nichols charts were the primary method of examining the data in the linear stability studies.

Interaction of the three engine control loops for the primary control mode was considered in the linear stability studies at the takeoff condition. Due to the complexity of evaluating interaction of a three-variable control (each having an inner servo loop and an outer loop through the engine) with standard servo analysis techniques, the design procedure was to establish control dynamics at takeoff conditions and then to use the hybrid simulation for stability evaluation at other conditions.

Control dynamics were selected to produce an integration-type control with lead compensation. The lead time constant compensates for the major lag in each loop's engine transfer function. This lead over an integration was accomplished by lagged-rate feedback in the inner servo loop of each control - rather than proportional-plus-integral dynamics in the forward path of each outer loop. Describing function analysis for torque motor and servovalve hysteresis predicted oscillation when using the proportional-plus-integral technique (specific results are cited later in this report section).

Historically, the stability analysis started with a simplified investigation. Each control loop (PS3/PTO-WF, N1K-βF, XM11-A18) was treated as a separate loop with the other loops open. This provided initial estimates for rate feedback, lag-time constants but did not answer questions about sampling rate or control loop interaction effects on stability.

To evaluate the sampling rate effect of the digital control, the A18 position loop of the manual control was studied because of its simplicity. Rate feedback and the initial lag-time constant estimate were used in the

inner servo loop. The A18 position loop stability was analyzed using a hybrid simulation of digital compensation, a conventional frequency domain analysis, and a z-plane sample data analysis. For the conventional frequency analysis, the sampling effect was considered to be equivalent to a delay of 1.5 times the digital control cycle time or a 0.015 second delay. This delay was inserted at the point of DA (digital-to-analog) conversion in the frequency analysis. The delay represents the digital cycle delay and the effect of a zero-order hold DA conversion. The zero-order hold may be approximated by a delay of half the digital cycle time if the control is of the "low pass" type and the sampling frequency is high (Reference 1). Since the sampling frequency is 628 radians/second and the rate feedback inner-loop bandwidth is 35 radians/second, this is a valid approximation. For the case studied, the simulation indicated an outer-loop gain margin of 22.7 dB compared to 21.5 dB for the frequency analysis and 21.8 dB for the z-plane analysis. The frequency analysis predicted a phase margin of 76° compared to 77° for the z-plane analysis. Thus, analysis in the frequency domain using 0.015 second delays at the DA conversions was felt to be reasonable for all loops since their bandwidths would be much less than the sampling frequency.

Before further analysis on the primary automatic control mode, a definition for the manual control mode was completed. The manual control mode will be used during tests to map engine characteristics. The objective was to have the same dynamic characteristics in the inner servo loops of both the manual and automatic control modes; the work was less complex when starting with the analysis of the manual mode. All inner loops were sized based on the assumption that separation between the inner- and outer-loop crossover frequencies would prevent loss of inner-loop stability margin due to outer-loop closure.

To finish the definition of the A18 manual control mode, a study was made considering hysteresis to be lumped at the interface between the digital control and the torque motor and servovalve. Using a describing function analysis, the outer-loop gain was sized to prevent undesirable low-frequency oscillations. The analysis of the A18 control loop took into consideration the minimum and maximum variations of servovalve gain due to load.

Proportional-plus-integral control was considered for the fan speed-fuel flow loop of the manual control mode. It was abandoned when a describing function analysis for torque motor servovalve hysteresis predicted oscillations of $\pm 1.63\%$ WF at 9 radians/second. Since the magnitude could not be greatly reduced and was greater than the $\pm 0.5\%$ objective, the proportional plus integral was abandoned in favor of lagged-rate feedback. After this analysis, lagged-rate feedback was used exclusively for both manual and automatic control modes. The manual mode core speed-fuel flow control loop was sized with the same rate feedback time constant (0.5 second) as the fan speed-fuel flow loop. The rate-feedback lag-time constant in the T41C fuel flow control was set at 0.1 seconds. The fan-pitch position control loop was sized with a 0.3-second rate feedback time constant considering maximum and minimum servovalve gains due to loading.

After the manual control mode dynamics had been determined, the dynamics for the automatic control mode were developed. The inner-loop dynamics of the manual modes were used as a starting point. The open-loop crossover frequencies of these inner loops were in the 12 to 18 radian/second range. Based on normal servo design procedures, this meant that the open-loop crossover frequencies for the automatic control loops (i.e., outer loops) must be lower by an octave or more than the crossover frequencies for the inner loop.

To determine which should be the fastest automatic control loop, frequency response data from the engine transfer functions $\Delta N1K/\Delta \beta F$, $\Delta(PS3/PTO)/\Delta WF$, and $\Delta XM11/\Delta A18$ were obtained for the maximum power setting at three points in the flight envelope:

	<u>ALTITUDE</u>	<u>AIRCRAFT</u>	<u>DELTA FROM</u>
	<u>(FEET)</u>	<u>Mach No.</u>	<u>STANDARD AMBIENT</u>
			<u>TEMPERATURE (°R)</u>
(1)	0	0	0
(2)	0	0.378	0
(3)	30,000	0.800	+18

2

For these three flight points, these data indicate that the magnitude variation of the βF to N1K engine response was significantly less in the frequency range above 5 radians/second. See Figure 30. The conclusion was that minimum change in the response of the N1K- βF engine control loop would be achieved at the above flight points if its open-loop crossover frequency were designed at 5 radians/second or greater. This conclusion, along with the above noted procedure of setting the outer-loop crossover frequency an octave or more less than the inner loop, led to the decision to make N1K- βF the fastest loop.

The decision to select the PS3/PTO-WF loop to be the next fastest and the XM11-A18 loop to be the slowest loop was based again on which would have the least variation in loop response at the above flight points. Data indicate that the magnitude variation of the A18 to XM11 engine frequency response was least in the frequency range below 2 radians/second. Whereas the gain change due to the WF metering valve (triangular port shape), in combination with the engine response from WF to PS3/PTO, would produce a sufficiently small net gain variation in the 2 to 3 radian/second frequency range. Therefore, the method used in the first linear analysis study was to size the N1K- βF open-loop crossover frequency in the 5 to 9 radian/second range with WF and A18 constant. Then, the open-loop crossover frequencies of the PS3/PTO-WF and the XM11-A18 loops were sized in the 2.0 to 3.0 and 1.0 to 1.5 radian/second range, respectively - in each case considering the closed-loop modulation effects of the other two automatic controls. For example, the PS3/PTO-WF loop was sized with both N1K- βF and XM11-A18 modulating. Using the dynamics of this linear study as a base, the procedure was then one of "boot strapping" between hybrid simulation and further linear studies to achieve the dynamic design for the first build of the UTW experimental engine.

During this hybrid simulation, linear analysis phase of design work, adjustments were made to the lagged-rate feedback time constants in the XM11-A18 loop and the PS3/PTO-WF loop from 0.278 seconds to 0.139 seconds and from 0.5 seconds to 0.25 seconds, respectively.

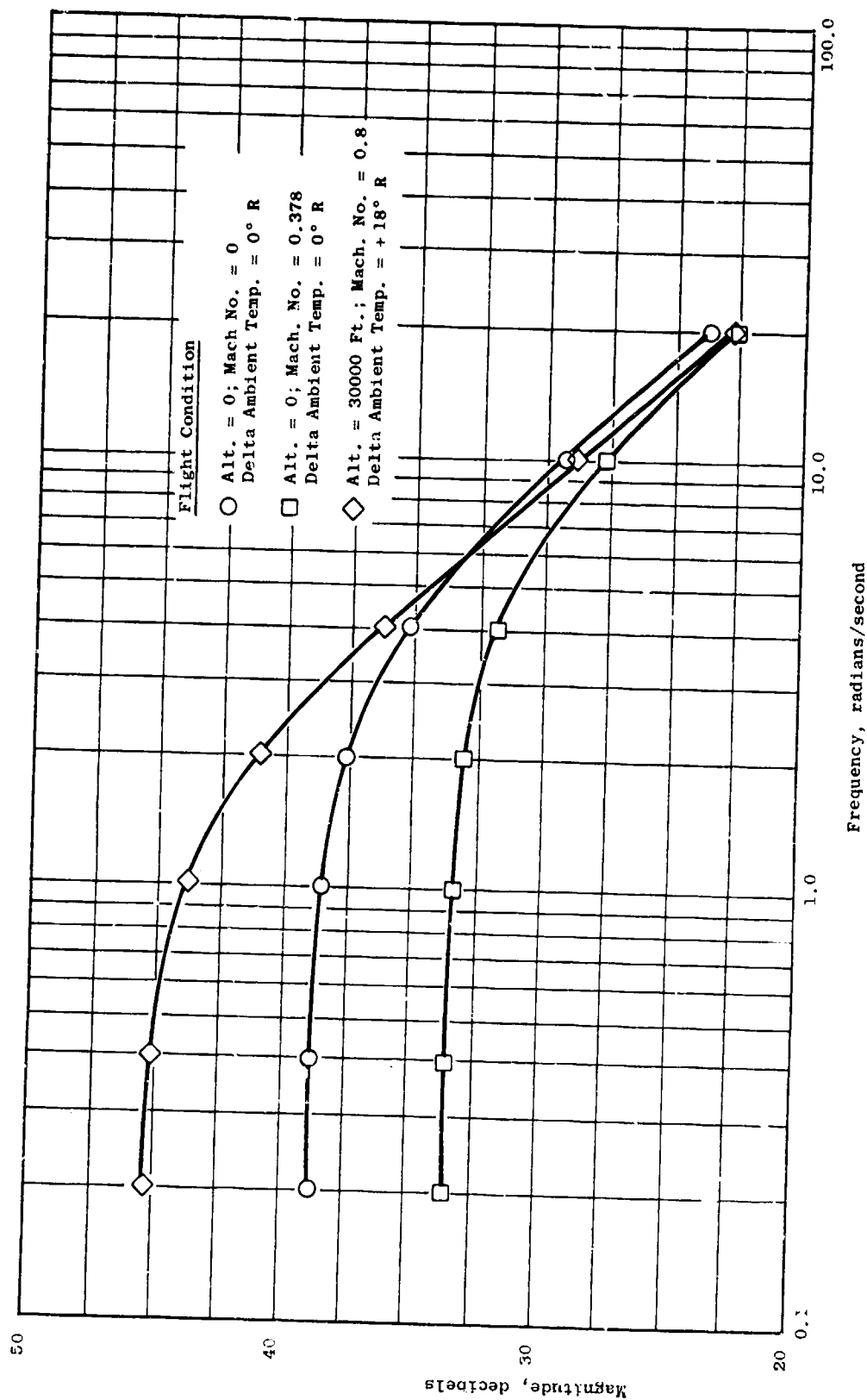


Figure 30. Magnitude of Engine Frequency Response from 0F to 1K at Maximum Thrust.

During the final phase of design, hybrid simulation results indicated that stability margin was inadequate for the PS3/PTO-WF inner loop at takeoff power, sea level static, standard day condition. Examination of inner-loop stability with the outer loop modulating showed a loss of 30 degrees of phase margin to 27° and 4.2 dB of gain margin to 4.4 dB. Inner-loop stability margin was restored by the addition of a 0.1-second lag in the forward gain portion of the outer loop. Results of this frequency analysis are illustrated in the Nichols chart of Figure 31.

With the outer loops modulating, an inner-loop stability check was made on the N1K- β F and XM11-A18 control loops. The XM11-A18 inner loop had adequate margin. To restore the stability margin for the N1K- β F inner loop, the forward outer-loop gain was reduced by 10%, and a 0.05-second lag was added to the forward outer-loop gain path.

Open-loop frequency response results for the primary automatic control mode of the UTW experimental engine at takeoff, sea level static, standard day, are shown in the Nichols charts in Figures 32 through 37. Figure 32 contains the open-loop frequency response plot for the N1K- β F outer loop, with the PS3/PTO-WF and XM11-A18 loops modulating. This figure shows that the maximum magnitude for the closed-loop response of the N1K- β F control is approximately 1.5 (as indicated by tangency of the open-loop frequency response plot with the $M = 1.5$ circle). It also shows that the gain margin is $1/0.4 = 2.5$ to 1 at an open-loop phase margin of zero degrees. These results indicate that the N1K- β F outer loop meets the criteria for adequate stability margin which was cited at the beginning of this report section.

Figure 33 shows the open-loop frequency response plot for the N1K- β F inner loop, with the PS3/PTO-WF and XM11-A18 loops modulating. The gain margin is more than adequate (i.e., $1/0.125 = 8$ to 1 at the open-loop phase margin of zero degrees). Figure 30 indicates that the magnitude for the closed-loop response exceeds the $M = 1.5$ maximum by a slight amount. However, 40 degrees of phase margin is maintained at the 7-radian-per-second cross-over frequency, and the stability margin of this inner loop is judged to be adequate.

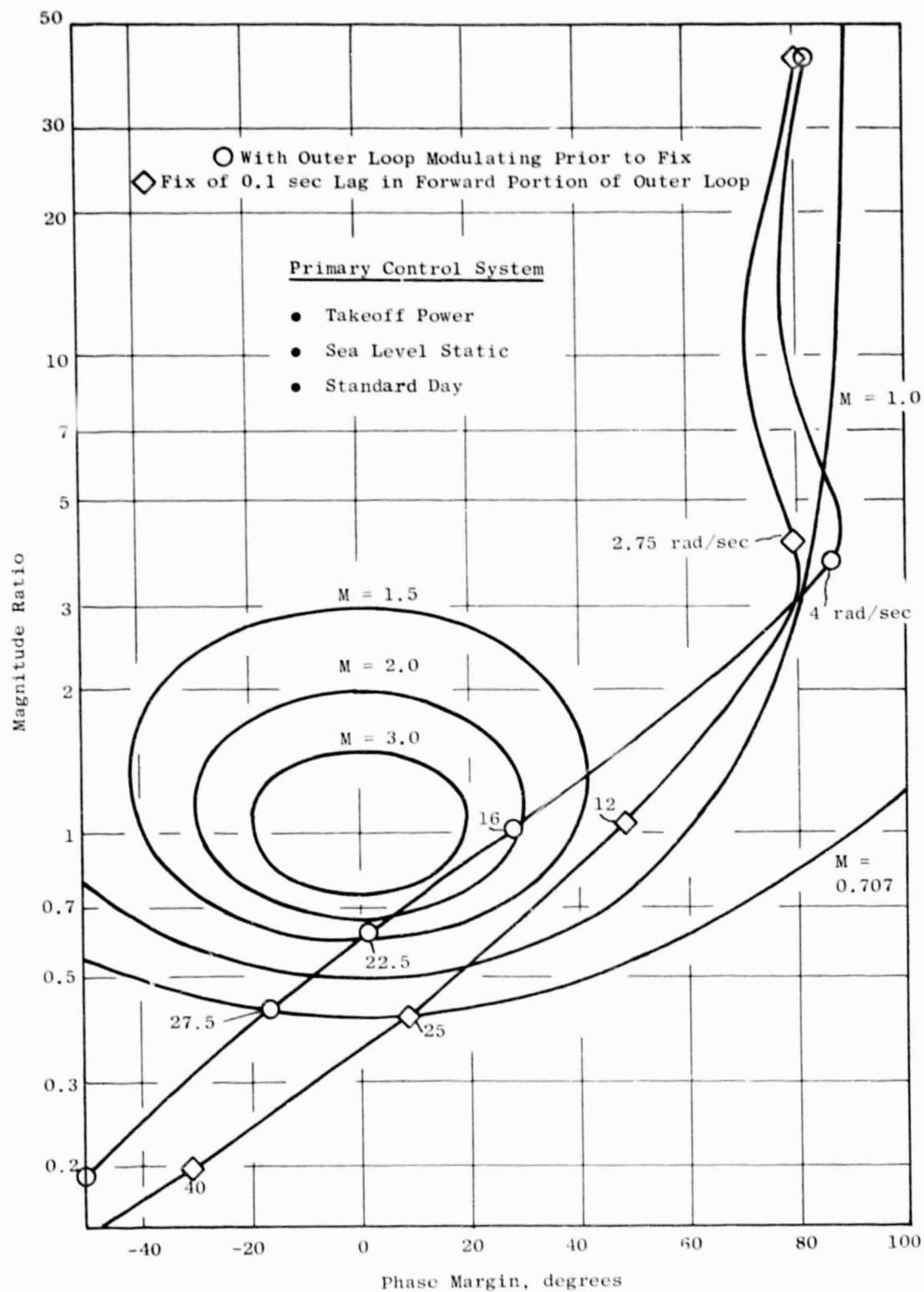


Figure 31. Phase-Magnitude Ratio Diagram PS3/PTO-WF Inner Loop Analysis.

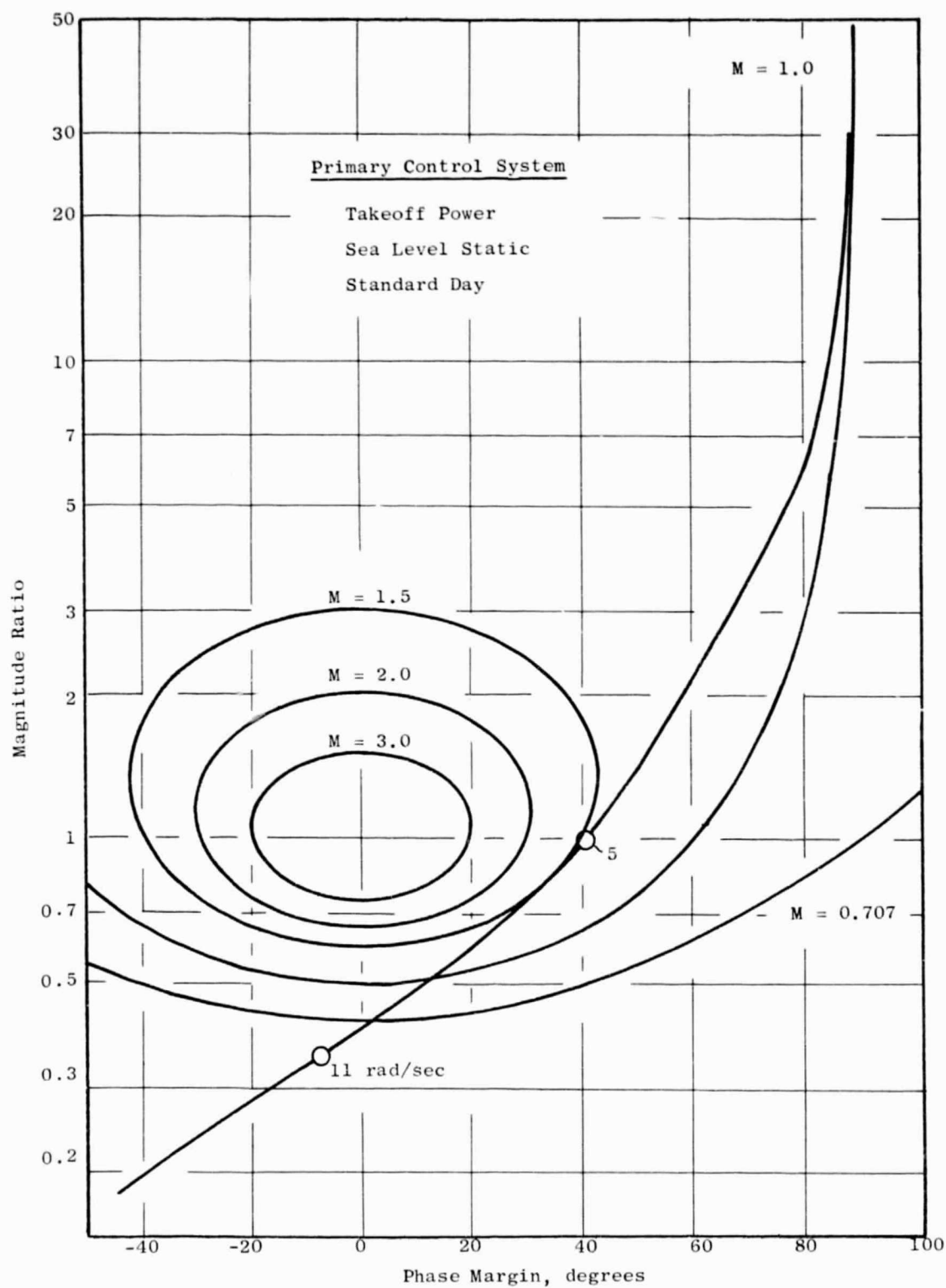


Figure 32. Phase-Magnitude Ratio Diagram Final N1K-8F Outer Loop.

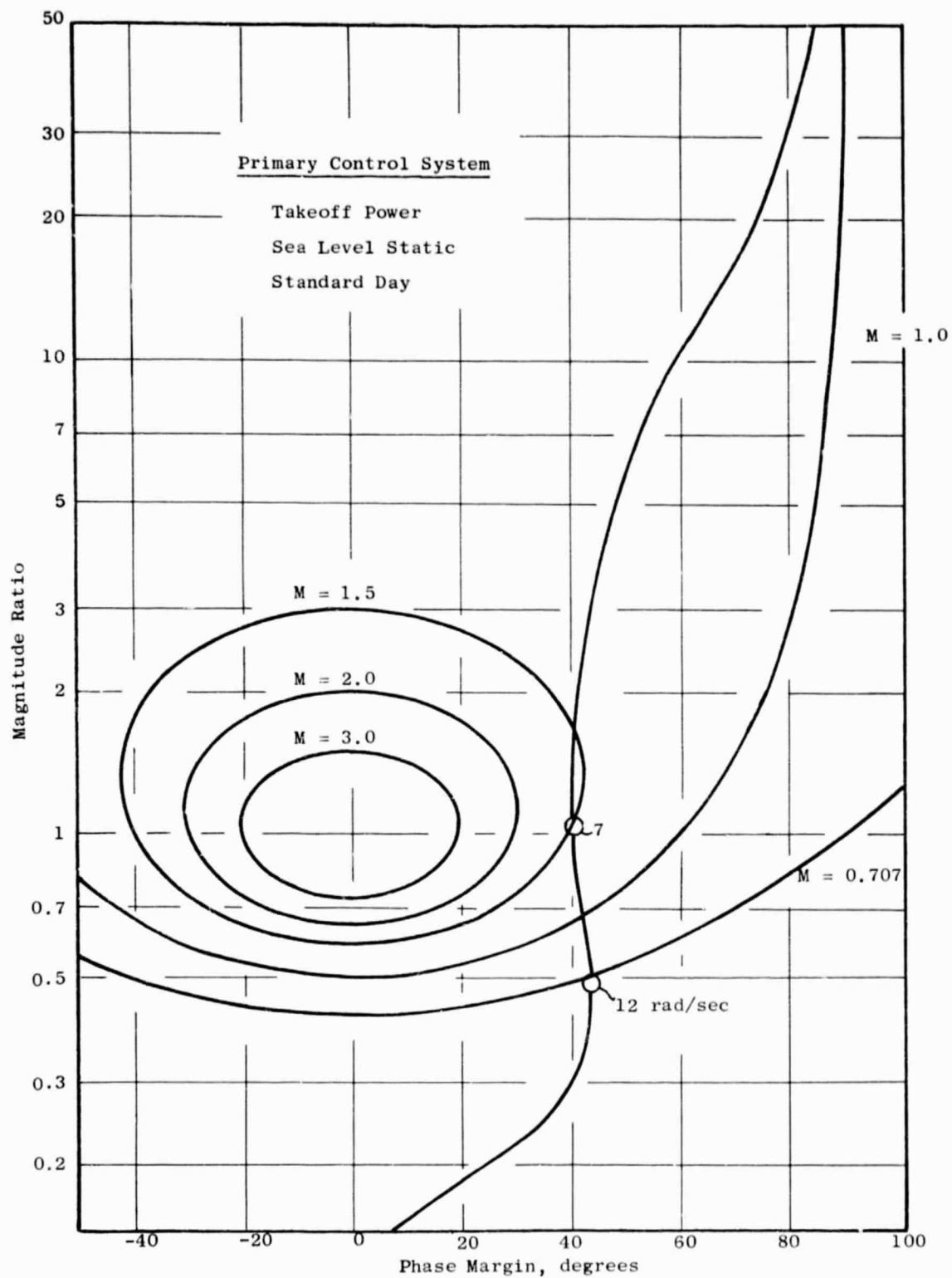


Figure 33. Phase-Magnitude Ratio Diagram Final N1K-8F Inner Loop.

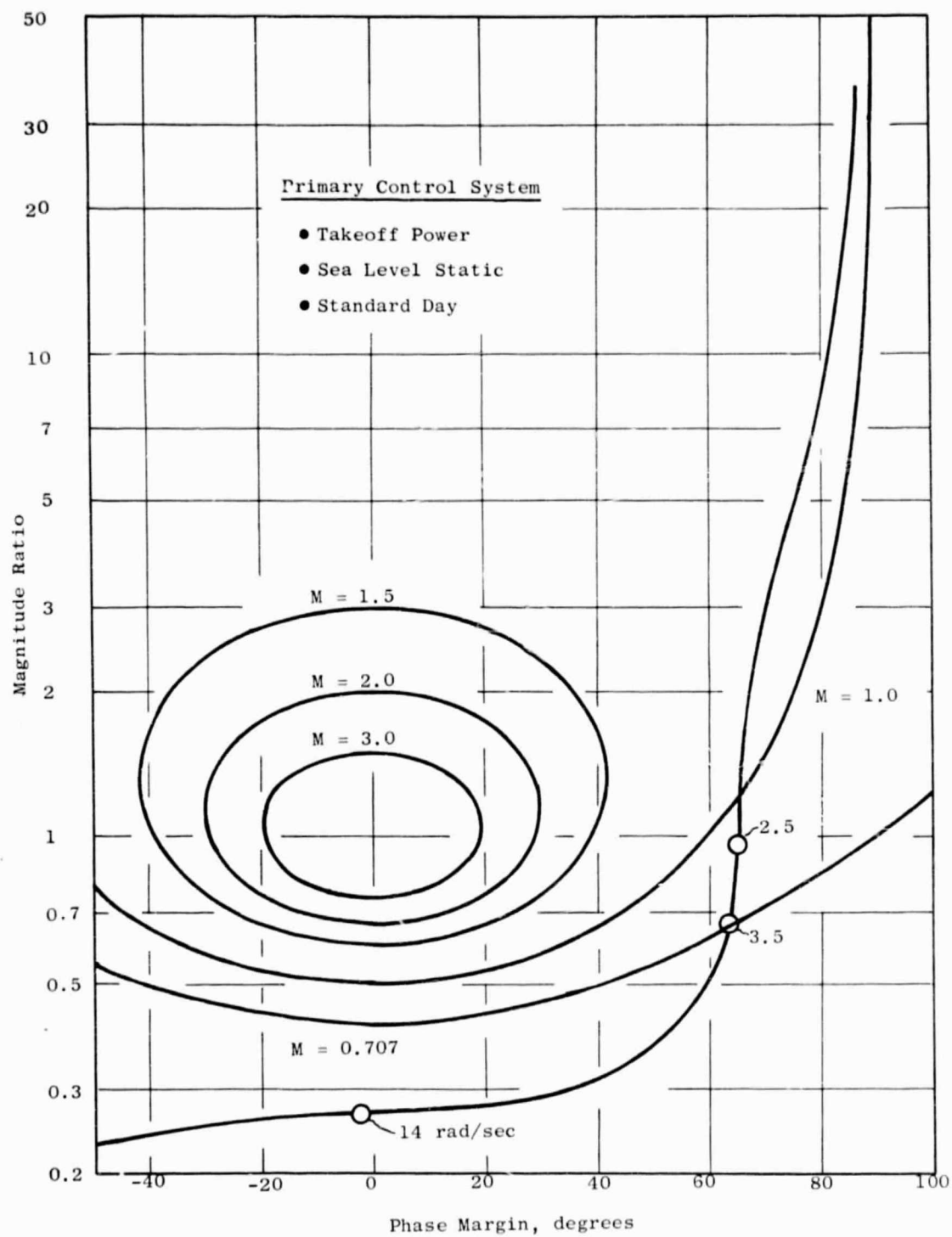


Figure 34. Phase-Magnitude Ratio Diagram Final PS3/PTO-WF Outer Loop.

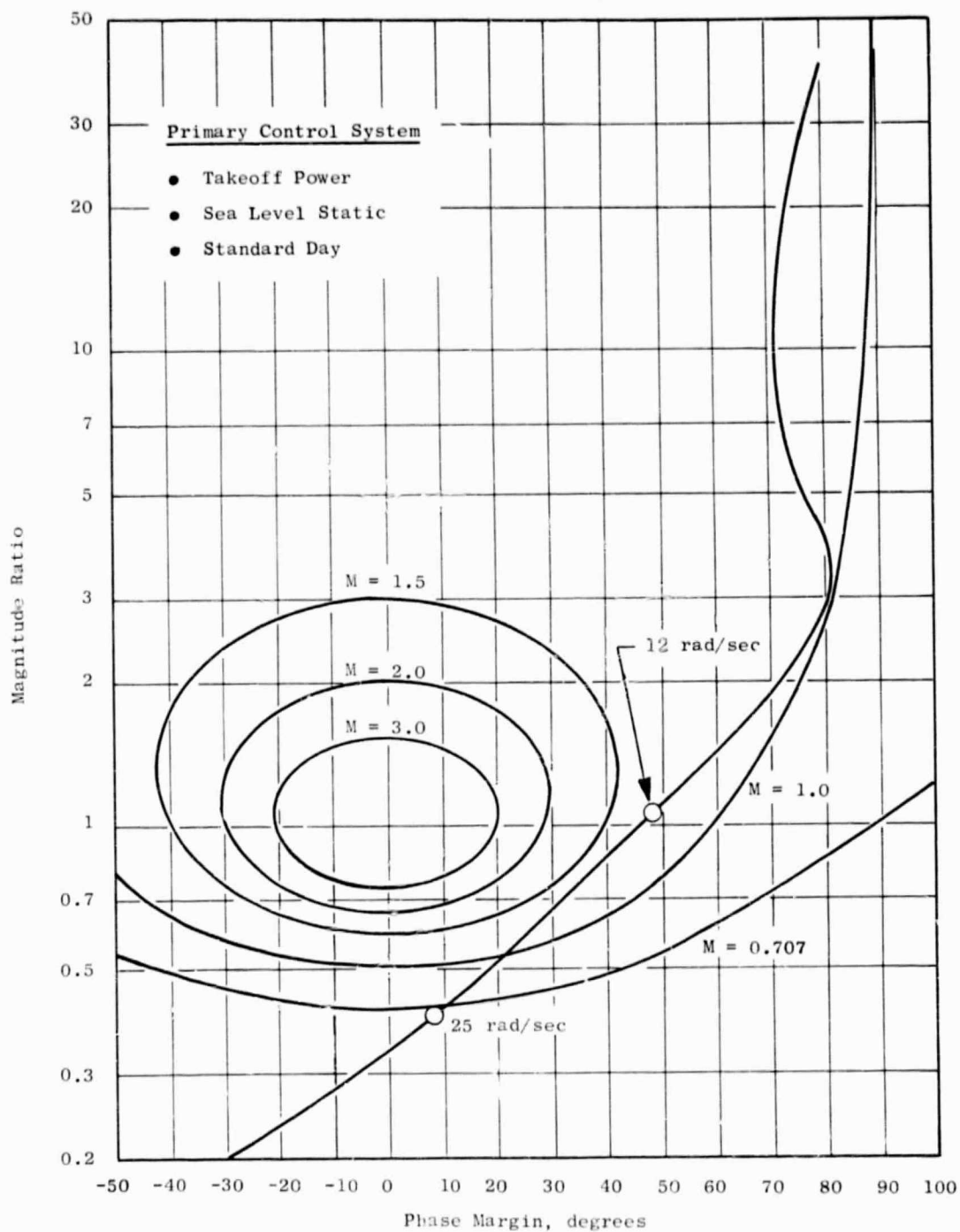


Figure 35. Phase-Magnitude Ratio Diagram Final PS3/PTO-WF Inner Loop.

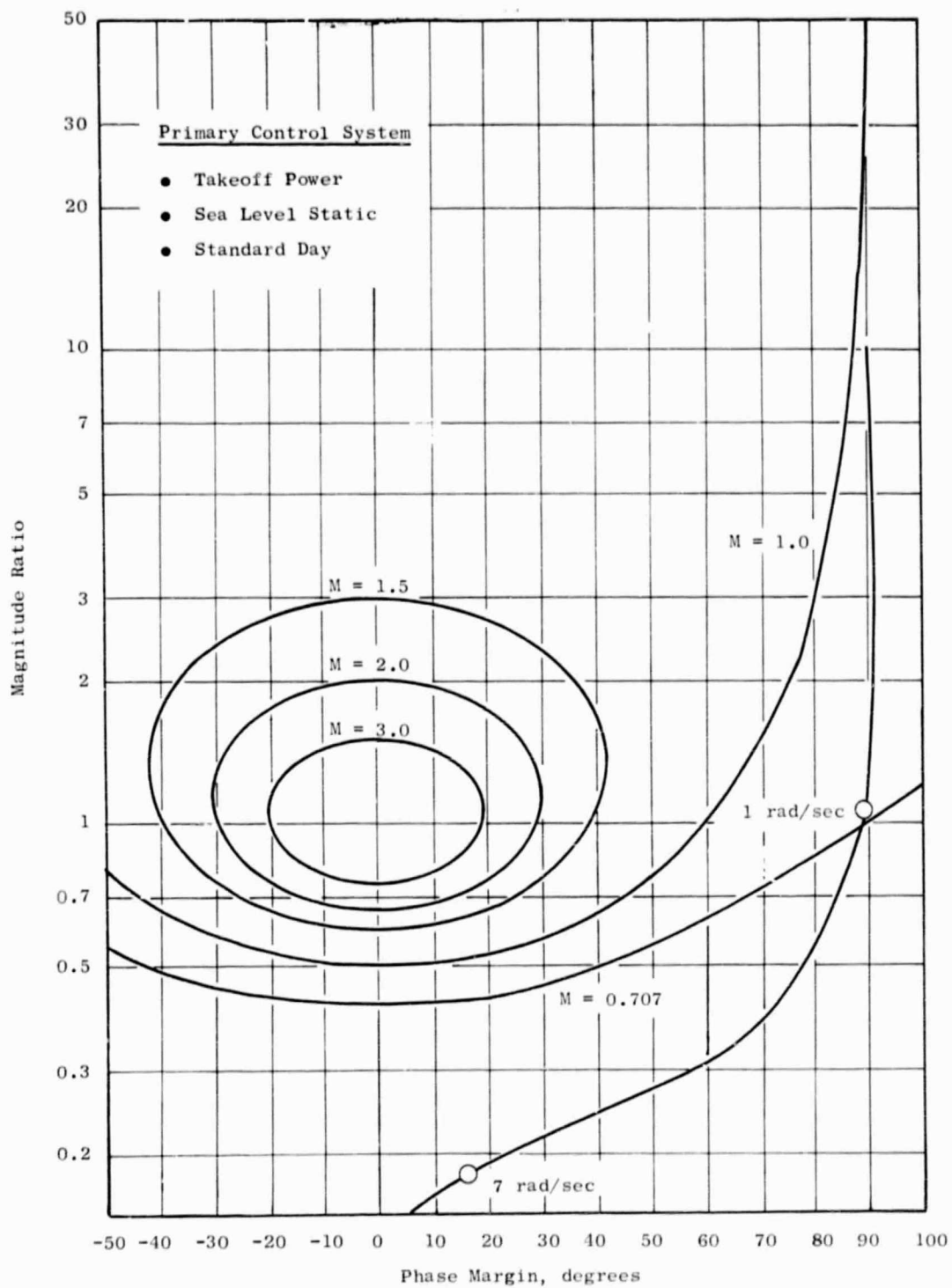


Figure 36. Phase-Magnitude Ratio Diagram Final XM11-A18 Outer Loop.

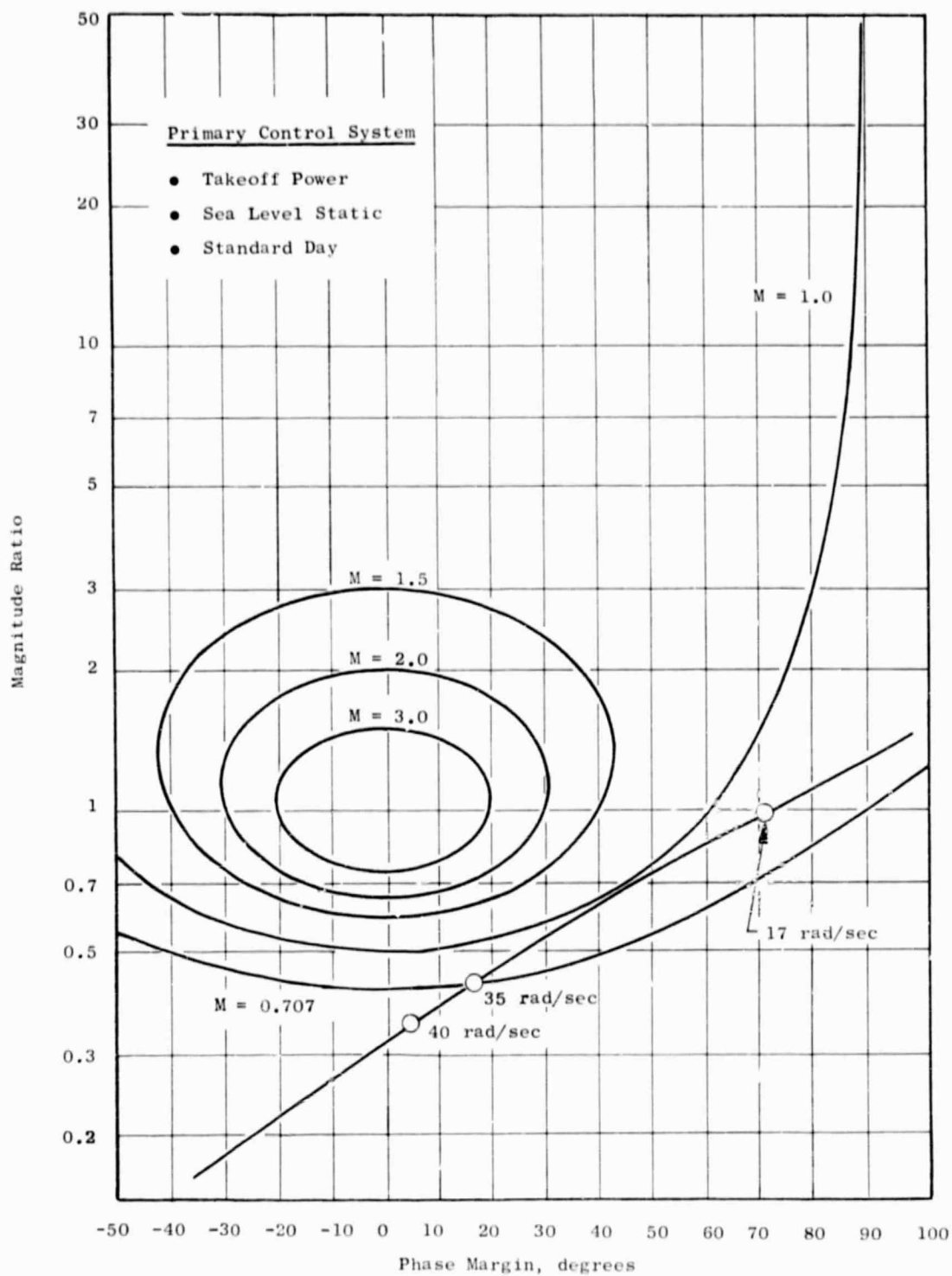


Figure 37. Phase-Magnitude Ratio Diagram Final XM11-A18 Inner Loop.

Figures 34 and 35 describe frequency response data for the PS3/PTO-WF outer and inner loops, with the N1K- β F and XM11-A18 loops modulating. Figures 36 and 37 contain the data for the XM11-A18 outer and inner loops, with the N1K- β F and the PS3/PTO-WF loops modulating. The results for these engine controls loops indicate closed-loop frequency response magnitudes (M) less than 1.5 and gain margins greater than 2 to 1. Therefore, adequate stability margin is demonstrated for each.

4.6.2 STEADY-STATE HUNTING INVESTIGATION WITH GE VARIABLE-PITCH ACTUATION SYSTEM

Another factor considered during the stability analysis of the primary automatic control mode was steady-state hunting due to nonlinearities in the control components. This was done using the hybrid-computer simulation of the engine and the primary control system. A simplified model of the GE variable-pitch actuation system was used in the simulation study; a description of this simplified actuation system model is contained in the UTW Engine Simulation Report (Reference 2).

In general, accurate, high-response, closed-loop, engine control systems will have some degree of thrust variation at a constant power setting. Also, control components and their outputs will usually exhibit some unwanted, more or less continual, motion or fluctuation; this is generally caused by nonlinearities such as friction, gear backlash, and parasitic leakages in hydromechanical components and also magnetic hysteresis in electromechanical components. The above mentioned variation (continual motion) and fluctuation are referred to as "hunting". The goal for this engine control system design has been peak-to-peak magnitudes of thrust hunting less than 0.1%. Control component wear also has been considered in establishing acceptable limits on control variables.

The hunting predicted for the UTW experimental engine and the primary automatic control mode was determined at 100% of takeoff thrust, sea level static, standard day condition. At this condition, closed loop control of fan speed, PS3/PTO, and inlet duct Mach number were maintained by automatic continuous adjustment of fan blade pitch angle, fuel flow, and fan exhaust

nozzle area. Nominal control gains were used. Recorded values of selected variables are shown in Figure 38. The initial portion of Figure 38 shows the sudden disturbance (retard to 60% power setting and immediately advance to 100%) which was quickly corrected in all the variables; the remaining portion shows the steady-state hunting associated with these variables. For the nominal system design, these recorded values indicate that hunting is maintained within 0.1% thrust, 0.1% on fan speed, 0.2% on fan nozzle area, 0.44% on fuel, 0.07° on fan blade position, and 0.001 on inlet Mach number. These values were judged to be acceptable.

Deliberate changes in twelve control variables were introduced (gains, hysteresis, loads, etc. as described in Table VIII) with their effect on hunting noted. As shown in Table VIII, ten of the control variables could be widely varied with negligible effect. One of the two variables which did affect hunting was fan variable-pitch position feedback hysteresis: magnitudes of hysteresis beyond 0.42° and up to one degree caused undesirable sustained oscillation at 0.5 to 1.0 Hz with up to 3.0% cyclic thrust variation and up to 1.5 Hz cyclic blade position variation, as shown in Figure 39. This is not a concern item because 0.03° hysteresis is expected to be easily maintained in the GE actuation system design.

Undesirable hunting was also indicated for metering valve position feedback hysteresis beyond 0.002 inches and up to 0.004 inches; Figure 40 shows that this hysteresis range caused oscillation at 1.25 Hz, up to 3.5% fuel flow variations, and up to 0.3% thrust variations. This is not a concern item since hysteresis less than 0.001 inches is expected to be easily maintained.

The above hunting investigation was performed prior to final "tuning" of the digital control gains and time constants. Changes to these gains and time constants were relatively minor but could cause some slight difference in the quantitative results reported above. This is not expected to be a concern item because of the margins reported in the above hunting investigation.

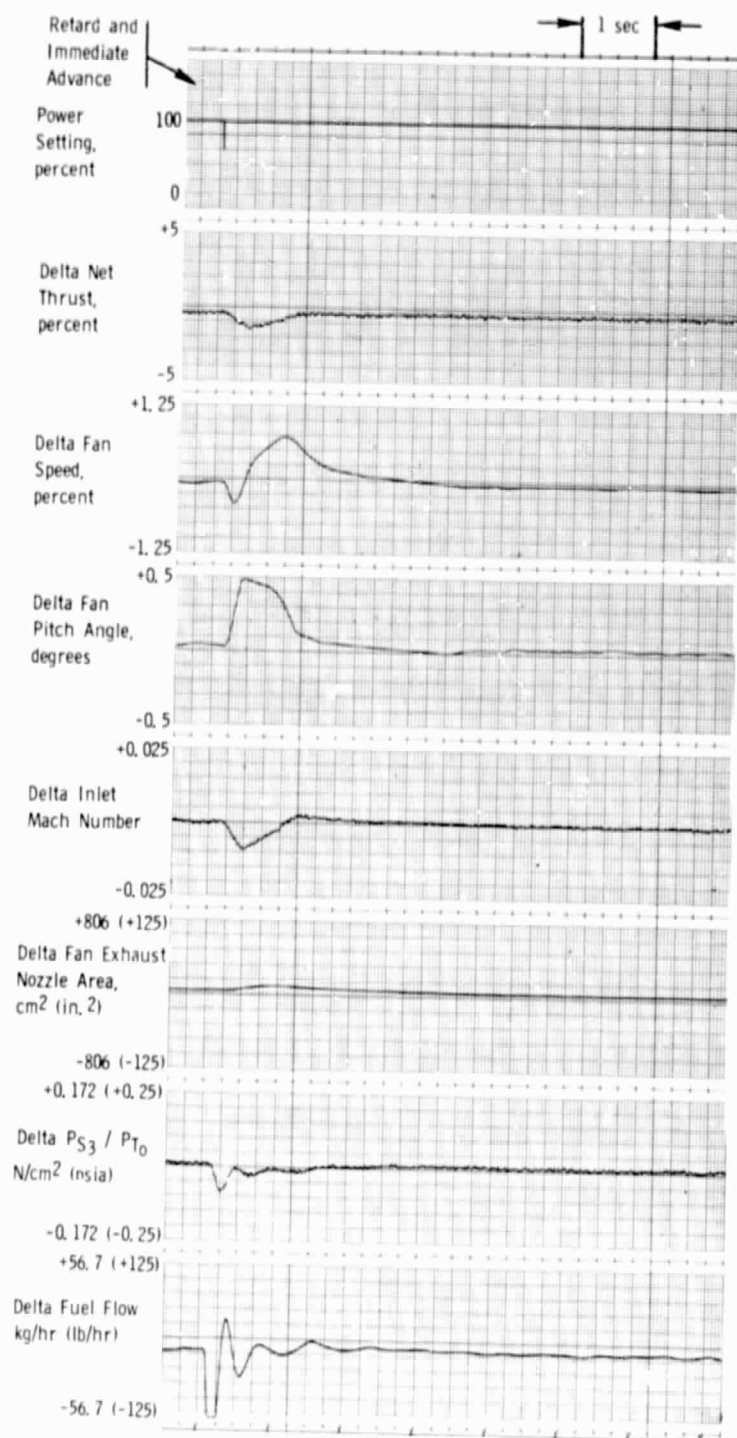


Figure 38. UTW Engine and Control System Hunting at Nominal Design Conditions, SLS, Standard Day.

ORIGINAL PAGE IS
OF POOR QUALITY

Table VIII. Effect of Control Variables on System Hunting.

Variable		Change From Nominal	Magnitude/Frequency of Hunting
1.	NIK-VP Digital Controller Gain	+20%	Within Limits
2.	VP Torque Motor Amplifier Gain	+20%	Within Limits
3.	VP Servovalve Hysteresis	+0.8 mA (NOM=0.8 mA)	Within Limits
4.	VP Position Feedback Hysteresis	+0.4 deg. to 1.0 deg. (NOM=0.03 Deg.)	Within Limits up to 0.42 Deg.; Out of Limits From 0.42 Deg. to 1.0 Deg.
5.	VP Blade Loads	-50%	Within Limits
6.	PS3/PTO-WF Digital Controller Gain	+20%	Within Limits
7.	WF Torque Motor Amplifier Gain	+20%	Within Limits
8.	WF Servovalve Hysteresis	+0.8 mA (NOM=0.8 mA)	Within Limits
9.	WF Position Feedback Hysteresis	+0.001 in. to 0.004 in. (NOM=0)	Within Limits up to 0.002 in.; Out of Limits from 0.002 in. to 0.004 in.
10.	XM11-A18 Digital Controller Gain	+20%	Within Limits
11.	A18 Torque Motor Amplifier Gain	+20%	Within Limits
12.	A18 Servovalve Hysteresis	+0.8 mA (NOM=0.8 mA)	Within Limits

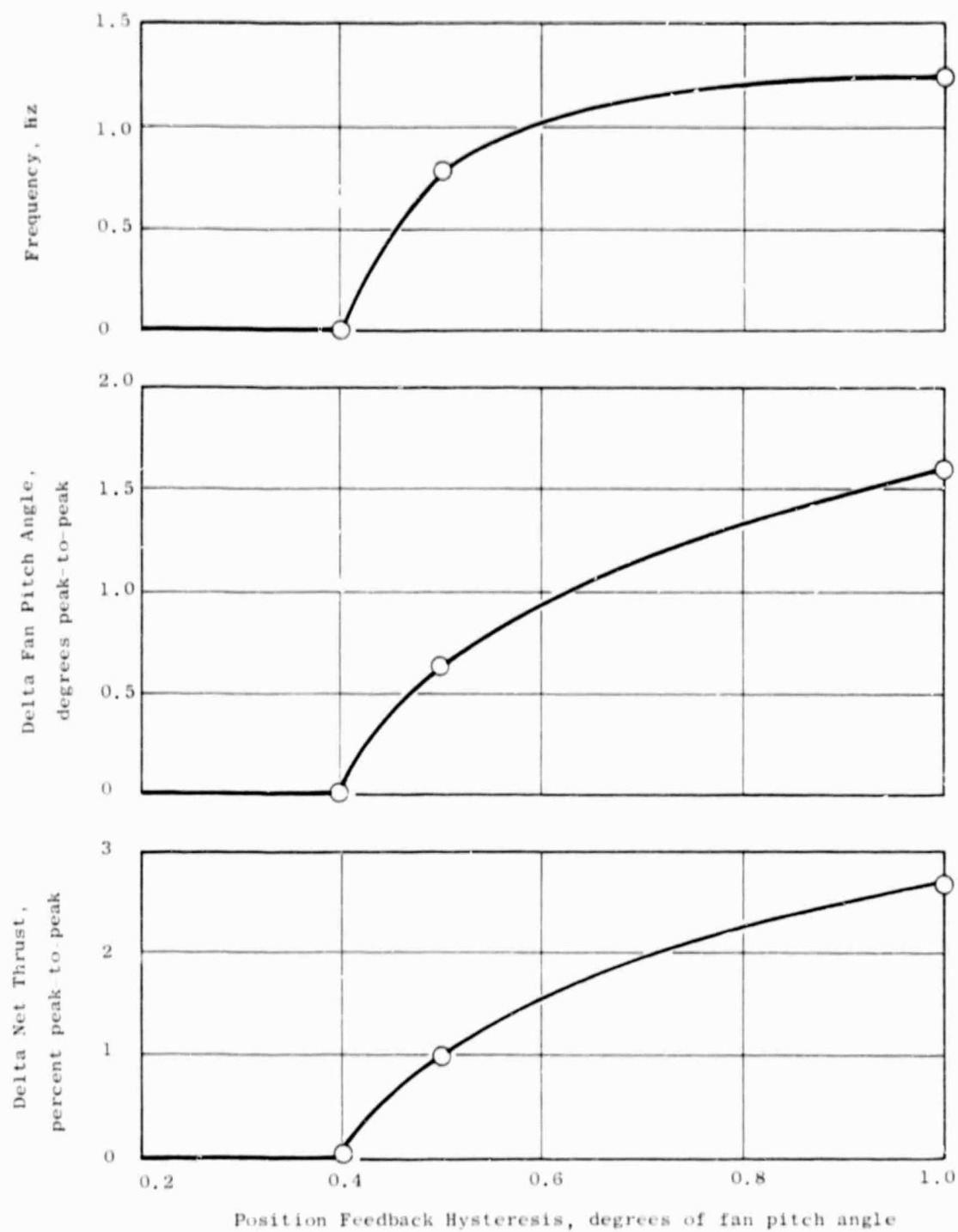


Figure 39. Hunting Due to Hysteresis in Feedback Sensing of Fan Pitch Hydraulic Motor Position at Takeoff, Sea Level Static, Standard Day.

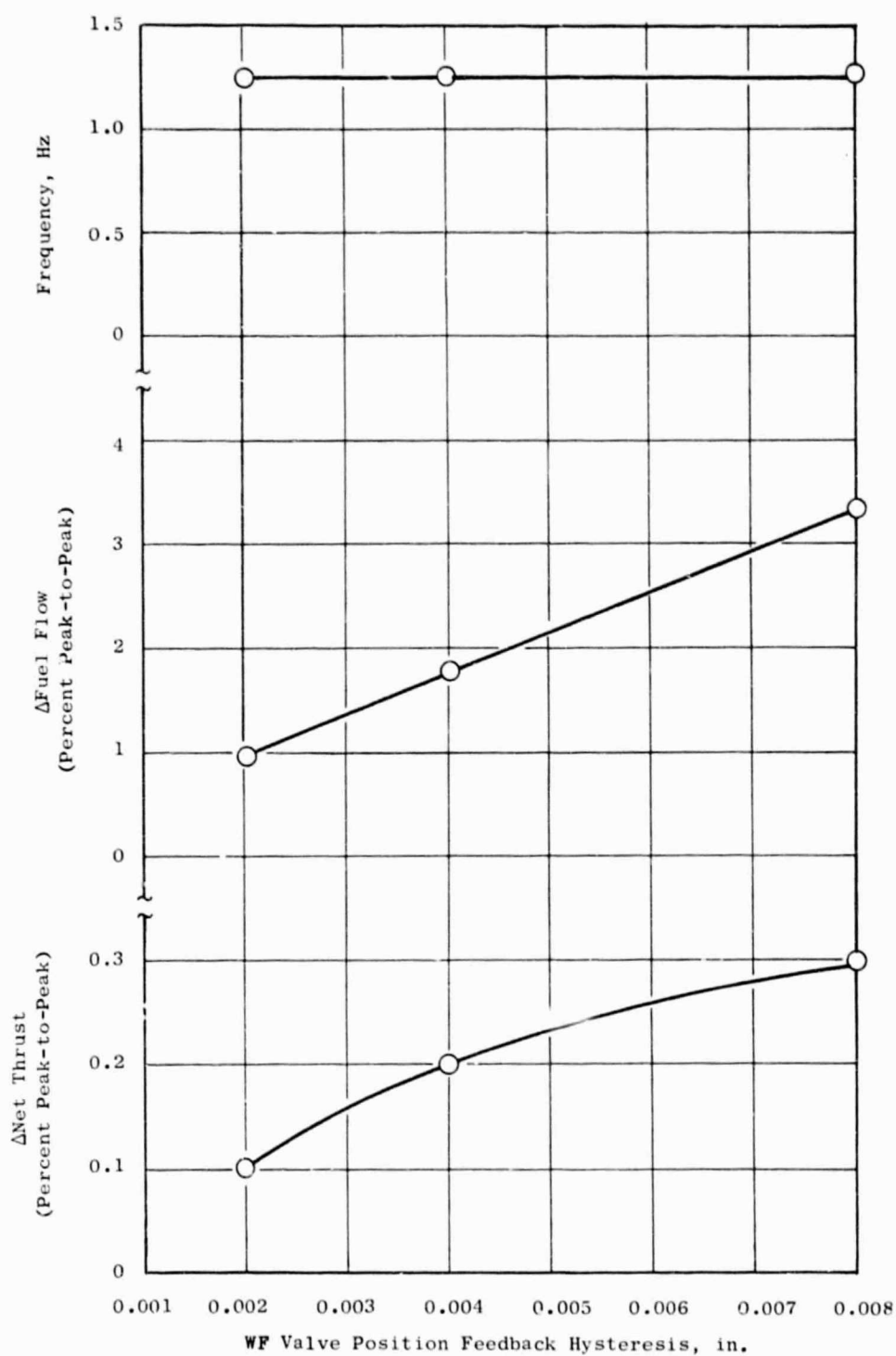


Figure 40. Hunting Due to Hysteresis in Feedback Sensing of Fuel Metering Valve Position at Takeoff, Sea Level Static, Standard Day.

4.6.3 STABILITY OF ALTERNATE AUTOMATIC CONTROL MODE

During the initial control mode analysis, TP5 was selected as a prime candidate for providing accurate thrust control. TP5 is a function of the inlet Mach number and the exhaust nozzle area, as defined by the following equation:

$$TP5 = \frac{1000 * XM11^2}{A18 * (1 + 0.2 * XM11^2)^6}$$

An alternate automatic control mode utilizing TP5 was selected in the initial mode analysis. It was TP5-WF, N1K-βF, and XM11-A18. A stability analysis was performed to establish the dynamic design for this control mode. Both linear-servo procedures and the hybrid simulation of the engine and controls were used in this stability analysis - in a manner similar to that reported in Section 4.6.1.

The first step in the design process was to size the TP5-WF, N1K-βF, and XM11-A18 control dynamics using linear stability studies at the takeoff, sea level static, standard day condition. Check out of these control dynamics using the hybrid simulation indicated stable operation at this take-off operating condition but not at 65% of takeoff thrust. Linear stability studies were repeated and the control dynamics were tuned to achieve adequate stability margin at both 65% and 100% takeoff thrust. These linear studies included an evaluation of the inner and outer loops for each control, with the other two control loops modulating. As an example, Figures 41 and 42 show the Nichols charts for the open-loop frequency response of the TP5-WF outer loop before and after tuning - at 65% and 100% of takeoff thrust, respectively - with the N1K-βF and XM11-A18 loops both modulating.

The tuned dynamics were then tested on the hybrid simulation of the engine and control system. The hybrid simulation verified that the system was stable at 65% and 100% of takeoff thrust; however, it was discovered that the system had inadequate stability margin at 80% of takeoff thrust. See simulation data in Figure 43 which is for a throttle chop from 100% to 80% thrust and illustrates inadequate stability margin as engine and control try to settle out at 80% thrust. The simulation data in Figure 44 show a

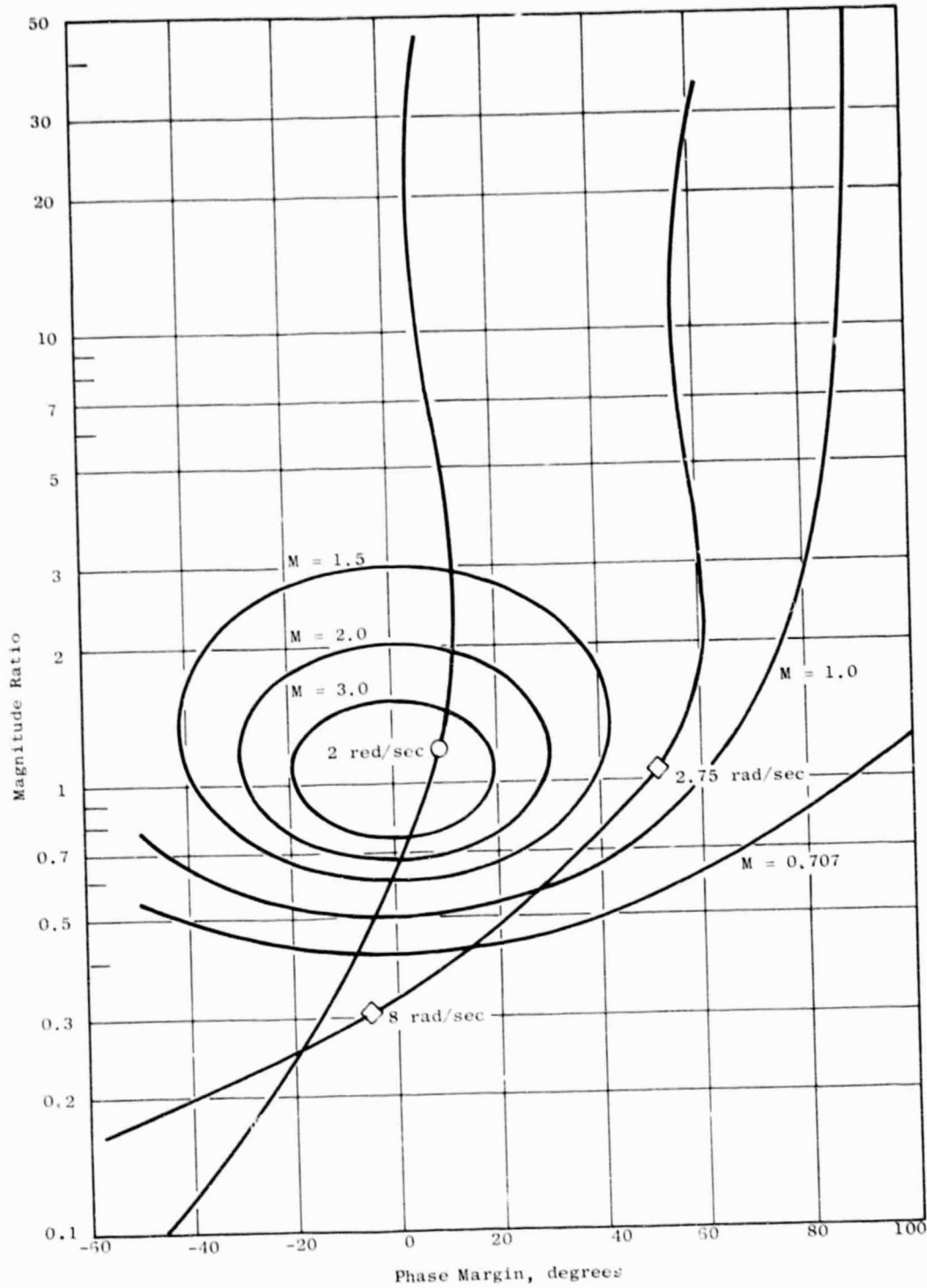


Figure 41. Phase-Magnitude Ratio Diagram TP5-WF Outer Loop.

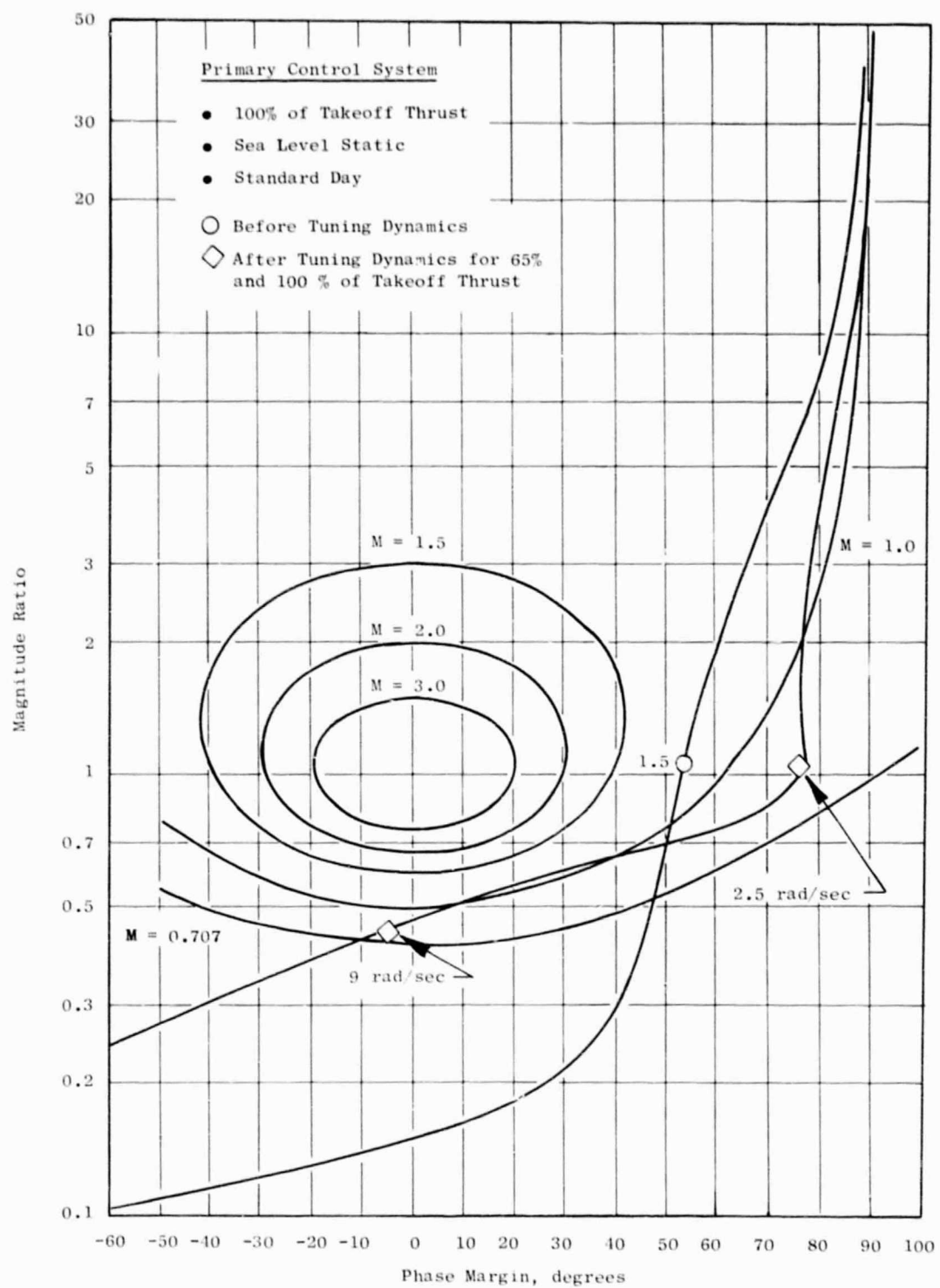


Figure 42. Phase-Magnitude Ratio Diagram TP5-WF Outer Loop.

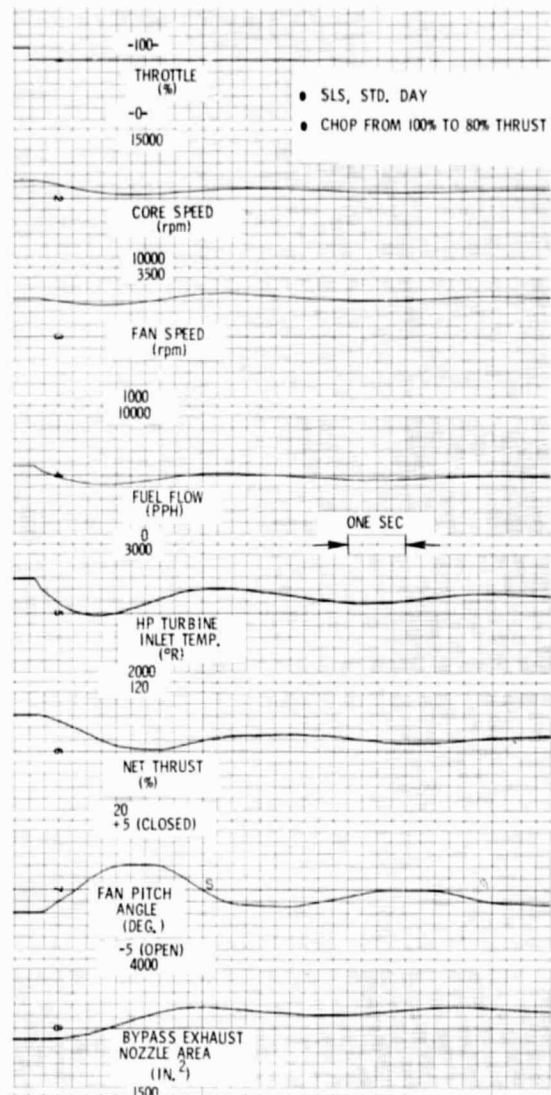
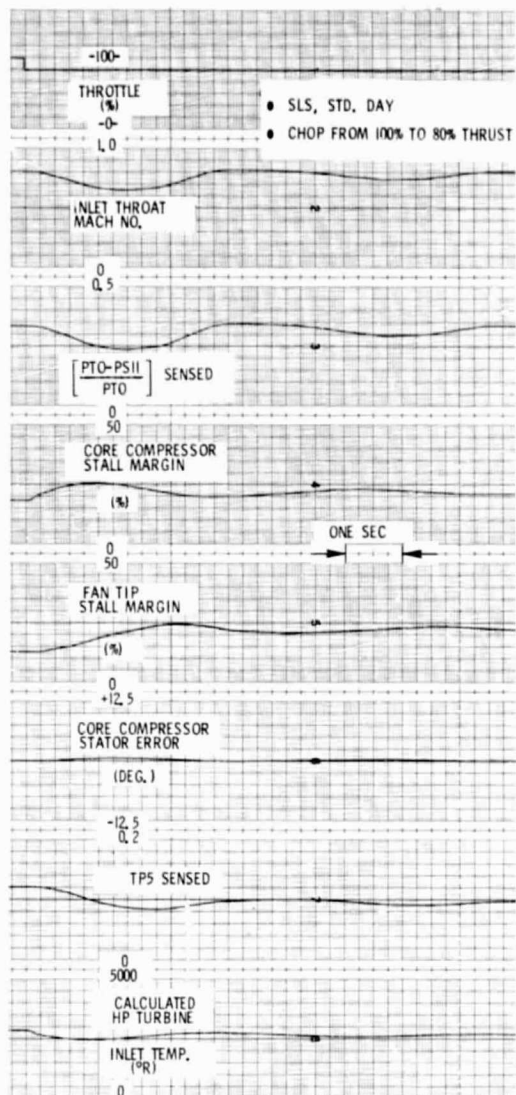


Figure 43. QCSEE UTW Engine Control System with TP5-WF Control Design.

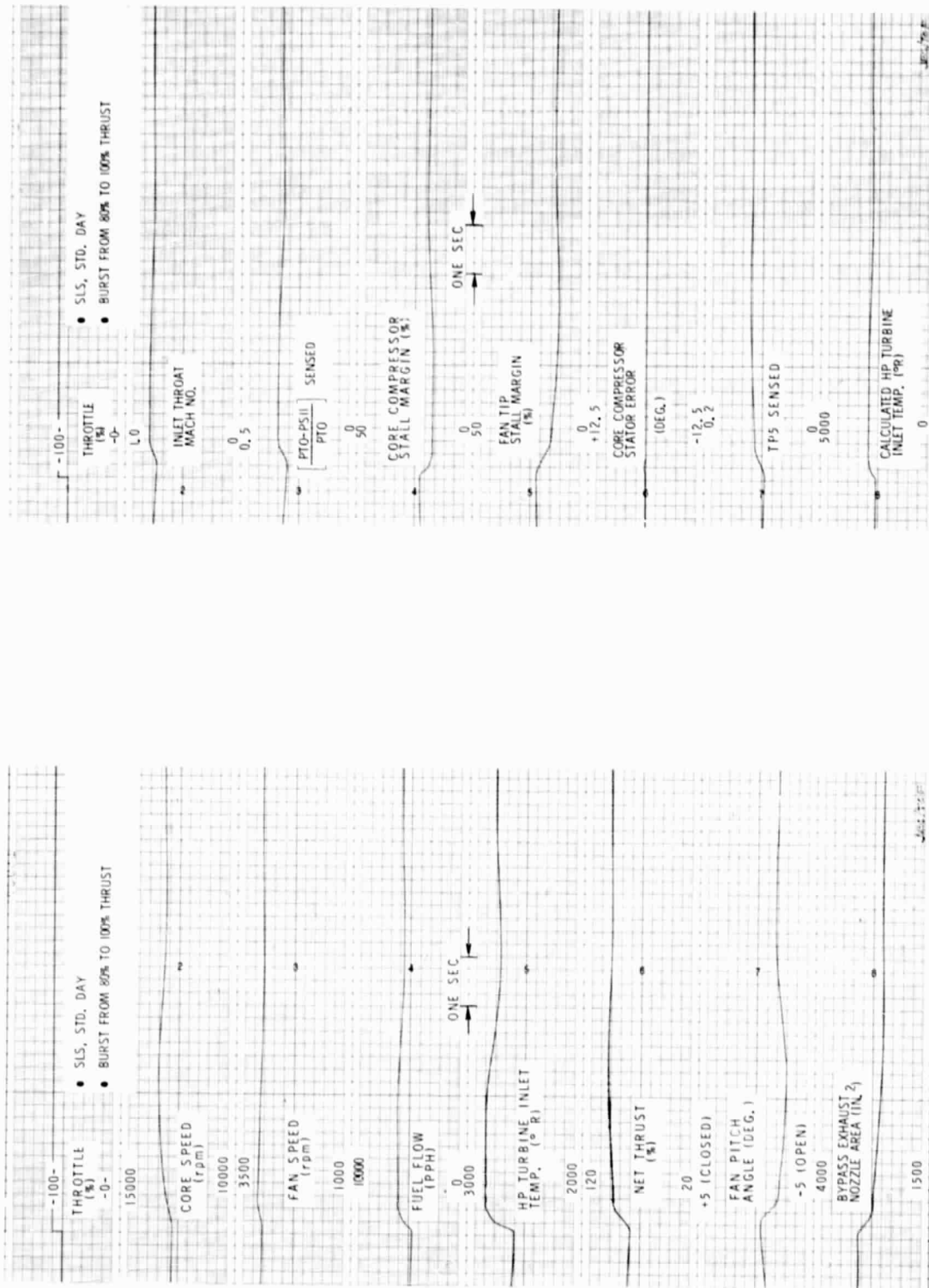


Figure 44. QCSEE UTW Engine Control System with TP5-WF Control Design.

ORIGINAL PAGE IS
OF POOR QUALITY

throttle burst from 80% to 100% thrust and illustrate the adequate performance at 100% thrust, which was predicted by the above linear stability study.

Both NASA and GE engineers reviewed the above analysis results on stabilizing the alternate control mode. It was noted that substantial effort had been directed to stabilizing this control mode - because initial control mode studies indicated potential benefits in using TP5 to provide accurate thrust control. However, analysis results predicted difficulties in achieving a consistently stable and fast responding control system in the part-power-setting range. The decision was that the alternate control mode could not be designed to work satisfactorily over a wide range of power settings on the UTW experimental engine. Furthermore, any future development of the alternate control mode should consider limiting the authority of the TP5-WF control to the 90% to 100% thrust range. For example, a possible configuration would be to use the primary control mode of PS3/PTO-WF, N1K-BF, and XM11-A18 below 90% thrust, and then transfer to the alternate control mode in the 90% to 100% thrust range.

4.7 FAILURE ANALYSIS

A QCSEE UTW control system failure analysis was undertaken when the system and component designs were essentially complete. Its purpose was to check on how well the system meets the design goal of having no failure modes which can cause serious engine damage or, in a flight design, cause flight safety problems. The failure analysis was supplemented by simulating certain key failures on the hybrid-computer model of the engine and control system. The basic failure analysis is included as Appendix B and the computer simulation of failures is included as Appendix C. Both are discussed below.

The analysis was conducted using the failure mode and effects technique in which a list is made of the various system element failures which might occur, and the effects of each failure on the system and engine are defined. The analysis verifies that most control system failures either have (1) little or no effect because of redundancy or backup limits or (2) they cause operational changes in a safe direction for an experimental engine or an engine on a multiengine aircraft. Failures which do not fall into one of these categories are discussed below.

Loss of A18 Feedback (Failure B2) - This results in a fully closed nozzle and, at some operating conditions, possible fan stall. Feedback redundancy would virtually eliminate this failure mode and would probably be applied to flight design. However, for the experimental engine system, the digital control hardware change necessary to add this redundancy was not felt to be justified because of the proven reliability of internally-mounted actuator LVDT's, the limited operating range in which this failure can cause stall, and the ability of the fan to tolerate stall without damage.

T3 Thermocouple Short Circuit (Failure C5) - This can cause turbine overtemperature but only when the engine is operating on the T41C limit. Under normal conditions this limit will not be encountered frequently and a method of protecting against this failure mode is not being pursued.

One other failure, the loss of the LPT speed signal (Failure B5), was identified in the analysis as one which has undesirable consequences and, as a result, a system change was made to provide protection. When operating in the automatic mode, loss of the LPT signal causes the fan pitch to close in an attempt to correct the false underspeed, while fuel flow remains essentially unchanged attempting to hold the thrust parameter level. The result is a fan speed increase, probably to the emergency overspeed limit. To prevent this,

logic has been added to the digital control program which reduces fuel flow by reducing the N2 limit to idle if the N1 signal (LPT) is lost. This function is only active when N2 is above 45% (approximately 5% below idle) so that it does not interfere during engine starts.

The hybrid-computer model simulation of failures was done after the analytical failure study and was directed primarily toward checking on operational safety for the experimental engine rather than for a flight design. The simulation results, which are shown in Appendix C, generally confirmed the analytical results indicating that safe operation will be maintained for most control system failures. Failures where simulation results indicate potential problems are discussed below.

Loss of A18 Feedback Signal (Failure B2) - The simulation verified a large fan stall margin loss as predicted in the analysis. The probability and impact of this failure are noted previously in the discussion of the analytical study.

PTO Sensor Open or Short Indicating Minimum PTO (Failure D2) - For Failure D2(a), the open or short in the PTO sensor is assumed to occur at a location which causes the digital calculation for PTO to be at the minimum value of 2 psia, causing the digital control to calculate in the following manner:

- PS3/PTO feedback goes to maximum scaled value of 20.47.
- The scheduled value of PS3/PTO increases.
- (PTO-PS11)/PTO feedback goes to maximum scaled value of 1.0.
- The scheduled value of fan speed increases.

The net effects on the control system (Figure 89)* are decreases in fuel flow (WF) and nozzle area (A18) and also closing of fan pitch. The engine decelerates and fan stall margin decreases to the 1% to 2% range as A18 closes to approximately 11,700 cm² (1800 in.²). These results indicate the possibility of a fan stall occurring before the fan has decelerated to a low speed condition. This potential problem is similar to the fan stall problem discussed in Failure B2 and the same comments apply.

Digital Control Fan Pitch Output Circuit to Maximum Close (Failure E6) - This failure pertains to a malfunction in the digital control which causes the electrical output to step to +80 mA. The simulation transient (Figure 97)* indicates that the fan pitch actuation system will slew closed to the mechanical stop in less than 0.2 seconds. The effect is a large and quick reduction in fan shaft power absorption, and the fan accelerates rapidly (reaches 3406 rpm, i.e., 105%, in less than 0.25 seconds). The

* Appendix C

fan speed limit control (limit reference set at 105%) reacts and causes fuel flow to decrease at about 0.35 seconds after the failure; however, by this time, the fan speed is greater than 110% (i.e., 3568 rpm) which will activate the Overspeed and Emergency Shutdown System. Since the simulation did not include a representation of this shutdown system, the transient is only valid in the first 0.35 seconds. The essential point of Figure 97 is to illustrate the potential for fan overspeed due to the above failure. Application of a fail-fixed servovalve in the control design would prevent the rapid fan pitch closure caused by this failure and thus prevent fan overspeed conditions which require activation of the Overspeed and Emergency Shutdown System.

Digital Control A18 Output Circuit to Maximum Open (Failure E8) - This failure pertains to a malfunction in the digital control which causes the electrical output to step to a maximum positive current. The simulation transient (Figure 98) shows that the nozzle area slews open to the mechanical stop ($A18 = 27,105 \text{ cm}^2$ [4170 in.²]) in 0.4 seconds. As the nozzle opens, PS3/PTO decreases; the PS3/PTO control causes fuel flow to increase until limited by the calculated turbine temperature control. Fan speed increases and the control opens the fan pitch in an attempt to return the fan to the takeoff speed of 3060 rpm (for this transient, the maximum open fan pitch limit was set at -8°). As a consequence, the inlet Mach number increases to 0.84 during the first 0.15 seconds of the transient. At 0.35 seconds after the step increase in the control output current, the increased fan speed and A18 result in improper operation of the simulation. (The high fan speed and low fan pressure ratio due to open nozzle cause operation in an ill-defined region of the fan component map; this causes the oscillation which is readily seen on the thrust recording channel.) Therefore, the subsequent inlet Mach number increase to 1.0 is certainly questionable. However, the essential point of Figure 98 is to illustrate that a digital control failure causing A18 to quickly open to the mechanical stop can result in high inlet Mach number and thus high inlet distortion. Application of a fail-fixed servovalve in the control design would remedy this potential problem.

Digital Control A18 Output Circuit to Maximum Closed (Failure E9) - This failure pertains to a malfunction in the digital control which causes the electrical output to step to a maximum negative current. The simulation transient (Figure 99) shows that the nozzle closed to approximately $11,700 \text{ cm}^2$ (1800 in.²); large nozzle aero loads (reflected as tension loads to the actuators) cause the closing rate of A18 to decrease as A18 approaches $11,700 \text{ cm}^2$ (1800 in.²). The fan and core engine rotors remain close to takeoff speed conditions during the transient. The significant effect is that fan stall margin decreases to the 1% to 2% range, which indicates the possibility of a fan stall at takeoff rotor speed conditions. For a flight control design, application of a fail-fixed servovalve will remedy this potential problem. No such action is planned for the experimental engine because of the ability of the fan to tolerate stall without damage.

One further indication from the failure simulation study pertains to the set-point of the power lever input to the hydromechanical fuel control. For testing the engine on a standard day, it is recommended that the power lever be set at a position which limits maximum core speed to 13,700 rpm. Otherwise, certain failures will cause the core to accelerate to corrected aero speeds greater than 105% where compressor characteristics begin to deteriorate rapidly.

4.8 PRESSURE SENSOR LOCATION STUDIES

Studies were conducted to determine the best method of sensing certain pressures which are important to the satisfactory operation of the UTW control system and some of which are not commonly sensed on transport aircraft engines.

One of the studies is related to choice of pressure sensing locations for the high-pressure portion of the engine pressure ratio thrust parameter. As stated in an earlier section, it was determined that total pressure rakes between the turbines were definitely out due to mechanical installation, cost, and reliability considerations. Static pressure was also considered between the turbines, but was rejected because of large total-to-static pressure variations to be expected in a high Mach flow channel with a very small LD (length-to-diameter) ratio and irregular wall surfaces. PS3 was chosen as the best alternative for an engine pressure ratio (EPR) signal. The pressure is physically a burner wall pressure taken in a region of very low flow velocity. Technically, the pressure is designated in the F101 cycle as PS3C. The pressure level is almost PT3 and there is extensive data (and experience of use in the F101 main and afterburner controls) for correlation of PS3C with PT3.

For the EPR reference pressure there were several possibilities considered: P12, the average fan inlet pressure; PS12, wall static pressure near the fan inlet; and PTO, a free-stream total obtainable either inside or outside of the inlet duct. P12 would be difficult to obtain and would offer no advantage over PTO. Extensive testing of scale model inlets have provided data showing an immersion of no more than 14.0 cm (5.5 in.) (full-scale inlet) is sufficient to get PTO at all conditions when the probe is as little

as 0.61 m (2.0 ft.) from the fan inlet. For reasons of noise generation (probe wake and fan blade interaction), ice shedding, and damage possibilities, the choice of an inside PTO measurement was rejected in favor of an outside PTO measurement. The outside location was chosen on the bottom at the nacelle maximum O.D.. This location was based on consultation with McDonnell Douglas. The final alternative of PS12 was rejected because, although it would be suitable for the EPR use, it would be marginal for use in the throat Mach control. With PS11-PS12 sensing, inlet duct losses at maximum flow and with high angles of attack would have an undesirable effect on control of throat Mach number. The throat Mach number would rise with increased losses (more than 1% for each 1% increase in pressure loss between sensing points). This is in the wrong direction with respect to our preference and is a regenerative process with effects greater than preliminary estimates. In conclusion, the choice for the engine inlet pressure is a free-stream total pressure (PTO) measured outside the nacelle at the location described above.

Data from NASA-Lewis acoustic suppression inlet testing with a 12-inch model inlet were used to establish the location for sensing the inlet static pressure (PS11) needed for control of inlet throat Mach number. Typical data from this testing are shown in Figures 45 and 46. These and similar data led to a decision to sense PS11 using two manifolded static taps in the inlet inner wall, axially located at $XL = 0.4$ (X = distance from inlet front face to sensing tap, L = distance from inlet front face to fan blade leading edge), and each on the inlet horizontal centerline 180° apart circumferentially. The $XL = 0.4$ location was chosen because it is affected little by aircraft angle-of-attack and crosswinds and it provides satisfactory accuracy.

4.9 STARTING STUDIES

An analysis of the QCSEE high-pressure rotor starting performance was conducted to support the selection of a starter for development engine testing. Since the QCSEE core is basically an F101 PFRT (preliminary flight rating test design) core, there is a great deal of factory- and field-starting experience on which to base this analysis.

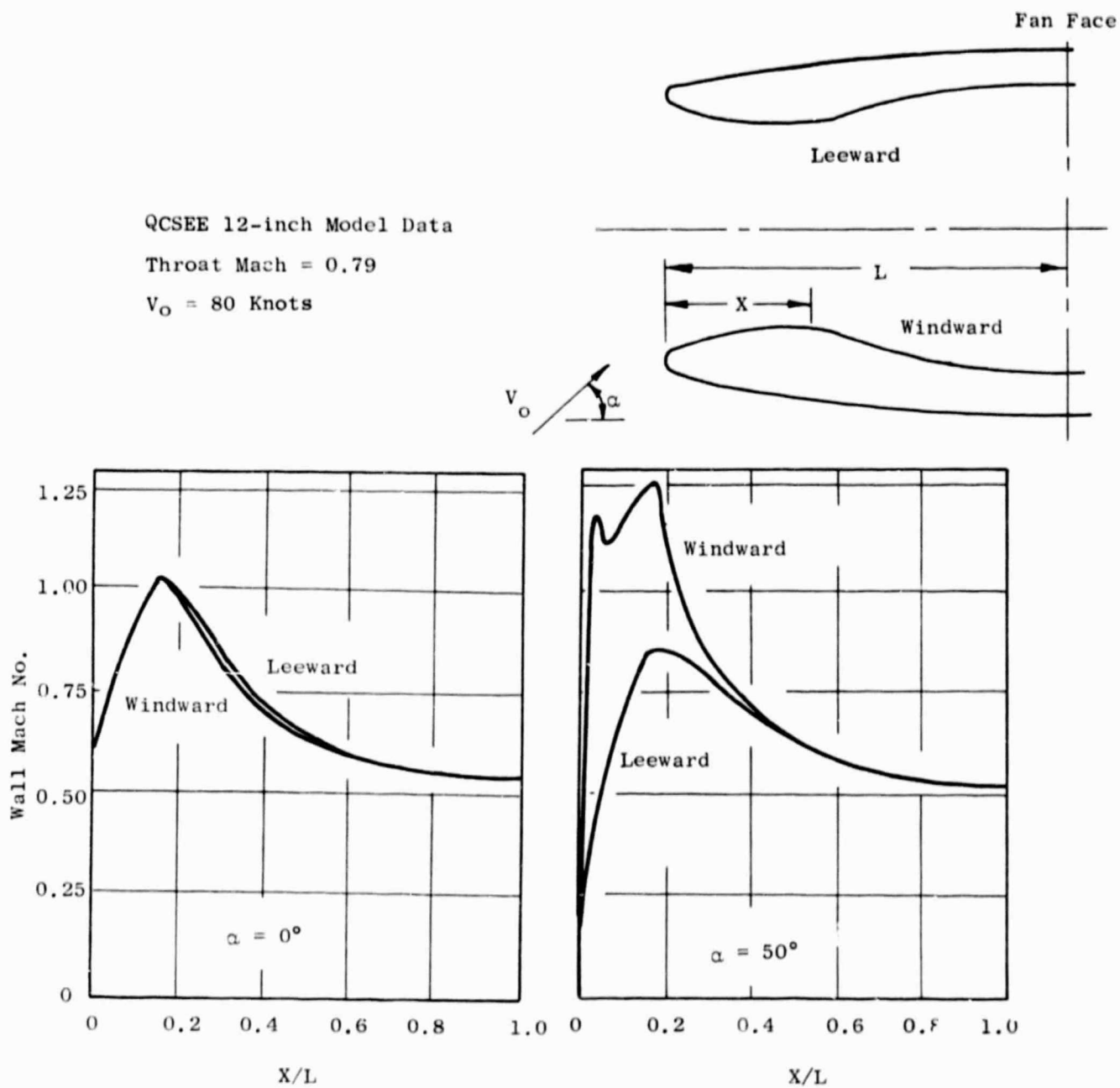


Figure 45. Inlet Pressure Sensing Data.

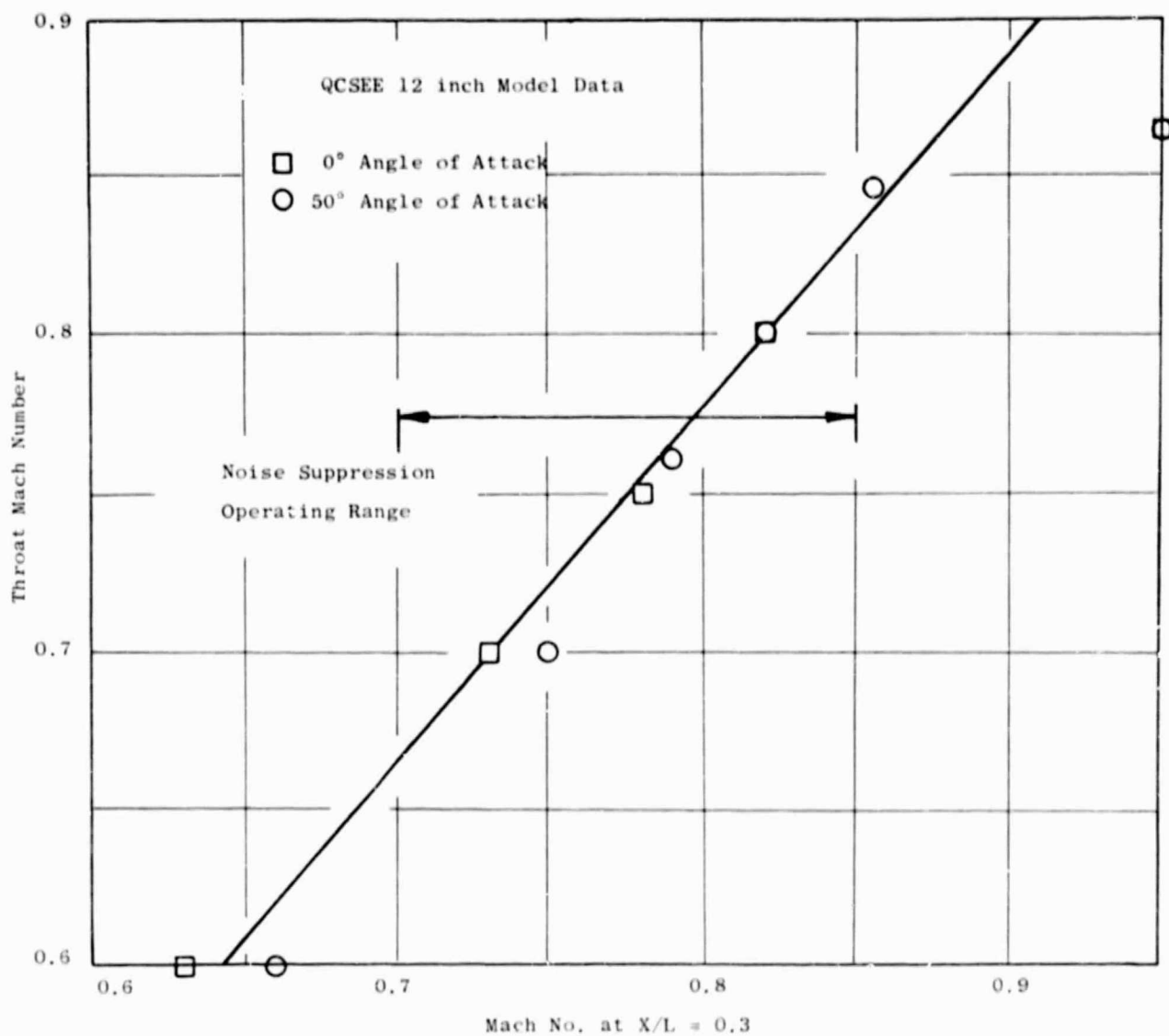


Figure 46. Inlet Mach Number Correlation Data.

During the successful completion of the F101 PFRT ground-starting torque test, a level of engine unfired and fired torque was demonstrated. It can be assumed that the QCSEE core engine will exhibit approximately the same level of unfired torque and be capable of the same level of fired torque as was demonstrated by the F101 PFRT engine. Consequently, the engine torques used for the QCSEE starter selection study reflect the F101 experience and are shown in Figure 47.

In addition to these torque requirements, other criteria considered in choice of a starter were cost, timing, installation envelope, 11,100 rpm idle requirement, a 4000-rpm maximum motoring speed goal, and the fact that there was no firm start-time requirement for this development engine. The base case for this study was the sea level static, standard day condition.

A start-time calculation program was constructed that combined the engine torques with typical air turbine starter characteristics. After examining a number of possible starters, a satisfactory characteristic was defined. This proposed starter was submitted to various starter vendors and their replies evaluated. This led to the selection of AiResearch Division's ATSl00-277A starter (Figure 48) for the QCSEE Program.

Estimates were made of the engine torques over a range of ambient temperatures and the corresponding start times calculated. These times are shown in Figure 49.

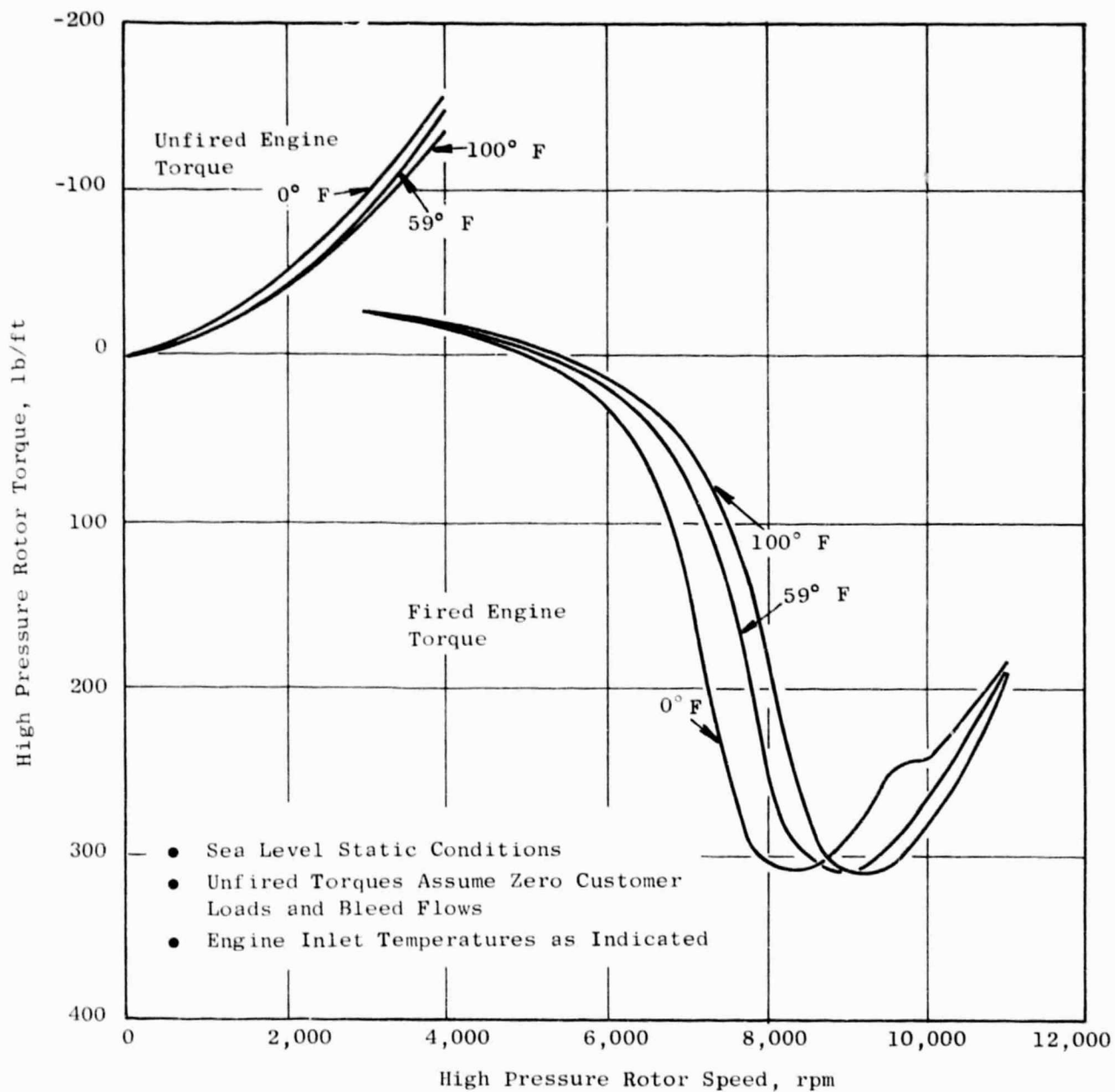


Figure 47. Estimated QCSEE Engine Torques.

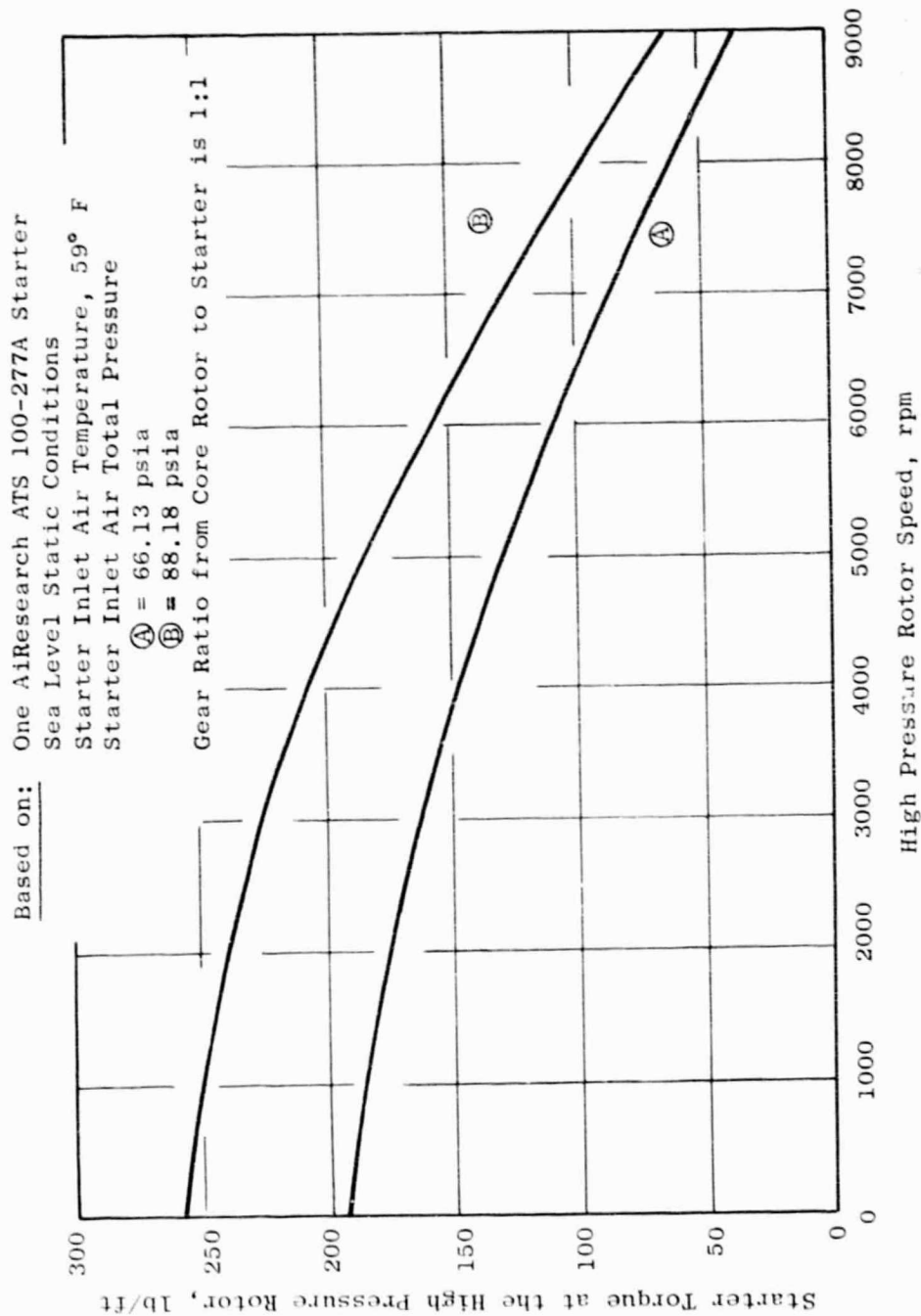


Figure 48. Expected Starter Torque for QCSEE Development Engine.

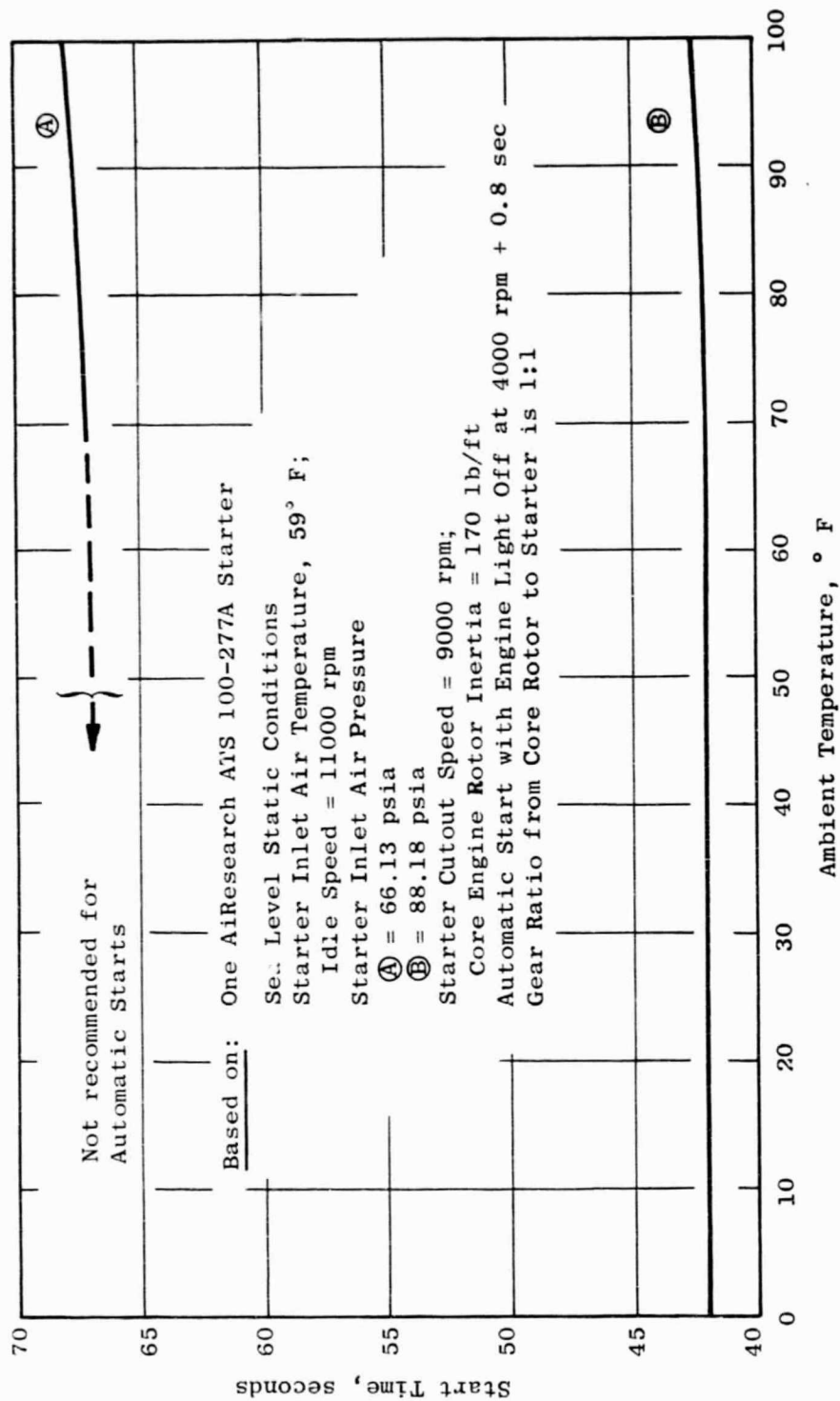


Figure 49. QCSEE Start Time Study of March 1975.

5.0 DIGITAL CONTROL SUBSYSTEM

5.1 GENERAL DESCRIPTION

The digital control subsystem, shown in Figure 50, is comprised of an engine-mounted digital control and command and monitor peripheral equipment located in the control room.

The digital control performs the computational requirements for the overall engine control system based on the demands received from the command and monitor equipment and other parameters received from engine-mounted sensors. In addition to generating control signals to manipulate fuel flow, fan pitch angle, and fan nozzle area, the digital control transmits engine and control data to the command and monitor equipment in the control room.

The command and monitor equipment approximates an aircraft interface in that it provides the command inputs to operate the engine, and the transmission process is the same from a hardware viewpoint as a flight-type system. That is, all command data are transmitted to the digital control in a time-shared digital format over a data link that could be adapted for a flight-type system. However, the command and monitor equipment have a number of added features to provide flexibility in testing an experimental engine. These include several modes of operations, provisions for manually controlling all manipulated variables, selected adjustment inputs to modify steady-state and dynamic characteristics of the control strategy, a fault indication and corrective action program, and a comprehensive control and engine parameter display system.

Fault indication and corrective action are part of the digital control strategy and are described in Section 3.3.3 of this report. Also, the control includes provisions for readout of 48 control and engine variables from the command and monitor equipment in the control room. These variables are listed in Table IX (also see Table X).

The Table IX data may be read out from a number of stations in the control room. Any one of the forty-eight parameters may be selected for display on a binary-coded decimal readout on the engineering control panel and all

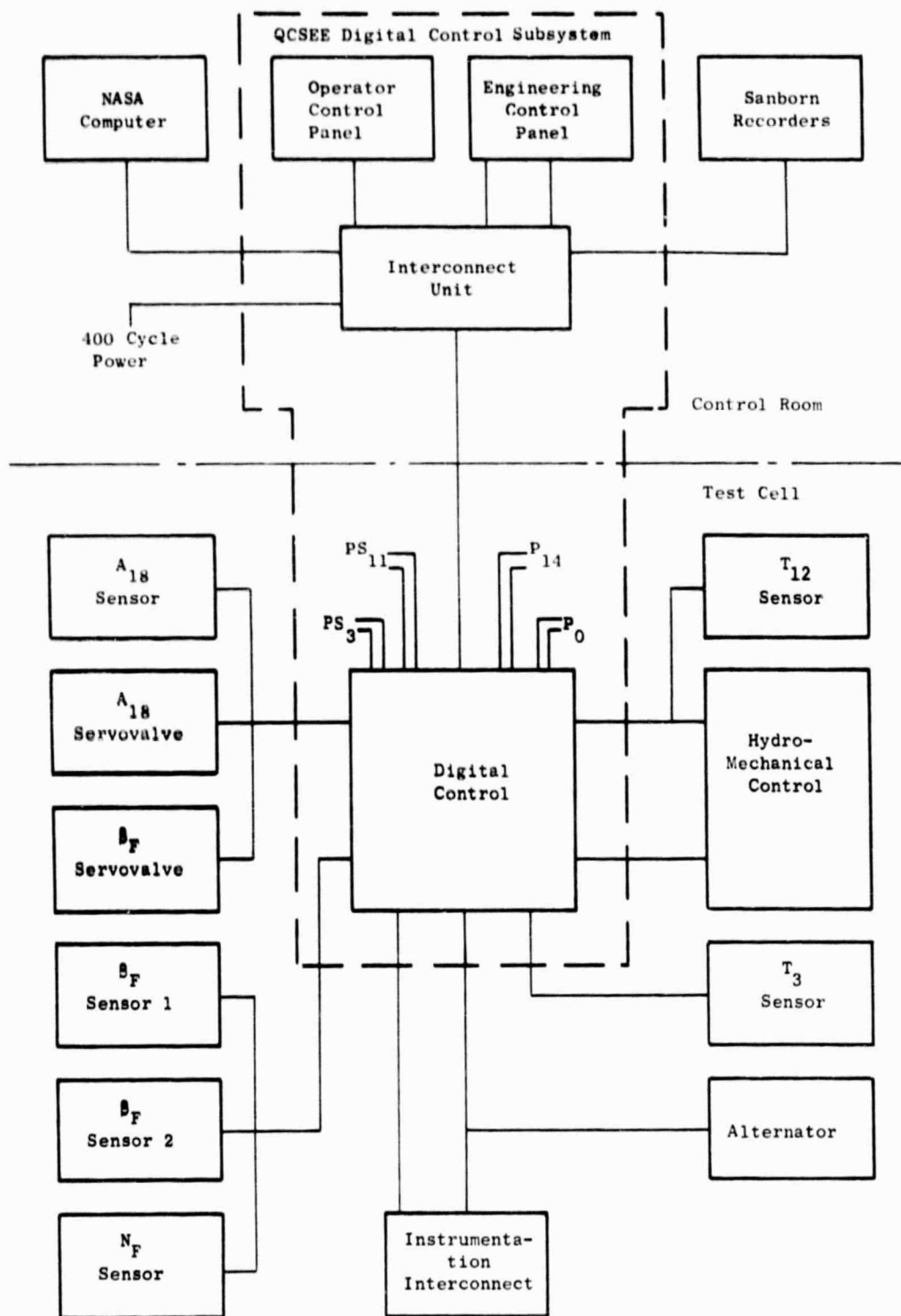


Figure 50. A Block Diagram of Digital Control System.

Table IX. Control and Engine Monitor Data.

Thumb Wheel Switch Position	Parameter	Full-Scale Range	Thumb Wheel Switch Position	Parameter	Full-Scale Range
00	A18 TMC	±100 mA	24	MVP	0 - 813 in.
01	BF TMC	±100 mA	25	BF1	-.414 to +.414 v/v exc.
02	WF TMC	±100 mA	26	BF2	-.414 to +.414 v/v exc.
03	WF	0 - 10K pph	27	BF Demand (auto mode)	0 to 3893 rpm NI
04	A18	-.247 to 4.753 in.	28	A18 Dem. (auto mode)	± 6 in./sec
05	BF	-.414 to +.414 v/v exc.	29	T3	-65 to 1090° F
06	FMP	0 to 800 psia	30	VSV Reset TMC	Normal/Reset
07	T41C	-0 to 3460 R	31	Mode Word	0 to 5000 psia
08	(PTO-PS11)/PTO	-0 to 1.0	32	Hyd. Pump Disc. Press	0 to 300° F
09	PS3/PTO	-0 to 20.47	33	WF Temp.	-30.8 to +30.8 v/v sec.
10	Power Demand	-0 to 100	34	BF Rate	0 to 2000° F
11	PLA	-0 to 130	35	EGT	0 to 250° F
12	N1	0 to 3893 rpm	36	Engine Oil Inlet Temp.	0 to 350° F
13	N2	-0 to 15,492 rpm	37	Scav. Oil Temp.	0 to 150 psig
14	VSV	-5 to 60 Degrees	38	Eng. Oil Inlet Press.	0 to 150 psig
15	WF Control Mode		39	Scav. Oil Press.	0 to 200° F
16	BF Control Mode		40	T25	0 to 25 psia
17	A18 Control Mode		41	P5	0 to 300° F
18	F.I. (See Table X)		42	Gearbox Innerrace	0 to 50 mils
19	T12	-40° to 160° F	43	Bearing Temperature	0 to 50 mils
20	PTO	0 to 19 psia	44	Horizontal Vib.	0 to 50 mils
21	P14-PTO	0 to 12 psid	45-47	Vertical Vib.	
22	PTO-PS11	0 to 12 psid		Spares	
23	PS3	0 to 300 psia			

Table X. Fault Indication (F.I.)*

No.	Fault	Data Word No. 18 Digital Output Value	Fault Indication
1	No Fault	0000	Off
2	Vib Hor. & Vert. > 40 mils	2048	On
3	Loss of Command Data Link	1024	On
4	Computer Fault Test	0512	On
5	N1 < 15% and N2 > 45%	0256	On
6	ESTMC > -60 mA	0128	On
7	Lub Supply Temp. > 180° F	0064	On
8	Lube Supply Pressure < 30 psia and N2 > 80%	0032	On
9	G/B Bearing Temp. > 264° F	0016	On
10	Hyd. Pump Pressure < 2500 psia and N2 > 45%	0008	On
11	-2.5° < $\beta F1 - \beta F2$ > +2.5°	0004	On
12	Computer Timing Oscillator Failure	0001	On

Sanborn Recorder Output (No. 18) Voltage = $\frac{\text{Digital Output}}{4095} \times 10 \text{ Volts}$

For multiple fault indication, the sum of the digital output values of the indicated failures shall be displayed.

* Parameter 18 on Table IX.

parameters are transmitted serially to the remote (NASA) computer in binary form. Parameters 00 through 14 are available for real time analog recording through instrumentation connections on the interconnect panel and any of the forty-eight channels may be selected for analog recording through a sixteenth instrumentation connection. In addition, parameters 04, 05, 07, 09, 10, 12, and 13, along with inlet Mach number calculated from 08 and turbine temperature calculated from 35, are displayed in engineering units on the operator control panel to aid in engine operation. Furthermore, the torque motor currents, items 00, 01, and 02, are displayed on engineering panel meters.

5.2 DIGITAL CONTROL DESCRIPTION

The digital control is an engine-mounted assembly that includes a special-purpose digital computer. The control accepts operational input demands and engine variable information in the form of a.c. and d.c. analog signals and digital signals and uses this information to generate engine control signals and engine condition monitoring data. Control inputs and outputs are given in Table XI and a block diagram is shown on Figure 51.

The digital computer is composed of three major sections: the program memory, the central processor, and the input-output unit. Basic operation is described below followed by a description of the key elements shown in Figure 51.

A group of instructions comprising one control cycle are stored in the program memory. Each instruction is sequentially transmitted to the central processor for execution. The central processor generates timing to operate the computer, executes the instruction, and transmits a ready-for-next-instruction command back to the program memory at the completion of each instruction except for the jump-and-branch instructions, in which case the central processor also provides a new address for the program counter. When all of the instructions are executed, the program is repeated. The flow of information into and out of the computer is handled by the input-output section under commands from the central processor. The input-output unit receives command digital data from the control room and analog input control parameter signals. Under the command of the central processor, the input-output unit digitizes the signals as they are required in the computational sequence and transmits them to the central processor as binary encoded numbers. The outputs to drive the servovalves are received in the input-output unit as binary encoded numbers from the central processor. Again, under the command of the central processor, the numbers are converted from digital to analog signals and are loaded and stored in sample-and-hold networks that are uniquely designated for each output. The sample-and-hold network outputs are processed using standard analog techniques to provide the output interface with the other components in the control system. The information contained in the sample-and-hold networks is updated once each cycle.

Table XI. Digital Control Inputs and Outputs.

I. INPUTS	II. OUTPUTS
<p>A. <u>Engine and Control Inputs</u></p> <ol style="list-style-type: none"> 1. Alternator - Power and Core Speed Sensing 2. Primary LP Turbine Speed Signal 3. Secondary LP Turbine Speed Signal 4. T12 Sensor 5. Compressor Discharge Gas Temperature Sensor 6. Fuel Metering Valve Position Transducer 7. Throttle Position Transducer 8. A18 Actuator Position Transducer 9. Fan Pitch (8F) Transducer 10. Fan Pitch (8F) Transducer 11. PS11 Sensor 12. PT0 Pressure 13. P14 Pressure 14. PS3 Pressure <p>B. <u>Instrumentation Inputs (0-10 V)</u></p> <ol style="list-style-type: none"> 1. Hydraulic Pump Outlet Pressure - psig 2. Fuel Temperature - °F 3. Fuel Manifold Pressure - psia 4. Exhaust Gas Temperature - °F 5. Fuel Flow - PPH 6. Engine Lube Oil Out Pressure - psig 7. Engine Lube Scavenge Pressure - psig 8. Engine Lube Oil Inlet Temperature - °F 9. Engine Scavenge Oil Discharge Temperature - °F 10. T25 - °F 11. Pressure Station 5 - psia 12. Gearbox Interface Bearing Temperature - °F 13. Engine Horizontal Vibration 14. Engine Vertical Vibration 15. Core Stator Position VSV, Degrees 16-20. Spares <p>C. <u>Operator Inputs</u></p> <p>Multiplex Digital Signals Ability to Receive Any Number</p>	<p>A. <u>Torque Motors</u></p> <ol style="list-style-type: none"> 1. WFTMC - Fuel Control 2. A18TMC - Fan Nozzle Area 3. 8FTMC - Fan Pitch Control 4. 8CTMC - Compressor Stator Reset 5. ESTMC - Emergency Shutdown <p>B. <u>LVDT Drives</u></p> <ol style="list-style-type: none"> 1. MVP 2. A18 3. 8F1 4. 8F2 5. PLA <p>C. <u>Other Outputs</u></p> <ol style="list-style-type: none"> 1. T12 Sensor Excitation 2. LPT Speed Indication 3. Multiplex Digital Data Link <p>Transmit any number of data words</p>

FOLDOUT FRAME

ORIGINAL PAGE IS
OF POOR QUALITY

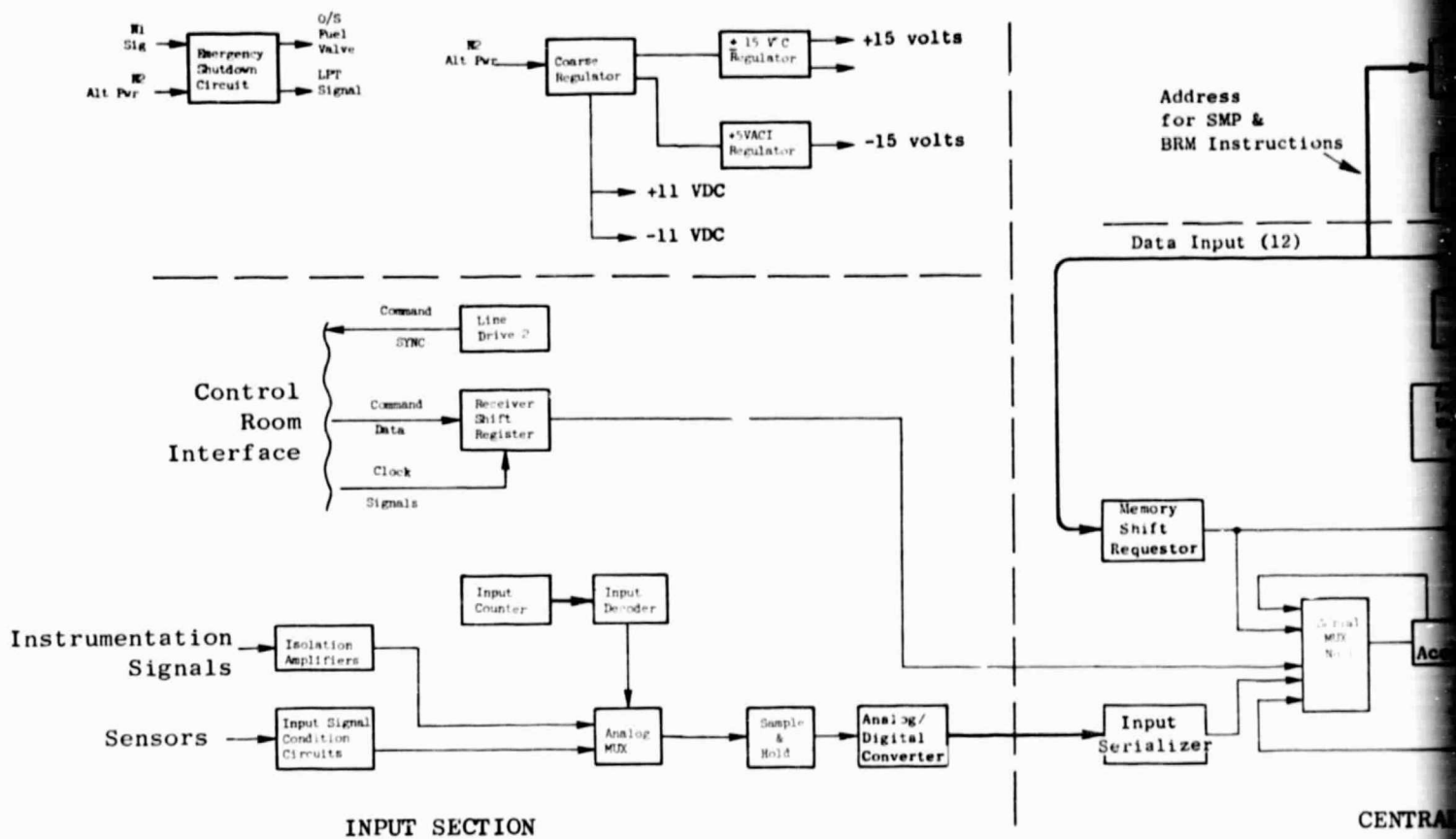


Figure 51. Digital Control

ORIGINAL PAGE IS
OF POOR QUALITY

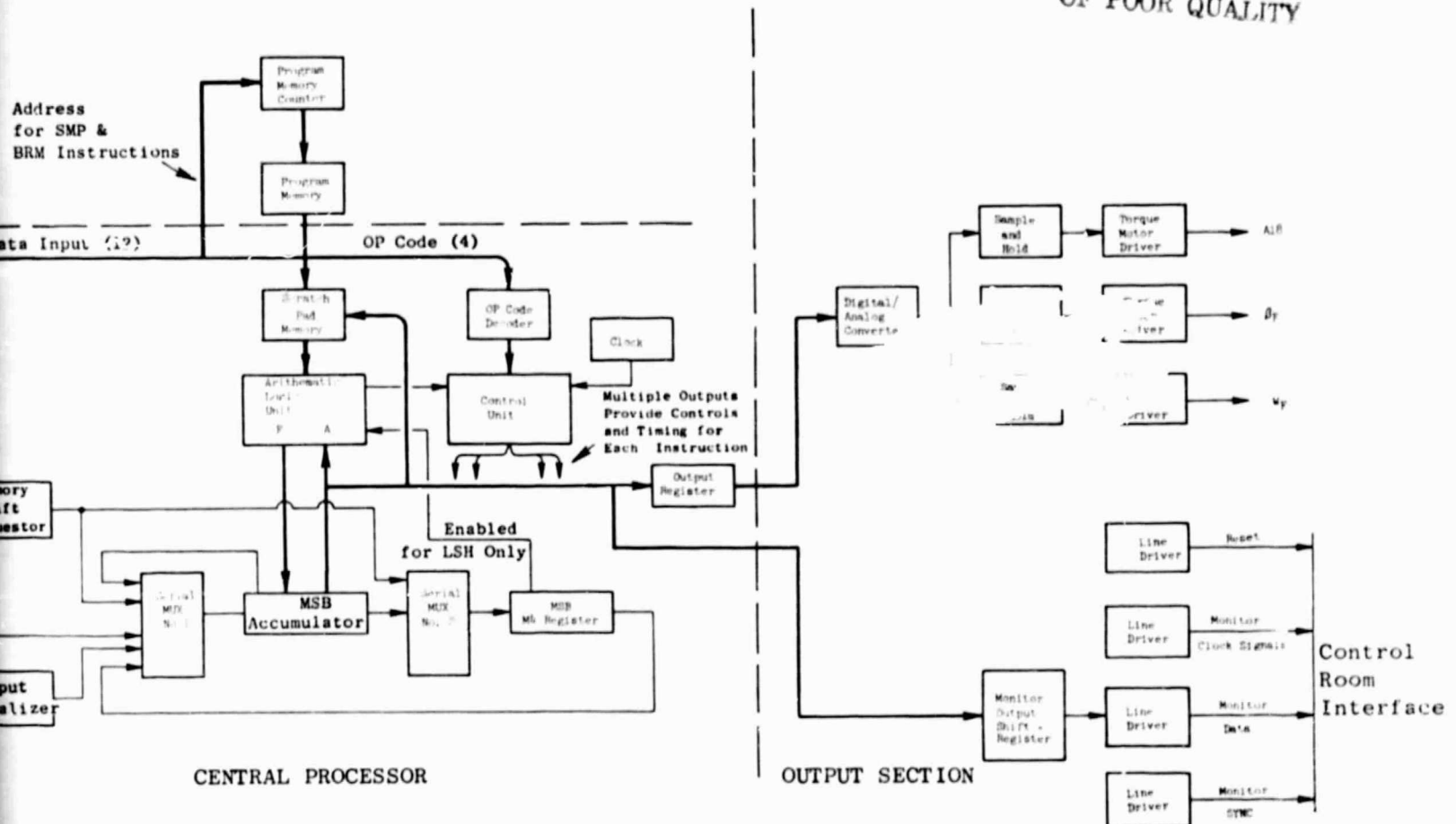


Figure 51. Digital Control Block Diagram.

The basic sections of the digital control are described separately below.

5.2.1 Program Memory

The memory has been organized to provide 16-bit words to the central processor. Each word contains four bits of operational code which, when decoded in the central processor, direct the central processor to perform one of the basic instructions. The specific instructions indicated by the operational codes are shown in Appendix D. The remaining twelve bits may be used to transmit binary numbers from the memory, address the scratch pad memory, or provide further instructional data depending on which instruction is contained in the operational code. The memory is composed of sixteen 512 x 8 chips to provide a 4096 word capacity.

The program counter receives an advance to the "next memory address" signal from the central processor when each instruction is complete and, for the jump-and-branch instructions. Each combination of high and low states of the counter outputs are decoded as a unique location in the program memory. The memory then outputs the word contained at that location. The OUT 15 instruction in the program memory is decoded in the central processor to reset all of the counters in the computer to zero and start the control cycle over.

5.2.2 Central Processor

The major functional blocks of the central processor are the Arithmetic and Logic Unit (ALU), the scratch pad memory, the control unit, the accumulator and MQ register. Figure 52 is a schematic showing the ALU, the accumulator register and the MQ register.

The function of the central processor is to carry out the instructions received from the program memory. The operational code portion of each word received from the program memory is decoded (op-code decoder) into 1 of the various instructions that the central processor has been designed to perform. The major elements of the central processor are described below.

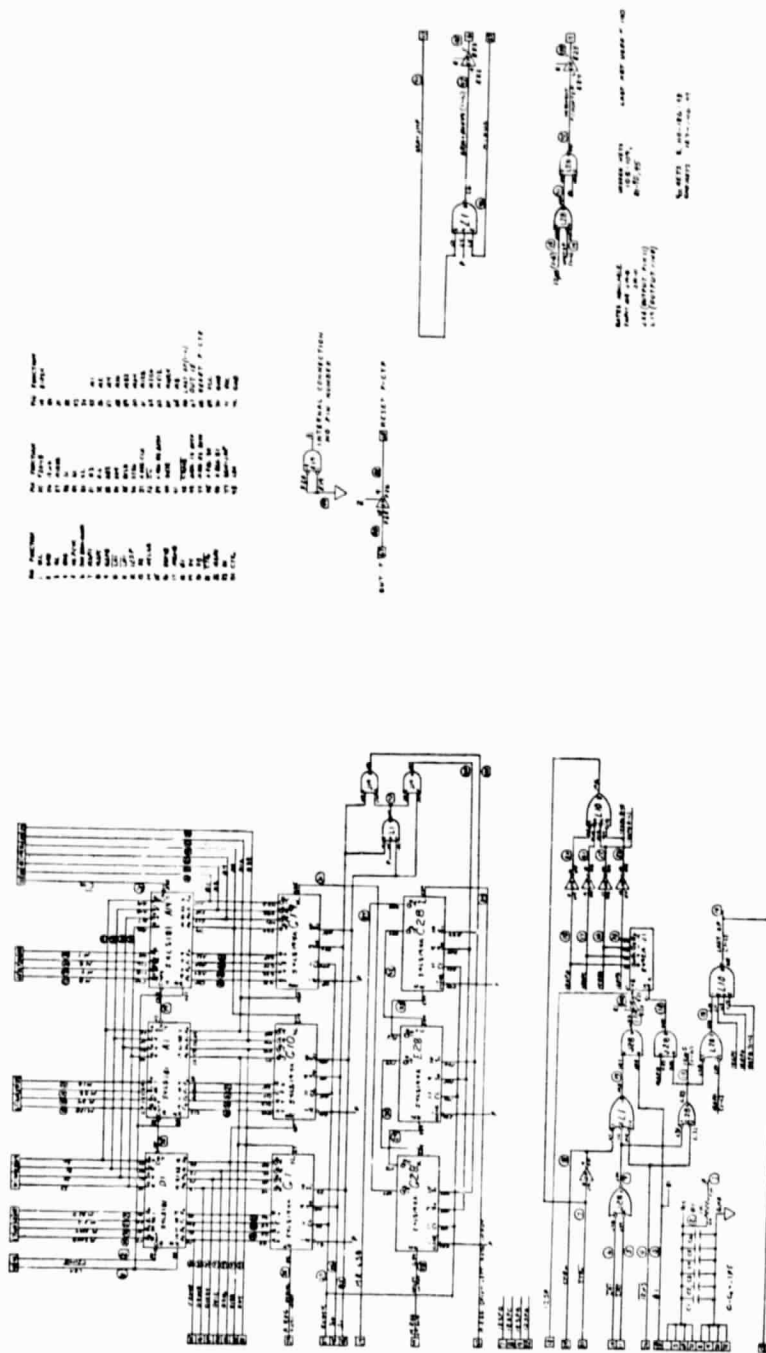


Figure 52. QCSEE Digital Control Arithmetic Elements.

1. Control Unit - The control unit contains the circuitry that generates control signals in the proper sequence to execute the instructions received from the op-code decoder. Control unit outputs are disbursed throughout the digital control to perform the required operations.
2. Arithmetic Logic Unit - The ALU is the heart of the digital control. All arithmetic operations employ the ALU in their execution. The ALU is comprised of D1, A1, and A14 as shown on Figure 52. The ALU operates on data received from the scratch pad memory at the "B" terminals and from the accumulator at the "A" terminals in accordance with control unit inputs received at the "S" terminals. Tables of the arithmetic and logic operation performed by the ALU are shown in Table XII. The results of the operations performed are presented at the "F" terminals of the ALU.
3. Scratch Pad Memory - The scratch pad memory is a 256-word random access memory (RAM) with read/write capability. The scratch pad memory is addressed from the program memory at the "A" terminals (Reference Figure 51). When the read mode is enabled from the control unit, data are output at terminal "O" to the ALU from the location addressed and when the read mode is enabled, data at terminal "O" are read into the location addressed.
4. Accumulator Register - The accumulator register, comprised of devices G1, G10, and G19 on Figure 52, is a very versatile register that is programmed by the control unit to accept inputs and provide outputs in either parallel or serial form. It accepts serial inputs from the sensors, instrumentation command inputs, MQ register, or program memory, and provides parallel outputs to the ALU, the scratch pad memory, and the output register as well as serial output to the MQ register. Data can be both left and right shifted in serial transmission of data through the accumulator. Point of input origin, destination of data outputs, as well as mode of operation, are established signals provided by the control unit.
5. MQ Register - The MQ register, comprised of devices G28, E28, and C28 as shown in Figure 52, is used as a shift register in conjunction with the accumulator. It is employed as a repository for data during the multiply, divide, and rotate instructions.

The remainder of the circuitry shown in Figure 52, and not discussed above, is a portion of the control unit circuitry.

5.2.3 Instructions

The digital control is programmed using the set of instructions defined below:

Table XII. Arithmetic Logic Unit (ALU) Operations.

Control CN ₊₄				Output Function With Mode Control CN ₊₄ & CN Low		Control CN ₊₄				Output Function With Mode Control CN ₊₄ High: CN Irrelevant	
S ₀	S ₁	S ₂	S ₃	Low Levels Active	High Levels Active	S ₀	S ₁	S ₂	S ₃	Negative Logic	Positive Logic
L	L	L	L	F = A minus 1	F = A	L	L	L	L	F = \bar{A}	F = \bar{A}
L	L	L	L	F = AB minus 1	F = A+B	L	L	L	L	F = $\overline{A+B}$	F = $\overline{A+B}$
L	L	H	L	F = \overline{AB} minus 1	F = A+B	L	L	H	L	F = $\overline{A+B}$	F = $\overline{A+B}$
L	L	H	H	F = minus 1 (2's complement)	F = minus 1 (2's complement)	L	L	H	H	F = Logical 1	F = Logical 0
L	H	L	L	F = A plus (A+B)	F = A plus \overline{AB}	L	H	L	L	F = $\overline{A+B}$	F = \overline{AB}
L	H	L	H	F = \overline{AB} plus (A+B)	F = (A+B) plus \overline{AB}	L	H	L	H	F = \bar{B}	F = \bar{B}
L	H	H	L	F = A minus B minus 1	F = A minus B minus 1	L	H	H	L	F = $\overline{A+B}$	F = A + B
L	H	H	H	F = A+B	F = \overline{AB} minus 1	L	H	H	H	F = A+B	F = \overline{AB}
H	L	L	L	F = A plus (A+B)	F = A plus AB	H	L	L	L	F = \overline{AB}	F = $\overline{A+B}$
H	L	L	H	F = A plus B	F = A plus B	H	L	L	H	F = A + B	F = A + B
H	L	H	L	F = \overline{AB} plus (A+B)	F = (A+B) plus AB	H	L	H	L	F = B	F = B
H	L	H	H	F = A+B	F = AB minus 1	H	L	H	H	F = A+B	F = B
H	H	L	L	F = A plus A*	F = A plus A*	H	H	L	L	F = Logical 0	F = Logical 1
H	H	L	H	F = AB plus A	F = (A+B) plus A	H	H	L	H	F = \overline{AB}	F = $\overline{A+B}$
H	H	H	L	F = \overline{AB} plus A	F = (A+B) plus A	H	H	H	L	F = AB	F = A+B
H	H	H	H	F = A	F = A minus 1	H	H	H	H	F = A	F = A

* Each bit is shifted to the next more significant position

For Positive Logic: Logical 1 = High Voltage
Logical 0 = Low Voltage

For Negative Logic: Logical 1 = Low Voltage
Logical 0 = High Voltage

Out 0 - The purpose of this instruction is to consume time while other functions are being performed in the control. No operation is performed as a result of the Out-0 command. When the Out-0 instruction word is received from the program memory the control unit generates the following:

- A signal to the program memory instruction counter that advances the count, sequencing the memory to the next instruction.

Out 1 - The purpose of the Out-1 instruction is to transfer calculated output data from the accumulator to the DA output register in the input-output unit to start the output process. When Out-1 instruction word is received from the program memory, the control unit generates two signals.

- A signal to the DA output register that enables a parallel transfer of data from the accumulator register.
- A signal to the program memory instruction counter that advances the count, sequencing the memory to the next instruction. The value in the output register is continuously converted to analog value by the digital-to-analog converter.

Outs 2 Through 6 - The purpose of these instructions is to load the output of the digital-to-analog converter into unique sample-and-hold networks designated for the data contained in the output register.

When one of these instruction is received, the control unit generates a signal to advance the output address counter and advance the program memory counter. Each output address count signal shall be decoded to select a specifically designated sample-and-hold network.

Out 13 - The purpose of this instruction is to transmit data to the off-engine equipment (simulated aircraft interface). When the Out-13 instruction is received the control unit generates the following signals:

- 12 clock pulses to the monitor output shift register to transmit the data serially to the off-engine equipment.
- 12 clock signals to the off-engine equipment to enable the off-engine equipment to receive the data.
- A monitor sync-pulse to the off-engine equipment at the conclusion of the message to update the off-engine message identification counter.

- A reset pulse signal to the off-engine equipment if the message transmitted was the last message of that control iteration to reset the off-engine message identification counter to zero.
- A signal to the program memory instruction counter that advances the program count.

Out 14 - When an Out-14 instruction is received, the control unit generates a command pulse signal to start an AD conversion and a command to advance the program memory instruction counter. The AD converter is a successive approximation type and requires 24 μ S to perform an AD conversion. Therefore, an Out-14 instruction will be inserted into the program far enough in advance of when the data are required to insure that 24 μ S have lapsed before it is required in a given computation. At the completion of the AD conversion, the converter generates a signal to advance the input counter. The input counter outputs are decoded to select 1 of 32 outputs. The counter outputs are coded by the order in which they will be used in the control cycle.

Out 15 - This instruction is used at the end of each computer cycle to recycle the computer. When an Out-15 command is received from the instruction decoder, the control unit generates a signal to reset the input, output, and instruction counters to zero and the computer cycle begins again. This positive reset at the end of each cycle insures that an occasional false trigger in the computer will not degrade the overall control system's performance.

INP \emptyset - The purpose of this instruction is to bring control inputs into the computer. This is accomplished in the following manner. After an AD conversion has been completed, the control parameter to be input to the computer is stored as a 12-bit binary number in an output register in the AD converter. The binary word is transmitted serially from the AD converter to the accumulator register through the use of a parallel serial converter via serial MUX No. 1. When an INP \emptyset instruction is received, the control unit generates the following signals to control the operation:

- A mode control signal (low level) to enable the accumulator to operate in the shift-right serial input mode.

- A strobe signal of the input serializer to enable the output.
- Four signals encoded to address the input serializer causing the serializer output to be sequenced through its inputs one bit at a time to transfer the 12-bit number serially from the DA converter in the order of least significant bit first.
- An enable signal to establish the gating path from the input serializer to the accumulator.
- A twelve-pulse clock signal to the accumulator that enables the serial data to be input from the multiplexer.
- An "advance the program memory" instruction countercommand signal.

INP 1 - The purpose of this instruction is to transfer data from the control room receiver shift register to the accumulator. When an INP 1 instruction is received the control unit generates the following signals to control the operation:

- Two enable signals to establish the gating path to the accumulator at serial MUX No. 1.
- A mode control signal (low level) to the accumulator to operate in the shift-right serial mode.
- A twelve-pulse clock signal to the control room receiver shift register and the accumulator to transfer the information from the shift register to the accumulator.
- An advance in the program memory instruction counter-command signal.

LAI - The purpose of the LAI instruction is to bring numerical constants from the program memory into the accumulator for use in a computational process. As in the previous instruction, a parallel to serial data conversion is made using the memory serial converter to transfer the data in the accumulator via MUX No. 1. When the LAI instruction is received, the control unit generates the following signals:

- A mode control signal (low level) to enable the accumulator to operate in the shift register-serial input mode.
- Three signals encoded to address the program memory serial converter causing the output to be sequenced through its inputs one bit at a time to transfer the 12-bit binary number serially from the program memory least significant bit first.

- Enable signals to the serial MUX No. 1 that establishes a transmission path from the memory serial converter to the accumulator.
- A twelve-pulse clock signal to the accumulator that enables the serial data to be input from the multiplexer.
- An advance in the instruction counter signal to the program memory.

LMI - The purpose of the LMI instruction is to transfer a numerical constant from the program memory to the MQ register for use in a computational process. The process is the same as the LAI instruction. The data are transferred serially using the program memory serializer except that the data are routed into the MQ register instead of the accumulator via serial MUX No. 2. The MQ register is a shift register with a shift-right or shift-left capability. When data are being transferred from program memory unit to the MQ register, zero's are loaded into the accumulator.

When an LMI instruction is received, the control unit generates the following signals that are applicable to this operation:

- An enable signal to serial MUX No. 2 that establishes the transmission path from the program memory serializer and the MQ register.
- A signal to the MQ register that places the register in the shift-right mode.
- A twelve-pulse clock signal to the MQ register that enables the serial data to be input from the multiplexer.
- Three signals encoded to address the program memory serializer causing the serializer output to be sequenced through its inputs one bit at a time to transfer the 12-bit binary number serially from the program memory, least significant bit first.
- A signal to advance the program memory to the next instruction.

LDA - The purpose of this instruction is to transfer data from a specific scratch pad memory location to the accumulator. The specific location in the scratch pad memory from which the data are to be transferred is determined by the data portion of the program memory instruction word. This is a parallel data transfer using the arithmetic and logic unit (ALU) as a transmission link.

Upon receipt of the LDA instruction, the control unit sends five control signals to the ALU to set up the control mode that will enable ALU to serve as a transmission link between the scratch pad memory and the accumulator. This control mode enables each of the 12 output lines of the ALU to be equal to the ALU "B" inputs only. In addition, the control unit generates the following signals that control the operation.

- A low-level signal to the accumulator that enables the parallel input mode of the accumulator.
- A signal to the scratch pad memory that enables the read mode of operation.
- A pulse signal to the accumulator that enters the data into the accumulator.

STO - The function of this instruction is to store a 12-bit number that is currently in the accumulator in the 256-word read/write scratch pad memory. The scratch pad memory work location at which the number is to be stored is selected by the program memory. The data portion of the program memory word is used to address the scratch pad memory and designate the scratch pad memory location. The transfer of data from the accumulator to the scratch pad memory is a parallel operation. When an STO instruction is received from the program memory, the control unit generates the following signals:

- A write command (low level) to the scratch pad memory enabling the write mode of operation of the scratch pad memory.
- An advance in the instruction counter signal to the program memory.

ROT - The purpose of this instruction is to interchange the data in the accumulator and the MQ register so that at the end of the operation the number contained in the accumulator will be in the MQ register and vice versa. To accomplish this, data paths are established between the serial outputs and inputs of the accumulator and MQ register. The accumulator and MQ register are placed in the serial right-shift mode of operation and the data are transferred by 12-pulse clock input.

When the ROT instruction is received, the control unit generates the following signals to control the operation:

- An enable signal that establishes the data transmission path between the serial output of the accumulator and the serial input of the MQ register via serial MUX No. 2.
- An enable signal that establishes the data transmission between the serial output of the MQ register and the serial input of the accumulator via serial MUX No. 1.
- Twelve-pulse clock signal to the accumulator and MQ register to shift the data in both one bit to the right for each clock pulse.
- An advance-the-counter signal to the program memory.

RSHM - The purpose of this instruction is to shift the data in the accumulator and MQ register one bit to the right. Execution of this instruction will cause the least significant bit in the accumulator to be shifted to the most significant bit location in the MQ register, the least significant bit in the MQ register to be lost, and a zero put into the most significant bit of the accumulator. When the RSHM instruction is received, the control unit generates the following signals to control the operation:

- A signal to the accumulator that enables the right-shift serial mode of operation of the accumulator.
- A signal to the MQ register that enables the right-shift serial mode of operation of the register.
- A transfer pulse to the accumulator and MQ register that transfers the data in both one bit to the right.
- An instruction counter advance signal to the program memory to start the next instruction.

RSH - This instruction is the same as RSHM except that it causes the most significant bit to be repeated in the accumulator in order to preserve the sign of the number. Control signals are also the same as with RSHM except there is a signal to shift the most significant bit in the MQ register back to the accumulator.

LSH - The purpose of this instruction is to shift data in the accumulator and the four most significant bits in the MQ register one bit to the left. Execution of this instruction will result in the most significant bit in the MQ register being transferred to the least significant location in the accumulator and the most significant bit in the accumulator being lost. The left shift is accomplished in the following manner. External wiring on the four most significant bits of the MQ register permits MQ register left-shift operation. The accumulator left-shift operation is obtained by operating in the parallel load mode and employing the arithmetic and logic unit in the $F = A+A$ mode. To obtain a left shift of the most significant bit in the MQ register to the least significant bit in the accumulator, a data path is established to carry the (CN) input of the ALU.

The control unit generates the following signals upon receipt of the LSH instruction.

- A high-level signal to the MQ register to enable the shift-left mode of operation.
- A low-level signal to the accumulator enabling the parallel load mode of operation.
- Five signals to the ALU establishing the $F = A+A$ mode of operation.
- A high-level signal to establish data path from MQ register to ALU through serial MUX No. 1.
- A clock pulse signal to the accumulator to transfer ALU outputs to the accumulator (left shift).
- A clock pulse signal to the MQ register to left-shift data in the MQ register.
- A signal to the instruction counter to advance to the next instruction.

ADD - The purpose of this instruction is to add a number stored in the scratch pad memory to a number stored in the accumulator using the ALU. The sum will be entered in the accumulator when the instruction is complete.

Add instructions are accomplished in the following manner. The data portion of the program memory word for this instruction is used to address the scratch pad memory location in which one of the numbers to be added is stored. The scratch pad memory is then placed in the read mode and the number is presented at the "B" inputs of the ALU. The other number which is contained in the accumulator is present at the "A" inputs of the ALU. The CN input will be set to indicate no carry. The ALU control inputs will be set to place the ALU in the ADD mode, $F = A+B$, and the sum is then gated into the accumulator replacing the "A" number.

When an ADD instruction is received, the control unit generates the following signals to control the operation.

- A high-level signal to the scratch pad memory enabling the read mode of operation.
- Five control mode signals to the ALU enabling the add mode of operation.
- A signal to the ALU carry input indicating zero carry input to this add function.
- A signal to the accumulator placing it in the parallel load mode of operation.
- A clock pulse signal to the accumulator that enters the sum from the ALU.
- A signal to the program memory to advance to the next instruction.

ADDC - The ADDC instruction is executed in the same manner as the ADD instruction. It is used to transfer a carry bit if one is generated in double-precision addition. Double-precision numbers (24 bits) are generated as a result of multiplications. To increase computational accuracy, it is sometimes necessary to add or subtract double-precision numbers. Addition of double-precision numbers is a two-step operation because the ALU can only accommodate 12-bit numbers at one time. The 12 least significant bits are added first. If a carry is generated from this addition at the carry output of ALU, it will be stored in a flip-flop in the control unit and will be added at the CN input of the ALU

during the next instruction when the most significant bits are added. The only change in the control unit's functions, as shown in the ADD instruction, is that ALU carry input may be high or low depending on the last carry out of the ALU.

SUB - The purpose of this instruction is to subtract a number stored in the scratch pad memory from a number in the accumulator. This instruction is accomplished in the same manner as the ADD instruction except that the ALU is placed in the subtract mode, $F = A - B - 1$, and the CN input of the ALU set to add a "one" to the result.

SUBC - This instruction is analogous to the ADDC instruction except that an overflow at the ALU carry output at the end of a subtraction now represents a "borrow" instead of a "carry".

MPYM - The purpose of this instruction is to multiply an unsigned number stored in the scratch pad memory by an unsigned number stored in the MQ register. At the end of this operation, a 24-bit product will be contained in the accumulator and MQ register combination.

The method of multiplying is as follows: The multiplicand, which is contained in scratch pad memory, is addressed by the data bits of the MPYM instruction and is present at the "B" inputs to ALU. At the start of multiplication, zero's are stored in the accumulator. Binary multiplication is accomplished through cumulative addition with a running total contained in the accumulator MQ register.

If the number stored in the least significant bit location in the MQ register is one, the number stored in both the accumulator and the MQ register are shifted one bit to the right. A zero will be shifted into the most significant location of the accumulator except if the sum of the accumulated total in the accumulator and the number stored in the scratch pad memory is greater than one. In this case, a one is generated at the ALU carry and is stored in the overflow flip-flop in the control unit. If the overflow flip-flop indicates a one, a one will serially input to the most significant bit of the accumulator during the shift-right operation.

If the number at the least significant bit of the MQ register is zero, then the addition does not take place and the numbers in the accumulator and MQ registers are right-shifted only. After 12 add-shift operations, the product, a 24-bit number, will be contained in the combination accumulator MQ register with the 12 most significant bits in the accumulator.

In order to perform the add-shift operation, the accumulator is placed first in the parallel mode of operation to add and then the serial mode of operation to right shift.

The control unit generates the following signals to control the operation:

- An accumulator mode control signal to add or shift. This signal is 12 μ S long and is 180° out of phase with IMC timing signal.
- A signal to establish the shift-right transmission path between the accumulator and the MQ register.
- A 12-pulse shift-right signal to the accumulator.
- An add signal to the accumulator each time the least significant bit in the MQ register is one. This signal is synchronized with the timing signal delayed by 0.5 seconds from the right-shift operation.
- A zero to the CN input of ALU.
- Five control signal inputs to the ALU to set up the ADD, F = A+B mode of operation.
- A signal to the scratch pad memory to enable the read mode of operation.
- A signal to the overflow flip-flop unit to zero output prior to each ADD in the ALU.
- A clock signal that sets a one in the overflow flip-flop if the ALU generates a carryout signal during the last add.
- A signal to the serial input of the accumulator when the overflow flip-flop output is one.

MPY - The purpose of this instruction is to multiply signed numbers.

The manner in which this is accomplished is exactly the same as the MPYM

instruction except for the following: For negative multiplicands (the number stored in the scratch pad memory), a one will be serially input to the accumulator whenever the most significant bit of the partial product in the accumulator and the most significant bit of the scratch pad memory are one.

DIV - The purpose of this instruction is to divide to a number in the accumulator by a number stored in the scratch pad memory. The DIV instruction is an accumulative subtraction shift-left operation that is performed in a manner similar to that of the multiplication instruction, the result again being a double-precision number stored in the accumulator and MQ register.

BRMA XXXX - The purpose of this instruction is to perform branching capability in the program when a BRMA (Branch on Minus Absolute) instruction is received. If the result of the last subtraction was negative, the program memory counter will be jumped to the address indicated by the data bits associated with BRM instruction denoted by XXXX. If the result of the last subtraction was positive, the program counter is simply incremented by one to the next instruction. The branching capability utilizes a timing signal delayed by 50% of the duty cycle of the normal clocking. When a BRM signal is received an "advance the counter" signal is generated by the control in time with the delayed signal if the result of the last subtraction was positive. Last subtraction resultant polarity was determined by a flip-flop in the control unit which monitors the carry out of the Arithmetic Logic Unit being set at the last subtraction instruction. If, however, the result of the last subtraction was negative the control unit generates the following signals to implement the branching in time with the normal clock.

- A control mode signal to place the program memory counter in the parallel load mode, and an enable signal that loads the data bit information to jump the memory address to that required.

BRMR XXXX - An instruction included for programming convenience (BRMR = Branch on Minus Relative) which is executed as BRMA.

JMP XXXX - The purpose of the jump instruction is to provide unconditional branching in the program address. It is executed identical to the BRM instruction where the result of the last subtraction was negative.

5.2.4 Input-Output Section

The input-output section of the digital control contains the signal condition circuits for inputs and distribution circuits for outputs and provides an interface with the central processor in an acceptable digital format. All data transfers to and from the central processor take place under the command of signals received from the control unit of the central processor.

Referring to Figure 51, the signal flow in the digital control is as follows: The instrumentation and sensor input signals are fed to an analog multiplexer circuit that is controlled by the central processor control unit. The input counter provides an address to the input decoder from which a single input signal is selected. The inputs are selected in a fixed order by increasing the count by one at the end of an analog to digital conversion. At the end of each control iteration cycle the counter is reset to zero.

The sample-and-hold output is connected to the analog-to-digital (AD) converter. The AD converter changes the analog signal to 12-bit digital word representing the analog signal. The 12-bit digital word is fed to the digital computer circuit via a serial digital multiplexer No. 1. Other signals into the digital multiplexer provide communication between the digital control and remote units located in the control room. The 12-bit word from the AD converter is operated according to the program instructions stored in the digital computer program memory.

Upon completion of this portion of the program, the central processor feeds the result of the computation to a digital-to-analog (DA) converter circuit and a data multiplexer circuit. The data multiplexer provides another communication link between the digital control and the control room. The DA converter signal goes to the analog output circuits which consist of flip-flops, sample and hold circuits, torque motor amplifiers, and driver circuits.

5.2.5 Other Circuits

Other circuits in the digital control include a power supply that provides the necessary regulated voltages for the control and circuits which provide transducer excitation. There is also an emergency shutdown circuit that cuts back fuel flow if the low-pressure turbine (LPT) acceleration rate is excessive or the LPT speed exceeds a given limit.

Figure 53 is an example of an analog signal conditioning circuit showing a pressure amplifier circuit, a typical analog circuit used in the digital control. The input to the amplifier is the output from a strain gauge bridge transducer. The excitation for the transducer is provided by the ± 15 volt power supply in the digital control. IC1 is used as a differential amplifier to provide some preamplification of the pressure signal. Resistors R13 through R19 comprise a temperature compensation network used to compensate offset and offset-drift over the temperature range. The output of IC1 goes to R7, the input resistor of IC2. IC2 is the second stage of the amplifier and sets the desired overall gain of the amplifier by selecting resistor R9, R10, and R11.

Another digital network which deserves mention here because it is part of a new development being applied to the QCSEE is the driver amplifier used to operate the fail-fixed servovalve described in Section 6.3. This is a unique application of digital technology in that it drives a hydraulic output power device without the need for digital-to-analog conversion.

As shown in Figure 54, a 12-bit word is generated and held by the processor as a function of the flow demand. The least significant bit (LSB) is ignored to generate a 11-bit signal "B". Simultaneously, the 2.048-MHz clock signal and three 4-bit series counters generate a continuously changing 12-bit word. The most significant bit (MSB) is excluded to create 11-bit word "A" that periodically counts from 0 to 2047. Signals A and B are compared by the three series 4-bit comparators to generate an output signal when $B > A$. The MSB (2^{12}) from the clock counter, through an inverter, and the next most significant bit (2^{11}) are fed to an AND gate to generate the 25% on signal; that is, a signal that repetitively is on 25% of the time of each count cycle from 0 to 4097.

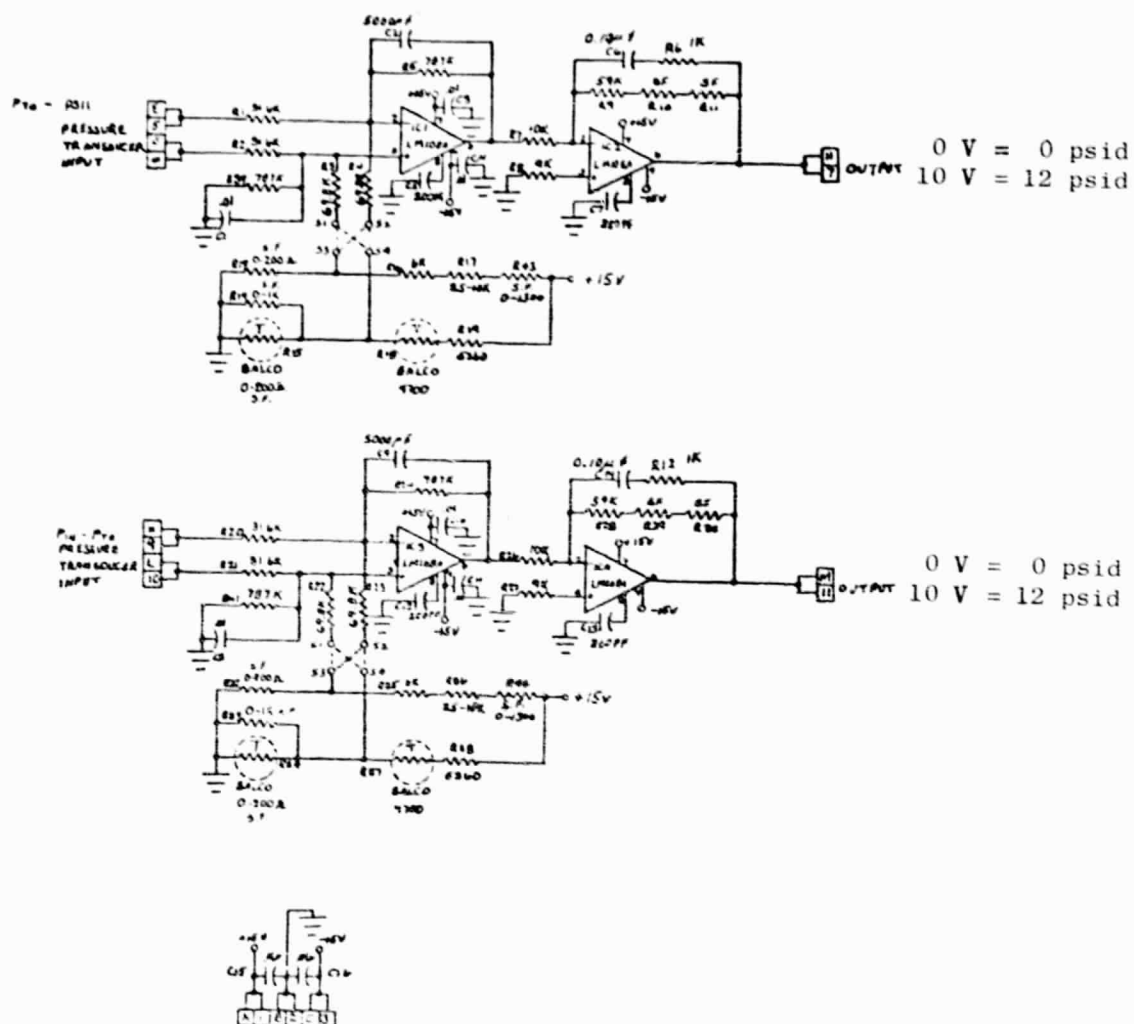


Figure 53. Typical Analog Circuit.

ORIGINAL PAGE IS
OF POOR QUALITY

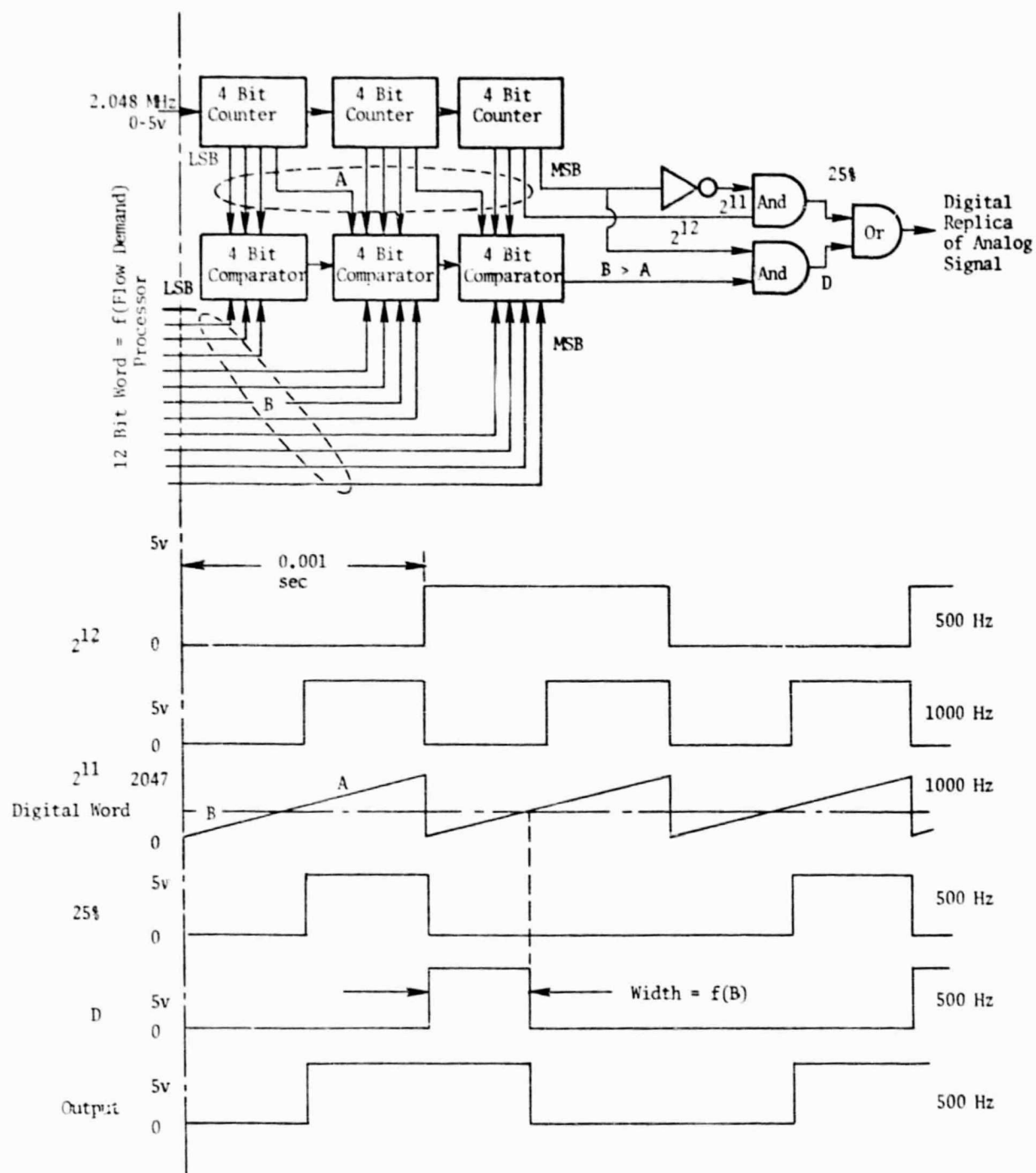


Figure 54. Digital Driver Amplifier for Fail-Fixed Servovalve.

The MSB (2^{12}) signal from the counter circuit and the $B > A$ signal from the comparator circuit are coupled through an AND gate to generate signal "D". As shown in Figure 54, the width of signal "D" is a function of "B", varying from 0% to 50% on time. The 25% signal and the "D" signal are logically summed through an OR gate to generate an output signal that is the replica of an analog signal of the flow demand. This signal is then treated by a conventional torque motor current amplifier stage to drive the servo-valve with a -80 mA to +80 mA, 500 Hz signal, whose on-time varies from 25% to 75% as a function of the digital flow word.

Circuit Components

Circuit components used in the digital control were selected on the basis of their ability to maintain the desired circuit accuracy under the stringent environmental conditions imposed upon them. Other considerations were cost, weight, power consumption, and availability. In order to achieve a state-of-the-art design, new components were investigated and used where possible. The major components are described below:

Low-Power Schottky TTL - Digital components used are primarily low-power Schottky TTL devices. These devices presently offer the best speed-power product of any high-speed family. Table XIII shows a comparison of the TTL circuits. The low-power Schottky family (54LS/74LS) features both Schottky-barrier-diode inputs and emitter inputs. Full Schottky-barrier-diode clamping is utilized to achieve speeds comparable to series 54/74 TTL at one-fifth the power. The Schottky-barrier-diode is connected in parallel with the base collector junction of the normal TTL transistor. Schottky-barrier-diodes have a lower forward voltage than the base collector junction and it clamps the transistor as base drive increases. Most of the excess base current is diverted and this prevents the transistor from reaching classic saturation. This effectively eliminates charge storage and subsequent recovery times.

Digital Memory Devices - Two other new integrated circuit devices are used in the computer section of the digital control. These are the 5340 programmable read-only memory (PROM) and the L5531D read/write random access memory (RAM). A description of each follows:

Table XIII. 54/74 Family Typical Performance Characteristics (TTL)

Series	GATES		
	Propagation Delay Time	Power Dissipation	Speed-Power Product
54LS/74LS	9.5 ns	2 mW	19 pJ
54L/74L	33.0 ns	1 mW	33 pJ
54S/74S	3.0 ns	19 mW	57 pJ
54/74	10.0 ns	10 mW	100 pJ
54H/74H	6.0 ns	22 mW	132 pJ

- The 5340 PROM is a 4096-bit memory arranged as 512 eight-bit words. The PROM contains logic circuits, decoders, buffers, and data storage circuits. The device is manufactured with all outputs high in all storage locations. Device programming is accomplished by making an output low for a particular word. To do this a Nichrome fusible link is changed from a low resistance to a high resistance. The outputs are programmed one at a time by applying the appropriate TTL levels to the enable and applying a voltage pulse to the output that is to be programmed. The voltage source must supply sufficient current to complete programming of the output. Since pulse techniques are used to program the PROM and it involves the use of the enable inputs and the output pins, the timing is critical and the pulses must occur as described by the device specification sheet. Programming equipment is available to simplify the procedure. Several PROMS can be connected to a common output bus and since the outputs are the open collector-type, pullup resistors must be used. The value of the resistor is determined in part by the number of PROMS used and the number of TTL loads the memory must drive. Sixteen PROMS are used in the digital control and are connected to form a 4096-by-16-bit word memory. The digital control program is stored in this memory and contains the instructions for the computations and data manipulations of the digital control.
- The L5531D RAM is a 256-bit memory device arranged in a 256-by-1 array. That is, there are 256 memory locations, each containing one bit of information. The RAM circuit chip contains logic circuits, decoders, buffers, and a memory array. The L5531D is a three-state device and is so called because the output has the high and low TTL states and third high impedance state. This third high impedance state allows the outputs of several L5531D's to be connected to a common bus. The memory is addressed using an 8-bit address word to select one of the 256-bit locations. With the write enable low, the data on the input pin of the RAM are written in the selected memory location. If the write enable is high and the RAM is enabled, the stored data are read out on the data-out pin. The data read-out is the complement of the data written into the memory location during the write cycle. The data will be retained in the selected memory location until new data are written in or the power is removed from the RAM. There are twelve L5531D's used in the digital control to form a 256-word memory with each word 12-bits long. These RAM's form the scratch pad memory of the computer and are used for temporary storage during computations and data manipulations.

Other New Components - Another device that is used is the Hewlett-Packard 5082-4365 optically-coupled isolator. These are used as interface components between the digital control and other circuitry where electrical isolation is desirable. The 4365 consists of a pair of inverting optically-isolated gates each with a light-emitting diode and high-gain integrated

photon detector. The output of the detector is an open collector Schottky clamped transistor. The input and output are TTL compatible.

Other new components used in the digital control consists of sample and hold circuits, voltage follower, and power op-amps all of which are standard op-amp-type circuits. They were selected because of improved characteristics (temperature drift, speed, etc.) over previously used components of the same type.

5.3 ELECTRICAL CIRCUIT CONSTRUCTION

General Description

In the QCSEE digital control, the signal processing and control are accomplished with a collection of interconnected electrical assemblies called modules. A module is a functional assembly of electronic components specifically designed to perform a precise sequence of desirable operations on one or more specified electrical inputs.

In general, modules constructed to meet on-engine environmental requirements consist of electrical components whose leads are soldered into printed circuit board (PCB) assemblies. The PCB provides the necessary electrical connections between components. These PCB assemblies are installed into an anodized aluminum module can with 0.081-cm-(0.032-in.) thick walls and encapsulated with filled, resilient potting compounds. The primary advantages of the potting compounds are (1) provide vibration damping and moisture protection, (2) improve steady-state and transient module thermal characteristics, and (3) protect the circuitry from contaminants.

QCSEE digital control module design consists of the following three basic module types:

- (1) Analog modules
- (2) Digital modules
- (3) Combination analog/digital modules

Each of the above designs is directed toward the packaging of a specific type or set of components. The analog module handles standard electrical components such as operational amplifiers, transistors, diodes, transformers, resistors, capacitors, and so on. The digital module is specifically designed to handle digital components in dual-inline package form. The analog/digital module is a necessary design compromise used where a separation of the analog and digital circuitry is not functionally possible due to electrical requirements.

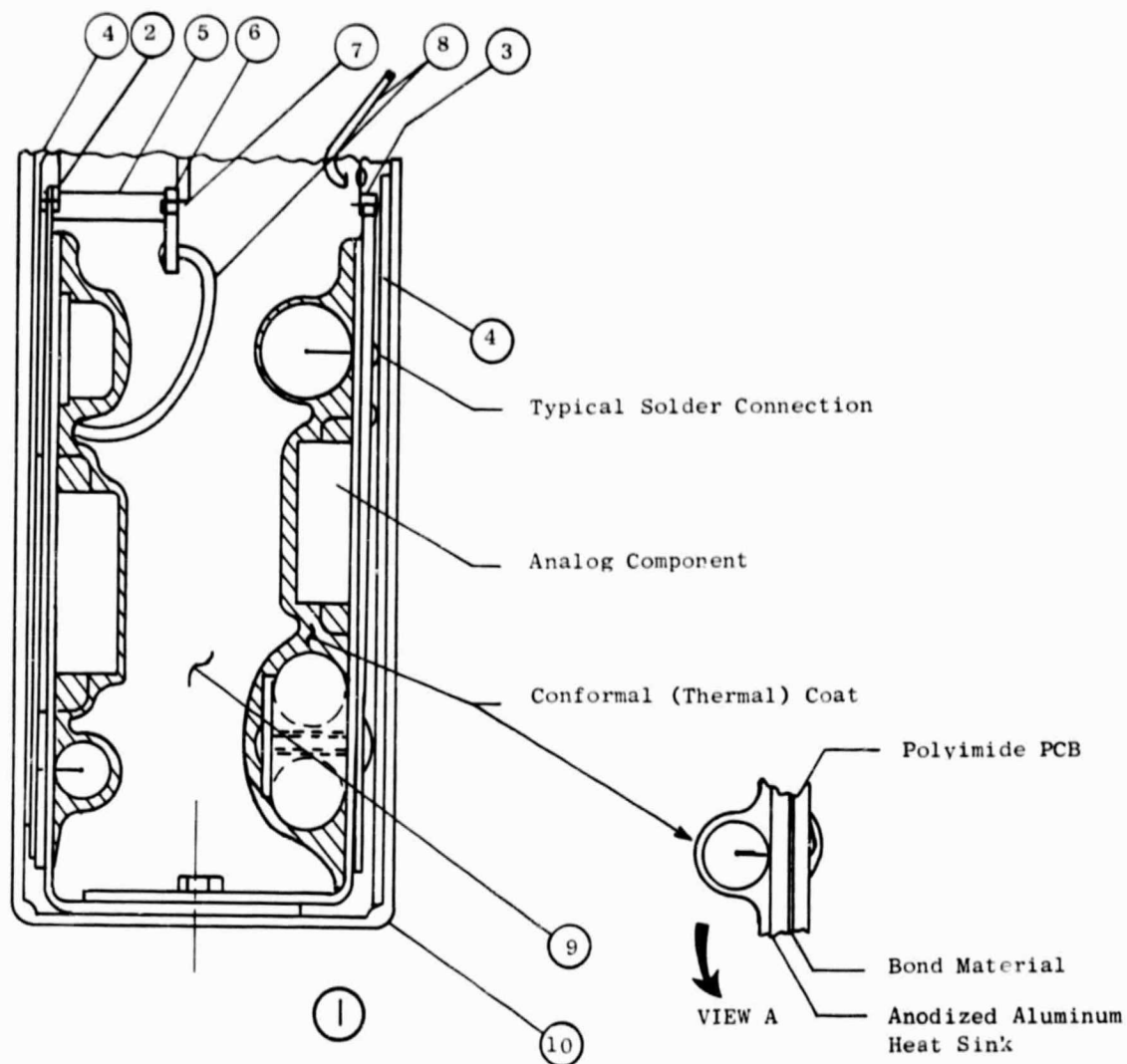
All of the module design approaches described below have been utilized on one or more successful engine programs. They are considered more than adequate to meet the QCSEE digital control design requirements.

Analog Module Design

An analog module consists of electrical analog components mounted to printed circuit boards (PCB's). A typical analog module requires two PCB's. All QCSEE analog PCB's utilize a 2 oz., double-sided copper, 0.079-cm (0.031-in)-thick polyimide boards bonded to an anodized heat sink made from aluminum sheet. The anodized aluminum heat sink is located between the bodies of the electrical components and the PCB component side surface and provides, via a nonanodized aluminum mounting flange, a low thermal resistance path to the module mounting surface (see Figure 55). The incorporation of the relatively low thermal resistance path permits the use of a lower density (lower thermal conductivity) potting compound which results in an overall weight reduction. The microsphere-filled RTV potting being used has a specific gravity of 0.7 compared to a specific gravity of 1.5 for the alumina-filled RTV potting compound normally used to thermally compensate module configurations not utilizing an anodized aluminum heat sink. Generally, these two module configurations are thermally equivalent and for most typical analog modules yield component-to-mounting-surface hot-spot temperature differences less than 25° F. Components having hot-spot temperature differences greater than this are provided with additional heat sinking capability to achieve the 25° F differential goal.

Digital Module Design

A digital module consists of digital electronic components mounted to automatically wire-wrappable digital boards. A typical digital module requires two wire-wrap boards. All QCSEE digital boards utilize 4-oz. copper for power and ground planes and are made from double-sided 0.127-cm (0.050-in.)-thick glass-epoxy PCB stock. The electrical connections required by the circuit being packaged are made with socket pins for digital component leads and Kapton insulated wire routed from pin to pin (see Figure 56). To reduce electrical noise and improve circuit reliability during operation, all electrical interfaces are soldered prior to final test and encapsulation. A typical digital module may have as many as 8 to 10 times more internal board-to-board common connections than a typical analog module. A special flexible interconnection circuit (see Figure 56) is designed to handle the relatively large number of common connections inherent in a digital module. The flexible



- | Item | |
|---------|------------------------------|
| 1----- | Typical Module Assembly |
| 2----- | Printed Wiring Bd. Assy. |
| 3----- | Printed Wiring Bd. Assy. |
| 4----- | Insulator (Electrical) |
| 5----- | Satellite Bd. Spacer |
| 6----- | Satellite Bd. |
| 7----- | Satellite Bd. Mounting Screw |
| 8----- | 24 AWG. Hookup Wire |
| 9----- | Lightweight Potting Compound |
| 10----- | Module Can |

Figure 55. Typical Analog Module.

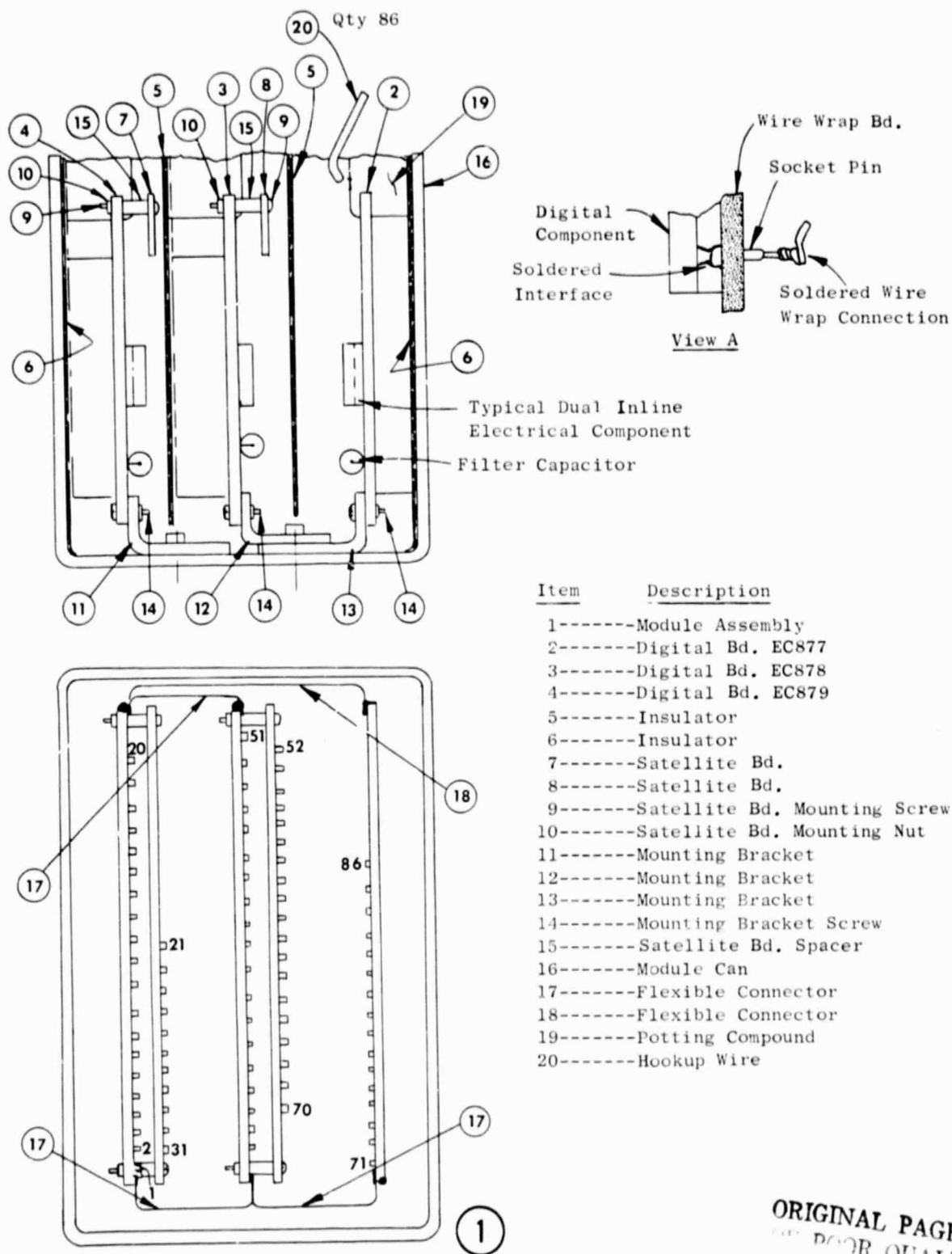


Figure 56. Typical Digital Module.

connector carries common signals and is routed around either end of the digital board. All flexible connector electrical interfaces are soldered in place prior to final test and encapsulation. Digital board assemblies are bracket-mounted to the base of the module can and the final module assembly is encapsulated in an alumina-filled potting compound. This compound is used in all digital and analog/digital modules to thermally compensate for the lack of an integral heat sink similar to the anodized aluminum heat sink utilized for analog PCB's. As in the case of analog modules, component-to-mounting-surface hot-spot temperature differences are held to less than 25° F with additional heat sinking capability added if necessary to achieve this goal.

Analog/Digital Module Design

An analog/digital module consists of one analog board coupled with one digital board. As in the digital module case the large number of board-to-board connections are made via a specially designed analog/digital board flexible connector and, as before, are soldered in place prior to final test and encapsulation. The final module assembly is encapsulated in an alumina-filled potting compound and subjected to the same component-to-mounting-surface hot-spot temperature evaluation as described for both the analog and digital modules.

5.4 DIGITAL CONTROL PRODUCT DESIGN

This section describes the manner in which the digital control circuit modules and other internal elements are mounted and enclosed to provide a unit suitable for engine-mounting and provide a means for connection of external inputs and outputs.

Installation

Figure 57 is a sketch showing the digital control and the manner in which it is mounted on the engine.

The control is basically a rectangular box with a raised section which incorporates the provisions for external electrical and pressure sensing

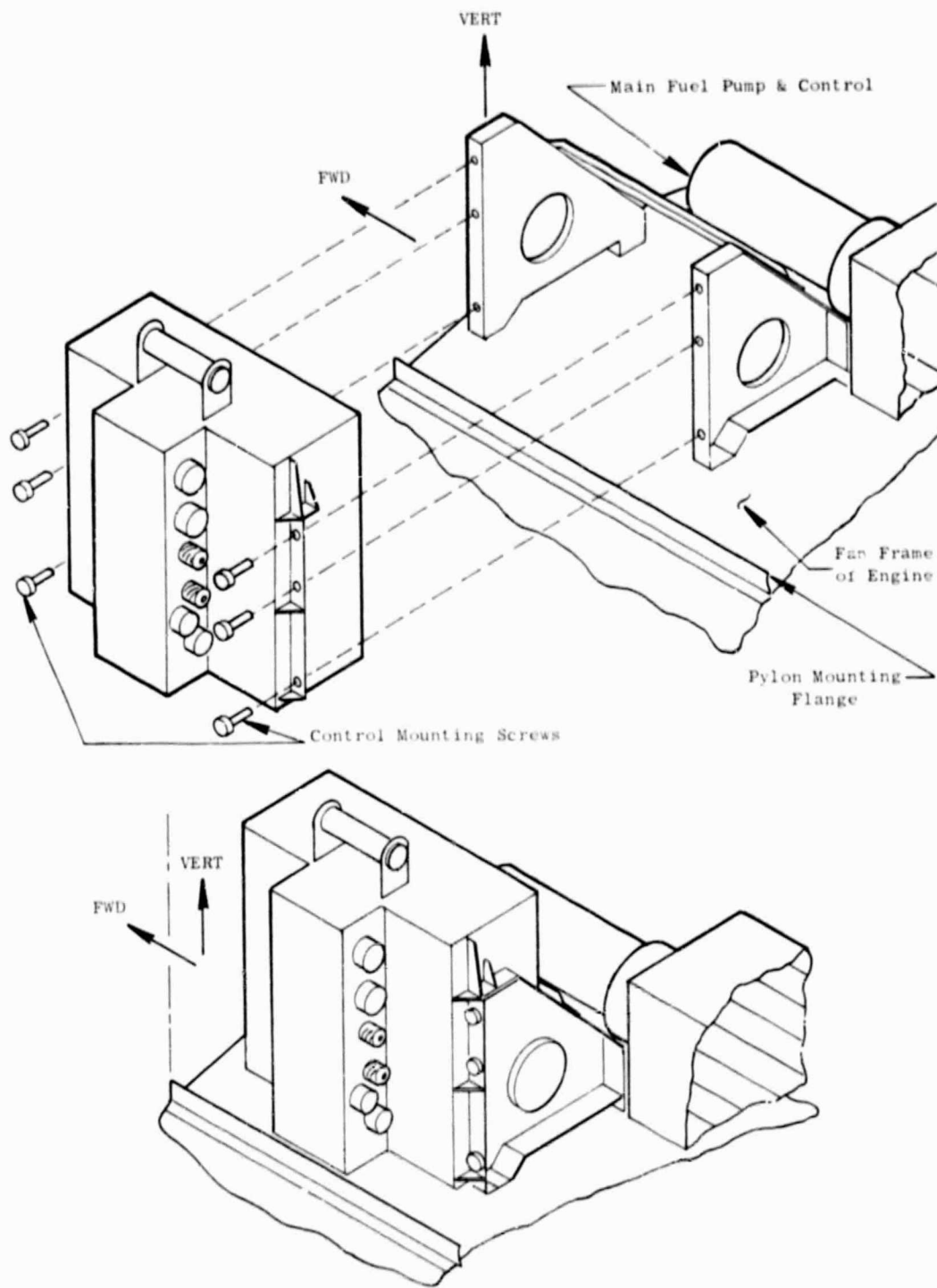


Figure 57. Digital Control Installation.

connections. The approximate dimensions are 33.0 x 38.1 x 12.7 cm (13 x 15 x 5 in.) - length, height, thickness as installed - with 5.08 cm (2.0 in.) additional thickness at the raised section (it should be noted that for this experimental control, excess space has been included for possible future experimental use).

Flanges are provided on the front and back surface of the control for mounting to two triangular brackets which in turn mount to pads on the engine fan frame. Four pads are provided, two for each triangular bracket.

A handle on top of the control is provided for carrying, installing, and removing the control. Resting tabs on the mounting surfaces help steady and support the weight of the control during installation or removal of mounting screws.

Vibration Considerations

Early in the control packaging design process a vibration study was performed assuming a 10-g vibratory input at the unit's calculated center of gravity, well above that expected on the engine (see Figure 58). The analysis identified weakness at several points in the initial design and changes were made to correct these weaknesses. The resulting design is anticipated to be satisfactory from a vibration standpoint.

To prove the vibratory capability of the unit, a chassis vibration test was performed over the spectrum shown on Figure 58 which is based on dynamic analyses performed on the complete engine.

Internal Construction

Definition of the internal construction details of the digital control primarily involved the definition of how best to arrange and mount the electrical circuit modules. The primary factors considered were: (1) module dimensions, (2) heat dissipation, (3) module interconnections, and (4) module connections to control inputs and outputs.

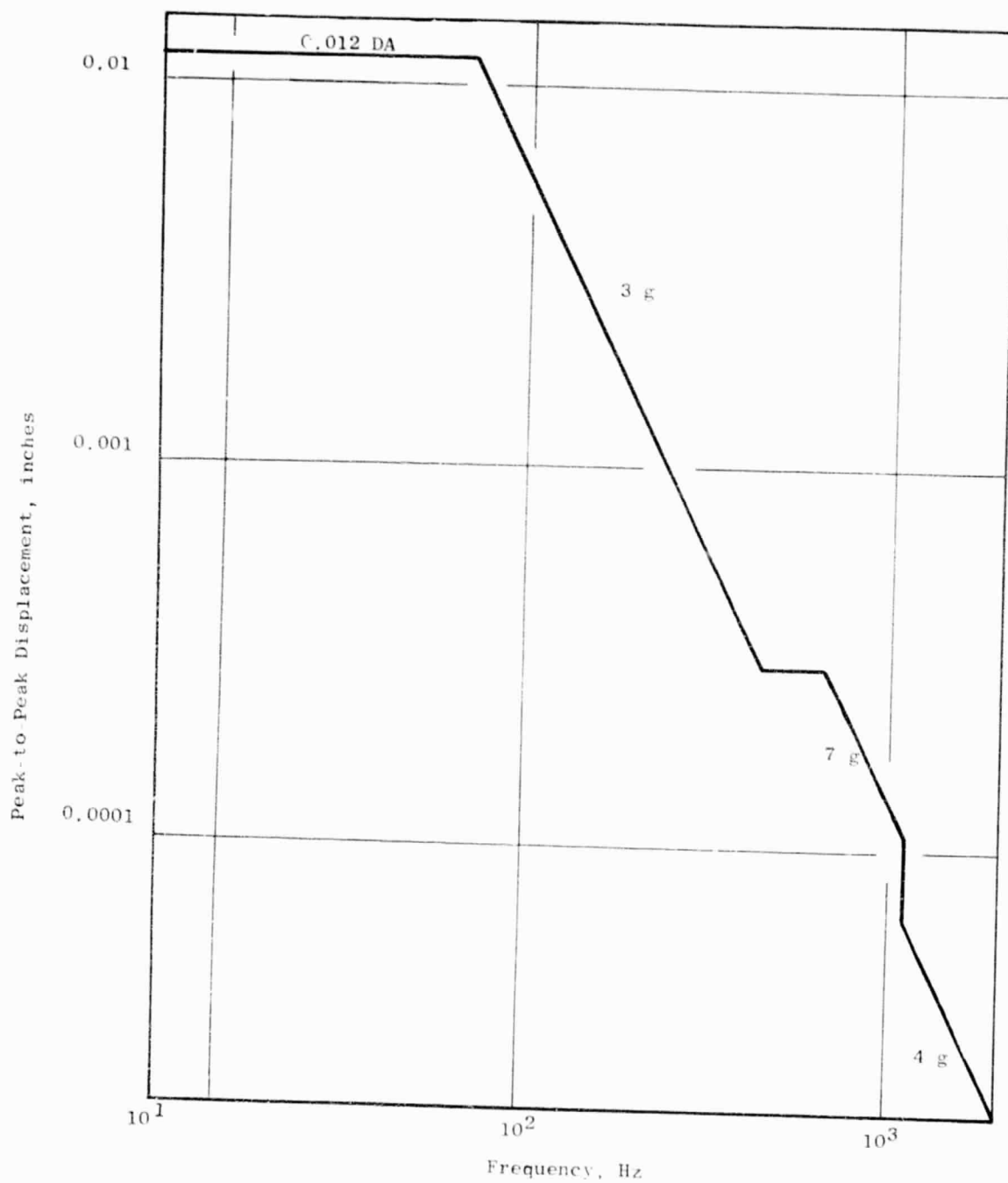


Figure 58. Vibration Testing.

The arrangement finally arrived at is shown on Figure 59 which is a view looking toward the side opposite the connector side with a cover removed. As noted previously, ample excess space has been provided for the addition of possible future experimental circuits.

The modules are bolted to aluminum plates which are part of the chassis and which serve to carry away heat as explained in more detail later. U-shaped channels between the rows of modules at their upper end furnish further support and also serve as channels for interconnecting wiring. Wires between modules are attached to pins at each module, routed through the appropriate channels, and tacked down with a clear silicon adhesive which provides waterproofing and reduces the chances of handling and/or vibration damage. Wires to external connections are passed through slots in the two channels and routed to the external connectors, input pressure transducers, or electrical input filters where they are connected. These wire bundles are coated with clear RTV.

Cooling

Approximately 100 watts of heat are generated by operation of the modules in the digital control. This heat is dissipated by conduction and convection utilizing air from outside the engine nacelle.

As noted earlier in the module design section, the heat generated by elements within each module flows through the thermally-conductive potting compound and anodized aluminum heat sink in the module to the mounting surface (see Figure 56). The heat is conducted through the bolted module mounting surface into the aluminum mounting plate and aided by a thermal grease applied at the interface. The heat is then conducted through the mounting plates and carried away by air passing over the plates on the side opposite the modules.

The air-cooling flowpath is shown in Figure 60. Air enters at the top (as mounted on the engine) and divides into 3 parallel ducts under the top rows of modules. The air from these ducts is collected, passed back across the lower portion of the module mounting surface, and discharged near the

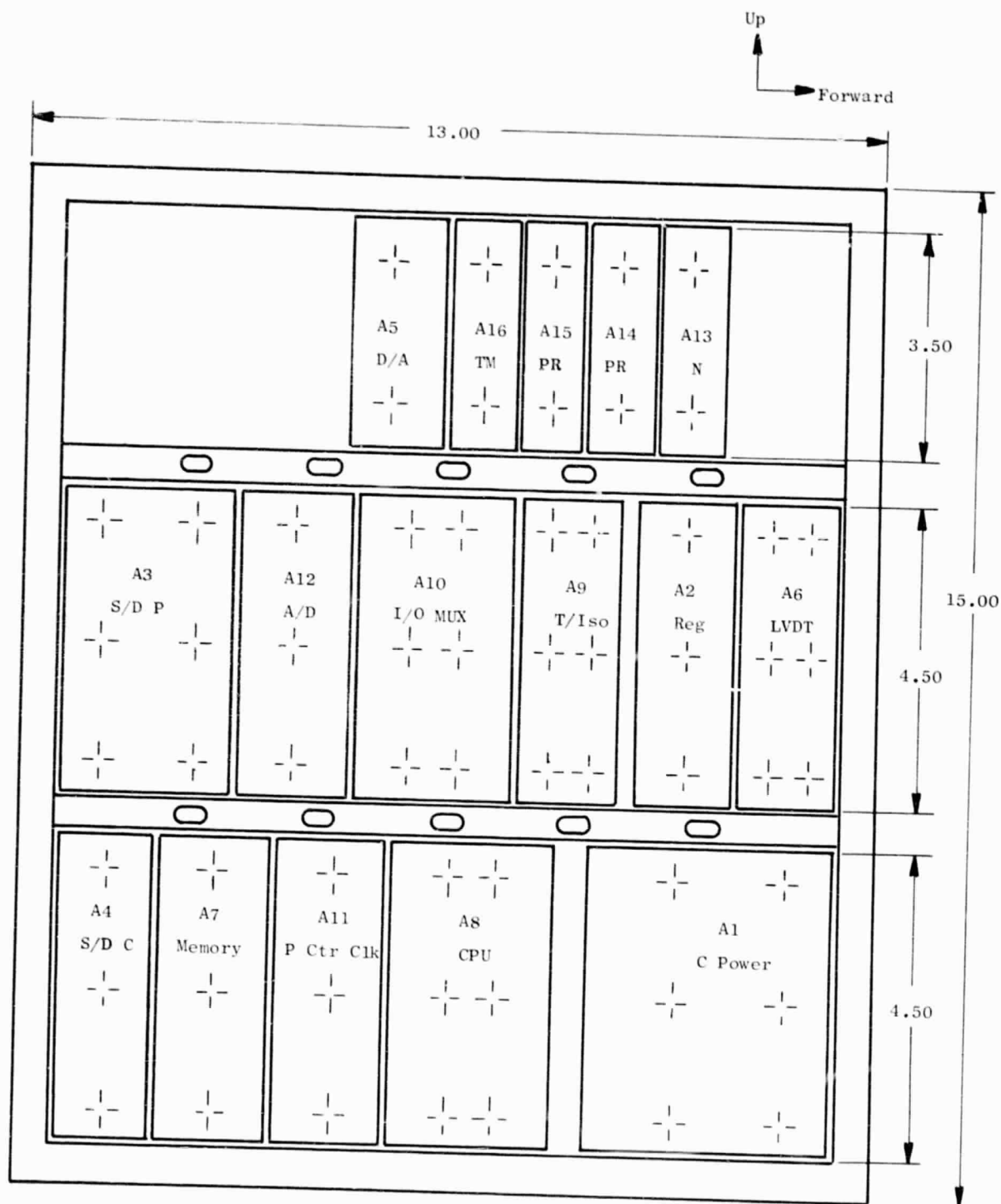
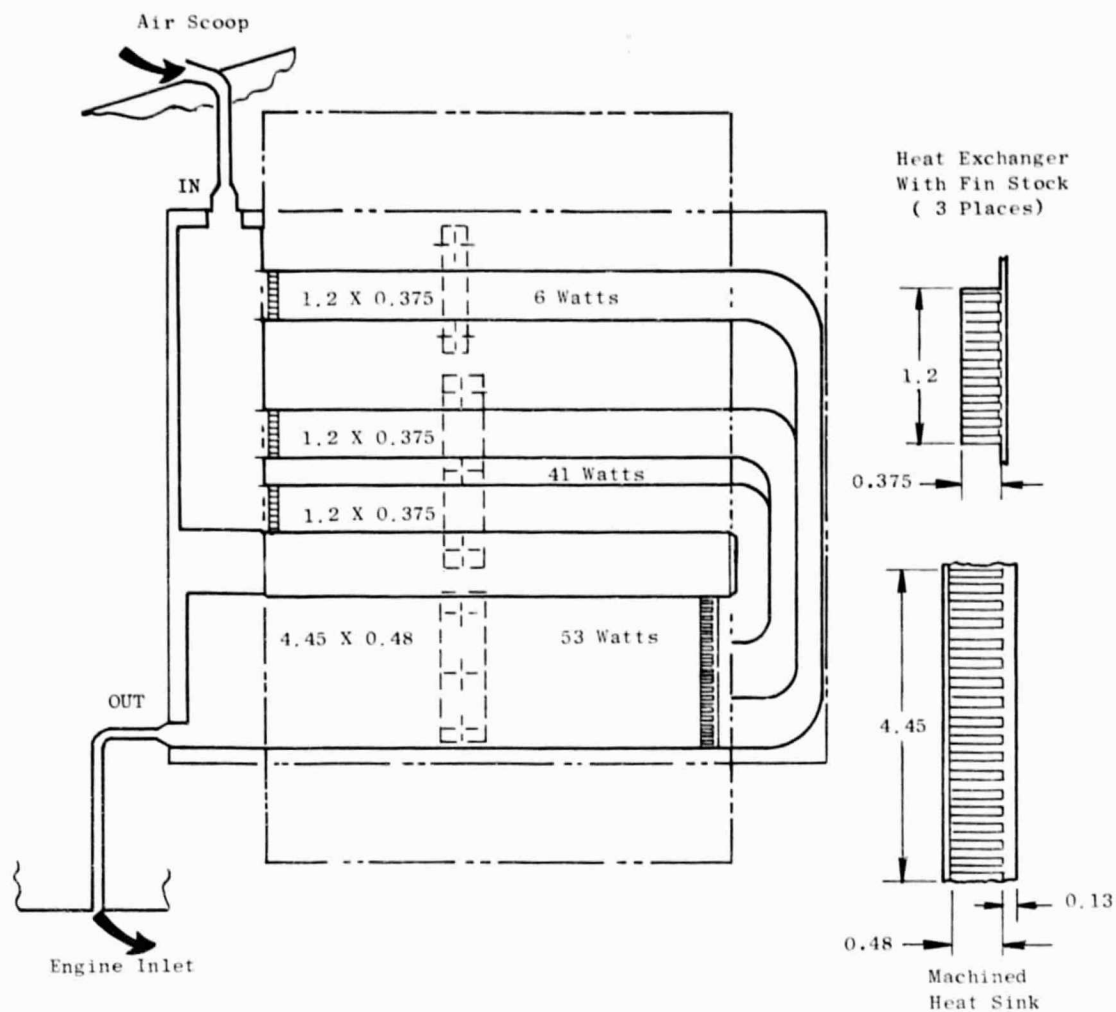


Figure 59. Module Arrangement Digital Control.



Minimum Pressure Drop.....0.288 psid
 Minimum Flow Rate.....0.026 lbm/sec
 Estimated Maximum ΔT43° F

Figure 60. Cooling Air Flow Path.

bottom of the control. Use is made of machined fins in parts of the cooling flowpath to get maximum heat transfer.

The air-cooling system is designed for an installed engine with an airscoop outside the nacelle serving as an inlet and a hole in the engine inlet duct flush with the duct wall serving as an exit. The pressure differential resulting from the lowered static pressure which will exist in the inlet duct during all forward operation will produce a flow sufficient to meet the design objective of having no elements in the control more than 43° F hotter than the cooling air supplied.

If any unusual installation conditions are encountered during the experimental engine test program which would eliminate the normal cooling air differential pressure, a pressurized air source will be used to cool the control.

5.5 SOFTWARE DESIGN

The computational section of the digital described in the previous paragraphs is a special purpose, stored program, single-address computer. Through appropriate electrical circuitry the central processor receives and processes input information to form the required outputs according to the instructions defined in the program memory. The computer has the capability to add, subtract, multiply, divide, and branch upon command. It is a fractional machine except for division which is done in integer form. The machine data word is twelve bits in length and may be treated as an unsigned binary or a signed two's complement number.

The term "software" applies to the set of statements which are contained in the program memory. The statements are made up using the set of instructions described in Section 5.1 and listed again in Appendix D, which also shows the execution time for each instruction.

The complete software program is listed in Appendix D with notes indicating key elements. The program basically follows the block diagrams of Figures 9 through 14 with statements generally grouped to correspond to the separate block diagrams and auxiliary functions. The major groups of statements are as follows:

- 0 - 72 Self-check and initialize for start of computations.
- 73 - 147 Decode and store input commands for future use.
- 148 - 1179 Variable-pitch block diagram
- 1180 - 2219 Fuel flow block diagram
- 2220 - 2308 Failure indication and corrective action
- 2309 - 2745 Exhaust nozzle (Al8) block diagram

Interwoven within these groups are operations related to engine sensor inputs and inputs from the off-engine equipment. Processing of information from the engine sensors is noted by the instruction INP Ø which transfers data in the AD register to the accumulator and STO XXX which stores the information in the accumulator in a selected location in the scratch pad

memory. This action is followed by the instruction OUT 14 which initiates the next AD conversion. The rate at which these engine data are read and stored is controlled by the speed of the AD converter. A software program spacing of approximately 25 to 30 microseconds is allowed for the conversion between reading and storing input data. Processing of information from the off-engine equipment is noted by the instruction INP 1 which transfers data from the command link register to the accumulator and STO XXX which transfers the data to the scratch pad memory for future use. This information is read into the scratch pad memory before it is required for use in the basic software program.

Transmittal of engine and control system operating point or condition information from the control to the off-engine equipment is also interwoven into the basic control software program. This processing is noted by the instruction LDA XXX which loads the accumulator with the data in scratch pad memory location XXX and OUT 13 which transmits the data in the accumulator to the off-engine equipment. Supplementary notes shown in Appendix D show where input-output data are woven into the software program.

Execution time for the complete 3071 statement QCSEE UTW program as shown in Appendix D is 7460 microseconds.

The following two examples of small program segments are described in more detail to aid in understanding program procedures. (Note: Circled numbers in the examples below refer to scratch pad memory addresses.)

Example 1 - This shows steps leading up to calculation of main fuel channel output from input stored in 7 and the desired gain, K_{WT} , of 2.1094 bits/bit. Because numbers cannot range beyond -2048 or +2047, the input signal must be limited to $2047/K_{WT}$ or 970, a value which is stored in 11. The steps in this computation are outlined below and charted on Figures 61 and 62.

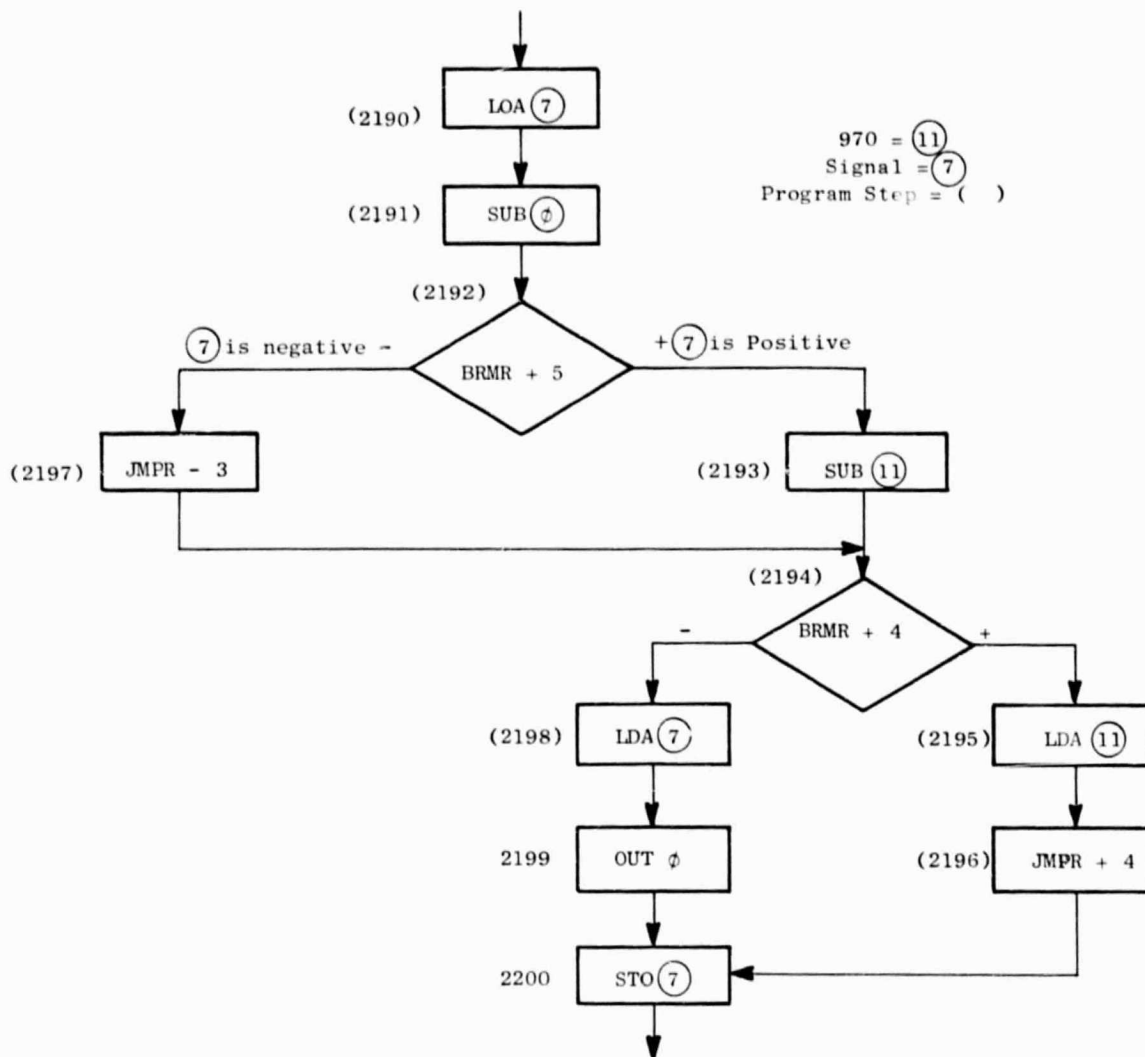


Figure 61. Flow Chart of Positive Circuit Check in Fuel Flow Channel.

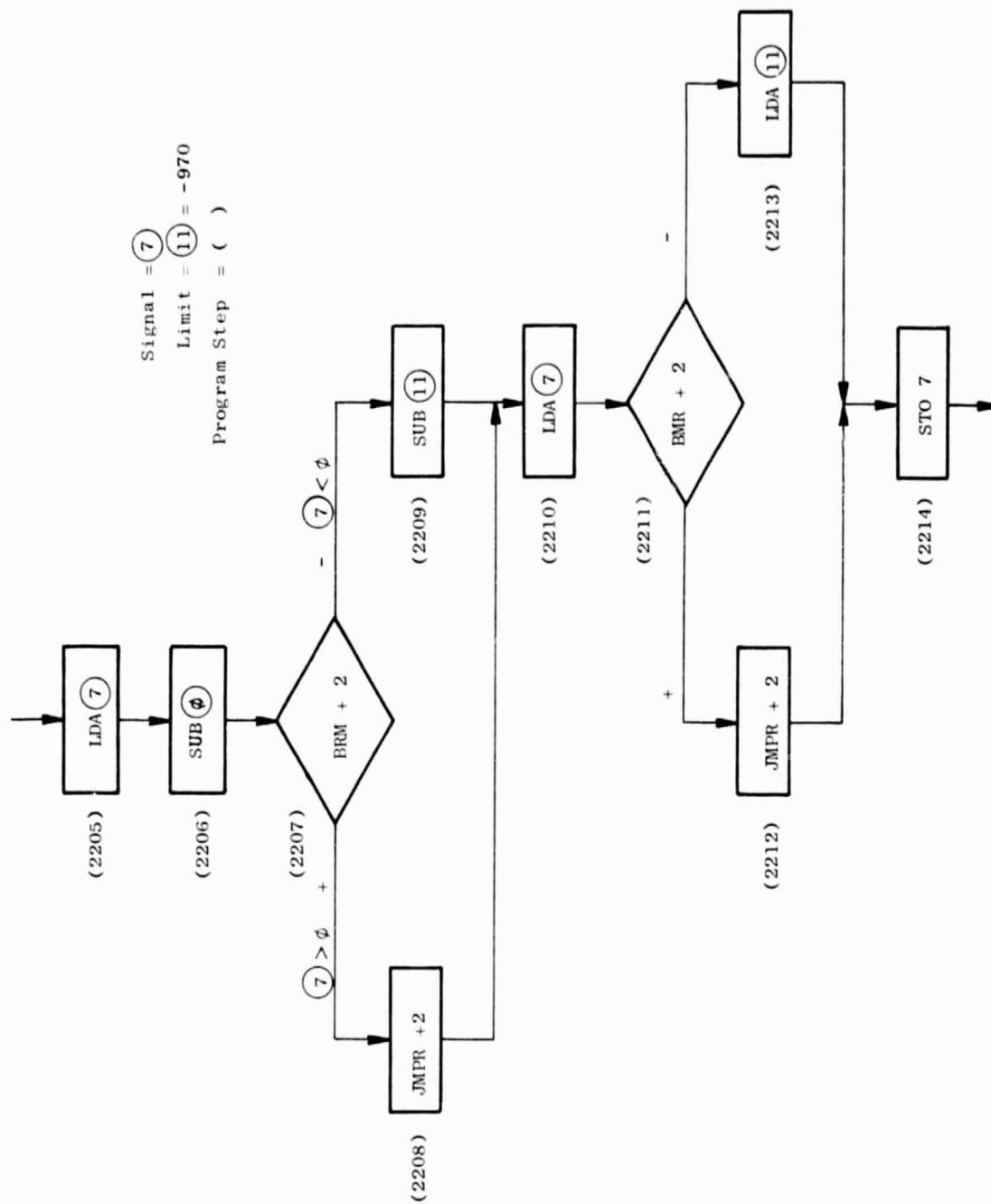


Figure 62. Flow Chart of Negative Limit Check in Fuel Flow Channel.

Line No.	Mnemonic	Comment	Minimum Value	Maximum Value
(First, limit to +970 - see Figure 61 for chart)				
		Input signal stored in (7) maximum and minimum values from previous program operations.	-1853	+2047
2190	LDA (7)	Load input signal in accumulator		
2191	SUB (0)	Test subtraction ((0) contains 0)		
2192	BRMR+5	Branch ahead 5 statements if (7) is negative		
2193	SUB (11)	Subtract 970 limit	- 970	+1077
2194	BRMR+4	Branch ahead 4 statements if result is < limit.		
2195	LDA (11)	Load accumulator with 970 limit		
2196	JMPR4	Jump ahead 4 statements		
2197	JMPR-3	Jump back 3 statements		
2198	LDA (7)	Load accumulator from memory		
2199	OUT (0)	No operation - kills time so path lengths remain equal		
2200	STO (7)	Store result in (7)	-1853	+ 970
(Next, limit to -970 - see Fig. 62 for chart)				
2203	LAI 3126	Enter (-970) in accumulator		
2204	STO (11)	Store (-970) in (11)		
2205	LDA (7)	Load input signal in accumulator	-1853	+ 970
2206	SUB (0)	Subtract zero	-1853	+ 970
2207	BRMR+2	Branch ahead 2 statements if result is negative		
2208	JMPR+2	Jump ahead 2 statements		
2209	SUB (11)	Subtract (-970)	- 883	+ 969
2210	LDA (7)	Load input signal in accumulator	-1853	+ 970
2211	BRMR+2	Branch ahead 2 statements if last subtraction (2209) was negative		
2212	JMPR+2	Jump ahead 2 instructions		
2213	LDA (11)	Load (-970) in accumulator		
2214	STO (7)	Store result in (7)	- 970	+ 970

Now the gain multiplication will be accomplished.

(The input signal or applicable limit is still stored in (7).)

<u>Line No.</u>	<u>Mnemonic</u>	<u>Comment</u>	<u>Minimum Value</u>	<u>Maximum Value</u>
2215	LMI 449	Load K _{WT} (449) in MQ register		
2216	MPY (7)	Multiply (7) by 449/4096	- 106	+ 106
2217	ADD (7)	Add (7) to accumulator	-1076	+1076
2218	ADD (7)	Add (7) to accumulator	-2046	+2046

Example 2 - This shows the logic routine which causes the forward mode reverse interlock signal described in Section 3.3.1 and shown as DBIF on Figure 9 to be operative in some control modes and not in others. Prior to this point in the program, the following scratch pad memory entries have been made: Zero in (0), 1 in (1), the DBIF signal (0 or 1) in (9), the local/remote switch position in (20) (remote = 1, local = 0), the "Full Manual" pushbutton status in (21) (manual = 1, not manual = 0), and the "Auto Reverse" pushbutton status in (23) (reverse = 1, no reverse = 0). Steps in the routine are outlined below and charted on Figure 63.

<u>Line No.</u>	<u>Mnemonic</u>	<u>Comment</u>	<u>Minimum Value</u>	<u>Maximum Value</u>
1507	LDA (20)	Load local/remote switch pos. into accumulator	0	1
1508	SUB (21)	Subtract "Full Manual" pushbutton status	-1	1
1509	LDA (0)	Puts zero in accumulator		
1510	BRMR+5	Skips to 1515 if result of 1508 was negative		
1511	SUB (23)	Subtracts "Auto Reverse" pushbutton status	-1	1
1512	BRMR+5	Skips to 1517 if result of 1511 was negative		
1513	LDA (9)	Puts DBIF in accumulator	0	1
1514	JMPR+5	Jumps to 1519		
1515	OUT 0	No operation (path equalization)		
1516	OUT 0	No operation (path equalization)		
1517	OUT 0	No operation (path equalization)		
1518	LDA (1)	Puts 1 in the accumulator		
1519	STO (9)	Store accumulator number in (9)	0	1

NOTE: "Full Manual" and "Auto Reverse" cannot exist simultaneously, so (21) and (23) cannot both be 1.

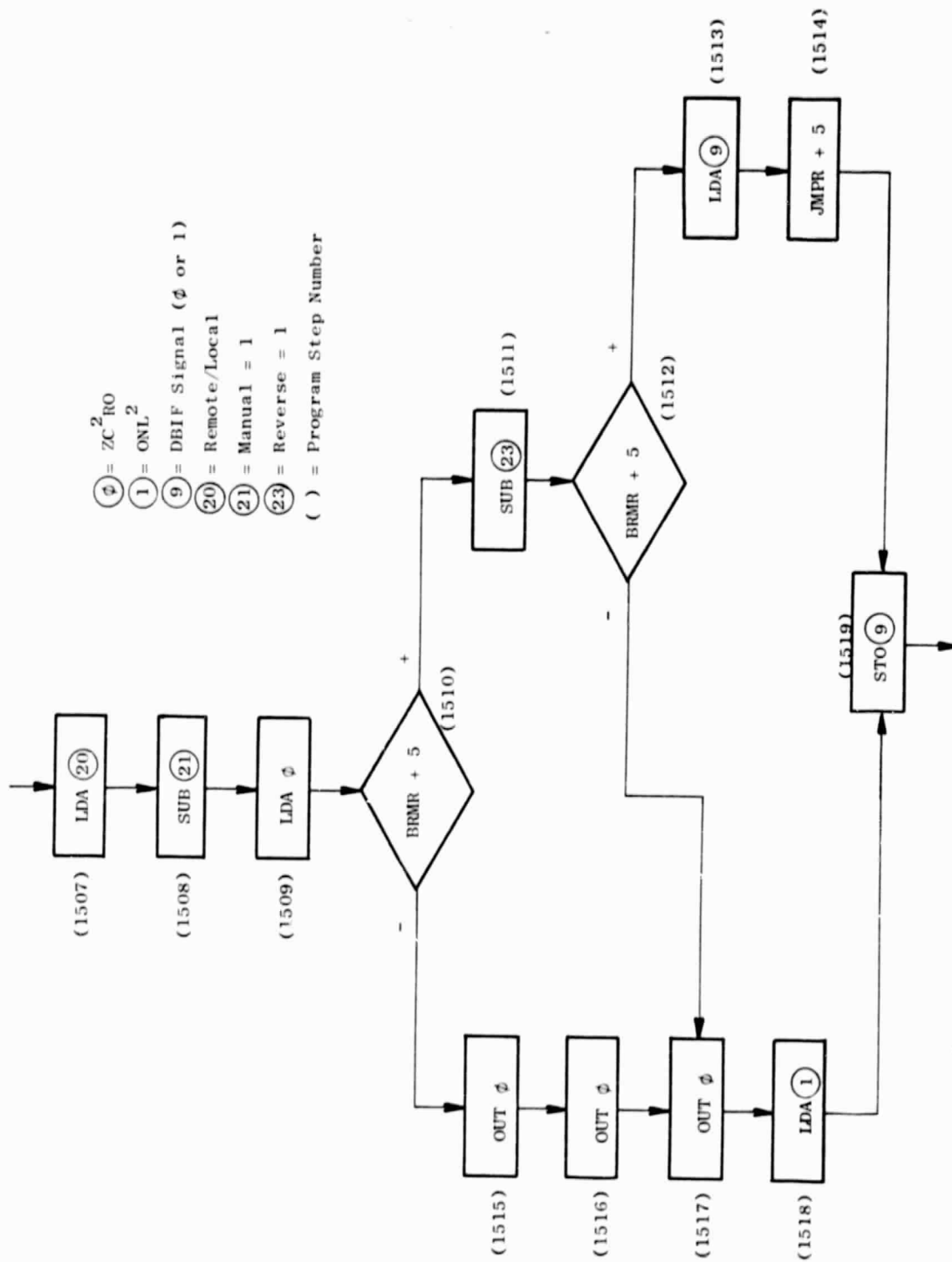


Figure 63. Flow Chart of Forward Mode Reverse Interlock Activation Logic.

5.6 VARIATIONS FOR FLIGHT DESIGN

For a flight design, the digital control would change significantly. One obvious change would be the elimination of the many extra functional features included in the experimental control providing testing flexibility and adjustability.

Also, development programs are currently being conducted to define advanced designs which take advantage of medium- and large-scale integrated chips (MSI and LSI) and advanced hybrid packaging techniques uniquely suited for on-engine environment.

Work is currently being done on an advanced packaging development program aimed at reducing the amount of internal wiring by using MSI and LSI chips and mounting them on alumina multilayer interconnection boards. The program also includes development of improved methods of transferring heat from electrical elements. This program is aimed primarily at improved reliability but will also offer weight and volume payoffs.

All things considered, it is estimated that the weight and volume of a flight-design digital control would be reduced approximately 40% from the current experimental design.

5.7 OFF-ENGINE DIGITAL CONTROL ELEMENTS

Description

The QCSEE digital control subsystem includes three off-engine components which furnish command and adjustment inputs to the engine-mounted digital control and display data transmitted from that unit. These three components, which will be located in the engine test control room, are designated the Interconnect Unit, the Operator Control Panel, and the Engineering Control Panel. Basic functions of the units are outlined below.

Interconnect Unit - This unit serves as a signal processing, coordinating, and switching device between the outer two off-engine digital control units, a remote digital computer supplied by NASA, transient data recorders, and the engine-mounted digital control.

Operator Control Panel - This unit is intended for use by the engine operating crew. The panel is arranged as shown on Figure 64 and includes the following features:

- Nine digital indicators which continuously display the variables shown.
- Six lighted segment pushbuttons for selecting the digital control operating mode.
- Lights which indicate whether an automatic or manual control mode is in effect.
- A light which indicates when digital control commands are originating from the remote NASA computer.
- Lights which indicate whether all manipulated variables are being controlled normally or if one of more is on a limit. When operation on a limit is indicated, the limit can be identified by means of a selectable digital readout on the Engineering Control Panel.
- A light which indicates when any of the faults of Table X have occurred. The fault or faults can be identified by means of a selectable digital readout on the Engineering Control Panel.
- A two-element pushbutton switch for switching to a recovery position which quickly introduces a predetermined set of control commands in case of emergency - or when desired for rapid transients during manual operation.
- A two-element pushbutton switch for operation of the VSV reset.
- Three potentiometers which provide independent control of fan pitch, fan nozzle, and power demand in manual operating modes.
- Two potentiometers for automatic mode power demand with push-buttons to allow instantaneous switching from one to the other, thus allowing power-demand step changes.

Engineering Control Panel - This unit is intended for use by an engineering test monitor. The panel is arranged as shown on Figure 65 and includes the following features:

- A selected digital display for indicating any one of the variables listed in Table IX.

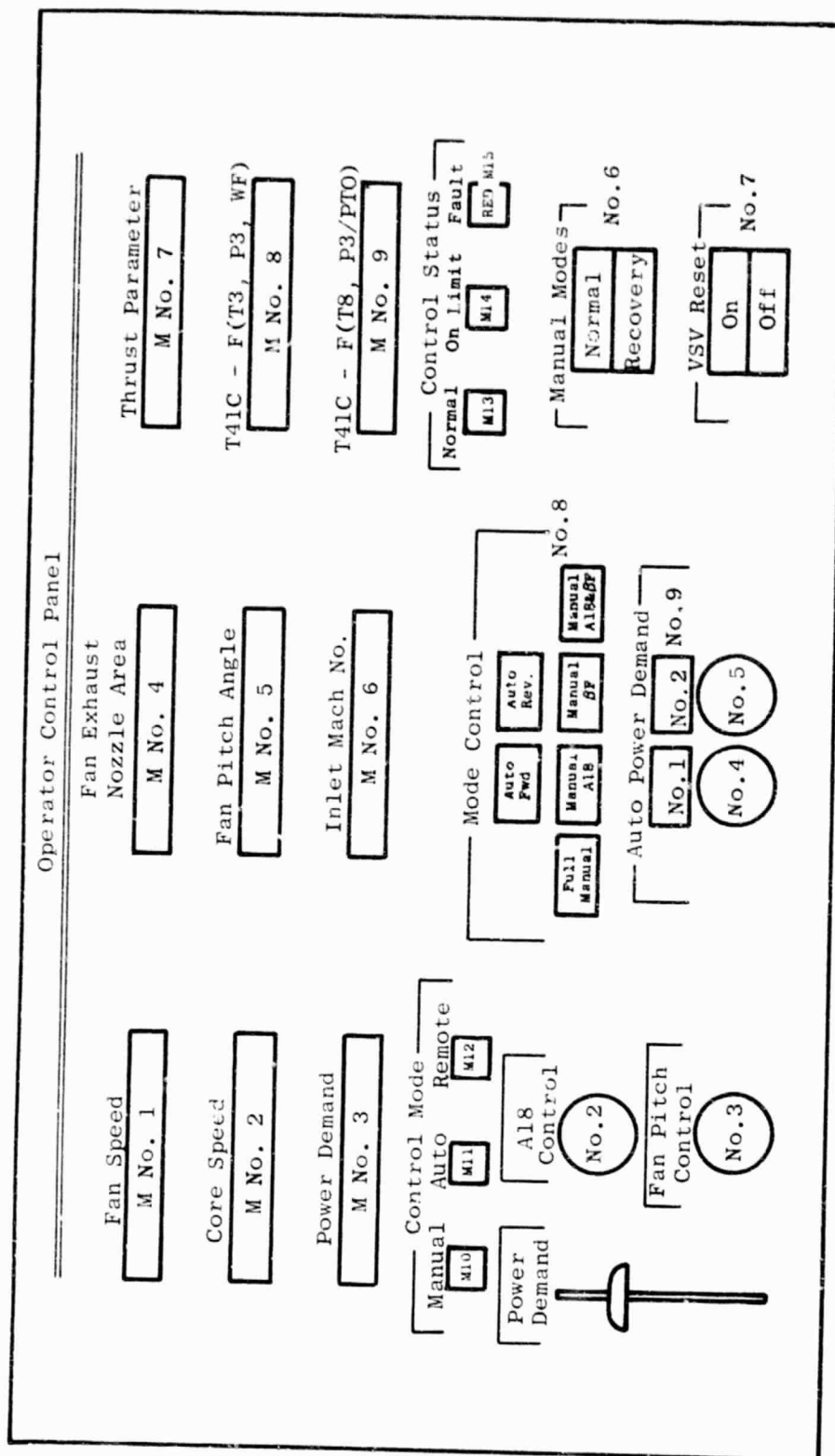


Figure 64. Operator Control Panel.

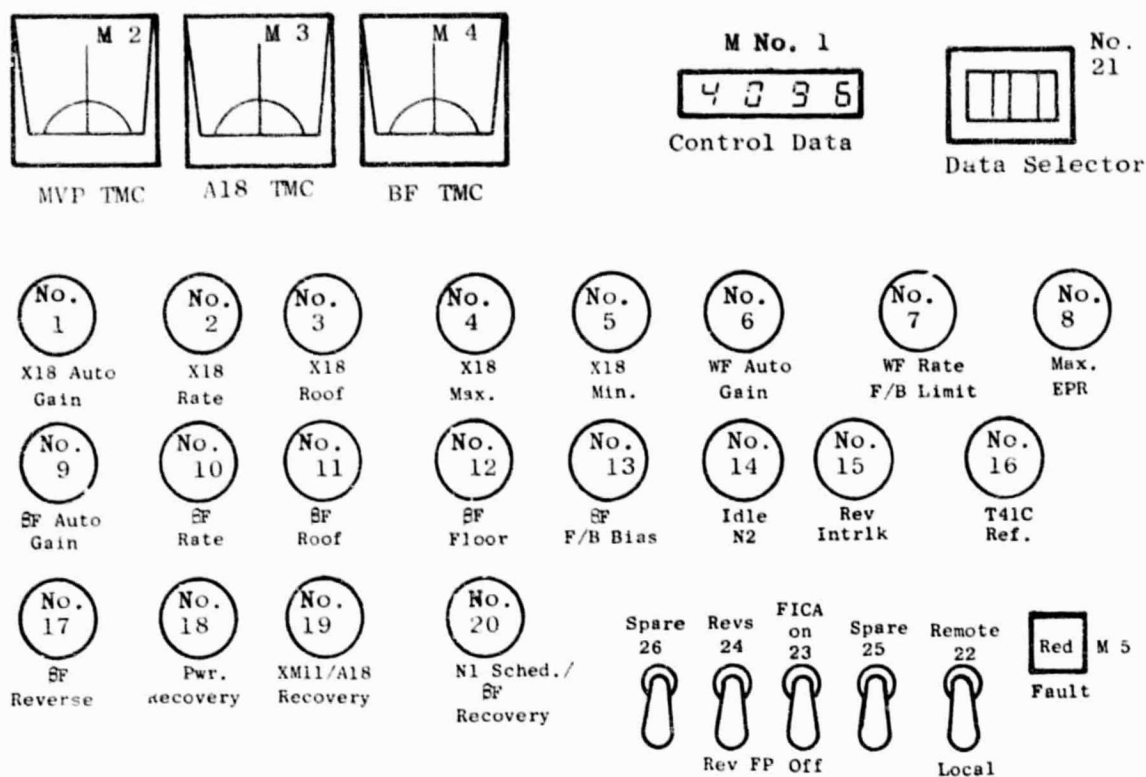


Figure 65. Engineering Control Panel.

- Three milliammeters which continuously indicate current to the torque motor servovalves controlling the manipulated variables.
- A fault light equivalent to the one on the Operator Control Panel.
- Five toggle switches, one for selecting the applicable fan pitch actuation configurations (i.e., reverse-thru-stall or reverse-thru-fault pitch), one for selecting the source digital control commands (i.e., remote NASA computer or "local" off-engine digital control units), one for activation of automatic fault correction features, and two spares.
- Twenty potentiometers for making on-line adjustments to the digital control logic.

Functional Design

A functional block diagram of the off-engine digital control components is shown on Figure 66 and a general functional description is given below.

Input signals to the off-engine components are in both analog and digital form. All digital signals are transmitted by differential line drivers and received by a differential line receiver over twisted wire pairs. All analog signals transmitted are buffered by low-output impedance amplifiers and received by operational amplifiers in a differential configuration.

The analog multiplexer located in the Interconnect Unit consists of two 16-channel multiplexer chips capable of handling all the analog inputs from the Engineering Control Unit and the Operator Control Unit. Each of the inputs are capable of being addressed separately in a predetermined sequence at a particular time determined by the digital control. The output of the multiplexer circuit goes to a sample-and-hold circuit and awaits AD conversion.

All analog signals coming into the Interconnect Unit are converted to a digital word upon command from the digital control just prior to being transmitted to the digital control.

Digital multiplexing at the data bus is accomplished by employing tristate logic devices to provide inputs to the bus. The three states are high output, low output, and high impedance. Placed in the high-impedance state, the devices can be essentially deactivated, while the other two states are used to define logic levels in the transmission mode. All but

one of the devices whose outputs are connected to the data bus shown in Figure 66 are placed in the high-impedance state; the remaining device will be in the transmission mode. In this manner, a single input to the data bus is made available to the digital serializer as a 12-bit parallel data word.

The digital serializer is a twelve-bit shift register which is parallel loaded upon command. Subsequently, the data are shifted one bit at a time into the transmission system.

The isolation of signal and signal grounds is accomplished by means of optical isolators. These devices convert electrical signals into light internally, and then reconvert the light signal back into electrical signals. This process breaks all electrical connection from input to output while maintaining the signal information. The purpose of the isolators is to assure that ground loops, power differences between systems, and signal noise are reduced to a minimum.

The power supply for the off-engine units is derived from a 400-Hz source of 300 volt-amps or more. In the Interconnect Unit, plus and minus fifteen volts are developed and routed to the Engineering Control Unit and the Operator Control Unit. Analog circuits requiring the use of ± 15 volts in any of the three units use this regulated supply.

The +5 volts supply is generated separately and used as a logic supply in each of the three units.

There are two isolated +5 volt logic supplies in the Interconnect Unit derived specifically to be used in the isolation technique used in this system.

The Operator Control Unit develops -10 V and -12 V for the scaling microprocessor. The +5 volts are developed for a logic supply and the 12-volts a.c. used to light the front panel pushbutton switches and indicators.

The Engineering Control Unit develops -10 V to reference the potentiometers. The +5 volts are used as a logic supply while the 10-volts a.c. is the deriving source as well as the supplier of the one lighted indicator

on the front panel. The ± 15 volts are used to derive the -10 volts as well as operating analog circuits.

The packaging of the off-engine digital control components is designed to operate in a control room environment. Both mechanical and electrical systems are designed for control room use only.

6.0 HYDROMECHANICAL CONTROL

6.1 PURPOSE

The purpose of the hydromechanical control is to provide backup control of engine fuel flow, to control core compressor stator vane position, and to provide the fuel-handling interface for operation of several engine limits utilized in the control system. The basic fuel flow control is provided by electrical signals to a torque motor on the hydromechanical control.

6.2 DESCRIPTION

The QCSEE hydromechanical control is an F101 main engine control which contains appropriate modifications applicable to the unique requirements of the QCSEE control system and engine. The control is capable of performing the computation (hydromechanical) and fuel metering necessary to control engine combustor fuel flow and compressor stator vane positioning. Woodward Governor Company is the vendor source for this control. The modified control is identified by General Electric Source Control Drawing 4013177-403P01.

The modified F101 control will perform the following subsystem functions:

- Modulate core engine fuel flow to govern core speed as a backup to the digital control.
- Schedule acceleration and deceleration fuel flow limits.
- Schedule variable stator vane position.
- Provide positive fuel flow shutoff and limit core engine overspeed.
- Limit compressor discharge pressure.
- Reduce fuel flow in proportion to electrical signal from the digital control as the primary fuel control method.
- Provide power lever position intelligence to the digital control.
- Provide minimum fuel system pressurization.
- Provide fuel flow shutoff to limit fan overspeed in response to electrical control signals from the digital control.

- Provide core stator vane reset in response to electrical control signals from the digital control.
- Provide electrical metering valve position intelligence to the digital control.

Hydromechanical Control Inputs and Outputs

The inputs to and outputs from the hydromechanical control are listed below:

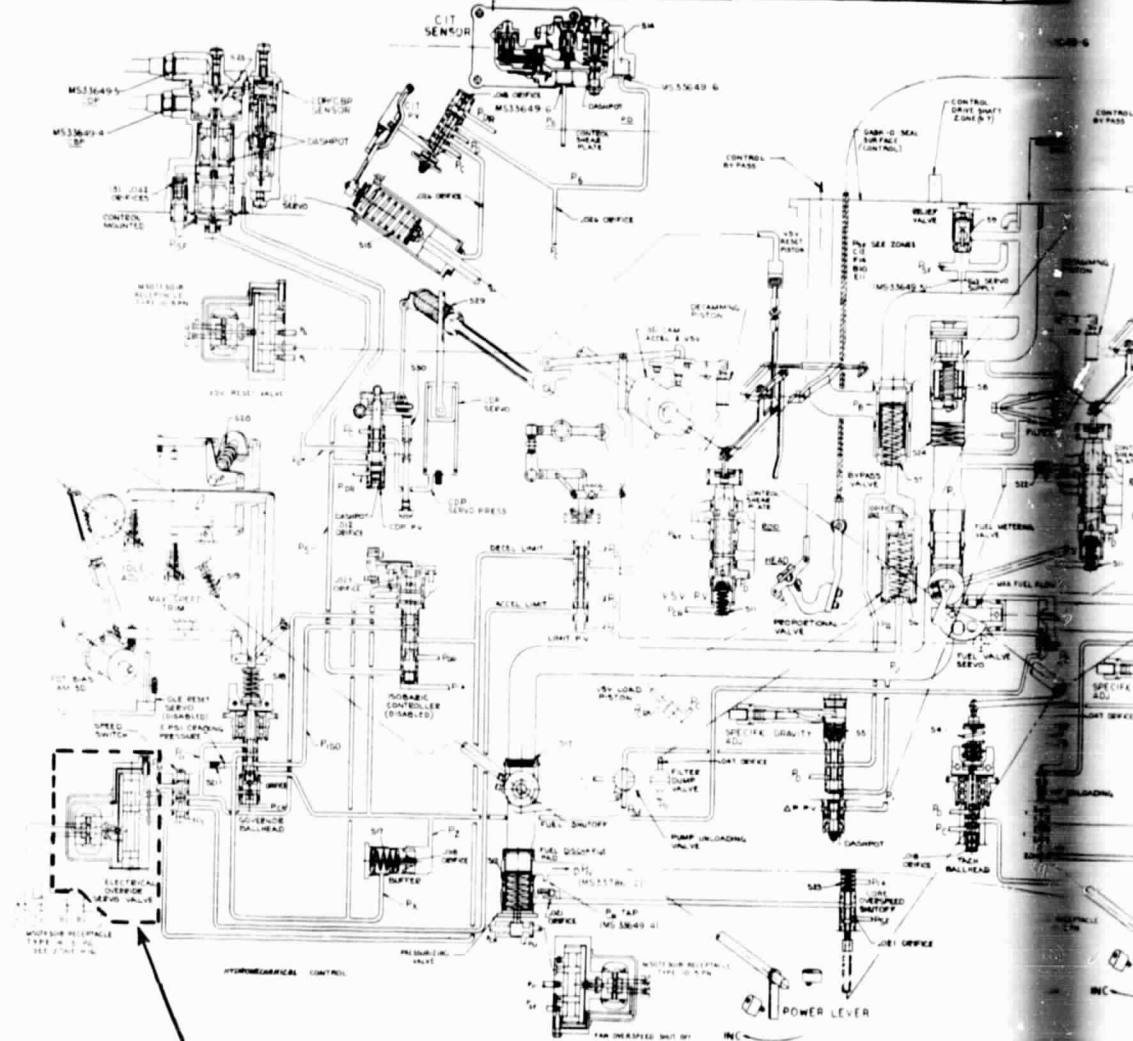
<u>Inputs</u>	<u>Outputs</u>
• Pump discharge fuel flow	• Metered engine fuel flow
• Power lever angle	• Bypass fuel flow
• Core engine drive speed	• Stator vane actuator control pressures
• Compressor discharge pressure	• Power lever electrical position signal
• Core inlet air temperature	• Metering valve electrical position signal
• Core stator actuator position	
• Electric fuel flow control signal	
• Electrical fan overspeed signal	
• Electrical stator reset signal	

6.3 OPERATION

The hydromechanical control mechanization arrangement which indicates implementation of the various control functions is depicted on Figure 67 for the modified F101 fuel control. The following functional description references Figure 67.

Backup engine speed control is accomplished with the same basic governing components that have been used in previous Woodward Governor Company units; a flyweight system that provides isochronous speed governing (Zone C-14). In normal operation, this system is overridden by use of a two-stage torque

ORIGINAL PAGE IS
OF POOR QUALITY



Fail-Fixed Servo Valve
Option Can Be Applied Here

Figure 67. Hydromechanical Co.

FOLDOUT FRAME /

motor servovalve to reduce engine speed in response to the electrical signal from the digital control (Zone B-15). Engine speed can only be reduced by action of the electrical torque motor override system, thereby requiring the throttle to be set at 100% to enable the system. This is important because, should any malfunction occur in the electrical subsystem, complete control of engine speed is still available with the hydromechanical system.

It should be noted at this point that the torque motor servovalve can be replaced later in the program with a fail-fixed servovalve which, for the most probable electrical malfunctions (i.e., zero signal or maximum signal), would cause the metering valve to remain fixed. This is described in more detail later.

The acceleration and deceleration limiting systems use a conventional WF/P3 3-D cam (Zone E-12) limiting schedule generated as a function of engine speed (Zone B-9), compressor inlet temperature (Zone J-12), and compressor discharge pressure (Zones F, H, J-13, and 14). The opposite side of this same 3-D cam also contains the reference schedule for the core stator vane servo. Stator servo position reference, a function of core speed and inlet temperature, is compared to actuator feedback position in a linkage system (Zone E-11), and the error positions the stator servo pilot valve (Zone E-11) to port flow and pressure to the stator actuation pistons.

The fuel metering system is designed to use simple control elements for multiple functions. The main metering valve is a variable area shoe and rotor (Zone D-10). A constant pressure drop is maintained across the metering valve by a bypass-type proportional-plus-integral regulator (Zones C, D, and E-10). The bypass system also provides the pump unloading function during shutdown (windmilling) conditions (Zone B-12). For reliability purposes, the unloading function is positively locked out during the normal engine operation between idle and maximum speed. The fuel shutoff valve (Zone B-12), similar to the fuel valve rotor, is integral with and actuated by the power lever shaft (Zone A-11). Movement of the power lever to the "off" position mechanically actuates the pump unloading function which provides a 1.72×10^6 N/m² (250 psi) pump discharge pressure during windmilling conditions for servosystem regulation purposes.

A pressurization valve (Zone B12), used to provide minimum back pressure to ensure adequate servosystem pressure during low metered flow conditions, is provided as part of the control package.

The temperature sensor (shown schematically, Zone J-12) provides the control with a hydraulic signal that is proportional to temperature. The sensor will be located to sense core engine inlet temperature for the QCSEE engine. To meet the response speed requirements, a high-conductivity zirconium alloy (Zircaloy II) is used for the gas-filled coil. The gas-filled coil senses temperature which expands a bellows inside the sensor body. The bellows applies a force at one end of the beam balance system which then changes the area at the variable metering orifice to produce a signal for control usage in acceleration and stator schedule computation. The sensor is designed for the following conditions:

- Temperature range -55.9° C to 260° C (-65° F to 500° F)
- Response 0.82 sec at $1.72 \times 10^2 \text{ kg/sec/m}^2$
 (35.2 pps/ft^2) airflow
- Accuracy $\pm 2.07 \times 10^4 \text{ N/m}^2$ ($\pm 3 \text{ psi}$) about a
 linear output schedule
- Sensitivity $2.02 \times 10^{-4} \text{ }^{\circ}\text{C/N/m}^2$ ($2.5^{\circ} \text{ F/psi}$)

Modifications to the control incorporated for QCSEE use will include the following:

- 3-D Cams - Cam schedule contours have been changed to match QCSEE engine requirements (Zone C-15 and E-12).
- Compressor Discharge Bleed Compensation - The acceleration schedule multiplier function of CDP/CBP ratio established by the CDP/CBP sensor (Zone H-14) has been altered by disabling the CBP function through removal of the CBP sensing bellows.
- Emergency Fuel Shutoff - An electrical-to-hydraulic torque motor servovalve has been added to the control to accomplish shutoff of engine fuel flow in response to an electric fan overspeed signal. This function is accomplished by switching pump discharge pressure into the reference chamber of the system pressurizing valve (Zone B-12). A similar action is taken in the event of core engine overspeed through the action of the existing overspeed shutoff valve (Zone B-10). A low-power torque motor operated switching valve is mounted on the pressurizing valve cover to accomplish the fan over-

speed protection. The flow gain of the output stage of the shutdown device has been selected to cause closure of the pressurizing piston within 20 milliseconds after the electrical overspeed signal is sensed. This shutdown action will temporarily place the fuel pump on pressure relief during the engine coast down.

- Stator Reset - The Block I F101 controls contain provisions for an electrically operated reset of core stator vane position. The reset is initiated by signalling a torque motor servovalve (Zone F-14). The stator reset servovalve switches reference pressures to the VSV reset piston (Zone F-11) to reset the stator control valve feedback linkage.
- Metering Valve Position Signal - The control provides an electrical rotary position transducer on the metering valve shaft to signal metering valve angle (Zone E-9). For the QCSEE units, a position transducer identical to the power lever position transducer (Zone H-17) is used for the metering valve transducer.
- Electrical Fuel Override Authority - The present F101 controls provide a core speed floor limitation on the electrical fuel flow override through the action of a speed switch valve (Zone C-14) which is actuated by the core speed tachometer (Zone B-9). This speed floor setting will be disabled for QCSEE by blocking the speed switch valve (Zone C-14) to the desired position, thereby providing for full fuel control by the digital control.
- Fail-Fixed Servovalve (later development, not on first control) - As seen by Figure 68, the fail-fixed servovalve is basically a standard two-stage electrohydraulic servovalve. It differs only in the configuration of the second-stage spool valve and its attendant porting. As with a conventional servovalve, spool position is a function of input current.

The valve is shown in the zero current condition. Both load lands of the spool valve have 0.015 cm (0.006 in.) overlaps thus hydraulically locking the actuator in position. As current is increased, the spool valve will stroke through the overlap and begin porting high-pressure flow to the metering valve actuator. Valve porting is timed so that at 50% rated current the areas of the metering valve port are equal to the areas of the supply and return ports, and will flow to and from the actuator effectively through two equal orifices in series. Flow is a maximum. As current is further increased, the metering valve land closes off: flow to the metering goes to zero, and a new fluid lock on the actuator is established. As the input current is reduced to zero, flow is again established to the actuator causing motion in the same direction as with increasing current. The actuator will be driven in small steps in one direction if the input is a series of square waves stepping from zero to rated current and back to zero. If the polarity of the input current is changed, the actuator will move in the opposite direction.

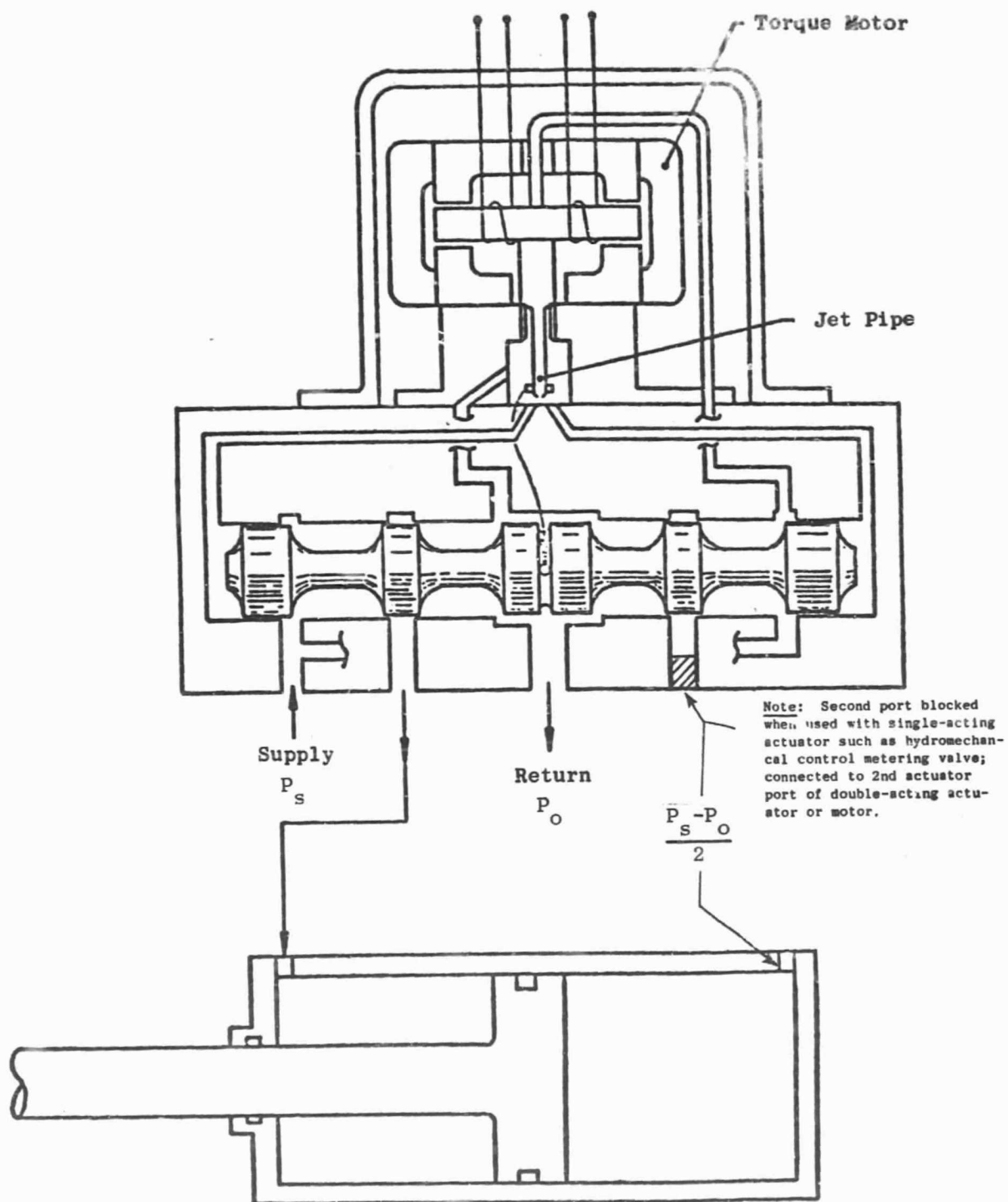


Figure 6b Fail-Fixed Servovalve.

C-3

The preferred mode of operation is to drive the servovalve at a constant input frequency (from -80 mA to +80 mA) above the frequency to which the valve can fully respond. The valve will average the plus and minus "on time". By limiting the minimum and maximum on-time to 25% and 75%, the valve will behave as an analog device in response to pulse-width modulation. Flow will be proportional from zero to maximum for a 25% to 75% pulse-width demand.

Should the valve receive a d.c. level zero current or a ± 80 mA current signal, indicative of an electrical failure, flow to or from the actuator will be stopped and a fluid lock condition established to hold the actuator to its position at the time of failure.

6.4 INSTALLATION

The hydromechanical control will be mounted on the F101 fuel pump similar to Figure 69. The pump is V-band flange-mounted to an F101 gearbox pump drive pad. Through-shafting is used to provide core speed input to the control drive spline.

The core stator vane position mechanical feedback interface will be used identical to the F101 control installation. All hydraulic and pneumatic piping interfaces to the control will be identical to the F101 configuration, except that the PCBP pressure port is unused.

6.5 VARIATION FOR FLIGHT DESIGN

The initial flight design QCSEE would have a hydromechanical backup to the primary digital electronic control, but it would be simplified significantly from the modified F101 fuel control being used on the experimental engine. The exact nature of the simplified backup hydromechanical unit will be the subject of further study with simplified elements being devised for speed governing, transient fuel control, and VSV control.

For a second-generation QCSEE, it is expected that the digital electronic technology would be developed (and proven by operational experience) to be better and more reliable than current hydromechanical controls and that the hydromechanical backup would be eliminated altogether.

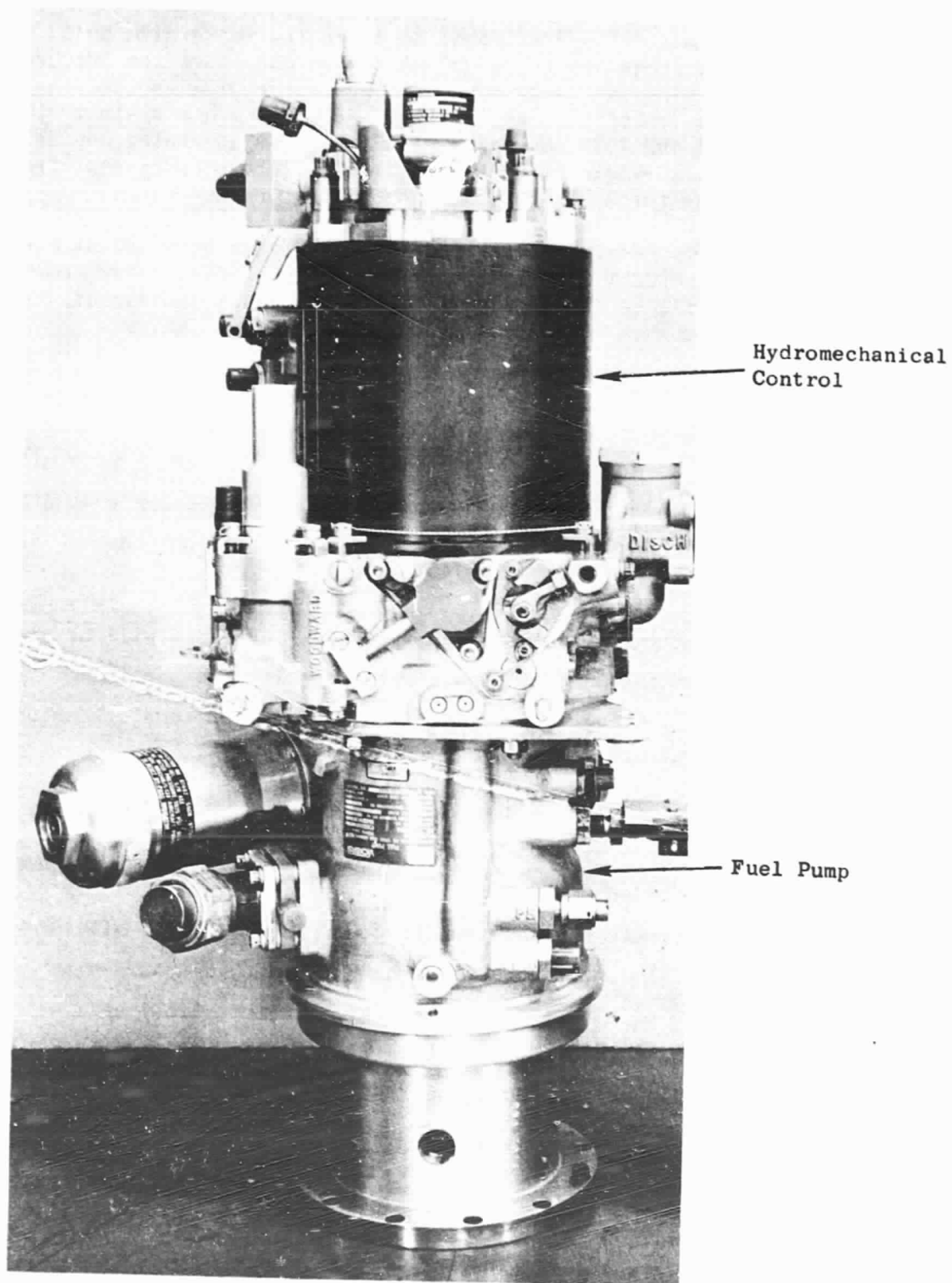


Figure 69. Hydromechanical Control and Fuel Pump.

7.0 FUEL DELIVERY SYSTEM

7.1 PURPOSE

The purpose of the fuel delivery system is to pump, filter, and meter the fuel flow required for core engine combustion at the pressures dictated by engine burner conditions and to provide a means of preventing fuel component overboard drain leakage.

7.2 DESCRIPTION

The QCSEE fuel delivery system is primarily based on F101 engine main fuel system components including the hydromechanical control and the temperature sensor described in Section 6.0. The fuel delivery system includes the following elements:

- Fuel Control (Metering Section)
- Main Fuel Pump
- Fuel Filter
- Drain Eductor and Flow Regulator

These elements are interconnected as shown in the schematic of Figure 70.

7.3 OPERATION

The fuel delivery system accepts fuel flow and pressure provided to the system pump intake by the test facility or aircraft fuel feed system and provides the pumping pressure rise required to deliver metered flow to the engine combustor as described in Section 7.6. Pump discharge flow is filtered by a 74 μ m absolute full-flow barrier filter prior to entering the hydromechanical control inlet. The metering section of the hydromechanical control sets the metering valve area in response to various control signals and limits as described in Section 6.0. Flow is metered by establishing a constant metering pressure drop across the metering valve area through the action of a fuel bypassing regulator which returns excess intake flow not required for metered demand to the fuel pump interstage pressure. Pump

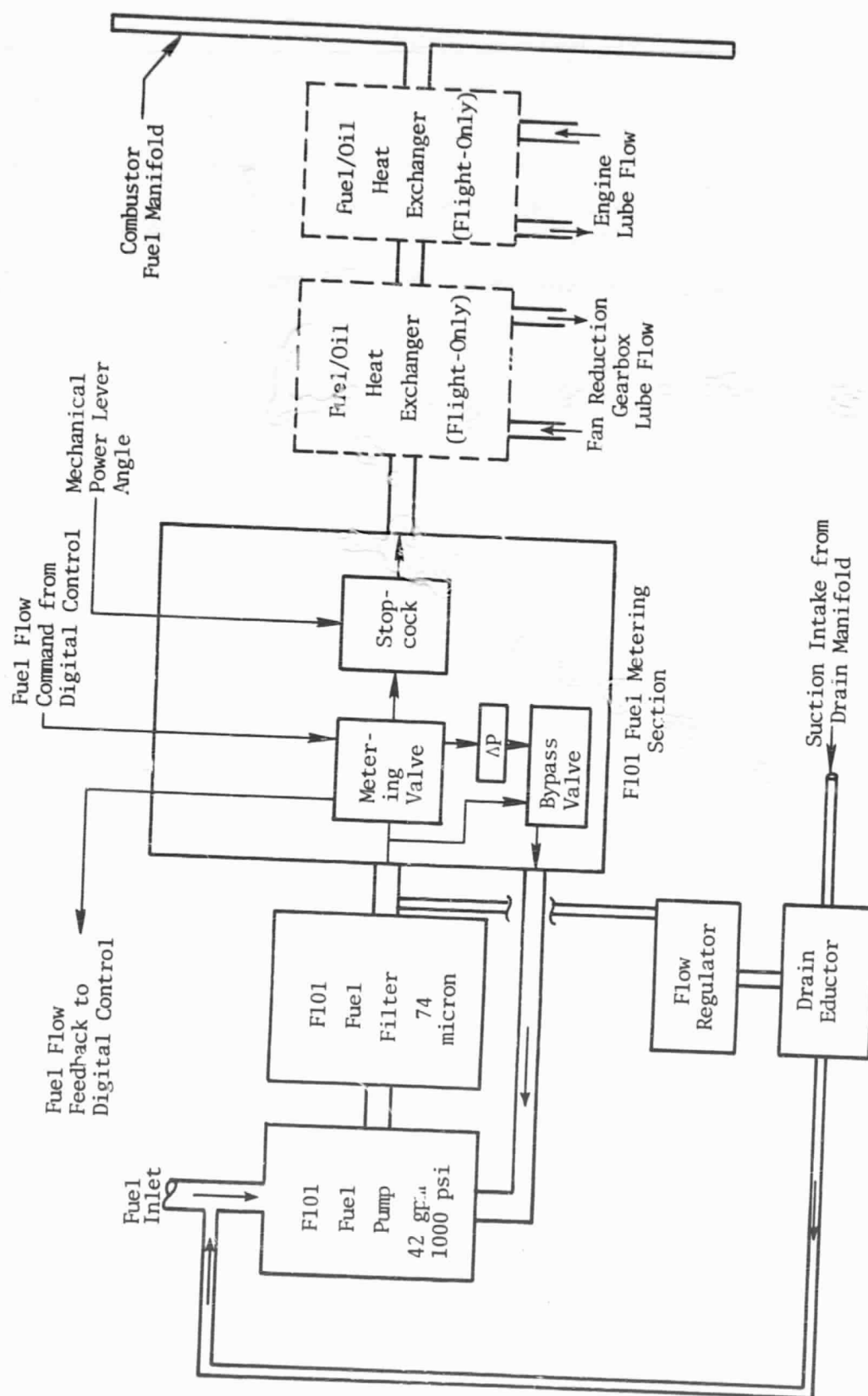


Figure 70. Fuel Delivery System.

discharge pressure in the system is established by the summation of engine burner pressure, injector pressure drop, and the maximum metering control pressure drop. A minimum control inlet pressure for servo pressure regulation is established by a control discharge pressurization valve as described in Section 6.3. The control contains a fuel cutoff valve downstream of the metering valve which is directly actuated by mechanical power lever input angle. A maximum metering flow area for the metering valve is established by a control mechanical stop which limits maximum metered flow to 10,350 pph.

The system also incorporates a jet-pump drain eductor which is powered by regulated jet flow extracted from pump discharge and which pumps jet flow and drain manifold leakage back to fuel pump inlet. The eductor maintains a partial vacuum at all times in the drain manifolds to prevent fuel seal leakage to overboard.

7.4 VARIATION FOR FLIGHT DESIGN

Variations within the fuel delivery system for a flight design would involve these component changes:

- Resize the fuel pump flow capacity downward to more exactly match the engine cycle requirements. The F101 fuel pump is oversized for QCSEE needs.
- Simplify the metering control as described in Section 6.5.
- Add an engine-mounted fuel-oil heat exchanger as described in Section 7.8. QCSEE experimental engines use slave heat exchangers for lube-oil cooling.
- Relocate the drain eductor to the core engine compartment below the lowest seal drain elevation and consolidate the flow regulator and jet pump into a single component package.

7.5 FUEL METERING SECTION

The metering section of the fuel control is as described in Section 6.0.

7.6 MAIN FUEL PUMP

The purpose of the fuel pump is to raise the pressure of metered system flow to a level suitable for metering control and delivery into the engine combustor.

The fuel pump is a standard F101 main fuel pump unmodified. It is a balanced vane design of fixed displacement and contains an integral centrifugal booster stage to charge the vane intakes. Sizing of the fuel delivery system is indicated by the fuel pump characteristics listed in Table XIV. A cross section view of the pump is shown on Figure 69 (Zone F-7).

The pump operates to provide the pumping performance ratings shown in Table XIV. (Pump installation was described in Section 6.4.)

7.7 FUEL FILTER

The purpose of the fuel filter is to filter pump discharge flow to a 74 μm level to protect the fuel control metering and injection system against larger foreign particles.

The main fuel filter is a barrier, through-flow-type of stainless steel wire mesh. It is mounted on the main fuel pump and has a clogged filter bypass valve, a service shutoff valve, and an impending bypass indication button. Design features are:

Rated Flow	50.4 gpm
Filtration (absolute)	74 μm
Impending Bypass Indication Pressure	22 psid
Bypass Valve Cracking Pressure	35 psid
Element Type	Disposable

Fuel enters the filter, flows through the element mesh, and is discharged from the center of the element. If the element is clogged, the bypass valve opens allowing unfiltered fuel to flow to the system. The impending bypass indicator button extends at a pressure level equivalent to approximately 80%

Table XIV. Fuel Pump Characteristics (FI01)

Main Fuel Pump

Boost Element	Vane Element
6690	6690
6891	6891
$2.7 \times 10^{-3} \frac{\text{m}^3}{\text{sec}}$ (42.8 gpm) at 107.2° C (225° F)	$2.7 \times 10^{-3} \frac{\text{m}^3}{\text{sec}}$ (42.8 gpm) at 107.2° C (225° F)
$2.76 \times 10^5 \text{ N/m}^2$ (40 psi) min.	$\approx 6.65 \times 10^6 \text{ N/m}^2$ (≈ 964 psi)
$3.45 \times 10^5 \text{ N/m}^2$ (50 psia)	$6.21 \times 10^5 \text{ N/m}^2$ (90 psia)
$1.49 \times 10^3 \text{ W}$ (2 hp) max.	Overall Efficiency = 0.72 at Design Point

Rated Speed, rpm

Maximum S.S. Speed, rpm

Rated Flow
(Delivered Flow at
Service Limit at
Rated Speed)

Rated ΔP at
Rated Flow

Rated Inlet Pressure at
Rated Flow and Speed

Power Loss at Rated Speed

of filter life. The service shutoff valve seals off both the inlet and the discharge fuel flowpaths through the filter to prevent fuel leakage when the filter bowl is removed to service the filter element.

Location of the fuel filter is shown on Figure 70.

7.8 FUEL-OIL HEAT EXCHANGER

The fuel-oil heat exchanger provides the means for transferring heat from the engine lube system, fan reduction gearbox, and hydraulic system to the fuel. In addition to cooling the oil, the heat exchanger serves to heat the fuel under cold operating conditions in order to avoid the possibility of fuel system icing.

An off-engine-mounted slave oil cooler will be used for the experimental engines. The slave cooler uses water for cooling instead of fuel. The unit is a stainless shell-and-tube design, qualified and in production for the GE LM2500 engine and used on shipboard applications. The slave cooler has a heat transfer capability approximately three (3) times the estimated heat load of the QCSEE engine. The unit consists of 332 0.953-cm (0.375-in.) dia. tubes (each 0.610 m [2.0 ft.] long) and 9 crossflow oil baffles. The cylindrical shell is 25.4-cm (10-in.) dia and 0.610 m (2.0 ft.) long. Drains are provided to avoid water freezing during winter operation.

Water is routed through the tubes and makes four passes. Oil flows over the tubes and makes 10 cross-counterflow passes. A waterflow of 100 gpm may be used at a pressure drop of 10 psid.

The slave oil cooler is located and mounted on the test stand superstructure above the engine.

The flight engine will use a fuel-oil heat exchanger located in the gearbox and accessories area of the engine. The heat exchanger will consist of two (2) cores with fuel flowing in series from one core to the other. Fan reduction gearbox oil operating at a lower temperature level than engine lube system oil will flow through the first core. Lube system oil will flow through the second core. At present, a nonbrazed (mechanical tube joint) aluminum shell-and-tube oil cooler is contemplated for a flight engine. Other

designs will be considered on the bases of reliability, cost, size, and weight. Current weight estimate is 13.61 kg (30 lb.) for the entire unit.

7.9 DRAIN EDUCTOR

The purpose of the drain eductor is to pump fuel component seal drain leakage back to the fuel pump intake and to prevent dumping leakage overboard.

The drain eductor consists of a production CF6-50 design used to pump aircraft drain can fuel back to the fuel pump inlet during engine coast down after stopcocking the engine. The CF6-50 part is identified as P/N 9070M89P02. A cross section view of the drain eductor is shown in Figure 71.

The drain eductor is used with an inline jet supply flow regulator which maintains a constant jet supply flow. The flow regulator is separately housed and is a standard Fluid Regulators Corp. design identified as P/N Q1547-01.

Pump discharge fuel pressure extracted from the filter discharge is supplied to inline flow regulator Q1547-01. The regulator maintains 550 pph constant flow to the drain eductor jet supply under varying pump discharge pressure conditions ranging from 250 psig to 1000 psig. Constant motive flow and pressure in the jet maintains constant jet-pumping characteristics in the eductor.

The constant motive pressure is applied to the jet supply port shown in Figure 71. Fuel drain manifolds are connected to the suction intake port; drain manifold flow is pumped through the suction check valve and into the suction chamber of the jet pump. Jet flow and suction flow mix in the jet diffuser and are returned to fuel pump inlet pressure at pressure levels up to 50 psig. A partial vacuum is maintained in the suction chambers and the drain manifold. The selector valve piston shown in Figure 71 is not used but is held to the right at all times by spring force, permitting continuous passage of the jet supply flow during pump operation. Seal leakage air and fuel vapor are continuously returned to fuel pump intake.

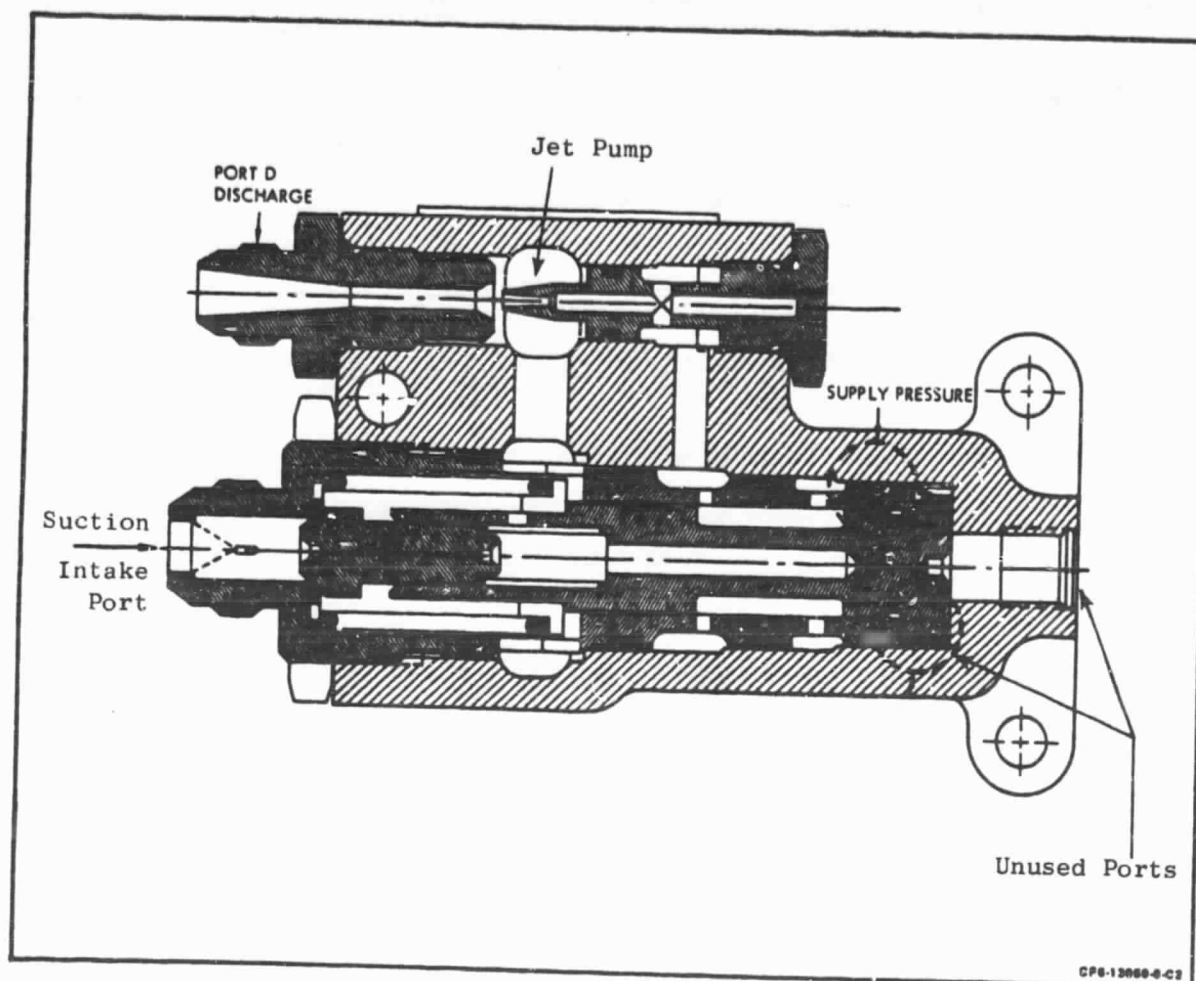


Figure 71. Drain Eductor Cross Section.

The flow regulator and drain eductor components are bolted to the fan cowl in the gearbox and accessory compartment. Stator actuator drain lines thus have a rise in elevation in order to reach the eductor system's suction manifold.

For a flight design, the eductor would be simplified to eliminate unused valving and to incorporate integrally regulated jet flow. The eductor would be relocated below the lowest drain point elevation in the core engine compartment.

8.0 VARIABLE GEOMETRY ACTUATION SYSTEMS

8.1 HYDRAULIC SUPPLY SYSTEM

The hydraulic supply system provides hydraulic motive power to the fan duct nozzle (A18) actuators and fan blade variable-pitch mechanism. The system consists of a hydraulic pump, boost pump element, filter, makeup filter, relief valve, and magnetic chip detector.

The UTW system is shown in Figure 72. A pressure-compensated hydraulic piston pump is driven by the accessory gearbox and provides varying flow output at constant pressure to servovalves which are part of the fan duct nozzle (A18) and variable-pitch systems. Pump output flow is determined by the demand from the servovalves, varying from actuator leakage at holding condition to maximum during the engine thrust reversal transient. The supply system is sized to provide peak transient flow for simultaneous operation of A18 and variable pitch at engine idle speed (65% of rated). Although pump maximum flow capability is proportional to engine speed, the output pressure is constant and virtually independent of speed or flow.

The hydraulic system receives and uses the same oil as the engine lube system. Once the hydraulic system is filled, however, it functions very nearly as an independent closed system. When oil leaves the pump to the servovalves at high pressure, oil is at the same time returning at low pressure from the servovalves. The servovalve incoming flow passes through a $1 \times 10^{-5} \text{ m}$ (10 μm) filter which provides a servovalve protection from hydraulic pump and engine lube system contaminants.

As the A18 actuators slew from head-end to rod-end position, there is differential displaced volume equal to the volume represented by the actuator piston rods. For a one second slew, this amounts to somewhat less than $1.89 \times 10^{-4} \text{ m}^3/\text{sec}$ (3 gpm) which must be made up from the engine lube system oil. Also, it is necessary to provide approximately $1.89 \times 10^{-4} \text{ m}^3/\text{sec}$ (3 gpm) to the pump during steady-state holding for pump cooling. Both of these functions, makeup and pump cooling, are provided by using an element in the engine lube pump as a makeup and boost pump to the hydraulic pump. A relief valve across

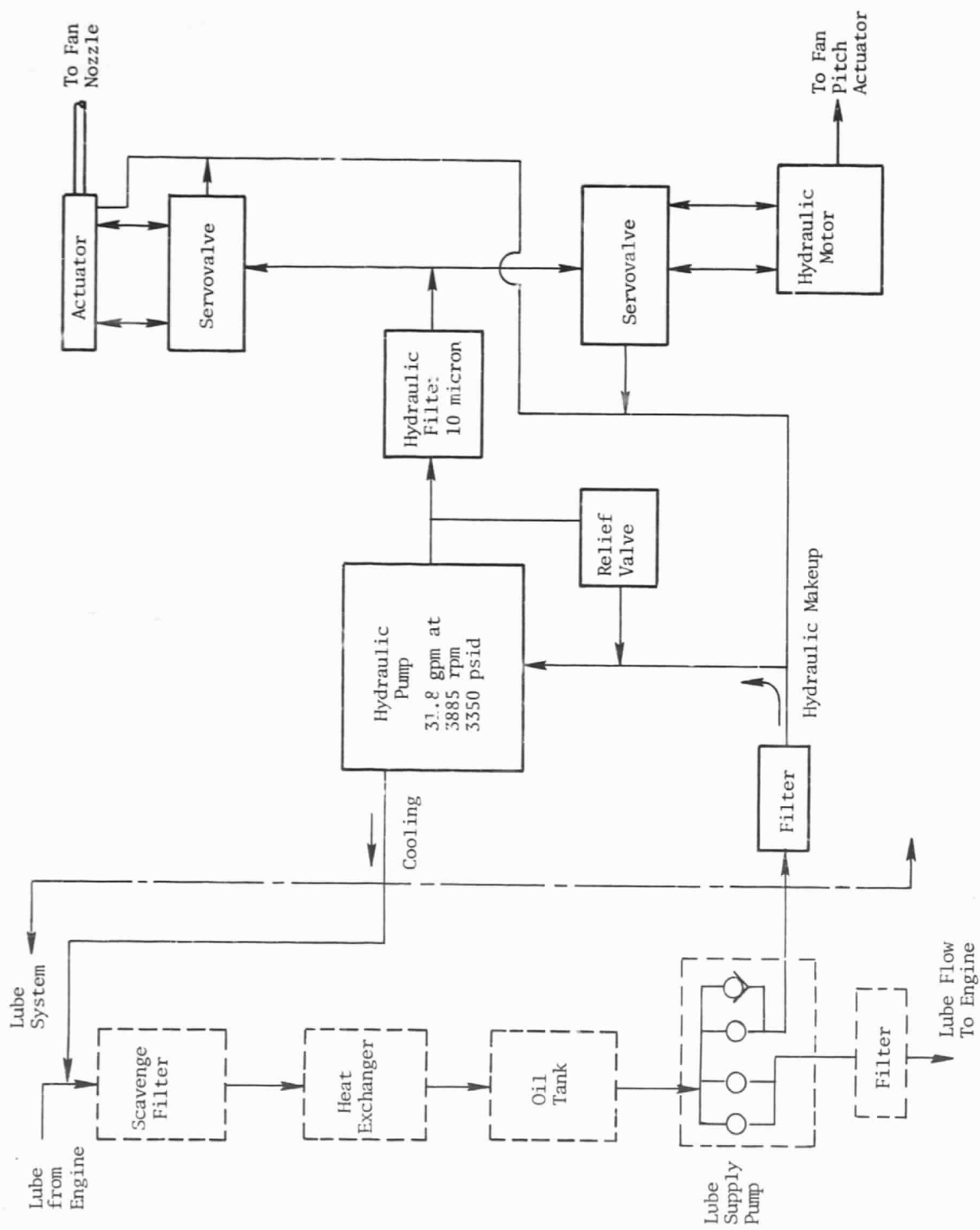


Figure 72. Hydraulic Supply System Schematic.

the lube pump elements acts as a pressure regulator so that the hydraulic pump inlet pressure is sufficiently high to avoid cavitation in the pump piston cavities. Hydraulic pump cooling is provided by virtue of mixing hydraulic oil with lube oil which passes through the engine oil cooler. Incoming hydraulic system makeup and cooling flow has been filtered to the 22 μ m level in an inline makeup flow filter. A magnetic chip detector is provided in the line returning cooling flow to the engine lube system so that any ferrous metal contaminants generated in the hydraulic system can be identified. A relief valve is provided to protect the high-pressure hydraulic components in the event of a pump pressure compensator failure.

As the engine is started, the hydraulic supply system flow output is at maximum in proportion to the engine speed. A servo demand decreases to zero, system pressure rises to a constant value independent of speed. With zero initial flow demand during start, the system pressure will reach rated value at approximately 2% engine speed resulting in a hydraulic pump input torque transient to approximately 1280 in.-lb. Torque will decrease to 200 in.-lb. at 20% speed and finally down to 100 in.-lb. at idle so long as flow demand is zero. At all conditions above idle speed, the hydraulic supply system will provide a near-constant pressure output (varying from 3350 psid minimum at maximum flow to 3500 psid at zero flow). Flow capability will be proportional to speed. Response time of the supply system, in terms of the time to establish rated output pressure after a step change in flow demand from minimum-to-maximum or maximum-to-minimum, is approximately 0.15 seconds.

8.2 HYDRAULIC PUMP

The pump provides varying flow output at constant pressure to servovalves which are part of the fan duct nozzle and variable-pitch systems.

The pump on the experimental engines is an ABEX Model AP12V-54 pressure-compensated piston pump. This model pump is an upgraded high-speed (6864 rpm) version of earlier model AP12V pumps qualified in production for the F-111 fighter aircraft and the CH-53 helicopter. The AP12V-54 was requalified in June, 1975 for use on a Boeing Vertol Co. application. The pump, shown in Figure 73, is compact in size and weighs 9.75 kg (21.5 lb.).

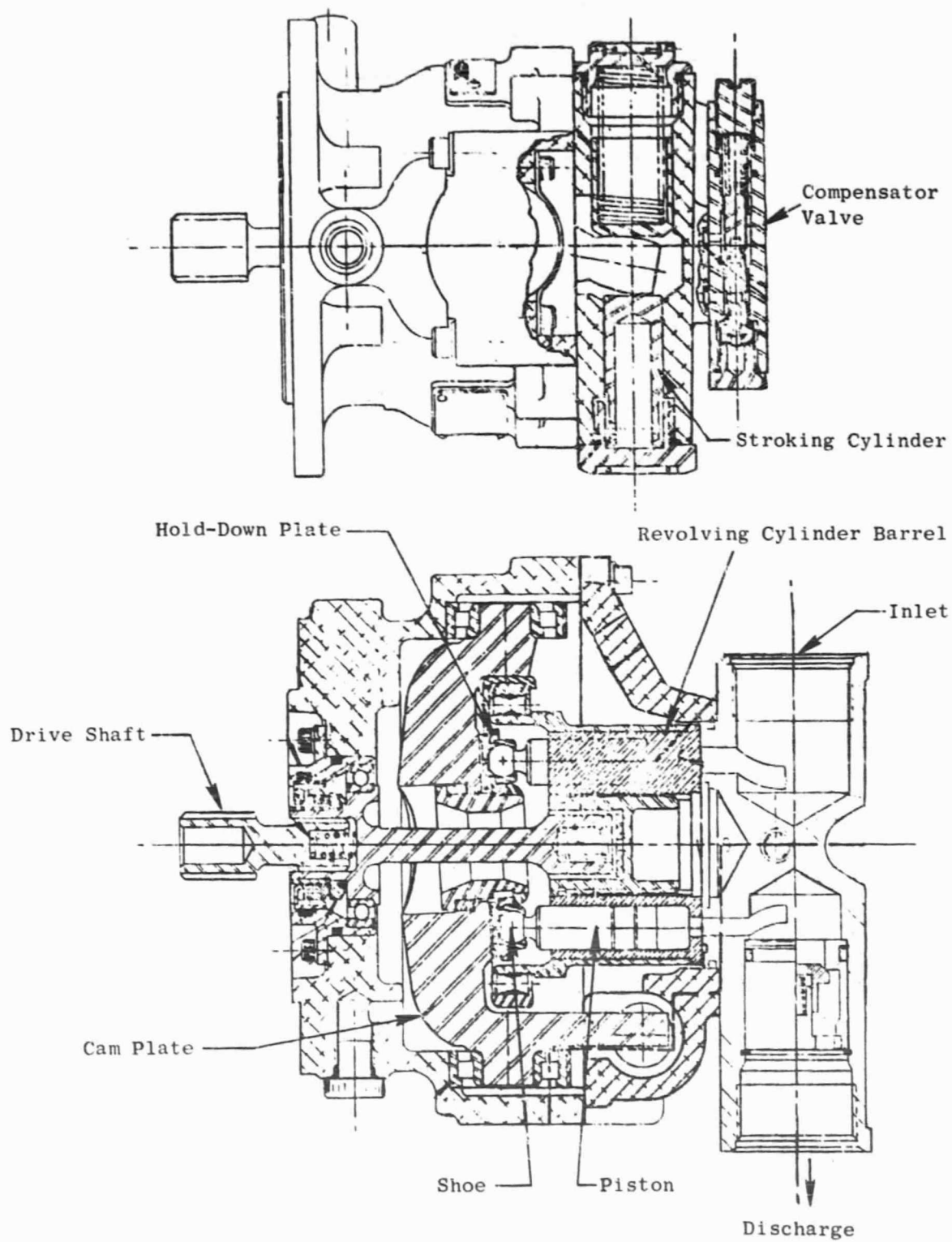


Figure 73. Hydraulic Pump.

ORIGINAL PAGE IS
OF POOR QUALITY

The pump is direct-driven off the engine gearbox through a splined shaft. Drive input is to a revolving cylinder barrel that contains nine (9) pistons. Pivoted shoes attached to the piston are supported on an inclined stationary cam plate which causes the pistons to reciprocate as the piston barrel revolves. A hold-down plate insures continuous contact of the piston shoes with the cam surface. By varying the angle of the cam plate, the stroke of the piston is changed, thereby increasing or decreasing the flow output of the pump.

Oil at approximately 60 psig is ported to the piston cylinders during their suction stroke and is expelled against high pressure during their discharge stroke. A pressure compensator regulates the volume delivered in accordance with the demand of the system, thereby maintaining a predetermined pressure. System pressure is directed to a compensating valve with a spool which is held in the closed position by an adjustable spring load. When system pressure exceeds the spring load, the spring moves the spool to vent oil in the stroking cylinder to the pump case. The stroking piston then retracts and an inherent force assisted by the rate piston spring moves the cam plate to a greater angle, increasing the volume pumped. Rated performance of the pump is tabulated below:

Speed	5977 rpm (100%)	
Output Flow, maximum	$3.08 \times 10^{-3} \text{ m}^3/\text{sec}$	(48.8 gpm) at 100% speed
	$2.01 \times 10^{-3} \text{ m}^3/\text{sec}$	(31.8 gpm) at 65% speed
Pressure Rise	$2.46 \times 10^7 \text{ N/m}^2$	(3500 psid) at zero flow
	$2.36 \times 10^7 \text{ N/m}^2$	(3350 psid) at full flow
Overall Efficiency	83%	
Shaft hp (100% speed, fuel flow)	$5.57 \times 10^4 \text{ W}$	(115 hp)
Starting Torque Transient (at 2% speed, 3500 psid and zero flow)	$1.45 \times 10^2 \text{ Nm}$	(1280 in.-lb.)
Inlet Pressure	$4.22 \times 10^5 \text{ N/m}^2$	(60 psig)
Case Drain Pressure	$9.14 \times 10^5 \text{ N/m}^2$	(130 psig)
Makeup and Cooling Flow	$3.78 \times 10^{-4} \text{ m}^3/\text{sec}$	(6 gpm)

Heat Rejection (at 100% speed)	$8.12 \times 10^3 \text{ W}$ $1.46 \times 10^4 \text{ W}$	(462 Btu/min) steady-state (829 Btu/min) transient
Discharge Pressure Stability	$\pm 2.46 \times 10^6 \text{ N/m}^2$	($\pm 350 \text{ psi}$)

The pump is mounted to the forward left-hand side of the engine gearbox. A bolt-in flange is used. Drive input is through a splined quill shaft having a shear section rating of $2.03 \times 10^2 \text{ N/m}$ (2600 in.-lb.).

The flight engine will use a pump which integrates several of the functions now handled by separate components. The pump package may include the servovalves, filter, relief valve, and chip detector. An electric operated depressurizing valve (EDV) which enables the pump to operate against a reduced discharge pressure level for unloading during engine starting may be incorporated if needed. A quick-attach/-detach mount may be used in place of the bolt-on arrangement. Oil flow jumper tubes may be used in conjunction with cored passages in the engine gearbox to eliminate external piping. A modular pump design which permits removal of separate pumping elements and valve elements without removing the entire pump would also be considered.

8.3 RELIEF VALVE

The relief valve is located in a line connecting the hydraulic pump discharge to the pump inlet. In the event of a pump malfunction in which the pump failed to destroke and maintain a maximum discharge pressure, the relief valve would open and permit excess flow to bypass back to the pump inlet. The relief valve is Fluid Regulators Corp. model C1376-04 and has the following characteristics:

Rated Flow	$3.03 \times 10^{-3} \text{ m}^3/\text{sec}$ at $3.16 \times 10^7 \text{ N/m}^2$	(48 gpm at 4500 psid)
Cracking and Reset Pressure	$2.53 \times 10^7 \text{ N/m}^2$	(3600 psid) minimum

8.4 FILTERS

The hydraulic supply filter is located inline downstream of the hydraulic pump (and relief valve). The filter protects the servovalves from contamin-

ants generated in the hydraulic system or introduced from the engine lube system. The filter also serves as a means of cleaning the hydraulic system after assembly or maintenance. The filter is Aircraft Porous Media (APM) model ACC-4081-1610Z and has the following characteristics:

Rating	$2.5 \times 10^{-5} \text{ m}$ $1 \times 10^{-5} \text{ m}$	(25 μm) absolute (10 μm) nominal
Pressure Drop	$1.72 \times 10^5 \text{ N/m}^2$ at $3.03 \times 10^{-3} \text{ m}^3/\text{sec}$	(25 psid max. at 48 gpm)
Capacity	$2.5 \times 10^{-3} \text{ kg}$	(2.5 grams)

An additional filter is provided in the line which routes makeup and cooling flow from the engine lube system. This filter provides protection for the hydraulic pump in the event of contaminants generated by failure of the lube supply pump or contaminants introduced into the oil tank. The use of a separate filter assembly is a convenience for the experimental engine and its function would be incorporated into the lube supply element for the flight engine. The unit is a J79 engine lube filter, APM model AC4208-123. Characteristics are as follows:

Rating	$4.6 \times 10^{-5} \text{ m}$ $2.2 \times 10^{-5} \text{ m}$	(46 μm) absolute (22 μm) nominal
Pressure Drop	$0.41 \times 10^5 \text{ N/m}^2$ at $3.79 \times 10^{-4} \text{ m}^3/\text{sec}$	6 psid at 6 gpm

8.5 CHIP DETECTOR

The chip detector is installed in the line which routes the hydraulic pump cooling flow back to the engine lube system. The purpose of the unit is to identify ferrous contaminants which might be generated by the hydraulic pump in the event of an engine failure. For example, a hydraulic pump roller bearing failure could be distinguished from a main engine bearing failure. The unit consists of a permanent-magnet collector plug immersed in the oil flowpath through an inline housing. The part is a TEDECO model A-495.

8.6 FLOW CONTROL VALVES

Hydraulic flow to the fan pitch and fan nozzle actuation is controlled by separate, 4-way, electrohydraulic, direction flow control valves mounted on a common manifold block which is mounted on the accessory gearbox. The valves control flow in response to a direct-current electrical signal from the digital control.

A schematic of the valve design is shown on Figure 74. The electrical signal is applied to parallel redundant coils of the flat armature torque motor which applies torque to the jet pipe causing it to deflect. This deflection unbalances the pressure on the opposite ends of the spool causing it to move until the jet pipe is returned to its center position by the feedback spring - the force of the spring just counteracting the torque generated by the electrical signal. In this manner, spool position is made proportional to the electrical signal current. The position of the spool determines the porting between the high pressure supply from the hydraulic pump (P), the actuation ports (1 and 2), and the low pressure return (R).

The valves are designed to operate with hydraulic fluid supplied from the hydraulic pump within the normal pressure range of 2.36×10^7 to 2.46×10^7 N/m² (3350 to 3500 psi). Flow ratings of the valves, based on a supply-to-return differential of 2.40×10^7 N/m² (3400 psi) and an actuation differential of 1.69×10^7 N/m² (2400 psi) are 0.63×10^{-3} m³/sec and 1.75×10^{-3} m³/sec (10 and 27 gpm) for the exhaust nozzle and fan-pitch valve, respectively.

For a flight design these valves would be replaced with fail-fixed valve designs similar to the one described for the fuel control (reference Section 6.3) except designed for a double-acting rather than a single-acting actuator or motor (i.e., two output ports rather than one).

8.7 FAN NOZZLE (A18) ACTUATION

The fan nozzle actuators position the four interlocking flaps of variable nozzle as a function of flow and pressure from the electrohydraulic servo-valve. Two of the six actuators contain an electrical transducer to feedback nozzle position (see Figure 75). Six actuators, three in each rear-cowling

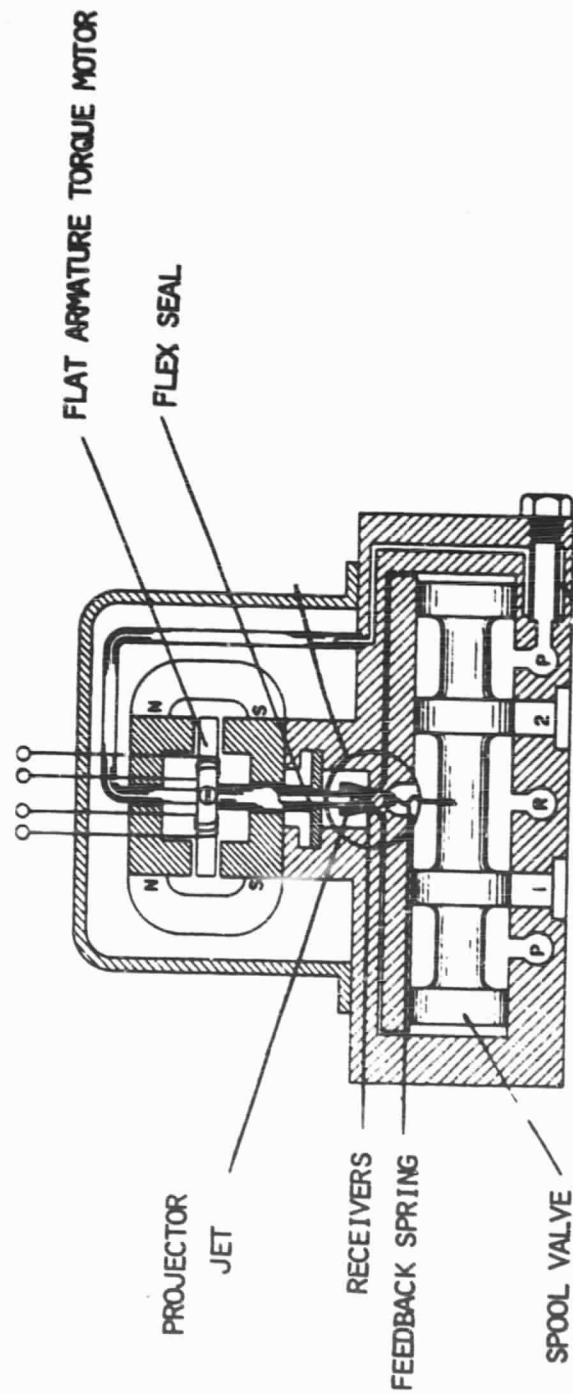


Figure 74. Electrohydraulic Servovalve.

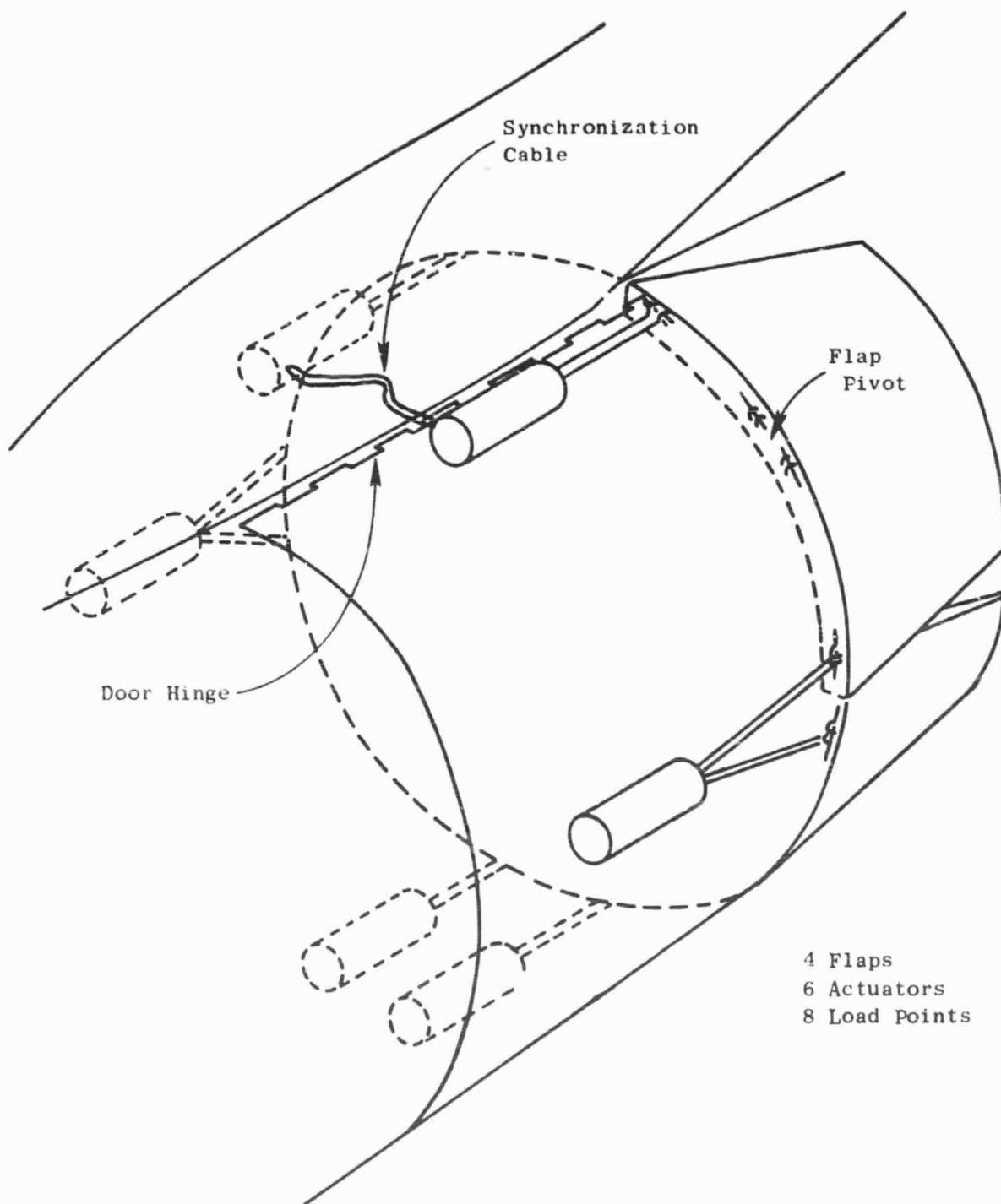


Figure 75. A18 Actuation.

half, are arranged circumferentially to hydraulically power the flaps through eight load-points. The center-mounted actuators in each half will power two load-points thus requiring twice the effective area of the four single-load-point actuators. These two larger area actuators will be synchronized through a worm screw mechanism in each actuator connected by an external flexible cable. The flexible cable contains a slip joint mounted in the pylon to allow the cable to lengthen as the cowl doors are opened.

Each actuation consists of a piston and rod contained in a hydraulic cylinder. A capped O-ring acts as a cross-piston seal while the rod contains a two-stage seal with the interstage cavity vented to the tank. Two actuators contain 1.94 in.² rod area (2.38 in.² head area) while the four single-load actuators contain 0.97 in.² rod area (1.33 in.² head area). Two of the single-load actuators contain LVDT's with the body grounded to the actuator and the core attached to the movable rod. The LVDT produces an electrical signal proportional to rod position. The two larger actuators contain the mechanical synchronization mechanism. Cross sections of the actuators are shown in Figure 76.

The actuators extend or retract as a function of rod or head port pressure and flow. The synchronous actuators produce a rotary mechanical output as a function of rod linear motion. Two actuators containing LVDT's produce an electrical output as a function of actuator position and input voltage.

The actuator rod end is threaded to a slider block and locked at the proper position. With the slider block installed in the nozzle track, the actuator is pinned to its head-end mount.

The hydraulic tubing, which has been previously installed through the cowl internal passages, is connected to the rod, head, and drain ports.

The synchronous cable is fed from the pylon through the internal cowl passages and inserted into the actuator worm gear. The cable outer sheath is then threaded to the actuator sync-port.

Hydraulic power is supplied by the constant pressure, variable-flow hydraulic pump common to the variable-pitch fan mechanism. Flow from the pump is controlled by an electrohydraulic servovalve. Upon an electrical

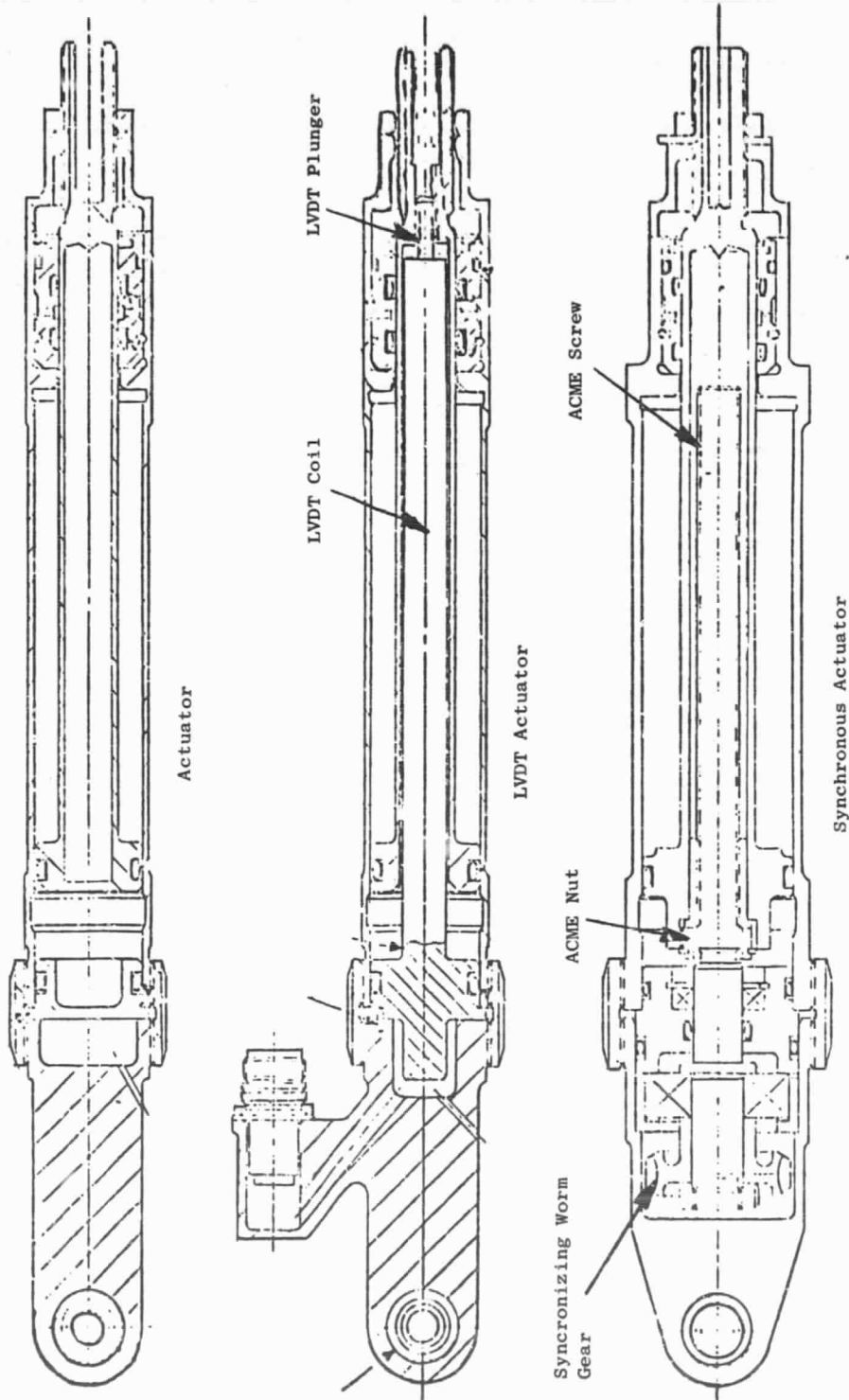


Figure 76. A18 Actuator Cross Section.

ORIGINAL PAGE IS
OF POOR QUALITY

demand to the servovalve, hydraulic flow positions the nozzle until the actuator electrical feedback satisfies the demand.

8.8 VARIABLE-PITCH ACTUATION

The purpose of the variable-pitch actuation is to position the variable-pitch fan blades which are a key feature of the UTW engine.

Two variable-pitch fan actuation systems are being developed as a part of the UTW experimental engine program. The cam harmonic drive system, illustrated in Figure 77, is being developed by the Hamilton Standard Division of United Technologies Corp. under subcontract to General Electric. Two hydraulic motors, which are part of the Beta regulator module mounted in the core cowl area, provide rotary mechanical input to the differential gear train through a flexible drive shaft which passes through the main reduction gear support. The rotary motion is then transmitted through a no-back, harmonic drive, rotating cam and cam follower arms to the blade trunnion.

The overall gear ratio from the blades to the flexible shaft is a nominal 773:1, with most of the ratio (201:1) provided by the harmonic drive. This permits the low torque power transmission elements between the Beta regulator and the harmonic drive to be designed for low weight and improved blade angle accuracy.

The planetary differential gear train provides a 5:1 ratio, and is utilized to cross the rotating boundary of the fan. The function of the bidirectional, spring-type no-back is to lock the fan blades in position in the absence of a pitch change command.

Two LVDT's located in the Beta regulator unit, and driven by hydraulic motor output, provide a blade angle feedback to the engine digital control system.

Utilization of a flexible drive capability permits the LVDT's and hydraulic motor to be remotely located in an engine area which permits ease of inspection and component replacement.

The ball spline actuation system shown in Figure 78 is being developed by General Electric. A hydraulic motor located on the fan centerline drives

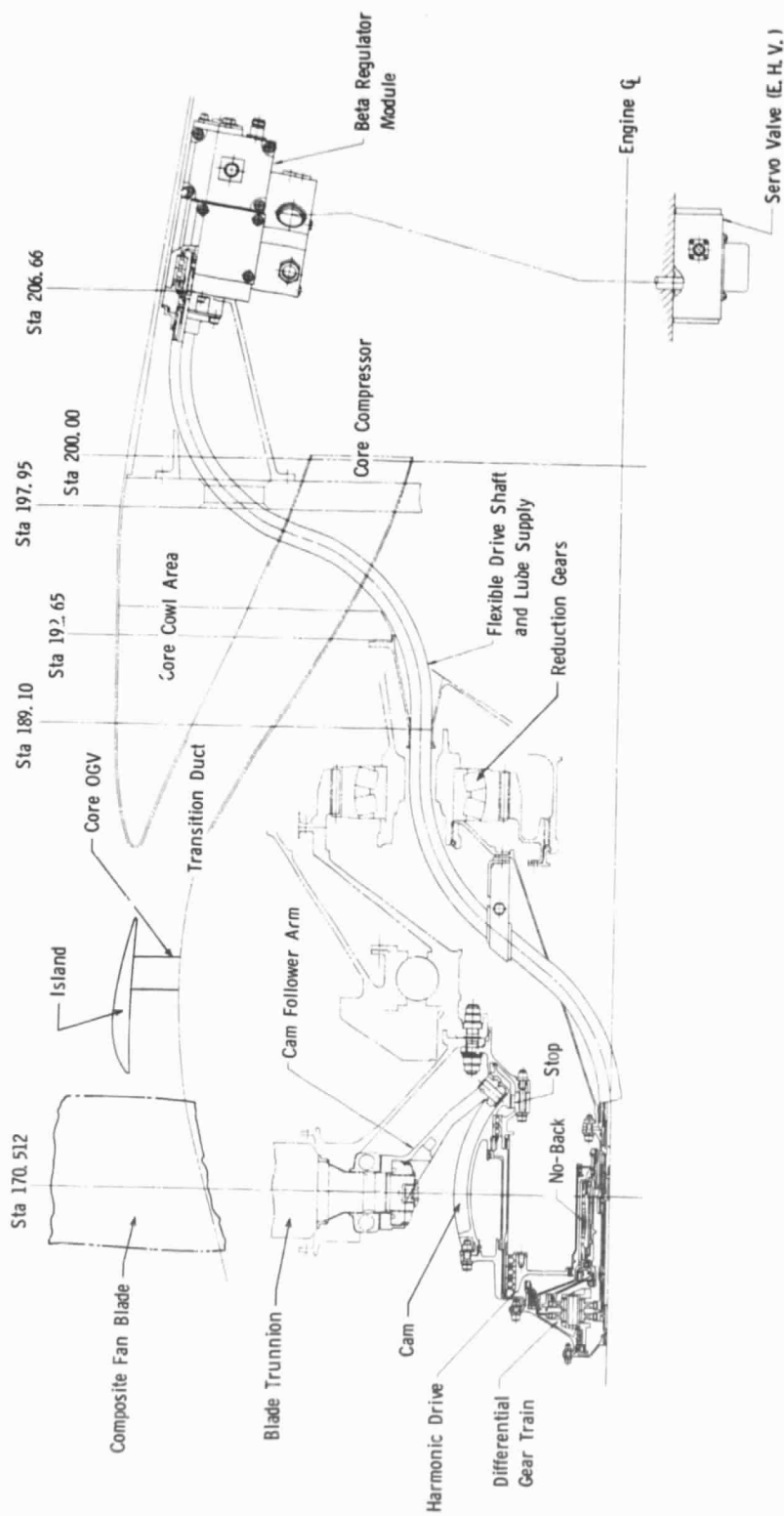


FIG. 77. Hamilton Standard Variable-Pitch System.

ORIGINAL PAGE IS
OF POOR QUALITY

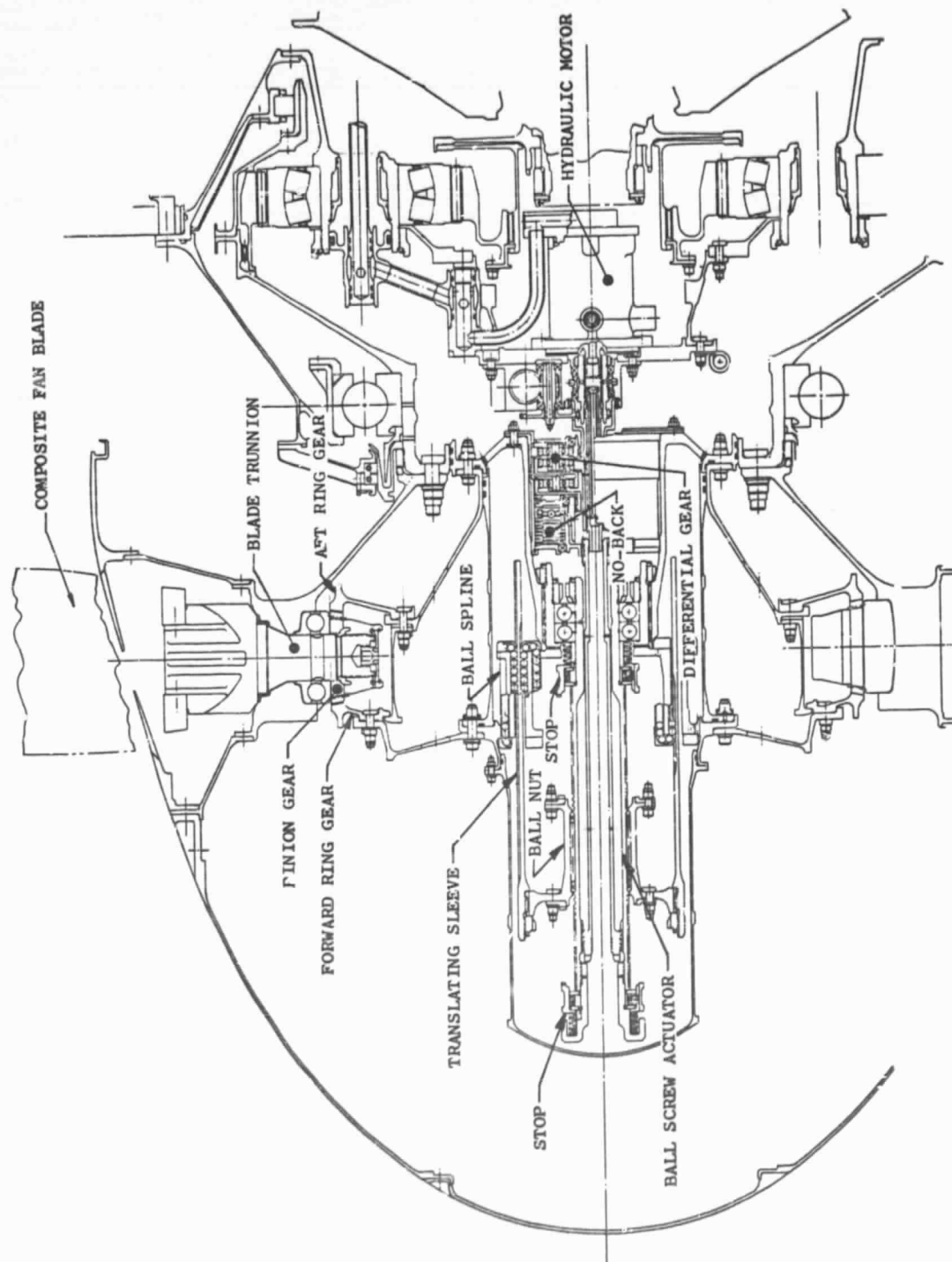


Figure 78. General Electric Ball Spline Actuator System.

a ball screw actuator through a differential gear and no-back. The linear motion of the ball nut of screw causes the sleeve (middle member) of a ball spline to translate in a fore or aft direction. The ball spline is a double-acting member with helical ball tracks between the sleeve and inner member, and straight ball tracks between the sleeve and the outer ball spline member. The inner member is attached to the aft ring gear while the outer member is attached to the forward ring gear. Translation of the ball spline sleeve, fore and aft, drives the two ring gears in tangentially opposite directions. The ring gears in turn are mated to 18 pinion gears that are splined to the fan blade trunnion.

The gear ratio between the hydraulic motor and the fan blade is 470:1. Two LVDT's driven by the hydraulic motor provide a blade angle feedback to the engine digital control system.

From a control system standpoint, operation of the two variable-pitch actuation system designs is essentially the same.

As described in Section 3.0, depending on control mode, the fan blades are either positioned in accordance with manual or automatic scheduling inputs or they are modulated to maintain desired fan speed. In either case, whenever the digital control computer detects that the blades are not in the correct position, it sends an electrical signal to the fan pitch servovalve (reference Section 8.6) which ports hydraulic fluid to the hydraulic motor to get the correct pitch angle (or fan speed if in the modulating mode).

8.9 CORE STATOR ACTUATION AND FEEDBACK

The F101 core compressor used in the QCSEE includes provisions for varying the angle of the inlet guide vanes and stator vanes in stages 1 through 3 to accommodate the relatively wide speed range in which the compressor must perform.

The variable vanes are connected through a system of levers, rings, and links which are actuated by two fuel-operated linear actuators mounted to the compressor casing on opposite sides of the engine. The actuator motions are synchronized through the inherent rigidity of the linkage system.

The QCSEE core stator actuators are F101 actuators (see Figure 79) modified to provide approximately 0.51 cm (0.2 in.) more stroke giving a total stroke of 8.446 cm (3.325 in.). This change is made by redimensioning the rod seal cartridge. The actuator vendor is Arkwin Industries, Inc.

The core stators are controlled by a position control loop including the actuators, a control valve and hydromechanical computing elements in the hydromechanical control, and a flexible push-pull cable which serves as a position feedback from the actuation system to the control. As described in Section 6.3, the hydromechanical control computes a desired stator vane position as a function of core speed and core inlet temperature and, by means of the control valve, controls flow to the actuators (as necessary) to make the vane position match the desired position.

The feedback consists of a flexible, fixed-length, push-pull cable in a flexible, fixed-length conduit providing a stroke path and protection for the cable. To eliminate inaccuracy due to lost motion, the cable is kept in tension by the hydromechanical control, aided by a Teflon lining in the conduit which minimizes friction. The QCSEE feedback is virtually the same as that used in the F101, the only significant difference being that the QCSEE cable is nearly twice as long and has a sleeve swaged to the conduit near its midpoint which serves as a firewall seal. Cablecraft, Inc. is the vendor source for the feedback.

For a flight design there would be little or no change to the core stator actuators but the feedback and control valve would probably change, depending on the nature of the simplified hydromechanical control discussed in Section 6.5.

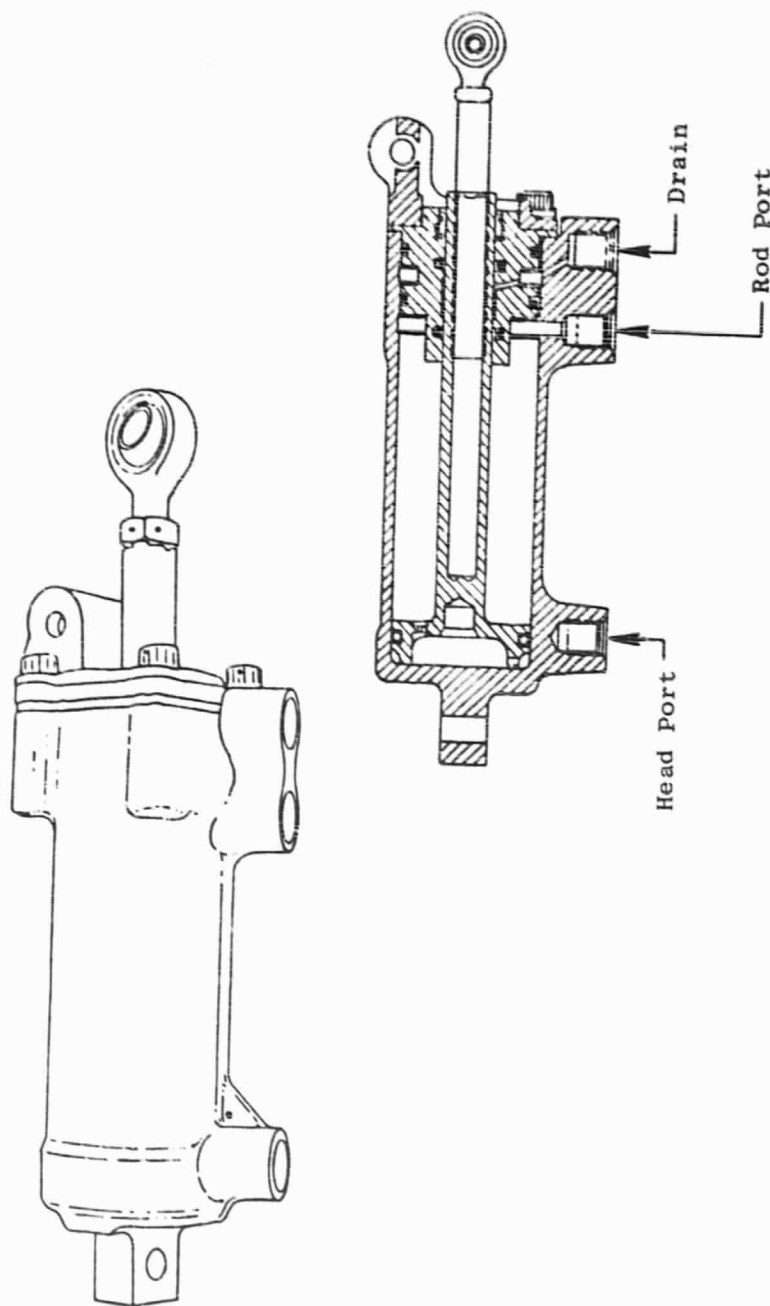


Figure 79. Core Stator Actuator.

ORIGINAL PAGE IS
OF POOR QUALITY

9.0 SENSORS

The engine sensors are the devices which change the variable to be measured into a form that can be used as an input signal to the engine digital or hydromechanical control or as an input signal to an indicator gage. The sensors include the following:

- Low Pressure Turbine (LPT) Speed Sensor
- Fan Inlet Temperature Sensor
- Core Inlet Temperature Sensor
- Compressor Discharge Temperature Sensor
- Absolute Pressure Transducers
- Differential Pressure Transducers
- Compressor Discharge Pressure Sensor

9.1 LOW PRESSURE TURBINE (LPT) SPEED SENSOR

The LPT shaft speed sensors produces two electrical signals that represent the rotational speed of the low pressure turbine shaft. One signal will be used for governing engine fan speed. The other signal will be used to limit the rate of speed change and maximum speed in the event of a loss of fan load, overspeed, or control failure. Each signal contains a signature which occurs once per revolution for dynamic balancing.

The speed sensor is very similar to that used on the F101 engine and is utilized as shown in Figure 80. The sensor consists of a curved metal tube containing lead wires with a magnetic pickup having a positioning flange on one end and an electrical connector (plus a mounting flange with a compression spring) on the other end. Design features are:

Rated speed (100%)	7996 rpm
Shaft acceleration	±1200 rpm/sec
Environmental temperature	-40° F to 350° F (-40° C to 176.7° C)

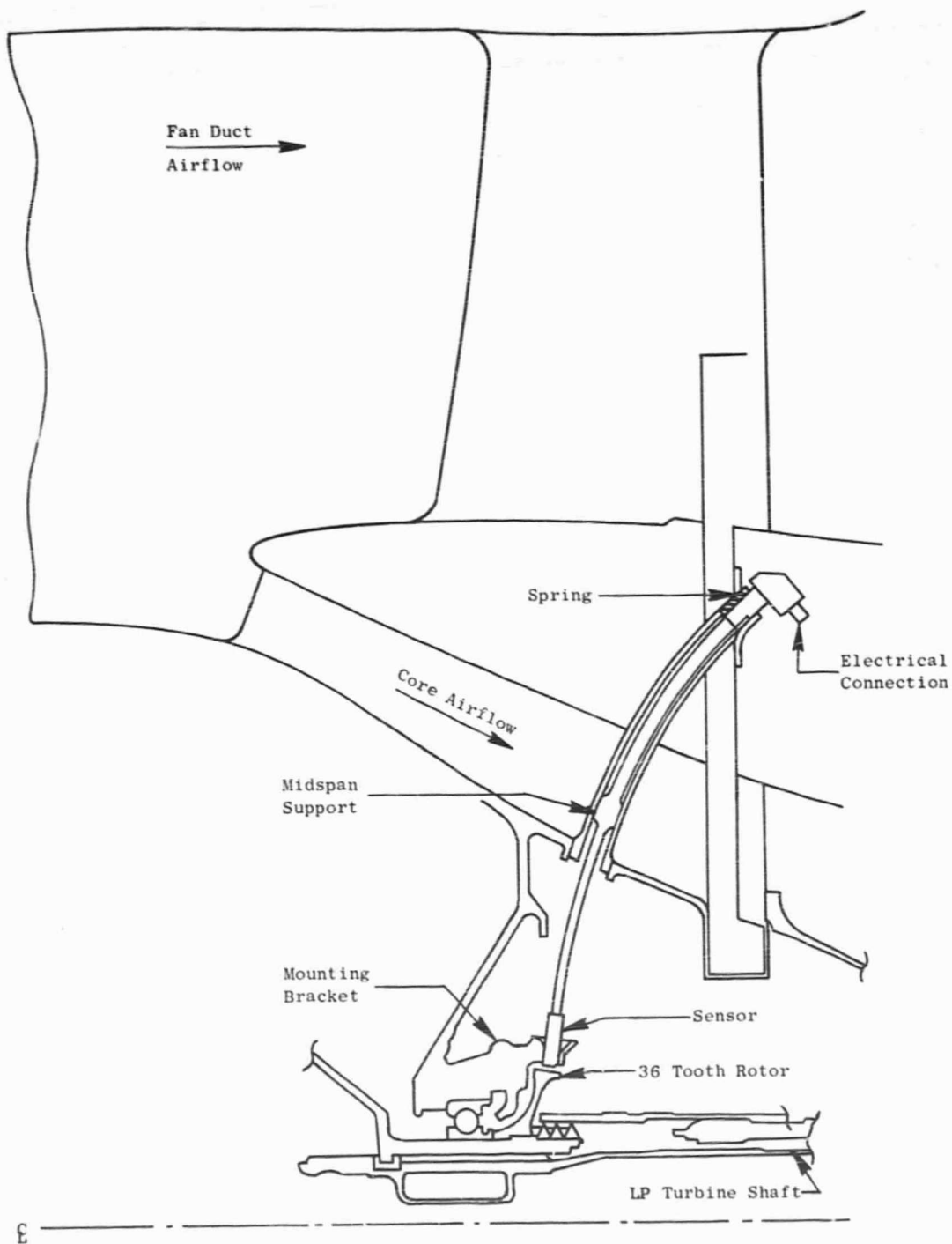


Figure 80. Low Pressure Turbine Speed Sensor.

Signal frequency	36 pulses/rev with a 1/rev signature
Signal amplitude (at 10% speed)	0.2 volts peak-to-peak minimum
Signal amplitude (at 100% speed)	10.0 volts peak-to-peak maximum
Balance signal (1/rev) amplitude ratio	2:1

The magnetic pickup consists basically of a permanent magnet behind a soft-iron pole piece containing a bobbin on which two coils have been wound. The magnetic flux linking the coil is high when a ferrous metal object (tooth) is placed in front of the pole piece and is low with no ferrous metal (slot) in front of the pole piece. The generated voltage is proportional to the rate of flux change in the pole piece, and the frequency of the a.c. signal is a product of the number of teeth and shaft speed in revolutions per second. The wave form of the signal is nearly sinusoidal depending upon the relative width of slots and teeth on the rotating disk and also the width of the pole piece relative to the slots and teeth. Signal output from the sensor is routed to a conditioner device in the digital control which produces a uniform voltage amplitude and wave form at varying speed so that ultimately the conditioned signal is interpreted in terms of frequency rather than voltage amplitude.

The sensor is installed (see Figure 80) in a fan frame strut by passing the pickup end through a tube in the strut until it is positioned in close proximity to a gear-like wheel located immediately aft of the LPT shaft front bearing. The spring-loaded mounting flange at the connector end is bolted to a pad on the aft side of the strut near the outside.

The flight design of the LPT speed sensor will be similar to that shown except for possible variations in external configuration.

9.2 FAN INLET TEMPERATURE (T12) SENSOR

The T12 sensor provides the engine control with an electrical signal representing the total temperature of the air entering the fan for use in scheduling and computing within the digital control.

The fan inlet temperature sensor shown in Figure 81 is identical to that used on the F101 engine. The sensor is a wire-wound resistance-type device mounted on and protruding through the inlet duct into the fan inlet air-stream. The sensor consists of a sensing element and housing. The sensing element contains a platinum wire wound on a cylindrical platinum mandrel. The wires are insulated from each other and from the mandrel by a ceramic insulant. The element is hermetically sealed in a capped platinum sheath and the connections are potted. The housing is a slotted airfoil which controls airflow so that the sensed temperature is that of the free stream. A series of small holes bleeds off the boundary layer and turns the stream, but not heavier particles, inward toward the sensing element. The boundary-layer air is exhausted out the top. Some of the diverted airstream flows through the first slot and carries the lighter liquid contaminants. The remaining portion of the diverted flow goes through the second slot and around the sensing element. Free-stream air, which flows around the sensing element, does not contact any portion of the sensor housing on airfoils.

The T12 sensor operates on the principle that the resistance of the platinum wire is a predictable function of temperature. A constant direct current of 12.5 mA is applied to the sensor coil and the voltage used as an indication of temperature.

Design Features

Temperature Range	-40° C to 7.1° C (-40° F to 160° F)
Resistance Range	168 to 256 ohms
Excitation	12.5 mA d.c. (constant)
Accuracy	±1.11° C (±2° F) max.
Recovery Error	Less than 0.5% at Mach 0.4
Response Time (to 63.2% of final value)	Less than 5 seconds to 48.8 kg/sec/m ² (10 pps/ft ²) airflow

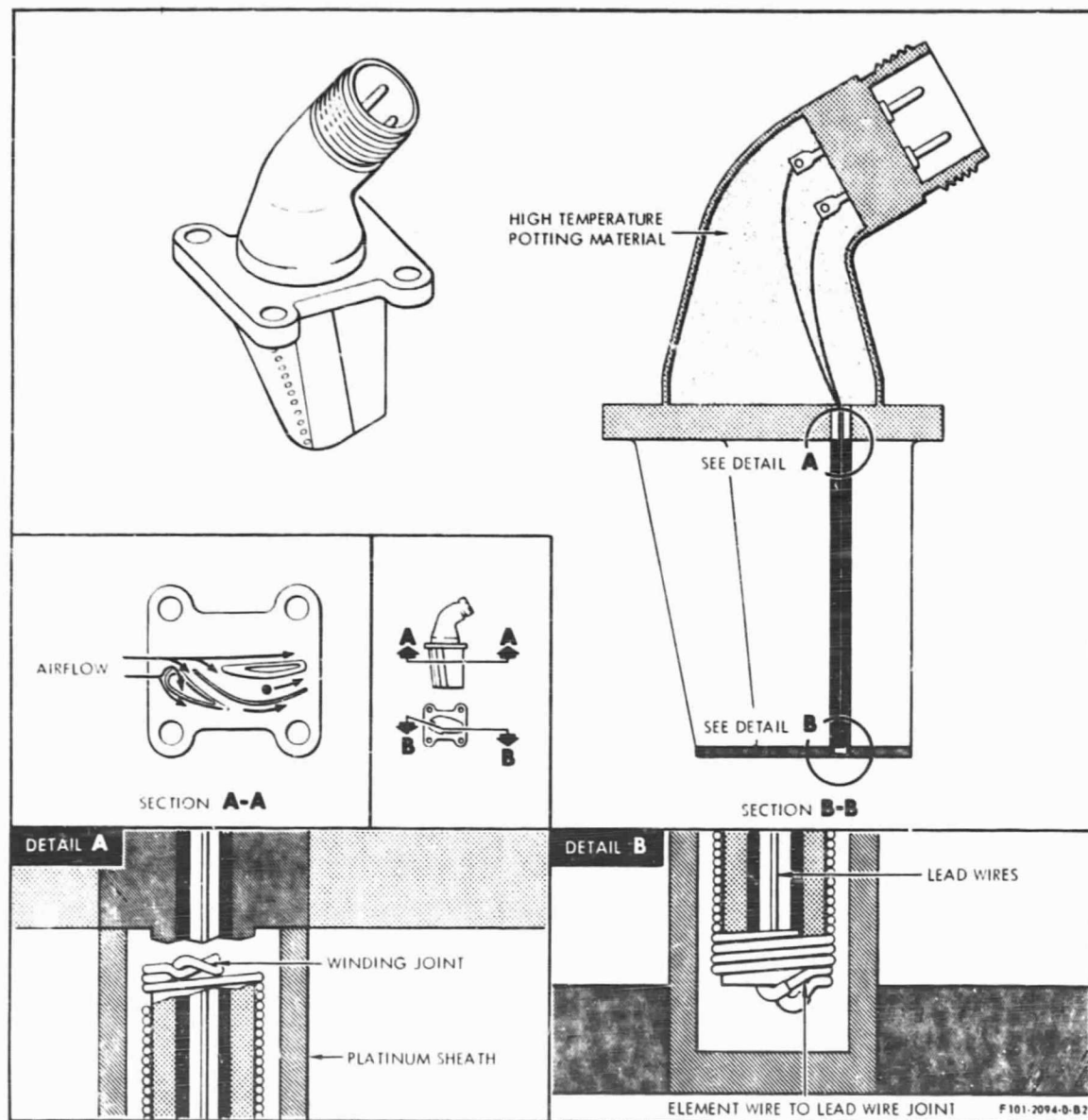


Figure 81. Fan Inlet Temperature (T12) Sensor.

9.3 CORE INLET TEMPERATURE SENSOR

Core inlet temperature is sensed hydromechanically by means of a gas-filled metal coil which protrudes into the core compressor inlet air flow-path. The coil is connected directly to a servomechanism which, in conjunction with the hydromechanical control, provides a fuel pressure proportional to core inlet temperature. Additional details on this sensor are given in Section 6.3.

9.4 COMPRESSOR DISCHARGE TEMPERATURE SENSOR (T3)

Compressor discharge temperature is sensed by a thermocouple located in the core air flowpath at the entrance to the combustor. The thermocouple signal is used in the digital control for calculation and control of turbine inlet temperature.

The temperature sensor shown in Figure 82 is similar to that used on the F101 and CFM56 engines. The sensor is mounted on the outer combustor case utilizing an existing engine borescope plug. The sensor will protrude through the inner combustor case and into the combustor outer-flow passage. The probe construction will be ruggedized for reliability utilizing a stainless steel sheathed-lead sealed at the sensor and connector ends. The design of the temperature sensor tip will optimize time response and repeatability of the measurement.

The probe consists of an ungrounded chromel-alumel thermocouple, encapsulated in a swaged magnesium-oxide tip which senses the air temperature surrounding the probe tip. The output signal from the sensor is routed directly to the digital control.

9.5 ABSOLUTE AND DIFFERENTIAL PRESSURE TRANSDUCERS

Two absolute-pressure transducers and two differential-pressure transducers are included within the QCSEE engine-mounted digital control to convert air pressure inputs into electrical signals for use in the control. Pressures sensed are:

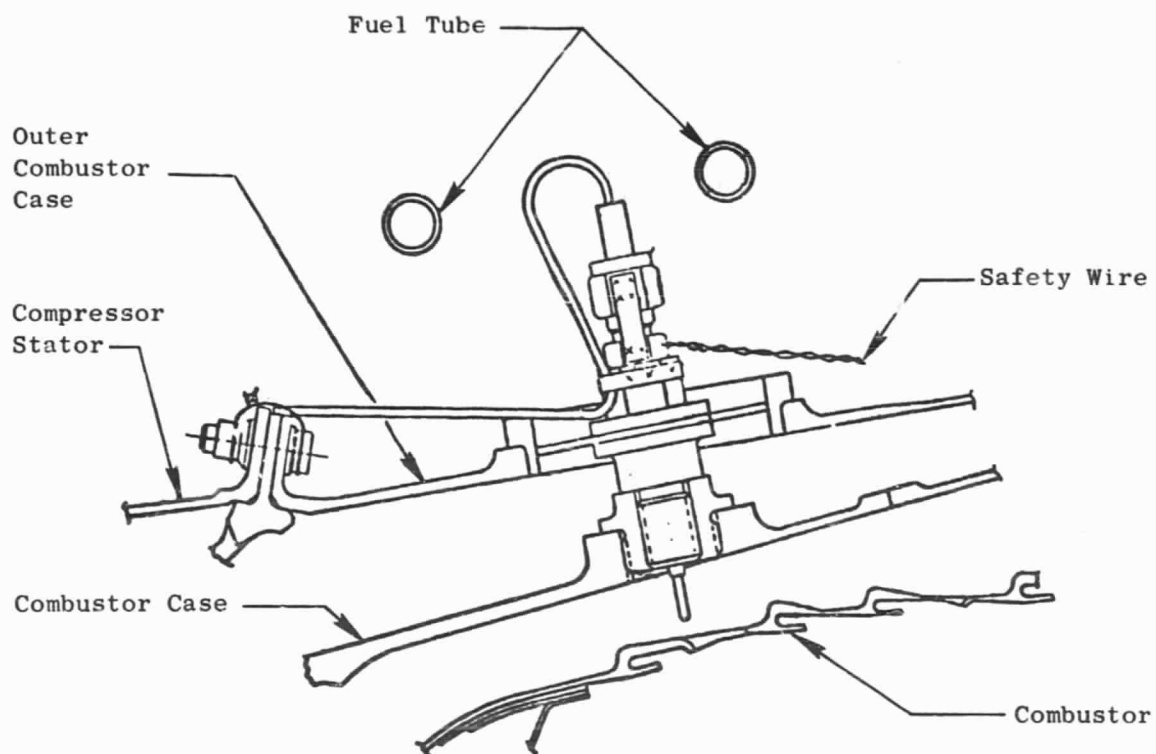


Figure 82. Compressor Discharge Temperature (T3) Sensor.

ORIGINAL PAGE IS
OF POOR QUALITY

Absolute

Compressor Discharge Static Pressure (PS3)

Free-Stream Total Pressure (PTO)

Differential

PTO-PS11 (Inlet Throat Static Pressure)

P14-PTO (P14 is Fan Discharge Pressure)

It should be noted that the P14-PTO sensor was included as a potential thrust parameter. As noted in Section 4.0, this is not the thrust parameter to be used during initial experimental engine testing, but the transducer has been retained and may be used at a later time.

Location of the source for these sensed pressures (except P14) was discussed in Section 4.8. Operating ranges are 0 to 300 psia for PS3, 0 to 20 psia for PTO, and 0 to 12 psid for both differential transducers.

All of these sensors are thin-film, strain gage bridge transducers identical to those used in the F101 engine. A typical cross section is shown in Figure 83. The sensors receive their electrical excitation from the control and change the ΔP and static pressure signals to electrical signals. They are located inside the digital control chassis.

The strain member is a cantilever beam on which a ceramic film is deposited for electrical insulation. The thin, metal film resistors forming a 4-element Wheatstone bridge are vacuum deposited on the ceramic insulator film. The beam is linked to a force-collector diaphragm which induces a strain on the beam proportional to applied pressure.

The sensors operate on the principle of a mechanical distortion producing a change in electrical resistance across a strain gage and, hence, a change in electrical current output from a bridge circuit. Referring to Figure 83, pressure is ported to the sensing diaphragm which deflects and drives a linkage pin against the sensing beam. The beam is shaped in such a way that it bends and causes "stretch" on the surface to which the strain gages are attached.

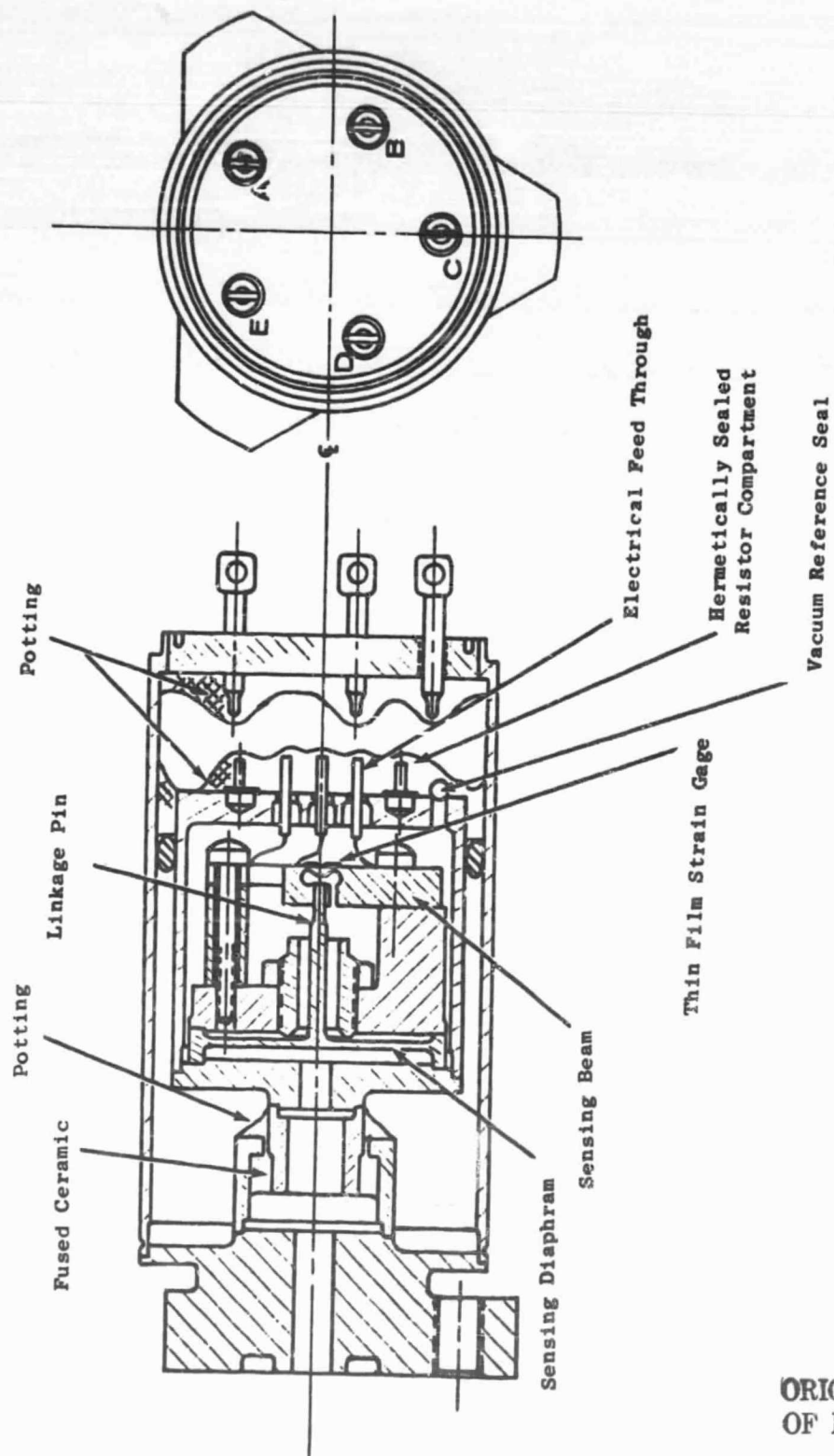


Figure 83. Pressure Transducer.

ORIGINAL PAGE IS
OF POOR QUALITY

9.6 COMPRESSOR DISCHARGE PRESSURE SENSING

Compressor discharge static pressure (PS3) is sensed both hydromechanically and electrically. The hydromechanical control includes a servomechanism which senses PS3 by means of a bellows and provides a fuel pressure for use within the control which is proportional to PS3. This servomechanism is shown as part of Figure 67.

The electrical PS3 transducer was described in Section 9.5.

10.0 MISCELLANEOUS

10.1 CONTROL ALTERNATOR

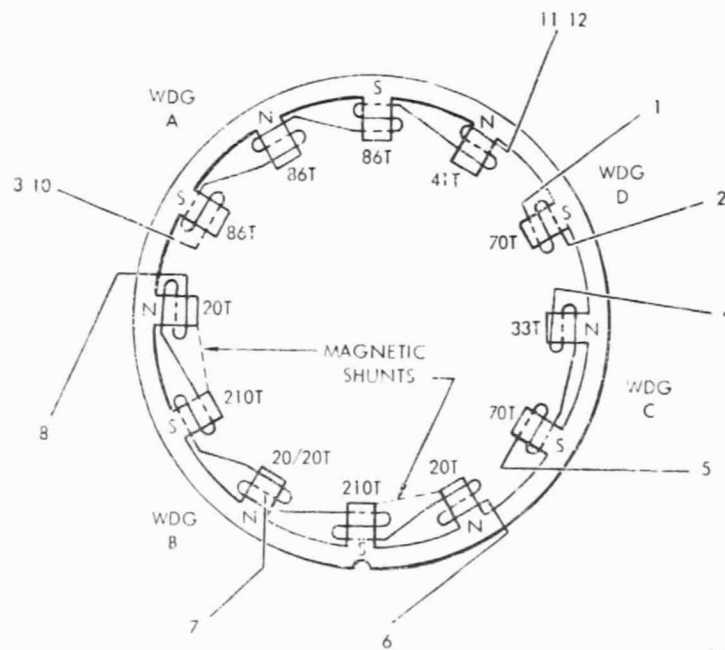
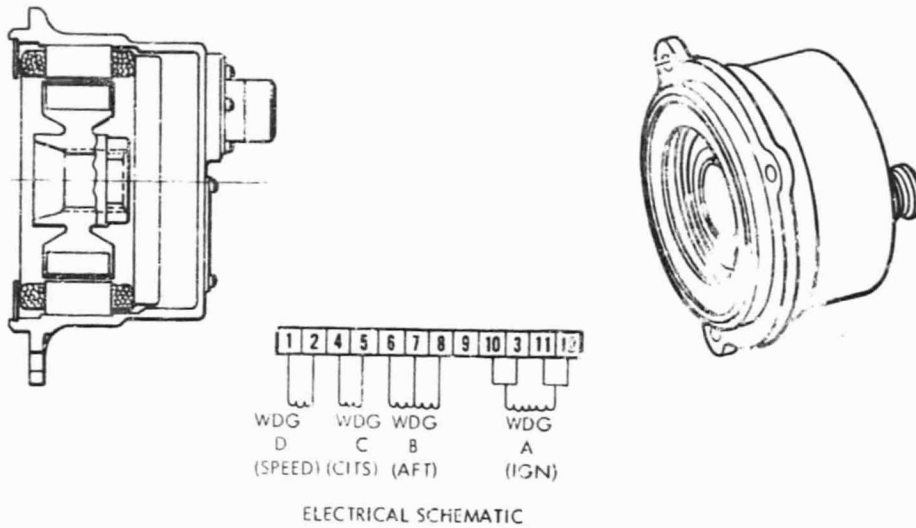
The QCSEE control system includes an engine-driven control alternator which provides primary power for operation of the digital control, power for an isolated emergency fan overspeed function in the digital control, and core speed indication both for the digital control and for remote indication.

The control alternator, which is identical to the one used on the F101 engine, is shown on Figure 84. It consists of a rotor containing 12 equally spaced permanent magnets with adjacent magnets having opposite polarity and a stator containing a laminated soft-iron core with 12 equally spaced poles wound with magnet wire. The coils are combined into four separate windings and utilized as shown on Figure 84. The voltage generated in each coil is proportional to the rate of flux change in the stator poles, and the frequency is proportional to the number of rotor pole pairs, both determined by speed of the rotor.

Outputs of the windings at 100% speed (24,903 rpm) are:

<u>Winding</u>	<u>Maximum Open Circuit Voltage (volts rms)</u>	<u>Maximum Short Circuit Current (amperes rms)</u>
A	310	3.5
B1 & B2	243	1.7
C	106	5.9
D	71	5.9

The alternator is mounted on the aft side of the accessory gearbox near the left end when looking forward. The rotor mounts to and is driven by a shaft protruding from and supported by bearings in the gearbox. The rotor hub threads (left-hand) onto the shaft until it seats and is positioned by a nonlocking taper. A left-hand thread locknut with a Vespel insert is used



ORIGINAL PAGE IS
OF POOR QUALITY

Figure 84. Control Alternator.

to secure the rotor. A pilot, with an O-ring seal, positions the stator radially. The stator is clamped to the gearbox by means of locknuts (and washers) threaded to three studs protruding from the gearbox pad.

10.2 ELECTRICAL INTERCONNECTIONS

Electrical interconnections in the QCSEE control system are accomplished using connector and cable designs essentially equivalent to those used on the F101. Stainless steel connectors are used on all connectors on and around the engine. Interconnecting cables are made up with wires combined in shielded, twisted pairs to minimize electromagnetic interface. Individual wires are virtually all stranded AWG 20.

An electrical interconnection schematic is shown on Figure 85.

10.3 WEIGHT

Weight estimates have been made for all system components, both for the designs to be used on the experimental engine and for predicted flight engine designs. The weight estimates are tabulated in Table XV.

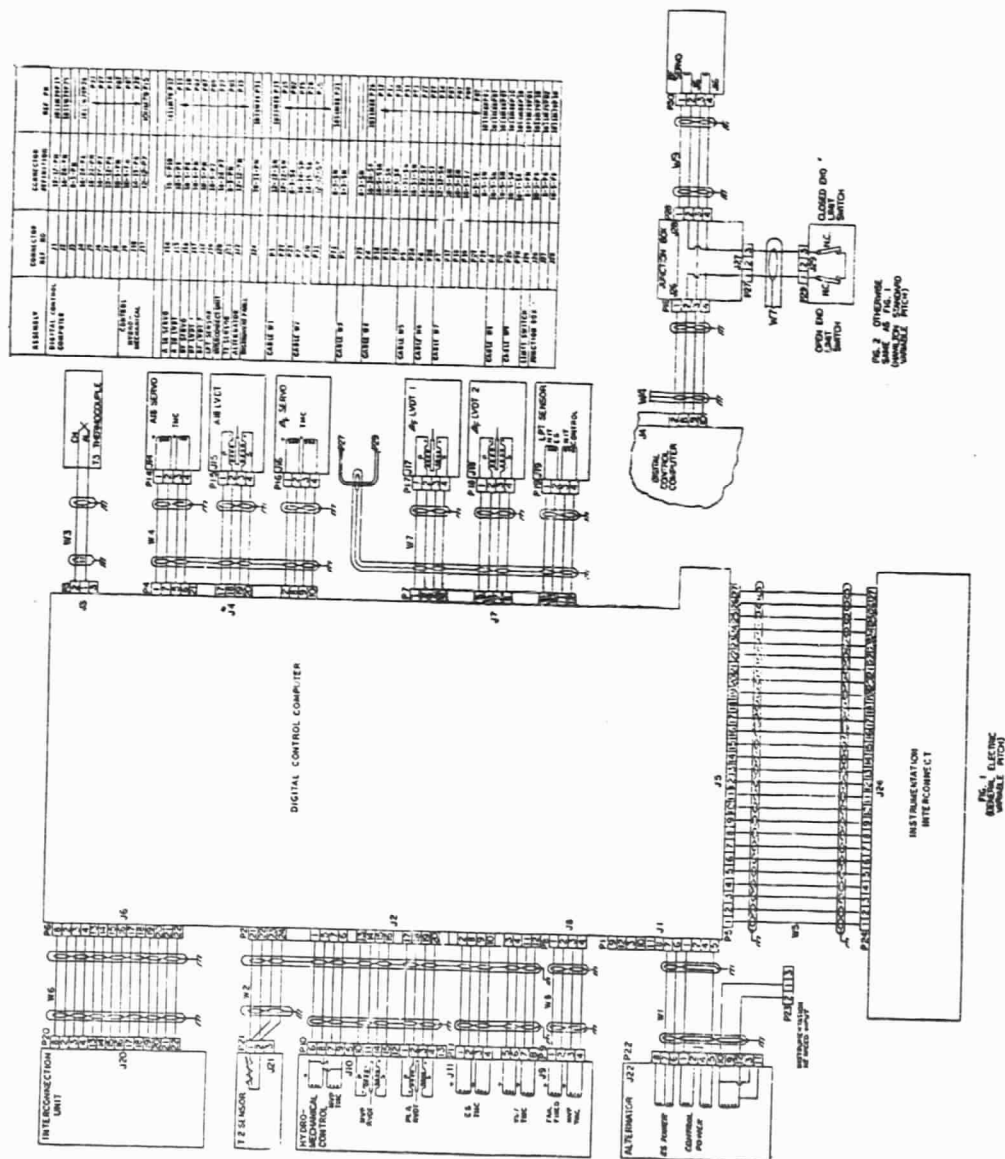
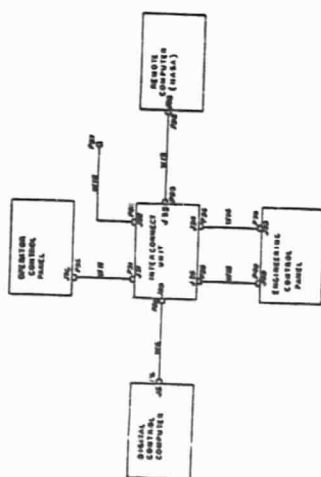


Figure 85. Electrical Interconnections.

ORIGINAL PAGE IS
OF POOR QUALITY



CONVENTION REPORT		FOOTNOTES	
FROM	TO		
1	1	1	1
2	2	2	2
3	3	3	3
4	4	4	4
5	5	5	5
6	6	6	6
7	7	7	7
8	8	8	8
9	9	9	9
10	10	10	10
11	11	11	11
12	12	12	12
13	13	13	13
14	14	14	14
15	15	15	15
16	16	16	16
17	17	17	17
18	18	18	18
19	19	19	19
20	20	20	20
21	21	21	21
22	22	22	22
23	23	23	23
24	24	24	24
25	25	25	25
26	26	26	26
27	27	27	27
28	28	28	28
29	29	29	29
30	30	30	30
31	31	31	31
32	32	32	32
33	33	33	33
34	34	34	34
35	35	35	35
36	36	36	36
37	37	37	37
38	38	38	38
39	39	39	39
40	40	40	40
41	41	41	41
42	42	42	42
43	43	43	43
44	44	44	44
45	45	45	45
46	46	46	46
47	47	47	47
48	48	48	48
49	49	49	49
50	50	50	50
51	51	51	51
52	52	52	52
53	53	53	53
54	54	54	54
55	55	55	55
56	56	56	56
57	57	57	57
58	58	58	58
59	59	59	59
60	60	60	60
61	61	61	61
62	62	62	62
63	63	63	63
64	64	64	64
65	65	65	65
66	66	66	66
67	67	67	67
68	68	68	68
69	69	69	69
70	70	70	70
71	71	71	71
72	72	72	72
73	73	73	73
74	74	74	74
75	75	75	75
76	76	76	76
77	77	77	77
78	78	78	78
79	79	79	79
80	80	80	80
81	81	81	81
82	82	82	82
83	83	83	83
84	84	84	84
85	85	85	85
86	86	86	86
87	87	87	87
88	88	88	88
89	89	89	89
90	90	90	90
91	91	91	91
92	92	92	92
93	93	93	93
94	94	94	94
95	95	95	95
96	96	96	96
97	97	97	97
98	98	98	98
99	99	99	99
100	100	100	100

UNIT		DATE		TIME		LOCATION		REMARKS	
001	001	001	001	001	001	001	001	001	001
002	002	002	002	002	002	002	002	002	002
003	003	003	003	003	003	003	003	003	003
004	004	004	004	004	004	004	004	004	004
005	005	005	005	005	005	005	005	005	005
006	006	006	006	006	006	006	006	006	006
007	007	007	007	007	007	007	007	007	007
008	008	008	008	008	008	008	008	008	008
009	009	009	009	009	009	009	009	009	009
010	010	010	010	010	010	010	010	010	010
011	011	011	011	011	011	011	011	011	011
012	012	012	012	012	012	012	012	012	012
013	013	013	013	013	013	013	013	013	013
014	014	014	014	014	014	014	014	014	014
015	015	015	015	015	015	015	015	015	015
016	016	016	016	016	016	016	016	016	016
017	017	017	017	017	017	017	017	017	017
018	018	018	018	018	018	018	018	018	018
019	019	019	019	019	019	019	019	019	019
020	020	020	020	020	020	020	020	020	020
021	021	021	021	021	021	021	021	021	021
022	022	022	022	022	022	022	022	022	022
023	023	023	023	023	023	023	023	023	023
024	024	024	024	024	024	024	024	024	024
025	025	025	025	025	025	025	025	025	025
026	026	026	026	026	026	026	026	026	026
027	027	027	027	027	027	027	027	027	027
028	028	028	028	028	028	028	028	028	028
029	029	029	029	029	029	029	029	029	029
030	030	030	030	030	030	030	030	030	030
031	031	031	031	031	031	031	031	031	031
032	032	032	032	032	032	032	032	032	032
033	033	033	033	033	033	033	033	033	033
034	034	034	034	034	034	034	034	034	034
035	035	035	035	035	035	035	035	035	035
036	036	036	036	036	036	036	036	036	036
037	037	037	037	037	037	037	037	037	037
038	038	038	038	038	038	038	038	038	038
039	039	039	039	039	039	039	039	039	039
040	040	040	040	040	040	040	040	040	040
041	041	041	041	041	041	041	041	041	041
042	042	042	042	042	042	042	042	042	042
043	043	043	043	043	043	043	043	043	043
044	044	044	044	044	044	044	044	044	044
045	045	045	045	045	045	045	045	045	045
046	046	046	046	046	046	046	046	046	046
047	047	047	047	047	047	047	047	047	047
048	048	048	048	048	048	048	048	048	048
049	049	049	049	049	049	049	049	049	049
050	050	050	050	050	050	050	050	050	050
051	051	051	051	051	051	051	051	051	051
052	052	052	052	052	052	052	052	052	052
053	053	053	053	053	053	053	053	053	053
054	054	054	054	054	054	054	054	054	054
055	055	055	055	055	055	055	055	055	055
056	056	056	056	056	056	056	056	056	056
057	057	057	057	057	057	057	057	057	057
058	058	058	058	058	058	058	058	058	058
059	059	059	059	059	059	059	059	059	059
060	060	060	060	060	060	060	060	060	060
061	061	061	061	061	061	061	061	061	061
062	062	062	062	062	062	062	062	062	062
063	063	063	063	063	063	063	063	063	063
064	064	064	064	064	064	064	064	064	064
065	065	065	065	065	065	065	065	065	065
066	066	066	066	066	066	066	066	066	066
067	067	067	067	067	067	067	067	067	067
068	068	068	068	068	068	068	068	068	068
069	069	069	069	069	069	069	069	069	069
070	070	070	070	070	070	070	070	070	070
071	071	071	071	071	071	071	071	071	071
072	072	072	072	072	072	072	072	072	072
073	073	073	073	073	073	073	073	073	073
074	074	074	074	074	074	074	074	074	074
075	075	075	075	075	075	075	075	075	075
076	076	076	076	076	076	076	076	076	076
077	077	077	077	077	077	077	077	077	077
078	078	078	078	078	078	078	078	078	078
079	079	079	079	079	079	079	079	079	079
080	080	080	080	080	080	080	080	080	080
081	081	081	081	081	081	081	081	081	081
082	082	082	082	082	082	082	082	082	082
083	083	083	083	083	083	083	083	083	083
084	084	084	084	084	084	084	084	084	084
085	085	085	085	085	085	085	085	085	085
086	086	086	086	086	086	086	086	086	086
087	087	087	087	087	087	087	087	087	087
088	088	088	088	088	088	088	088	088	088
089	089	089	089	089	089	089	089	089	089
090	090	090	090	090	090	090	090	090	090
091	091	091	091	091	091	091	091	091	091
092	092	092	092	092	092	092	092	092	092
093	093	093	093	093	093	093	093	093	093
094	094	094	094	094	094	094	094	094	094
095	095	095	095	095	095	095	095	095	095
096	096	096	096	096	096	096	096	096	096
097	097	097	097	097	097	097	097	097	097
098	098	098	098	098	098	098	098	098	098
099	099	099	099	099	099	099	099	099	099
100	100	100	100	100	100	100	100	100	100

STATE CONTROL REGISTRATION NUMBER 12-27-1978	
STATE	REGISTRATION NUMBER
ALABAMA	12-27-1978
ALASKA	12-27-1978
ARIZONA	12-27-1978
ARKANSAS	12-27-1978
CALIFORNIA	12-27-1978
COLORADO	12-27-1978
CONNECTICUT	12-27-1978
DELAWARE	12-27-1978
FLORIDA	12-27-1978
GEORGIA	12-27-1978
HAWAII	12-27-1978
IDaho	12-27-1978
ILLINOIS	12-27-1978
INDIANA	12-27-1978
IOWA	12-27-1978
KANSAS	12-27-1978
KENTUCKY	12-27-1978
LOUISIANA	12-27-1978
MAINE	12-27-1978
MARYLAND	12-27-1978
MASSACHUSETTS	12-27-1978
MICHIGAN	12-27-1978
MINNESOTA	12-27-1978
MISSISSIPPI	12-27-1978
MISSOURI	12-27-1978
MONTANA	12-27-1978
NEBRASKA	12-27-1978
NEVADA	12-27-1978
NEW HAMPSHIRE	12-27-1978
NEW JERSEY	12-27-1978
NEW MEXICO	12-27-1978
NEW YORK	12-27-1978
NORTH CAROLINA	12-27-1978
NORTH DAKOTA	12-27-1978
OHIO	12-27-1978
OKLAHOMA	12-27-1978
OREGON	12-27-1978
PENNSYLVANIA	12-27-1978
RHODE ISLAND	12-27-1978
SOUTH CAROLINA	12-27-1978
SOUTH DAKOTA	12-27-1978
TENNESSEE	12-27-1978
TEXAS	12-27-1978
UTAH	12-27-1978
VIRGINIA	12-27-1978
WASHINGTON	12-27-1978
WEST VIRGINIA	12-27-1978
WISCONSIN	12-27-1978
WYOMING	12-27-1978

SCHEDULE		PAGE	
NO.	DATE	NO.	DATE
1	1/1/1971	1	1/1/1971
2	2/1/1971	2	2/1/1971
3	3/1/1971	3	3/1/1971
4	4/1/1971	4	4/1/1971
5	5/1/1971	5	5/1/1971
6	6/1/1971	6	6/1/1971
7	7/1/1971	7	7/1/1971
8	8/1/1971	8	8/1/1971
9	9/1/1971	9	9/1/1971
10	10/1/1971	10	10/1/1971
11	11/1/1971	11	11/1/1971
12	12/1/1971	12	12/1/1971
13	1/1/1972	13	1/1/1972
14	2/1/1972	14	2/1/1972
15	3/1/1972	15	3/1/1972
16	4/1/1972	16	4/1/1972
17	5/1/1972	17	5/1/1972
18	6/1/1972	18	6/1/1972
19	7/1/1972	19	7/1/1972
20	8/1/1972	20	8/1/1972
21	9/1/1972	21	9/1/1972
22	10/1/1972	22	10/1/1972
23	11/1/1972	23	11/1/1972
24	12/1/1972	24	12/1/1972
25	1/1/1973	25	1/1/1973
26	2/1/1973	26	2/1/1973
27	3/1/1973	27	3/1/1973
28	4/1/1973	28	4/1/1973
29	5/1/1973	29	5/1/1973
30	6/1/1973	30	6/1/1973
31	7/1/1973	31	7/1/1973
32	8/1/1973	32	8/1/1973
33	9/1/1973	33	9/1/1973
34	10/1/1973	34	10/1/1973
35	11/1/1973	35	11/1/1973
36	12/1/1973	36	12/1/1973
37	1/1/1974	37	1/1/1974
38	2/1/1974	38	2/1/1974
39	3/1/1974	39	3/1/1974
40	4/1/1974	40	4/1/1974
41	5/1/1974	41	5/1/1974
42	6/1/1974	42	6/1/1974
43	7/1/1974	43	7/1/1974
44	8/1/1974	44	8/1/1974
45	9/1/1974	45	9/1/1974
46	10/1/1974	46	10/1/1974
47	11/1/1974	47	11/1/1974
48	12/1/1974	48	12/1/1974
49	1/1/1975	49	1/1/1975
50	2/1/1975	50	2/1/1975
51	3/1/1975	51	3/1/1975
52	4/1/1975	52	4/1/1975
53	5/1/1975	53	5/1/1975
54	6/1/1975	54	6/1/1975
55	7/1/1975	55	7/1/1975
56	8/1/1975	56	8/1/1975
57	9/1/1975	57	9/1/1975
58	10/1/1975	58	10/1/1975
59	11/1/1975	59	11/1/1975
60	12/1/1975	60	12/1/1975
61	1/1/1976	61	1/1/1976
62	2/1/1976	62	2/1/1976
63	3/1/1976	63	3/1/1976
64	4/1/1976	64	4/1/1976
65	5/1/1976	65	5/1/1976
66	6/1/1976	66	6/1/1976
67	7/1/1976	67	7/1/1976
68	8/1/1976	68	8/1/1976
69	9/1/1976	69	9/1/1976
70	10/1/1976	70	10/1/1976
71	11/1/1976	71	11/1/1976
72	12/1/1976	72	12/1/1976
73	1/1/1977	73	1/1/1977
74	2/1/1977	74	2/1/1977
75	3/1/1977	75	3/1/1977
76	4/1/1977	76	4/1/1977
77	5/1/1977	77	5/1/1977
78	6/1/1977	78	6/1/1977
79	7/1/1977	79	7/1/1977
80	8/1/1977	80	8/1/1977
81	9/1/1977	81	9/1/1977
82	10/1/1977	82	10/1/1977
83	11/1/1977	83	11/1/1977
84	12/1/1977	84	12/1/1977
85	1/1/1978	85	1/1/1978
86	2/1/1978	86	2/1/1978
87	3/1/1978	87	3/1/1978
88	4/1/1978	88	4/1/1978
89	5/1/1978	89	5/1/1978
90	6/1/1978	90	6/1/1978
91	7/1/1978	91	7/1/1978
92	8/1/1978	92	8/1/1978
93	9/1/1978	93	9/1/1978
94	10/1/1978	94	10/1/1978
95	11/1/1978	95	11/1/1978
96	12/1/1978	96	12/1/1978
97	1/1/1979	97	1/1/1979
98	2/1/1979	98	2/1/1979
99	3/1/1979	99	3/1/1979
100	4/1/1979	100	4/1/1979

INVESTIGATIVE DIVISION HAS DISCLOSED WITH REFERENCE TO THE
COMMUNIST INFLUENCE AT BUREAU

Figure 85. Electrical Interconnections (Concluded).

Table XV. Control System Weight.

	<u>Experimental</u>	<u>Predicted</u> <u>Flight</u>
	(lbs.)	
Fuel Pump	16.5	14.5
Fuel Filter	2.7	3.4
Hydromechanical Control	41.0	20.0
T25 Sensor	1.9	-
Core Stator Actuators (2)	4.0	4.5
Core Stator Feedback	3.0	-
Drain Eductor	3.0	-
Eductor Flow Regulator	3.0	3.0
Fuel System Total	75.1	45.4
Digital Control and Mounting Hardware	51.6	26.0
Alternator	3.5	4.5
LPT Speed Sensor	1.1	1.1
T12 Sensor	0.5	0.5
T3 Sensor	1.0	1.0
Electrical System Total	57.7	33.1
Hydraulic Pump	21.5	21.5
Hydraulic Filter	2.5	2.5
Hydraulic Relief Valve	1.5	1.5
Chip Detector	0.4	0.4
A18 Actuators (6)	30.3	30.3
A18 Synch. Cables	8.0	8.0
A18 Synch. Slip Joint	1.5	1.5
A18 Servovalve	0.9	0.9
Servovalve Manifold	3.0	3.0
Hydraulic System Total	69.6	69.6

APPENDIX A

NOMENCLATURE DEFINITION

A18	Fan Exhaust Area
A41	High Pressure Turbine Inlet Area
A49	Low Pressure Turbine Inlet Area
β_C	Core Stator Vane Angle
β_F	Fan Blade Pitch Angle
FD	Ram Drag
FG	Gross Thrust
FN	Net Thrust
HP	High Pressure
LP	Low Pressure
MO	Aircraft Mach Number
M11	Inlet Throat Mach Number (Same as XM11)
N1K	Same as PCNLR
N1T	Percent Fan Turbine rpm
NH	Core rpm
NL	Fan rpm
PAMB	Ambient Pressure
PCBP	Compressor Bleed Pressure
PCNH	Percent Core rpm
PCNHR	Percent Corrected Core rpm ($PCNH/\sqrt{T25/518.7}$)
PCNL	Percent Fan rpm
PCNLR	Percent Corrected Fan rpm ($PCNL/\sqrt{T12/518.7}$) [Equivalent to N1K]
PLA	Power Lever, Angle
PS3	Compressor Discharge Static Pressure
PS3QOT	PS3/PTO
PS8	Core Exhaust Nozzle Throat Static Pressure
PS11	Inlet Throat Static Pressure
PS14	Fan Discharge Static Pressure
PTO	Free-Stream Total Pressure
P14	Fan Discharge Total Pressure
P14QOT	P14/PTO
P49	Low Pressure Turbine Inlet Total Pressure
P49QOT	P49/PTO
SM12	Fan Stall Margin
TP1, TP2, Etc.	Thrust Parameters as Defined in Section 4.2.1
T0	Ambient Temperature
T2	Fan Inlet Total Temperature (Hub)
T3	Compressor Discharge Total Temperature
T8	Core Exhaust Total Temperature
T8QT2	Same as T8/T12
T12	Fan Inlet Total Temperature
T12R	Fan Inlet Reference Total Temperature (Figure 7)

Appendix A (Continued)

T25	Core Inlet Total Temperature
T41	High/Low Pressure Turbine Inlet Total Temperature
T41C	T41 Calculated from T3, WF, and PS3
T41CT2	Same as T41C/T2
T49	Low Pressure Turbine Inlet Temperature
T49QT2	Same as T49/T12
UTW	Under the Wing
VSV	Variable Stator Vane Position (Equivalent to βC)
WC	Cooling Bleed Airflow
WF	Engine Fuel Flow
W25	Core Air Flow
XM11	Same as M11

APPENDIX B

CONTROL SYSTEM FAILURE ANALYSIS

<u>Failure</u>	<u>Control System Effects</u>	<u>Engine Effects</u>
<u>A. Electrical Power Supply Failure</u>		
1. Lose digital control power supply (alternator, lead, or connection failure).	WF decreases to minimum, βF doesn't change, A18 drifts to aerodynamic balance position (approximately fan duct discharge area).	Thrust is lost.
2. Loss emergency overspeed circuit power supply (alternator, lead, or connector failure).	Lose overspeed protection. Fault light will notify engine operator.	No immediate effect. Emergency overspeed protection lost, normal maximum N1 limit retained.
3. Lose power to control room elements of digital control.	Lose commands to digital control. Fault will be detected through test word and control revert to next-to-last set of commands.	Remains at prefault condition. Manual thrust reduction possible with hydro-mechanical control.
<u>B. Electrical Feedback Failures</u>		
1. Lose WF metering valve feedback signal.	Electrical fuel control loop stability compensation lost and T4LC error in upward direction introduced (zero feedback is high WF).	WF instability, thrust loss due to false high T4LC.
2. Lose A18 feedback signal.	Indicates actuator at midstroke. Results are: <u>Manual Mode - Forward, Thrust Operation</u> A18 goes to min. stop, WF increases to hold N1. <u>Automatic Mode - Forward</u> A18 goes to min. stop, βF closes to hold N1. <u>Reverse Mode</u> A18 goes to reverse stop which is just slightly beyond the normal reverse position.	Fan stall margin reduced approximately 80% Fan stall margin reduced approximately 50%. Negligible effect.

<u>Failure</u>	<u>Control System Effects</u>	<u>Engine Effects</u>
3. Lose one βF feedback signal.	Continues normal operation on second feedback. Fault light notifies operator of loss in redundancy.	No effect.
4. Lose both βF feedback signal.	Indicates pitch at midposition. Results are:	
	<u>Reverse-Through-Stall Configuration -</u>	
	<u>Manual Mode - Forward, βF Demand</u>	Thrust reduction.
	βF goes to closed stop, WF maintains proper N1.	
	<u>Manual Mode - Reverse, βF Demand</u>	Negligible; stop is near normal reverse position.
	βF goes to open stop.	N1 increases to maximum limit.
	<u>Automatic Mode - Forward</u>	Negligible; stop is near normal reverse position.
	βF goes to closed stop.	
	<u>Automatic Mode - Reverse</u>	
	βF goes to reverse stop.	
	<u>Reverse-Through-Flat-Pitch Configuration -</u>	
	<u>Manual Mode - Forward βF Demand</u>	Thrust increases.
	βF to open stop.	
	<u>Manual Mode - Reverse βF Demand</u>	Negligible; stop is near normal reverse position.
	βF to reverse stop.	
	<u>Automatic Mode - Forward</u>	Reduced N1, thrust maintained.
	βF to open stop.	
	<u>Automatic Mode - Reverse</u>	Negligible; stop is near normal reverse position.
	βF to reverse stop.	

<u>Failure</u>	<u>Control System Effects</u>	<u>Engine Effects</u>
5. Lose LPT speed signal to digital control.	<p>Manual and Reverse Modes Senses N1 loss, reduces max. N2 limit to idle.</p> <p>Automatic Mode - Forward Senses N1 loss, actuates βF to flat pitch limit, reduces maximum N2 limit to idle.</p>	Engine decels to idle N2.
6. Lose LPT speed signal to emergency overspeed circuit.	Lost emergency overspeed protection. Loss of N1 readout notifies operator.	No immediate effect. Emergency overspeed protection lost, normal maximum N1 limit retained.
C. <u>Electrical Input Failures</u>		
1. Command data link	Lose commands to digital computer. Fault will be detected through test word and computer will revert to next-to-last set of commands.	Remains at prefault condition. Manual thrust reduction possible with hydromechanical control.
2. T12 sensor open circuit	<p>Manual and Reverse Modes No effect, T12 not used.</p> <p>Automatic Mode - Forward Sensed T12 goes to 160° F causing scheduled thrust parameter level to decrease and scheduled N1 to increase.</p>	<p>No effect.</p> <p>Thrust reduction (0 to 20%).</p>
3. T12 sensor element short circuit	<p>Manual and Reverse Modes No effect. T12 not used.</p> <p>Automatic Mode - Forward Sensed T12 goes to -40° F causing scheduled thrust parameter level to increase and scheduled N1 to decrease.</p>	<p>No effect.</p> <p>Thrust increases, possibly to T41C or N2 limit.</p>

<u>Failure</u>	<u>Control System Effects</u>	<u>Engine Effects</u>
4. T12 sensor circuit shorted to ground.	<p>Manual and Reverse Modes No effect. T12 not used.</p> <p>Automatic Mode - Forward Sensed T12 shifts a small amount or to 40° F, depending on location of short. Scheduled thrust parameter level and N1 change.</p> <p>T41C low resulting in loss of over-temperature protection.</p>	<p>No effect.</p> <p>Thrust change (20% maximum).</p>
5. T3 thermocouple circuit open, shorted lead-to-lead or shorted to ground.	<p>T41C low resulting in loss of over-temperature protection.</p>	<p>Turbine overtemperature if operating on T41C limit. If not on limit, no immediate effect but overtemperature protection lost. Low T41 indication alerts operator.</p>
6. Throttle RVDT failed.	No effect. Currently used only for indication.	No effect.
D. <u>Pressure Sensing Failures</u>		
1. PTO sensing line leaks.	<p>Manual and Reverse Modes No effect. PTO not used.</p> <p>Automatic Mode - Forward Negligible SLS effect. At simulated flight conditions, sensed PTO will be low causing upward shifts in the thrust parameter feedback and N1 schedule and opening A18.</p>	<p>No effect.</p> <p>Thrust reduction.</p>

<u>Failure</u>	<u>Control System Effects</u>	<u>Engine Effects</u>
2. PTO sensor open or short	<p><u>Manual and Reverse Modes</u> No effect. PTO not used.</p> <p><u>Automatic Mode - Forward</u> Sensed PTO near maximum or minimum extreme depending on location of fault. The thrust parameter and N1 will shift up or down and A18 will open to roof or close to floor schedules.</p>	<p>No effect.</p> <p>Thrust change, safety limits retained.</p>
3. PS11 sensing line leaks.	<p><u>Manual and Reverse Modes</u> No effect. PS11 not used.</p> <p><u>Automatic Mode - Forward</u> Sensed PS11 shifts upward resulting in a downward shift in sensed inlet Mach which causes A18 to open to the roof schedule. WF and βF modulate to maintain constant thrust parameter level and N1.</p>	<p>No effect.</p> <p>Inlet mach increase, more inlet distortion, probable decrease in compressor stall margin.</p>
4. PTO-PS11 sensor open or short circuit	<p><u>Manual or Reverse Mode</u> No effect. PTO-PS11 not used.</p> <p><u>Automatic Mode - Forward</u> Sensed PTO-PS11 shifts to near maximum or minimum extreme depending on location of fault. A18 open to roof or closes to floor limits.</p>	<p>No effect.</p> <p>Either increase or decrease inlet mach. Increase gives probable stall margin reduction, decrease gives noise increase.</p>

<u>Failure</u>	<u>Control System Effects</u>	<u>Engine Effects</u>
5. PTL4 sensing line leaks.	<u>Manual or Reverse Mode</u> No effect. PTL4 not used. <u>Automatic Mode - Forward, PTL4/PTO Thrust Parameter</u> Sensed level of thrust parameter decreases causing increase in WF. βF and A18 modulate to maintain N1 and inlet Mach. <u>Automatic Mode - Forward, Other Thrust Param.</u> No effect. PTL4 not used.	No effect. Thrust increase, safety limits retained. No effect.
6. PTL4-PTO sensor open or short circuit	<u>Manual or Reverse Mode</u> No effect. PTL4-PTO not used. <u>Automatic Mode - Forward, PTL4/PTO Thrust Parameter</u> Sensed PTL4-PTO shifts to near maximum or minimum extreme depending on location of fault. WF decreases or increases, βF and A18 modulate to maintain N1 and inlet Mach. <u>Automatic Mode Forward, Other Thrust Parameter</u> No effect. PTL4-PTO not used.	No effect. Thrust decrease or increase, safety limits retained. No effect.

Failure

7. PS3 sensing line leak.

Control System Effects

Low PS3 sensed by both digital and hydro-mechanical controls. Effects are:

Automatic Mode - Forward, PS3/PTO Thrust Parameter

Small leak will cause WF to increase to regain demanded PS3/PTO. Large leak causes WF reduction because of false high T41C or low acceleration schedule.

Other Modes

Small leak has no effect. Large leak causes WF reduction because of false high calculated T41 or low acceleration schedule.

Engine Effects

Thrust increase with small leak, thrust decrease with large leak.

No effect from small leak, thrust decrease with large leak.

<u>Failure</u>	<u>Control System Effects</u>	<u>Engine Effects</u>
8. PS3 sensor open or short circuit	Sensed PS3 shift to near maximum or minimum extreme depending on fault location. Results are: <u>Automatic Mode - Forward, PS3/PTO Thrust Parameter --</u> <u>Shift to Maximum</u> False low T4LC and false high level of thrust parameter. <u>Shift to Minimum</u> False high T4LC and false low level of thrust parameter.	Thrust decrease. Thrust decrease.
E. Digital Control Failures	<u>Other Modes -</u> <u>Shift to Maximum</u> False low T4LC.	No effect if not operating on T4l limit, overtemperature if operating on limit. Low T4l indication alerts operator.
	<u>Shift to Minimum</u> False high T4lc resulting in T4lc limit takeover at less than actual T4l limit.	Thrust decrease.
1. WF output circuit to zero output.	WF goes to minimum hydromechanical limit.	Decel to less than idle.
2. WF output circuit to maximum increase.	WF increases until limited by hydromechanical N2 schedule or by emergency overspeed shutdown.	Accel to N2 limit or emergency overspeed shutdown limit.

Failure	Control System Effects	Engine Effects
3. WF output circuit to maximum decrease.	WF goes to minimum hydromechanical limit.	Decel to less than idle.
4. βF output circuit to zero output.	No effect. No-back maintains βF in position.	No immediate effect. Subsequent βF change not possible.
5. βF output circuit to maximum open.	<u>Reverse-Through-Stall Configuration</u> βF goes to reverse region stop. Interlock logic reduces WF to set flight idle N1. <u>Reverse-Through-Flat-Pitch Configuration</u> βF goes to maximum open stop. WF and A18 maintain thrust and inlet Mach number.	Engine goes to flight idle N1 in reverse thrust. N1 decreases, thrust and inlet Mach unchanged. Possible fan stall margin reduction.
6. βF output circuit to maximum closed.	<u>Reverse-Through-Stall Configuration</u> βF goes to maximum closed stop. <u>Reverse-Through-Flat-Pitch Configuration</u> βF goes to reverse region stop. Interlock logic reduces WF to flight idle N1.	N1 increases, probably to normal maximum limit. Engine goes to flight idle N1 in reverse thrust.
7. A18 output circuit to zero output.	A18 drifts to aerodynamic balance position: βF and WF attempt to maintain N1 and thrust.	βF opens, inlet mach increases. High inlet distortion at high power settings.
8. A18 output circuit to maximum open.	A18 driven to reverse (diverging) position: βF and WF attempt to maintain N1 and thrust.	βF opens, inlet mach increases. High inlet distortion at high power settings.

Failure	Control System Effects	Engine Effects
F. Hydraulic System Failures		
1. Hydraulic pump output lost.	βF remains in position, A18 drifts to aerodynamic balance position.	Thrust decreases, inlet Mach increases. High inlet distortion at high power settings. βF and A18 lag on transients.
2. Hydraulic pump compensator failed to minimum displacement condition.	No steady-state effect. βF and A18 transients slow.	No immediate effect but shutdown necessary when oil temperature reached limit. βF and A18 lag on transients.
3. Hydraulic pump compensator failed to maximum displacement condition.	Full pump flow bypassed through relief valve, oil heats up rapidly, controlled variables unaffected.	No effect.
4. Relief valve sticks open.	No steady-state effect, βF and A18 transients slow.	No effect.
5. A18 (or βF) servovalve coil open circuit.	No effect. Operation continues on redundant coil. Redundancy lost.	No effect.
6. A18 (or βF) servovalve feedback spring failed.	Servovalve proportional characteristic lost, A18 (or βF) unstable.	A18 (or βF) unstable.
7. A18 servovalve spool stuck.	Servovalve will not respond to input change, remains at condition existing when spool stuck.	If steady-state, A18 remains in position or drifts open to aero. balance point. If transient, A18 goes to stop.
8. βF servovalve spool stuck.	Servovalve will not respond to input change, remains at condition existing when spool stuck.	If steady-state, βF remains in position. If transient, βF goes to stop.

<u>Failure</u>	<u>Control System Effects</u>	<u>Engine Effects</u>
9. A18 servovalve jet pipe plugged.	Servovalve spool tends to stay at condition existing when plugging occurred.	If steady-state, A18 remains in position or drifts open to aero. balance point. If transient, A18 goes to stop.
10. β F servovalve jet pipe plugged.	Servovalve spool tends to stay at condition existing when plugging occurred.	If steady-state, β F remains in position. If transient, β F goes to stop.
G. <u>Hydromechanical Control System Failures</u>		
1. T25 sensor coil leak; gas charge lost.	Sensed T25 reduces to below -65° F, lowering the hydromechanical N2 schedule and causing core stators to go to a fail-safe schedule.	Thrust decrease probable; amount depends on relative settings of throttle and electrical power setting signal.
2. T25 sensor variable orifice plugged.	Sensed T25 shifts to high-temperature extreme, causes core stators to shift in the closed direction.	Thrust decreases.
3. Core stator feedback cable breaks.	Core stators go to full-closed position.	Thrust decreases.
4. Hydromechanical control fuel metering valve fails open.	WF increases, increasing rotor speed until operator or emergency overspeed function cuts off fuel flow.	Acceleration to overspeed limit and then shutdown.
5. Hydromechanical control fuel bypass valve goes closed.	Fuel control loop closes metering valve maintaining schedules and limits. Excess fuel is bypassed through relief valve causing fuel temperature rise.	Possible WF instability. Shutdown required to prevent excessive fuel heating.

Failure	Control System Effects	Engine Effects
6. WF trim servovalve coil open circuit.	No effect. Operation continues on redundant coil. Redundancy lost.	No effect.
7. WF trim servovalve feedback spring failed.	Servovalve proportional characteristic lost. WF unstable unless being controlled by hydromechanical governor.	WF unstable if in electrical control mode. Can be corrected by PLA retard to N2 governor takeover.
8. WF trim servovalve spool stuck.	Servovalve will not respond to input changes, remains at condition existing when spool stuck.	Probable WF drift; can be controlled by PLA/N2 governor at reduced power. Emergency overspeed limit still active.
9. WF trim servovalve jet-plugged.	Servovalve tends to stay at condition existing when plugging occurred.	Probable WF drift; can be controlled by PLA/N2 governor at reduced power. Emergency overspeed limit still active.
10. Emergency overspeed servovalve coil open circuit.	Lose emergency overspeed; fault light alerts operator.	No immediate effect. Emergency overspeed protection lost, normal maximum N1 limit retained.
11. Emergency overspeed servovalve spool stuck or jet-plugged.	Servovalve will not respond to overspeed signal; lose emergency overspeed protection.	No immediate effect. Emergency overspeed protection lost, normal maximum N1 limit retained.

APPENDIX C

COMPUTER SIMULATION of
CONTROL SYSTEM FAILURES

Failure Simulation Study

Failure*	Control System Effects	Engine Effects
B.1. Lose WF metering valve feedback signal (see Figure 86).	WF feedback path in digital control indicates maximum metering valve position (i.e., XMV = 0.816 in.). This causes calculated T41 to increase to maximum scaled value of 660° R above T41 at takeoff, which exceeds the T41C reference limit by 460° R; as a consequence, the T41C control causes WF to decrease to the deceleration schedule. During deceleration, fan pitch closes to floor schedule limit of +2° and A18 opens to roof schedule limit of 1.71 m ² (2650 in. ²). After engine deceleration, the core idle speed control modulates WF. Because of the failed feedback signal, the control gain is high and the phase lead compensation has been lost.	Core engine decelerates to the idle speed reference of 11,000 rpm which decreases fan speed and thrust. Core speed, fan speed, and thrust oscillate at this idle power condition because of the failed feedback signal. Frequency of oscillation is 0.5 Hertz. Fan stall margin oscillates in the 8% to 10% range.
B.2. Lose A18 feedback signal (see Figure 87).	A18 feedback path in digital control calculates that A18 actuators are at the midstroke position, which indicates that A18 is further open than the roof schedule. Therefore, the A18 digital control causes A18 to close to 1.06 m ² (1800 in. ²). Fan pitch closes to the fan pitch floor schedule, as the fan speed-pitch control tries to maintain takeoff fan speed.	The fan speed decreases about 25 rpm, due to the +2° fan pitch floor schedule limit. Thrust decreases to 92% of takeoff thrust. Fan stall margin decreases to the 1% to 2% range.

*Identification numbers (i.e., B.1., B.2., etc.) match failure analysis numbers in Appendix B.

Failure Simulation Study (Continued)

Failure	Control System Effects	Engine Effects
C.3. T12 sensor element short circuit (see Figure 88).	Indicates sensed T12 at 420° R (i.e., -40° F). Causes reduction in fan speed reference. Fan pitch opens to reduce fan speed.	Fan speed decreases from 3060 rpm (takeoff) to 2750 rpm. Thrust decreases 2% below takeoff. Fan stall margin decreases to about 7% transiently and settles to a steady-state level of 9% stall margin.
D.2.(a) PTO sensor open or short indicating minimum PTO (see Figure 89).	Sensor fails at location which indicates PTO = 2 psia. Causes (1) PS3/PTO feedback calculation to go to maximum scaled value of 20.47; (2) scheduled PS3/PTO to increase; (3) PTO-PS11/PTO feedback calculation to go to 1.0; and (4) scheduled fan speed to increase. Net effect is decrease in WF and A18 and closing of fan pitch to floor schedule.	Engine decelerates; fan stall margin decreases to the 1% to 2% range; inlet Mach number decreases to 0.25.
D.2.(b) PTO sensor open or short indicating maximum PTO (see Figure 90).	Fails at location which indicates PTO = 19 psia. This causes (1) digital calculation for sensed PS3/PTO to decrease; (2) scheduled PS3/PTO to decrease; (3) PTO-PS11/PTO feedback calculation to decrease; and (4) scheduled fan speed to decrease. Net effect is fuel flow increasing until limited by calculated T41 control, fan pitch closing, and A18 closing 0.065 m ² (100 in. ²). Acceleration of core engine rotor is eventually limited by the hydromechanical core speed governor at 13,700 rpm.	Core engine accelerates to 13,700 rpm. Turbine temperature increases 130° R. Inlet Mach number decreases to 0.74 and fan stall margin decreases to 5%.

Failure Simulation Study (Continued)

Failure	Control System Effects	Engine Effects
D.7. PS3 sensing line leak (see Figure 91).	Sensed PS3 sensing line leak of 2% was assumed (≈ 4 psi). PS3/PTO feedback decreases causing WF to increase. Fan pitch opens about 0.4° to hold fan speed at 3060 rpm. AL8 closes about 0.032 m^2 (50.0 in.^2) to hold inlet Mach number at 0.79.	Core speed increases from 13,200 rpm to 13,300 rpm. Turbine temperature increases 40° R ; thrust increases from 100% to 102%. Fan stall margin decreases about 0.5%. In general, minor effect on engine operation.
D.8.(a) PS3 sensor open or short indicating minimum PS3 (see Figure 92).	Sensor fails at location which indicates PS3 = 0. This causes feedback calculation for PS3/PTO to go to zero and calculated T41 to go to 660° R above the takeoff temperature (which exceeds the T41C reference limit by 460° R). As a consequence, the T41C control demands a decrease in WF to the deceleration schedule. After engine deceleration, the core idle speed control modulates WF. During deceleration, fan pitch closes to floor schedule of $+2^\circ$ and AL8 opens to roof schedule of 1.71 m^2 (2650 in.^2).	Core engine decelerates to 11,000 rpm, which is the digital control core idle speed reference. Fan decelerates and thrust decreases to 29% of takeoff thrust. Fan stall margin decreases from 14.5% to 8.5%.

Failure Simulation Study (Continued)

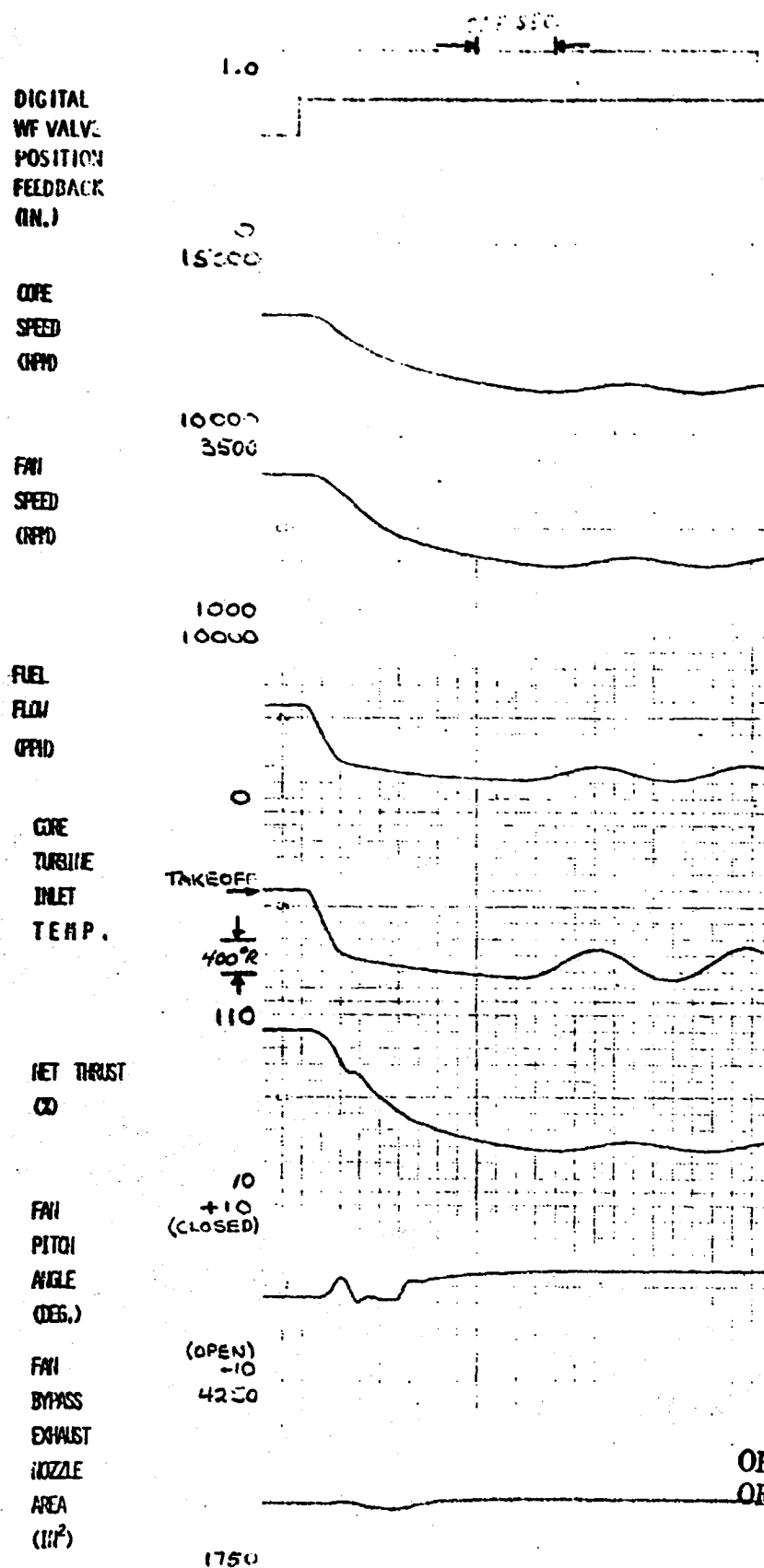
Failure	Control System Effects	Engine Effects
D.8.(b) PS3 sensor open or short indicating maximum PS3 (see Figure 93).	Sensor fails at location which indicates PS3 = 300 psia. This causes (1) PS3/PTO feedback calculation to go to maximum scaled value of 20.47; (2) calculated T41 feedback to decrease; (3) fan pitch to close to floor schedule of +2°; and (4) A18 to open to roof schedule 1.71 m ² (2650 in. ²). Calculated PS3/PTO exceeds the reference to the PS3/PTO-WF digital control which causes WF to decrease to the deceleration schedule. The core speed control modulates WF after the engine decelerates.	Affects engine in the same manner as described in D.8.(a) above.
E.2. WF output circuit to maximum increase (see Figure 94).	WF control output current goes to +80 mA. WF increases to hydromechanical acceleration schedule; fan pitch opens to hold fan speed; and A18 closes to hold inlet Mach number. Acceleration of core engine rotor is eventually limited at 13,700 rpm by hydromechanical core speed governor.	Core engine accelerates to 13,700 rpm. Turbine temperature increases 135° above takeoff temperature. Thrust increases from 100% to 108%. Fan stall margin decreases to 9.5%. Inlet Mach number increases from 0.79 to 0.80.
E.3. WF output circuit to maximum decrease (see Figure 95).	WF control output current goes to -80 mA. WF decreases to hydromechanical deceleration schedule; calculated T41 decreases; fan pitch closes to floor Schedule of +2°; A18 opens to roof schedule of 1.71 m ² (2650 in. ²).	Engine will decelerate to less than idle.

Failure Simulation Study (Continued)

Failure	Control System Effects	Engine Effects
E.5. Fan pitch output circuit to maximum open (see Figure 96).	Fan pitch control output current goes to -80 mA. Fan pitch slews through stall to mechanical stop. At -10°, the interlock logic switches WF digital control from PS3/PTO to core idle speed mode (reference is 11,000 rpm); this causes WF to decrease.	Fan and core rotor speeds decrease; engine goes to reverse thrust. (Note: For this simulation transient, minimum fan shaft power absorption during transition to reverse fan pitch was assumed to be 5500 hp.)
E.6. Fan pitch output circuit to maximum closed (see Figure 97).	Fan pitch control output current goes to +80 mA. Fan pitch slews closed to mechanical stop. WF goes to deceleration schedule because fan accelerates above 3406 rpm (105% N1). Overspeed and Emergency Shutdown System will be activated at 3568 rpm (110% N1).	Fan speed increases to 3568 rpm in about 0.3 seconds. Since Overspeed and Emergency Shutdown System was not included in the simulation, the transient beyond 0.3 seconds is not valid; however, it does provide an indication of fan overspeed without the above shutdown system.

Failure Simulation Study (Concluded)

Failure	Control System Effects	Engine Effects
E.8. A18 output circuit to maximum open (see Figure 98).	A18 control output current goes to +76 mA. A18 slews open to actuator stop. PS3/PTO decreases, causing WF to increase until limited by the T41C-WF digital control. Fan pitch opens in attempt to return fan speed to 3060 rpm (takeoff). WF decreases to final value when acceleration of core engine rotor is limited by the hydromechanical core speed governor at 13,700 rpm. For this simulation transient, maximum open fan pitch limit was set at -8°.	Inlet Mach number increases to 0.84 during first 0.15 seconds of the transient. Subsequently, the inlet Mach number increases to 1.0 (simulation results are questionable after the first 0.4 seconds due to operation in ill-defined region of fan component map). Thrust decreases to 78%.
E.9. A18 output circuit to maximum closed (see Figure 99).	A18 control output current goes to -76 mA. A18 slews closed to approximately 1.16 m ² (1800 in. ²). Fan pitch closes to floor schedule of +2° in an attempt to maintain fan speed at 3060 rpm. WF decreases about 150 pph to hold PS3/PTO at the takeoff reference value.	Large decrease in fan stall margin to 1% to 2% range. Thrust decreases from 100% to 92%.



ORIGINAL PAGE IS
OF POOR QUALITY

Figure 86. UTW Experimental Engine Transient When WF Metering Valve Position Feedback Signal Fails (Takeoff, SLS, Std. Day).

DIGITAL
WF VALVE
POSITION
FEEDBACK
(IN.)

INLET
THROAT
PACH
NO.

[PTD-PSII]
[PTD] SENSED
(PSIA/PSIA)

CORE
COMPRESSOR
STALL
MARGIN
(%)

FAN
TIP
STALL
MARGIN
(%)

CORE
COMPRESSOR
STATOR
ERROR
(DEG.)

[PS3]
[PTD] SENSED
(PSIA/PSIA)

CALCULATED
CORE
TURBINE
INLET
TEMP.

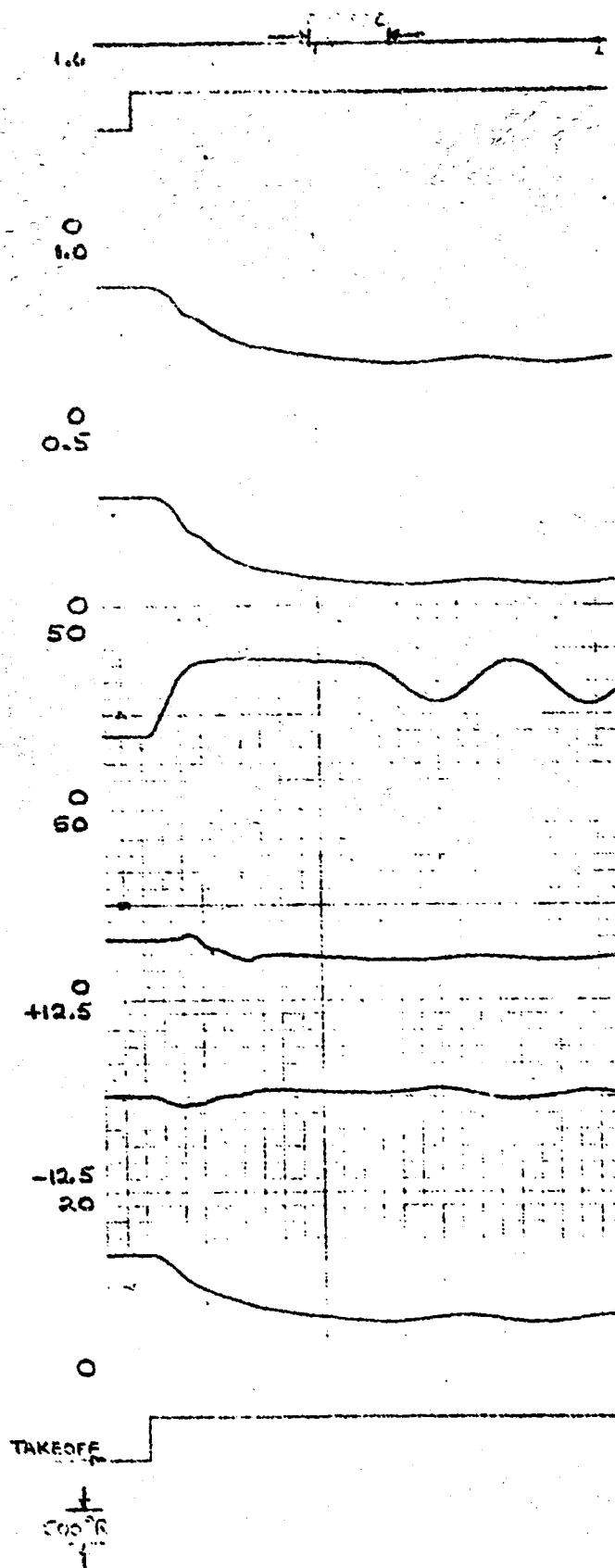


Figure 86. UTW Experimental Engine Transient When WF Metering Valve Position Feedback Signal Fails (Takeoff, SLS, Std. Day) (Concluded).

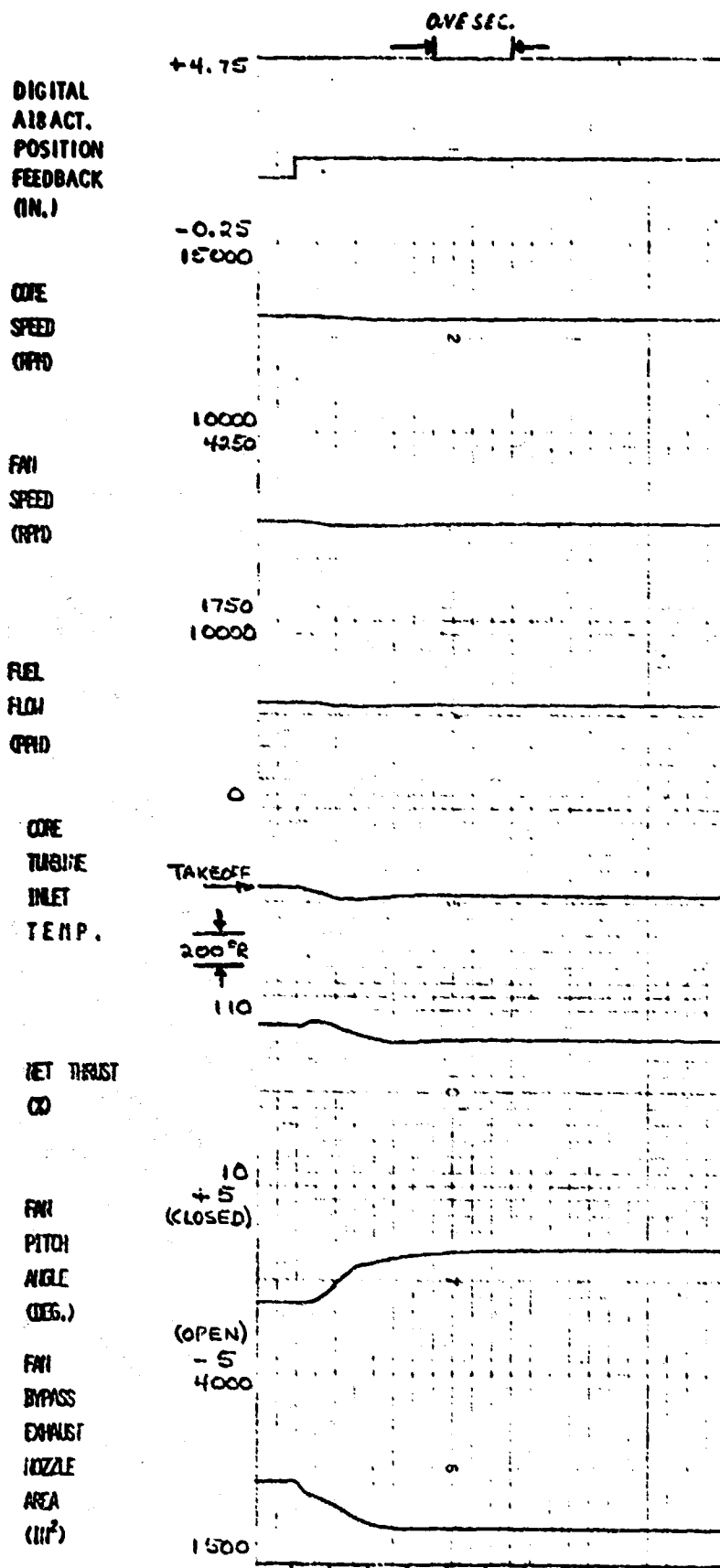


Figure 87. UTW Experimental Engine Transient When A18 Feedback Signal Fails (Takeoff, SLS, Std. Day).

ORIGINAL PAGE IS
OF POOR QUALITY

DIGITAL
A18 ACT.
POSITION
FEEDBACK
(IN.)

DILET
THROAT
PNOI
NO.

[PTD-PSII]
PTD SENSED
(PSI/PSIA)

CORE
COMPRESSOR
STALL
PNOI
CO

FMI
TIP
STALL
PNOI
CO

CORE
COMPRESSOR
STATOR
ERROR
(DEG.)

[PSI]
PTD SENSED
(PSI/PSIA)

CALCULATED
CORE
TURBINE
INLET
TEMP.

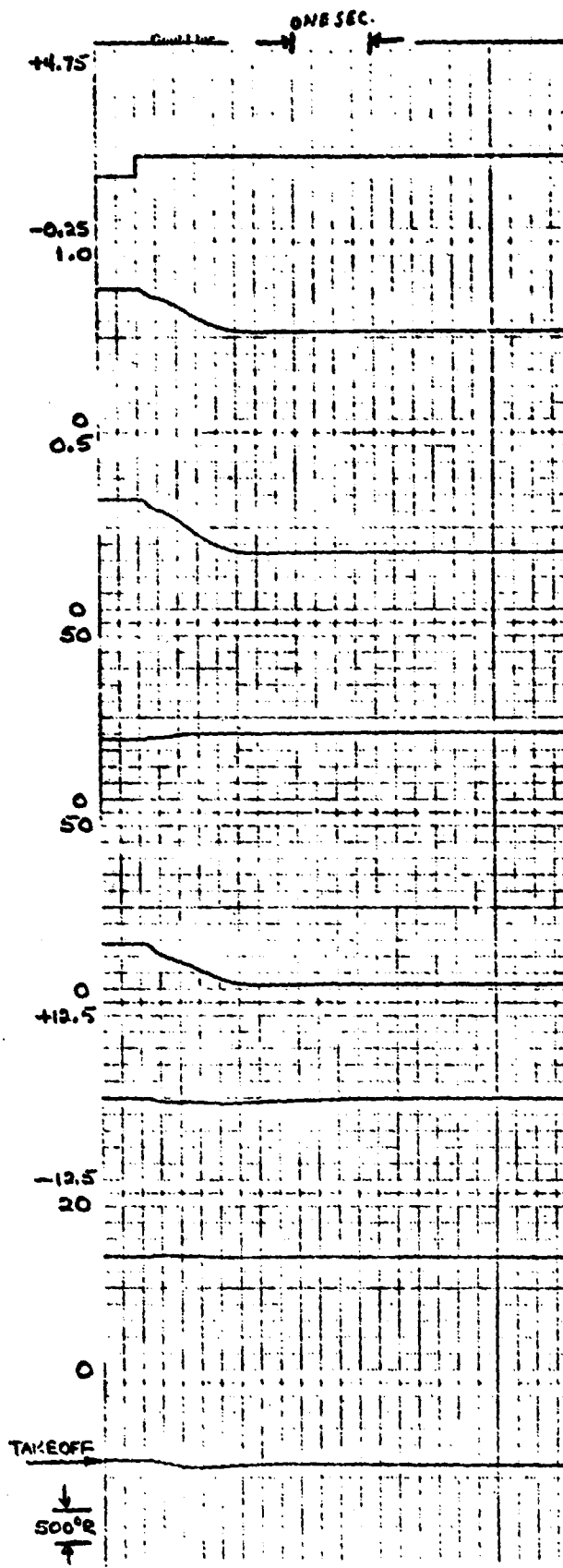


Figure 87. UTW Experimental Engine Transient When A18 Feedback Signal Fails (Takeoff, SLS, Std. Day) (Concluded).

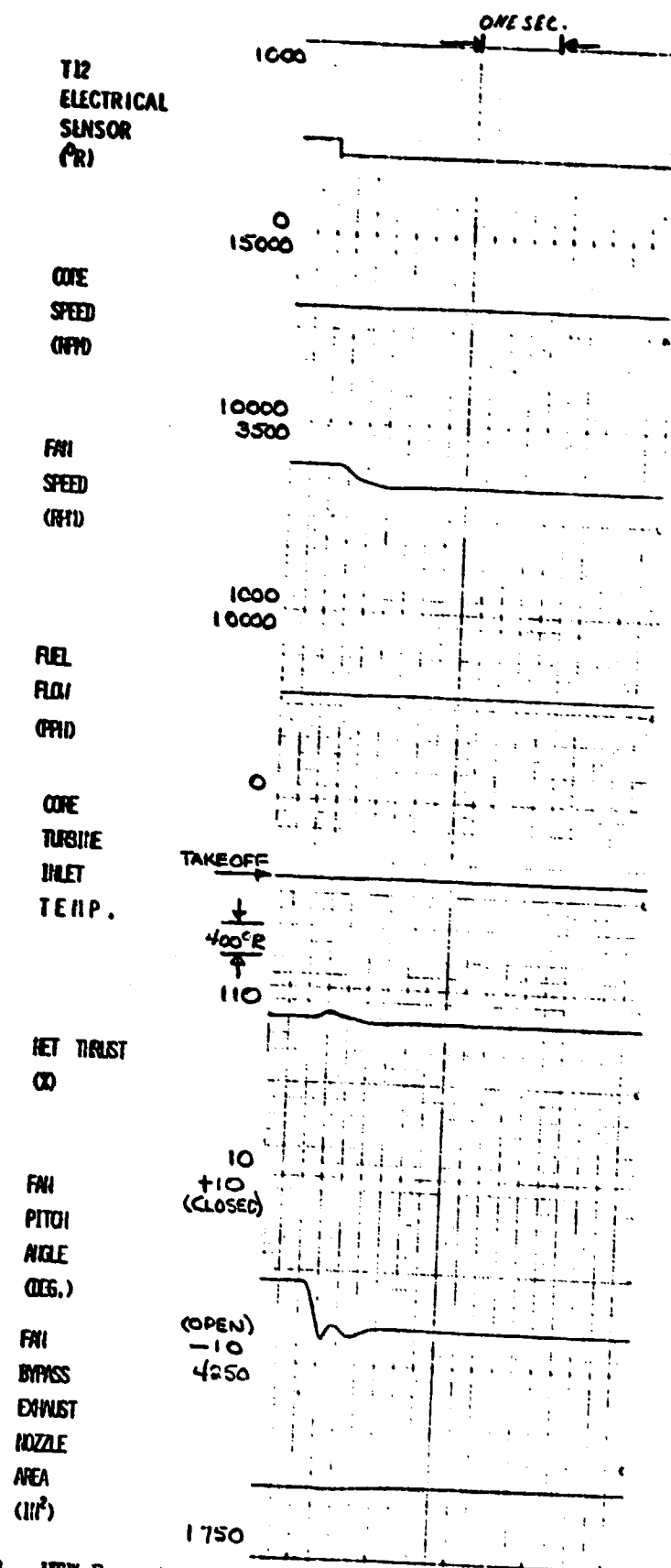


Figure 88. UTW Experimental Engine Transient When T12 Sensor Element Short Circuits (Takeoff, SLS, Std. Day).

ORIGINAL PAGE IS
OF POOR QUALITY

T12
ELECTRICAL
SENSOR
(R)

INLET
THROAT
PACH
NO.

PTO-PS11
PTO SENSED
(PSIA/PSIA)

CORE
COMPRESSOR
STALL
MARGIN
CO

FAN
TIP
STALL
MARGIN
CO

CORE
COMPRESSOR
STATOR
ERROR
(DEG.)

PS3
PTO SENSED
(PSIA/PSIA)

CALCULATED
CORE
TURBINE
INLET
TEMP.

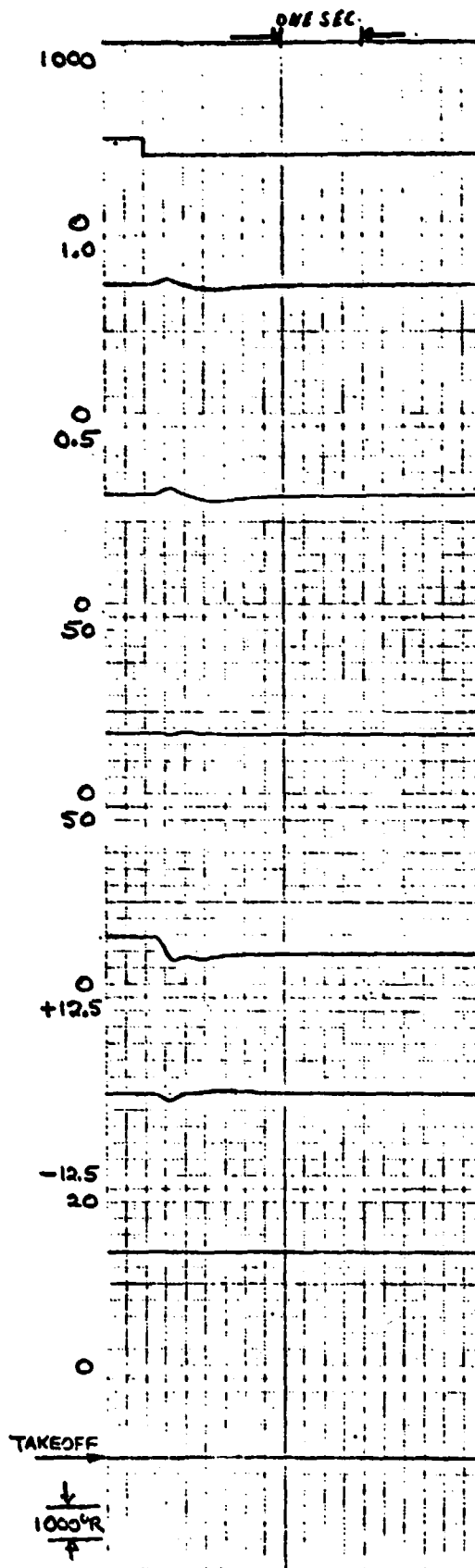


Figure 88. UTW Experimental Engine Transient When T12 Sensor Element Short Circuits (Takeoff, SLS, Std. Day) (Concluded).

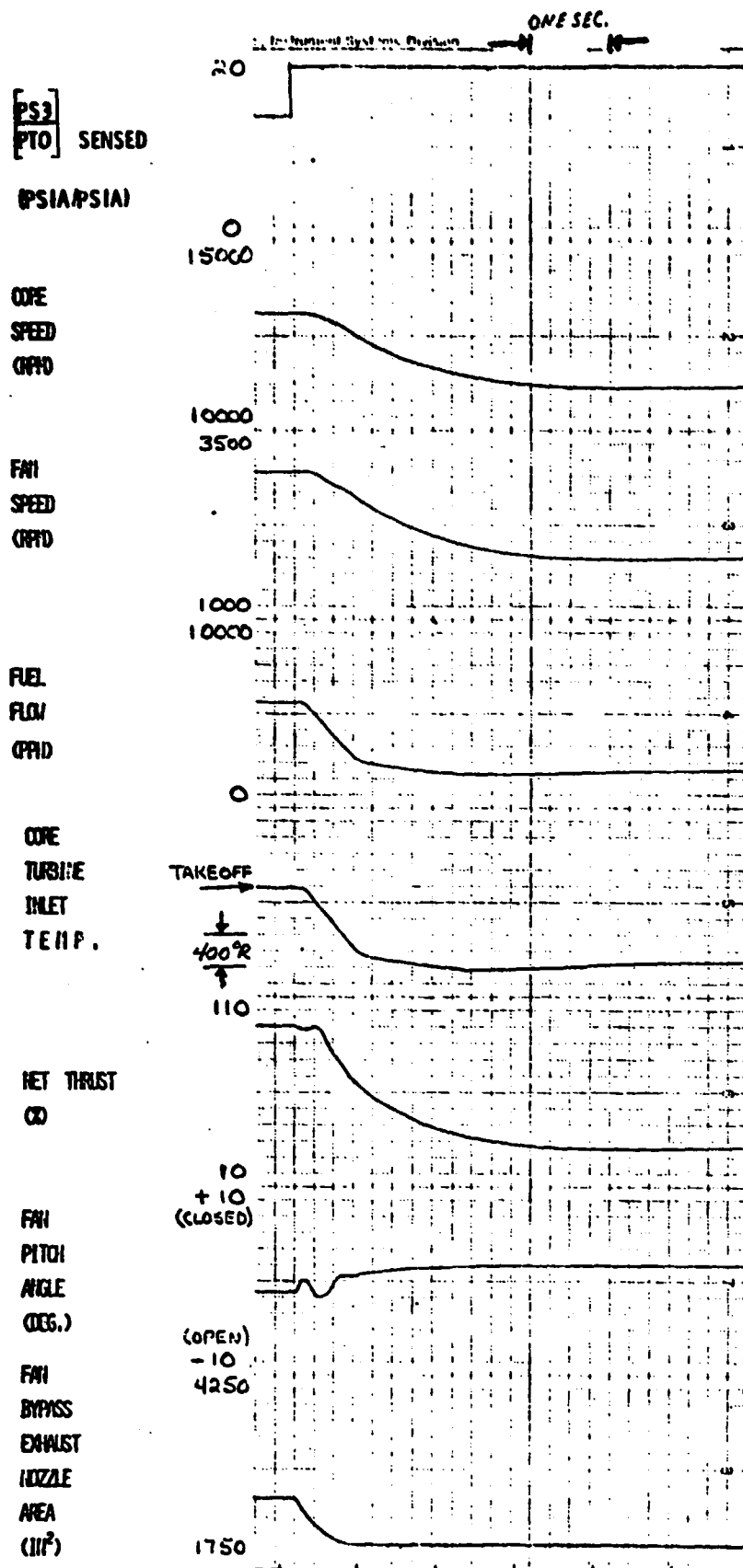


Figure 89. UTW Experimental Engine Transient When PTO Sensor Opens or Shorts and Indicates Minimum PTO (Takeoff, SLS, Std. Day).

ORIGINAL PAGE IS
OF POOR QUALITY

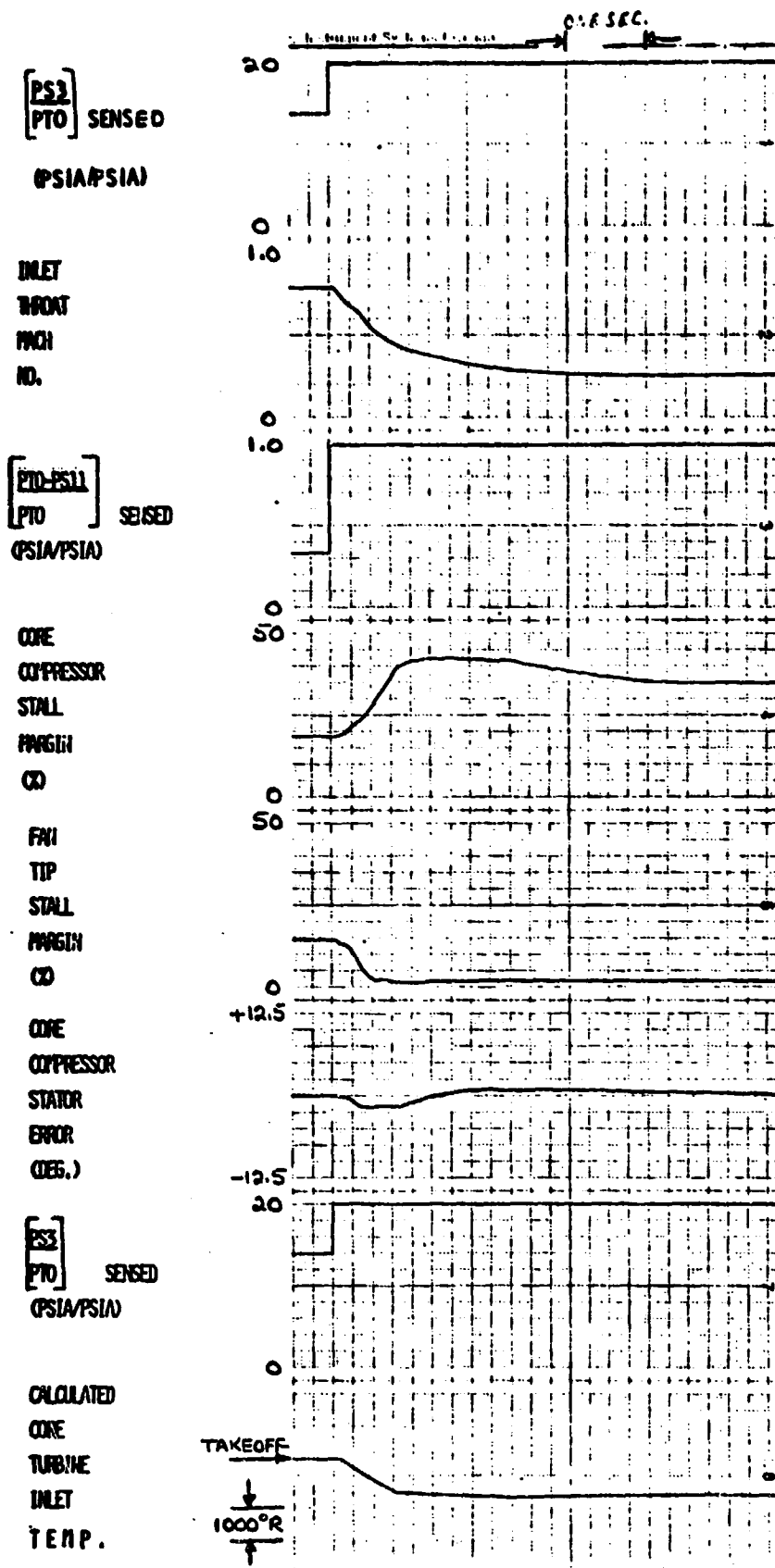


Figure 89. UTW Experimental Engine Transient When PTO Sensor Opens or Shorts and Indicates Minimum PTO (Takeoff, SLS, Std. Day) (Concluded)

ORIGINAL PAGE IS
OF POOR QUALITY

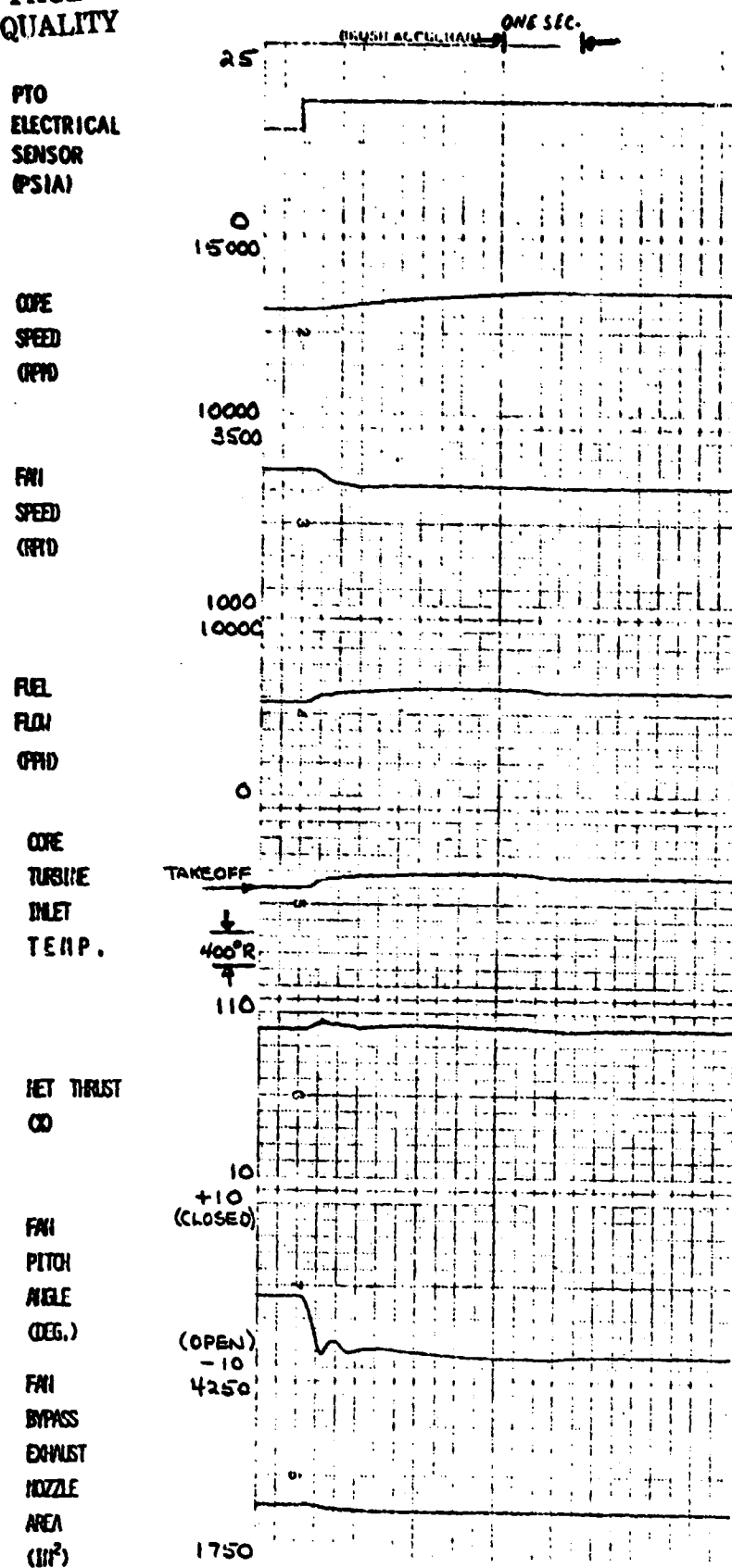


Figure 90. UTW Experimental Engine Transient When PTO Sensor Opens or Shorts and Indicates Maximum PTO (Takeoff, SLS, Std. Day).

PTO
ELECTRICAL
SENSOR
(PSIA)

INLET
THROAT
MACH
NO.

PTO-PS11
PTO SENSED
(PSIA/PSIA)

CORE
COMPRESSOR
STALL
MARGIN
(%)

FAN
TIP
STALL
MARGIN
(%)

CORE
COMPRESSOR
STATOR
ERROR
(DEG.)

PS1
PTO SENSED
(PSIA/PSIA)

CALCULATED
CORE
TURBINE
INLET
TEMP.

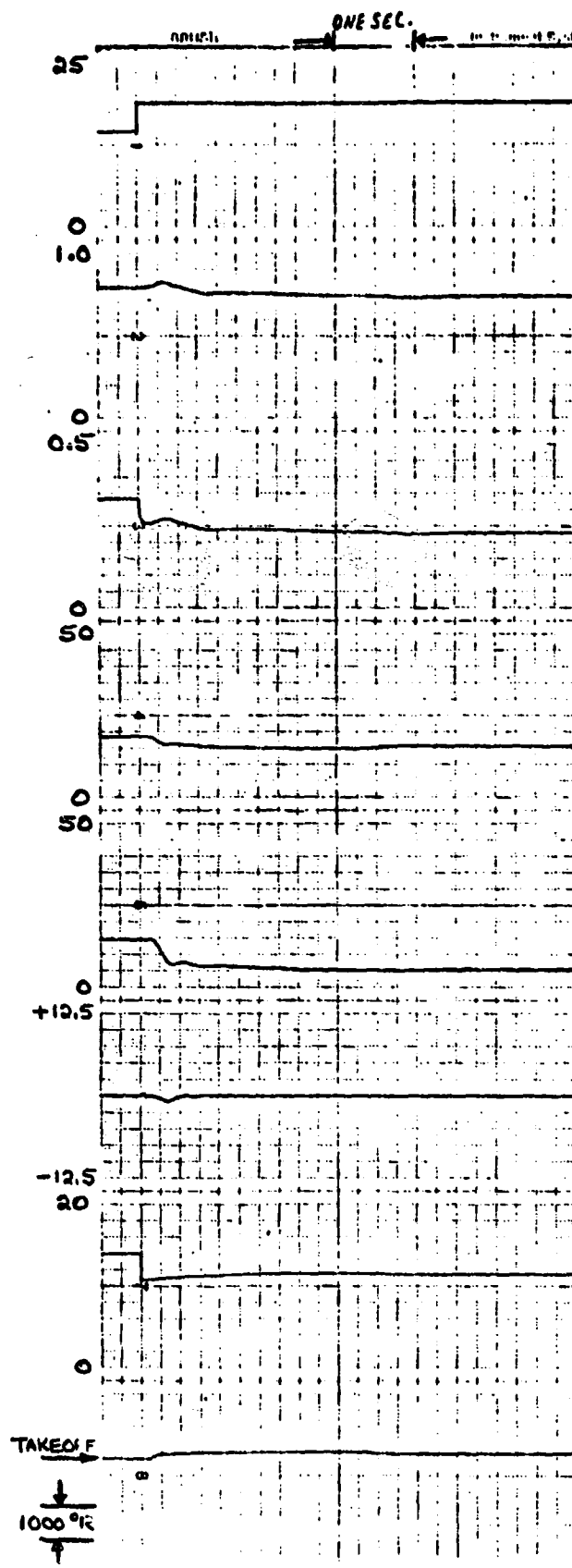


Figure 90. UTW Experimental Engine Transient When PTO Sensor Opens or Shorts and Indicates Maximum PTO (Takeoff, SLS, Std. Day) (Concluded).

ORIGINAL PAGE IS
OF POOR QUALITY

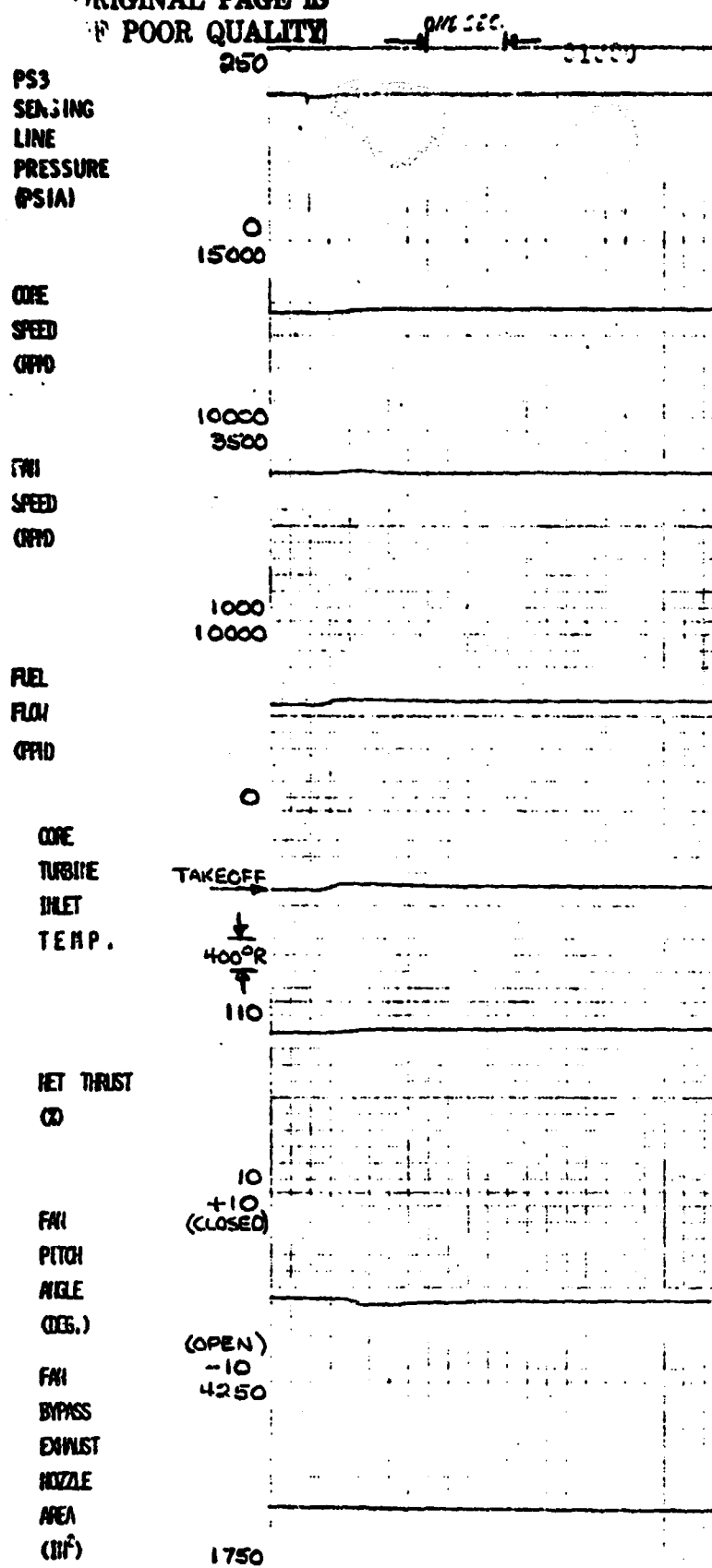


Figure 91. UTW Experimental Engine Transient When PS3 Sensing Line Leaks (Takeoff, SLS, Std. Day).

PS3
SENSING
LINE
PRESSURE
(PSIA)

INLET
THROAT
FACH
NO.

$\left[\begin{array}{c} \text{PTO-PS11} \\ \text{PTO} \end{array} \right]$ SENSED
(PSIA/PSIA)

CORE
COMPRESSOR
STALL
MARGIN
(%)

FAN
TIP
STALL
MARGIN
(%)

CORE
COMPRESSOR
STATOR
ERROR
(DEG.)

$\left[\begin{array}{c} \text{PS3} \\ \text{PTO} \end{array} \right]$ SENSED
(PSIA/PSIA)

CALCULATED
CORE
TURBINE
INLET
TEMP.

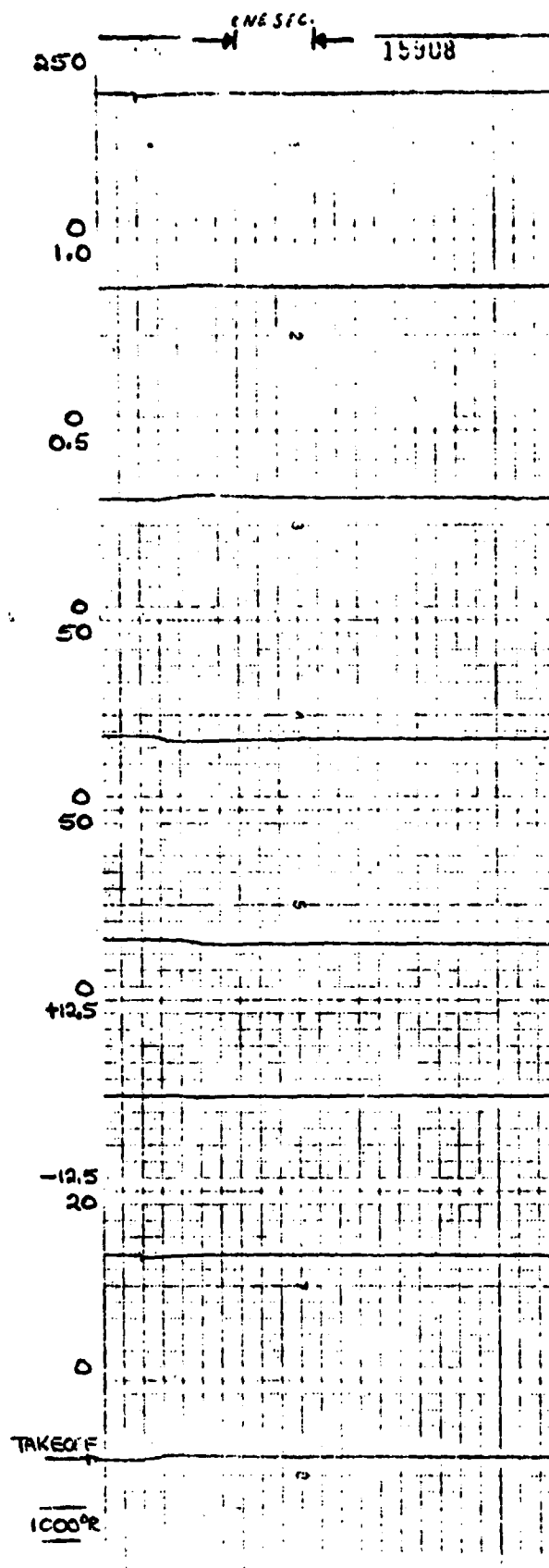


Figure 91. UTW Experimental Engine Transient When PS3 Sensing Line Leaks (Takeoff, SLS, Std. Day) (Concluded).

ORIGINAL PAGE IS
OF POOR QUALITY

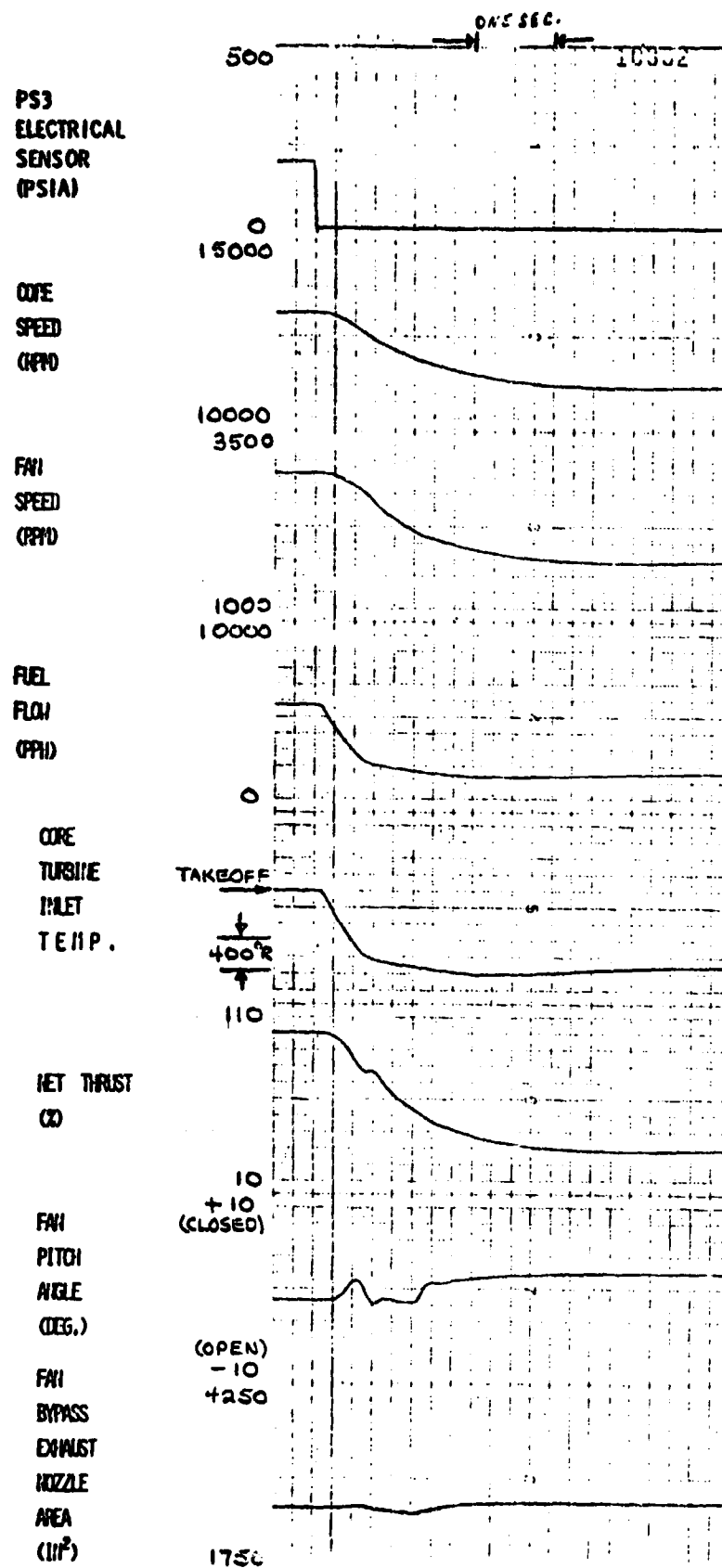


Figure 92. UTW Experimental Engine Transient When PS3 Sensor Opens or Shorts and Indicates Minimum PS3 (Takeoff, SLS, Std. Day).

PS3
ELECTRICAL
SENSOR
(PSIA)

GILET
THROAT
MACH
NO.

$\left[\frac{P_{T0}-P_{SLL}}{P_{T0}} \right]$ SENSED
(PSIA/PSIA)

CORE
COMPRESSOR
STALL
MARGIN
(%)

FAN
TIP
STALL
MARGIN
(%)

CORE
COMPRESSOR
STATOR
ERROR
(DEG.)

$\left[\frac{P_{S3}}{P_{T0}} \right]$ SENSED
(PSIA/PSIA)

CALCULATED
CORE
TURBINE
INLET
TEMP.

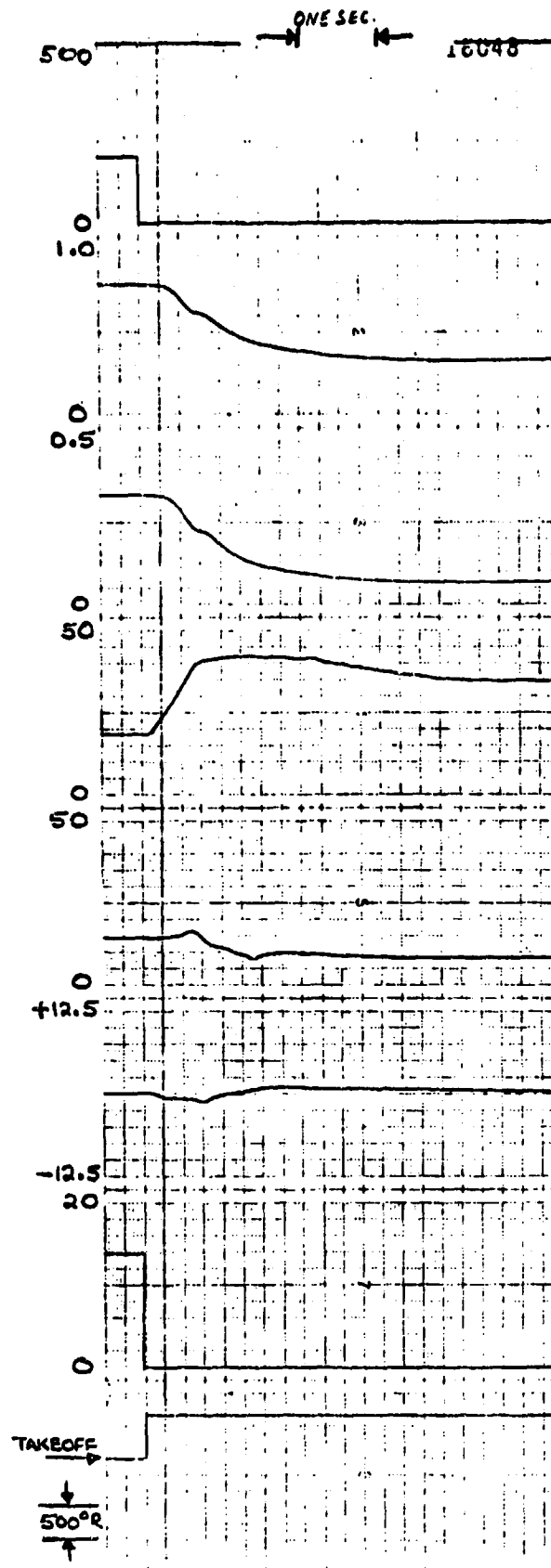


Figure 92. UTW Experimental Engine Transient When PS3 Sensor Opens or Shorts and Indicates Minimum PS3 (Takeoff, SLS, Std. Day) (Concluded).

ORIGINAL PAGE IS
OF POOR QUALITY

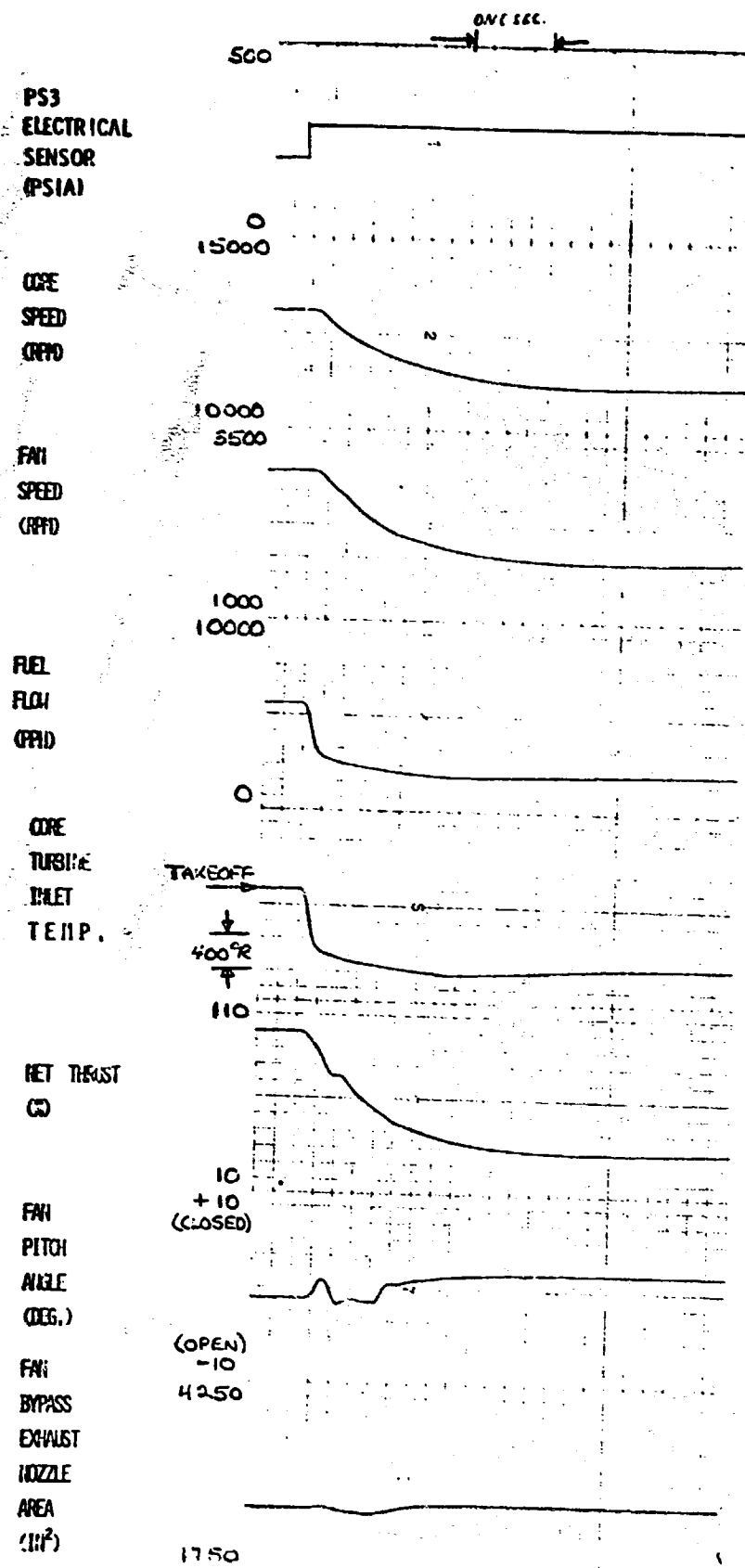


Figure 93. UTW Experimental Engine Transient When PS3 Sensor Opens or Shorts and Indicates Maximum PS3 (Takeoff, SLS, Std. Day).

PS3
ELECTRICAL
SENSOR
(PSIA)

INLET
THROAT
PNOI
NO.

$\left[\frac{P_{T0}-P_{S11}}{P_{T0}} \right]$ SENSED
(PSIA/PSIA)

CORE
COMPRESSOR
STALL
MARGIN
(%)

FAN
TIP
STALL
MARGIN
(%)

CORE
COMPRESSOR
STATOR
ERROR
(DEG.)

$\left[\frac{P_{S3}}{P_{T0}} \right]$ SENSED
(PSIA/PSIA)

CALCULATED
CORE
TURBINE
INLET
TEMP.

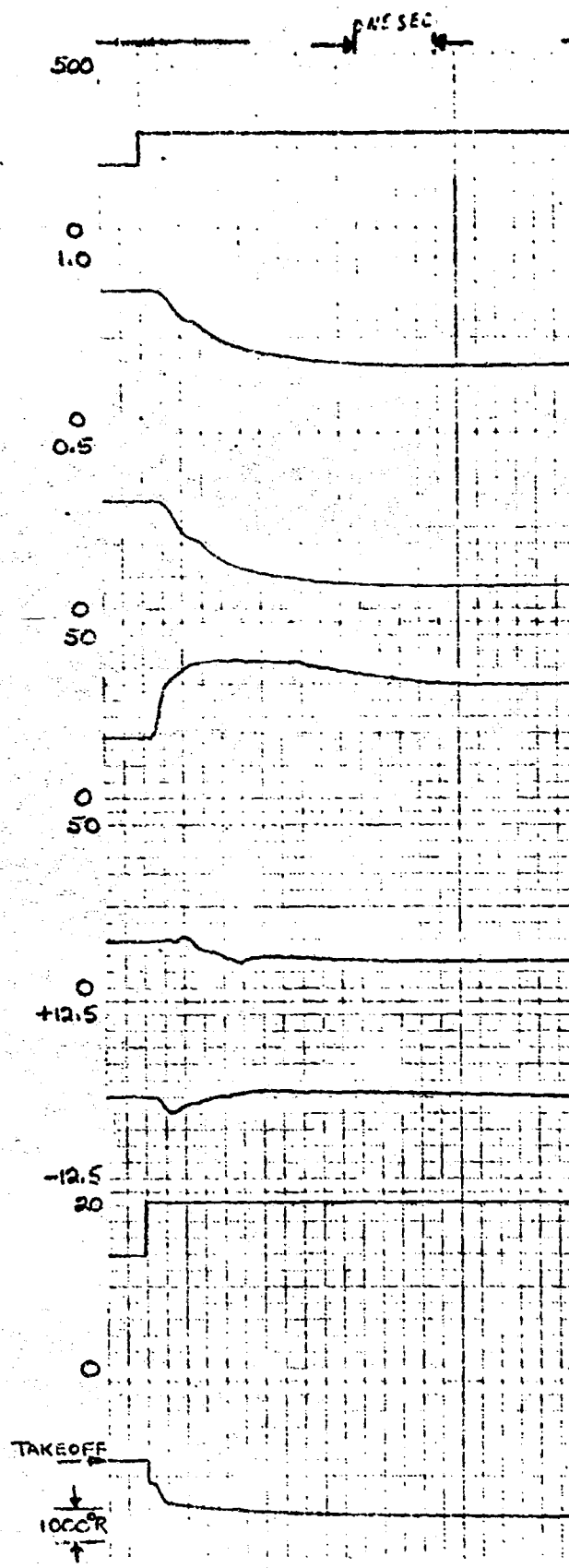


Figure 93. UTW Experimental Engine Transient When PS3 Sensor Opens or Shorts and Indicates Maximum PS3 (Takeoff, SLS, Std. Day) (Concluded).

ORIGINAL PAGE IS
OF POOR QUALITY

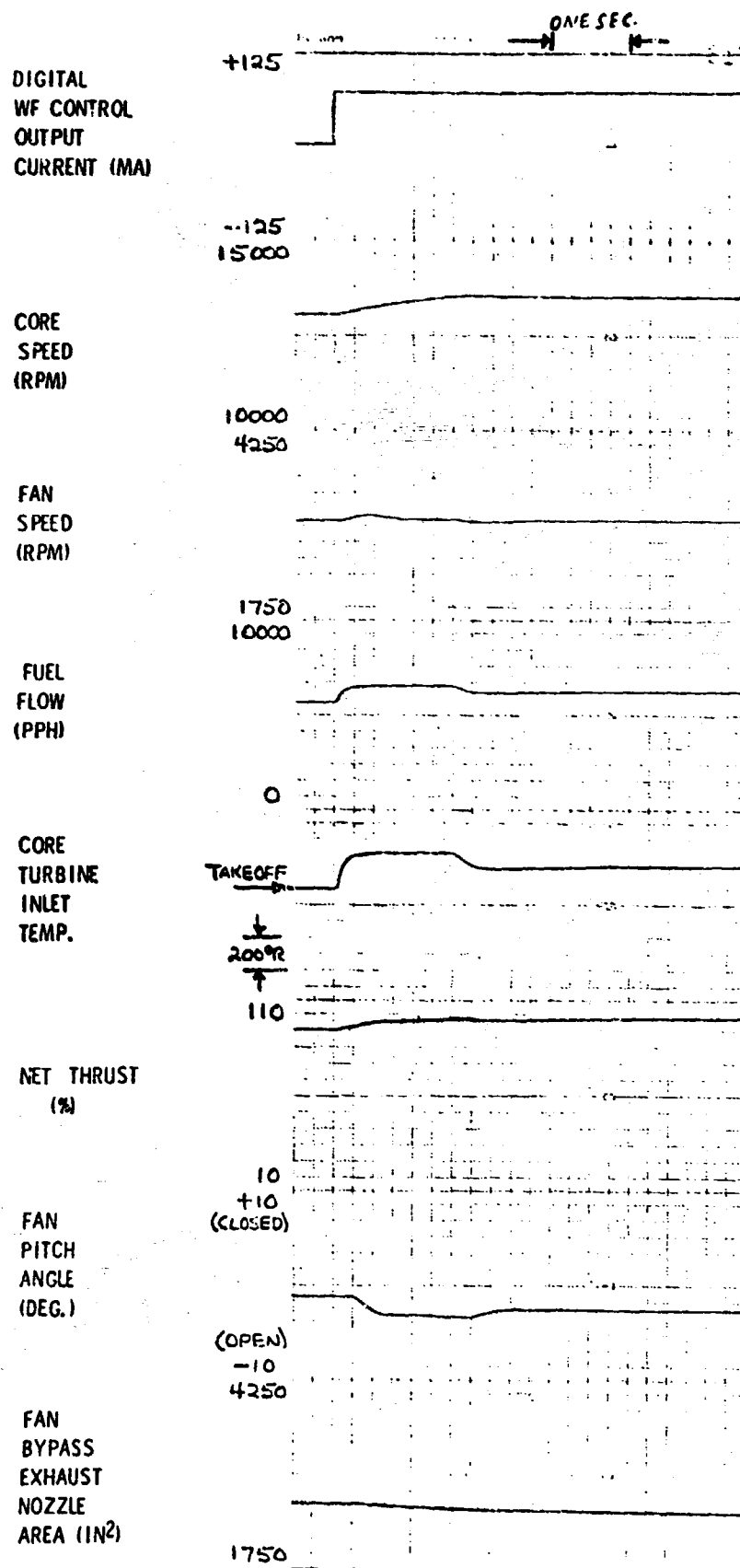


Figure 94. UTW Experimental Engine Transient When Digital Control WF Output Circuit Fails to Maximum Increase (Takeoff, SLS, Std. Day).

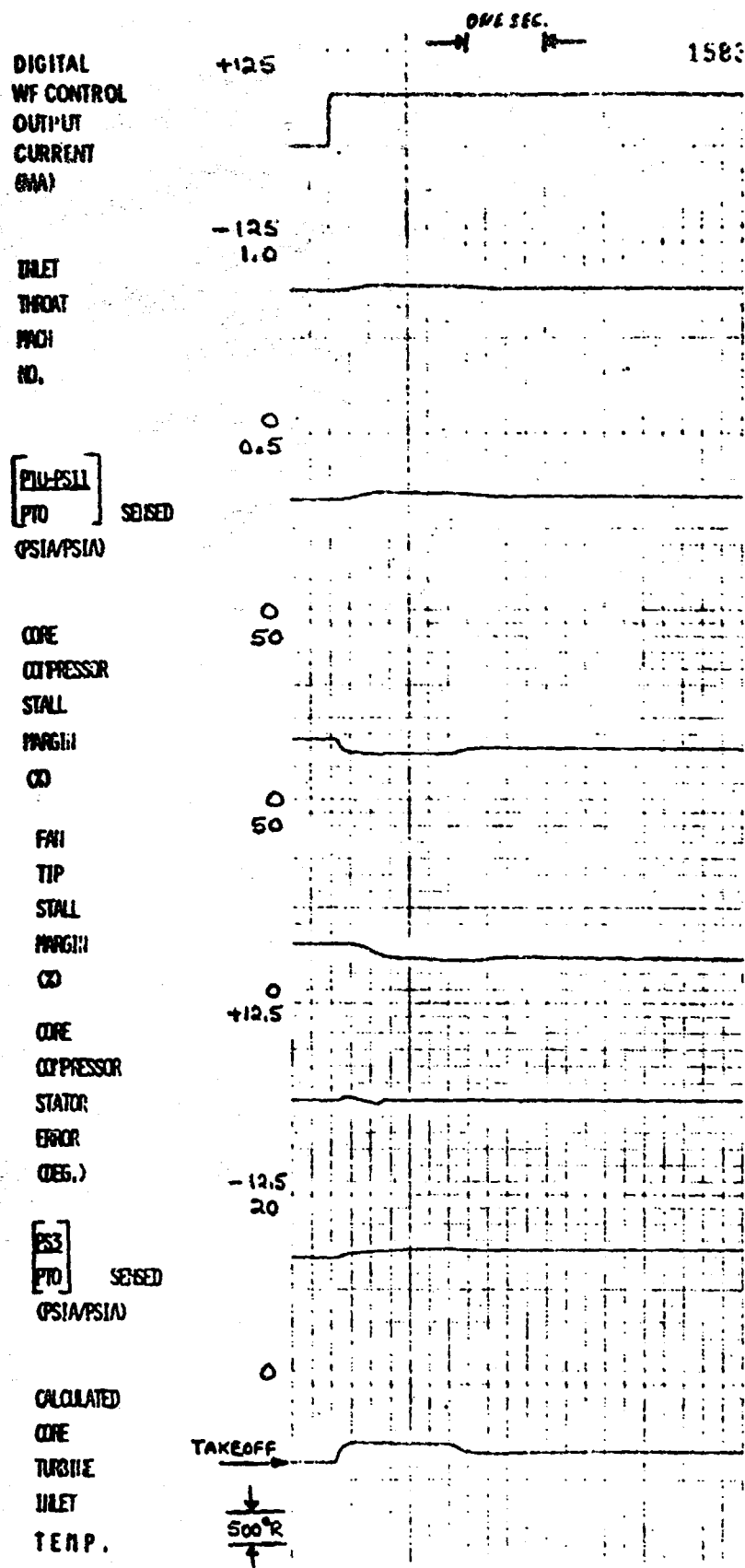


Figure 94. UTW Experimental Engine Transient When Digital Control WF Output Circuit Fails to Maximum Increase (Takeoff, SLS, Std. Day) (Concluded).

ORIGINAL PAGE IS
OF POOR QUALITY

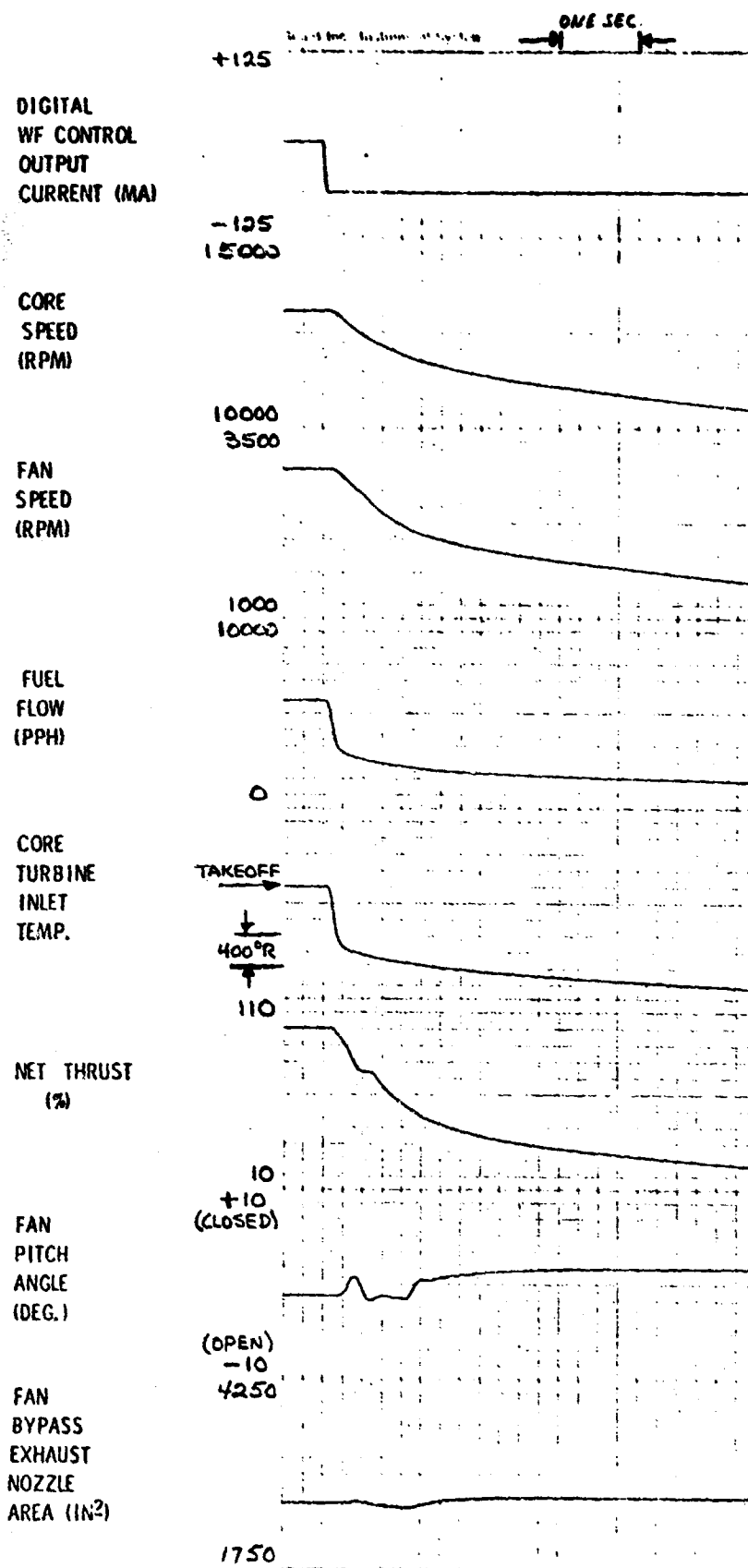


Figure 95. UTW Experimental Engine Transient When Digital Control WF Output Circuit Fails to Maximum Decrease (Takeoff, SLS, Std. Day).

DIGITAL
WF CONTROL
OUTPUT
CURRENT (MA)

INLET
THROAT
MACH
NO.

$\left[\frac{\text{PTO-PSII}}{\text{PTO}} \right]$ SENSED
(PSIA/PSIA)

CORE
COMPRESSOR
STALL MARGIN
(%)

FAN
TIP
STALL
MARGIN
(%)

CORE
COMPRESSOR
STATOR
ERROR
(DEG.)

$\left[\frac{\text{PS3}}{\text{PTO}} \right]$ SENSED
(PSIA/PSIA)

CALCULATED
CORE
TURBINE
INLET
TEMP.

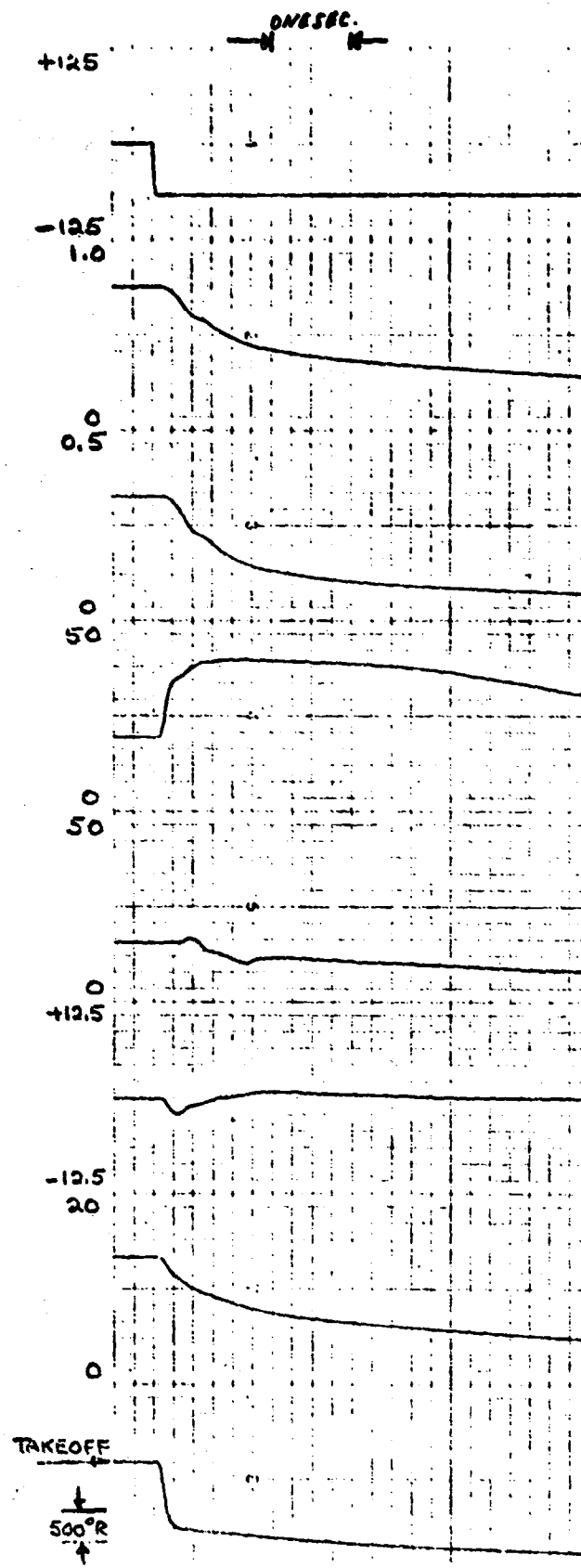
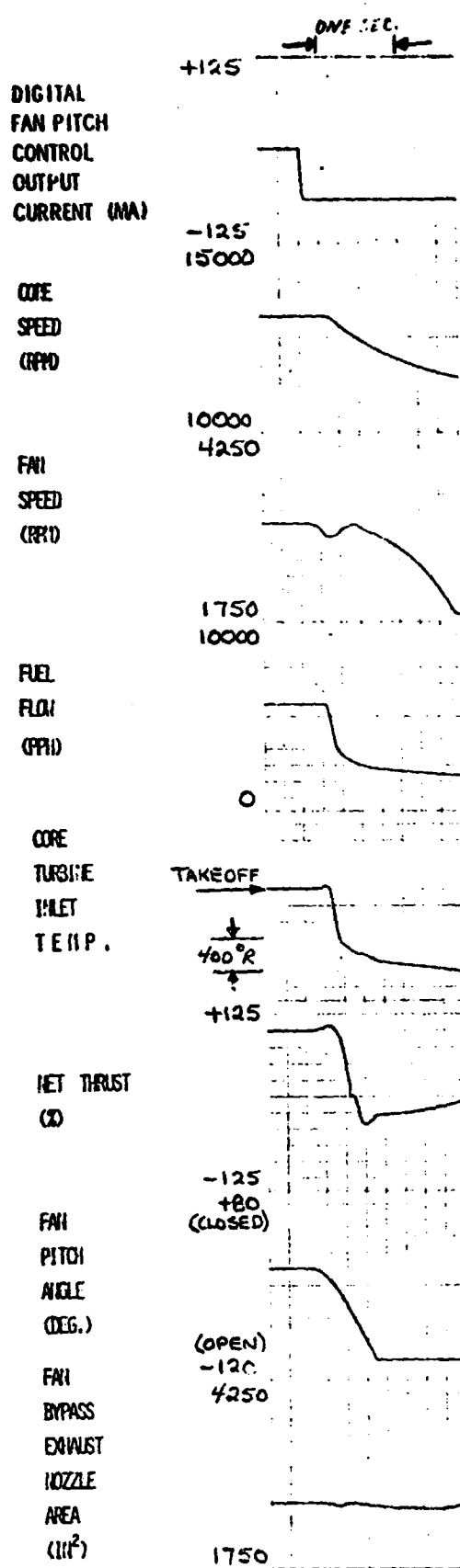


Figure 95. UTW Experimental Engine Transient When Digital Control WF Output Circuit Fails to Maximum Decrease (Takeoff, SLS, Std. Day) (Concluded).

ORIGINAL PAGE IS
OF POOR QUALITY



DIGITAL FAN PITCH CONTROL OUTPUT CURRENT (MA)

INLET THROAT MACH NO.

PTO-PS11
PTO SENSED
(PSIA/PSIA)

CORE COMPRESSOR STALL MARGIN (X)

NOT USED

CORE COMPRESSOR STATOR ERROR (DEG.)

PS3
PTO SENSED
(PSIA/PSIA)

CALCULATED CORE TURBINE INLET TEMP.

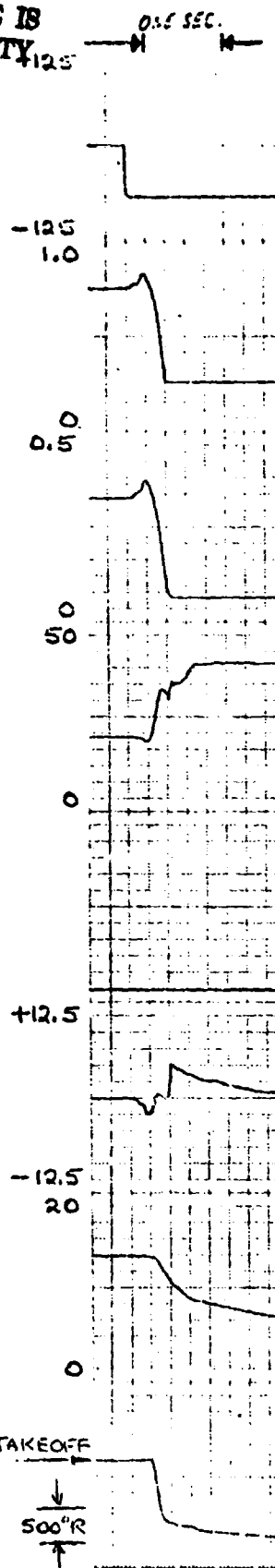


Figure 96. UTW Experimental Engine Transient When Digital Control Fan Pitch Output Circuit Fails to Maximum Open (Takeoff, SLS, Std. Day).

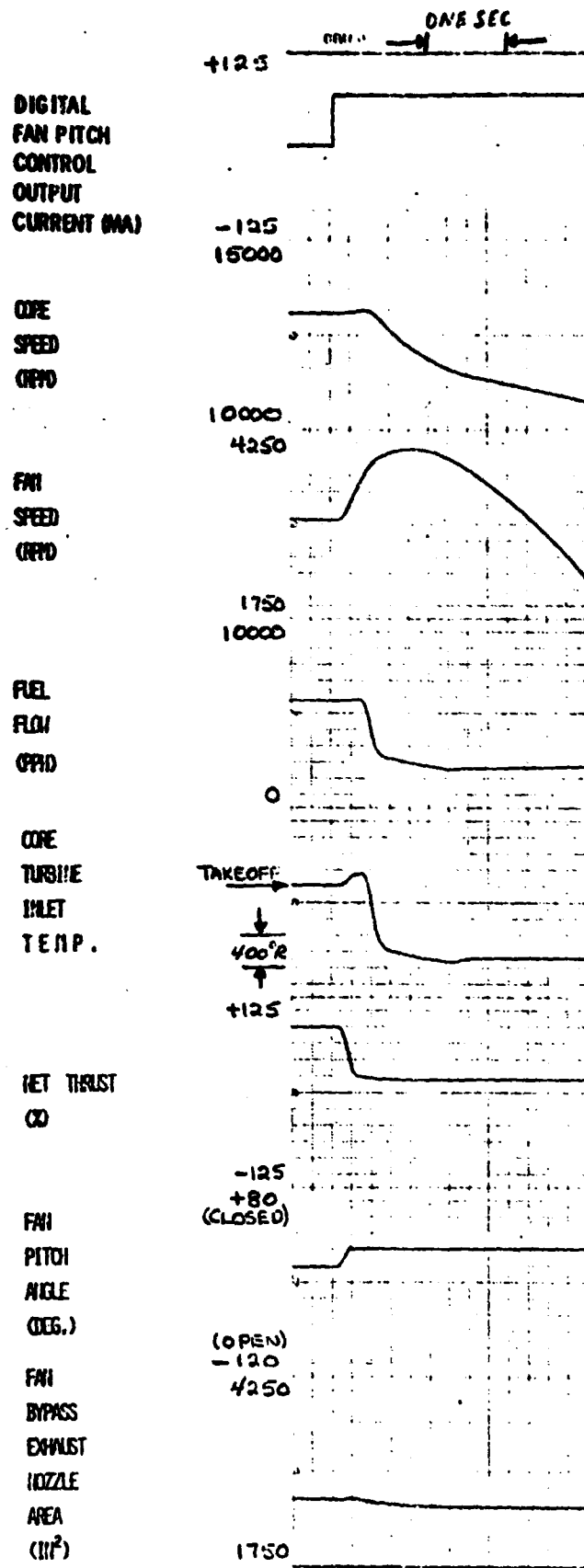


Figure 97. UTW Experimental Engine Transient When Digital Control Fan Pitch Output Circuit Fails to Maximum Close (Takeoff, SLS, Std. Day).

ORIGINAL PAGE IS
OF POOR QUALITY

DIGITAL
FAN PITCH
CONTROL
OUTPUT
CURRENT (MA)

INLET
THROT
PITCH
NO.

PTD-PS11
PTD SENSE
(PSIA/PSIA)

CORE
COMPRESSOR
STALL
MARGIN
CO

NOT
USED

CORE
COMPRESSOR
STATOR
ERROR
DEG.)

PS3
PTO SENSED
(PSIA/PSIA)

CALCULATED
CORE
TURBINE
INLET
TEMP.

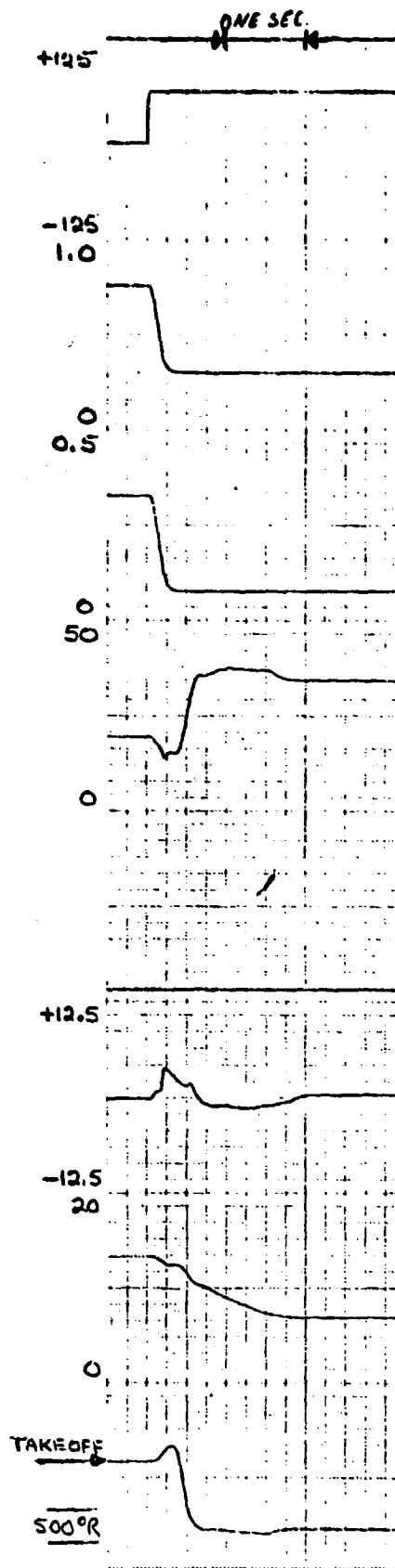


Figure 97. UTW Experimental Engine Transient When Digital Control Fan Pitch Output Circuit Fails to Maximum Close (Takeoff, SLS, Std. Day) (Concluded).

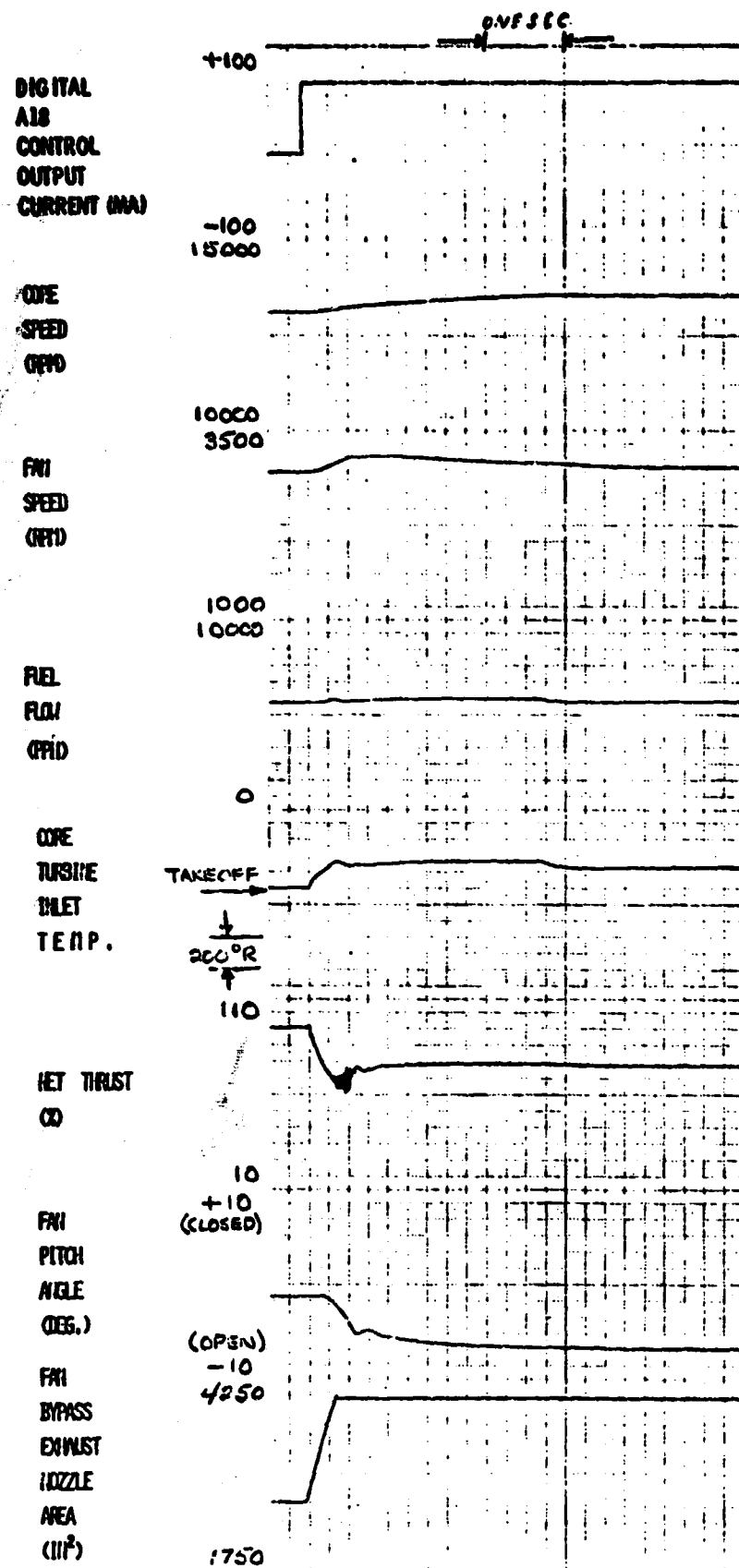


Figure 98. UTW Experimental Engine Transient When Digital Control A18 Output Circuit Fails to Maximum Open (Takeoff, SLS, Std. Day).

ORIGINAL PAGE IS
OF POOR QUALITY

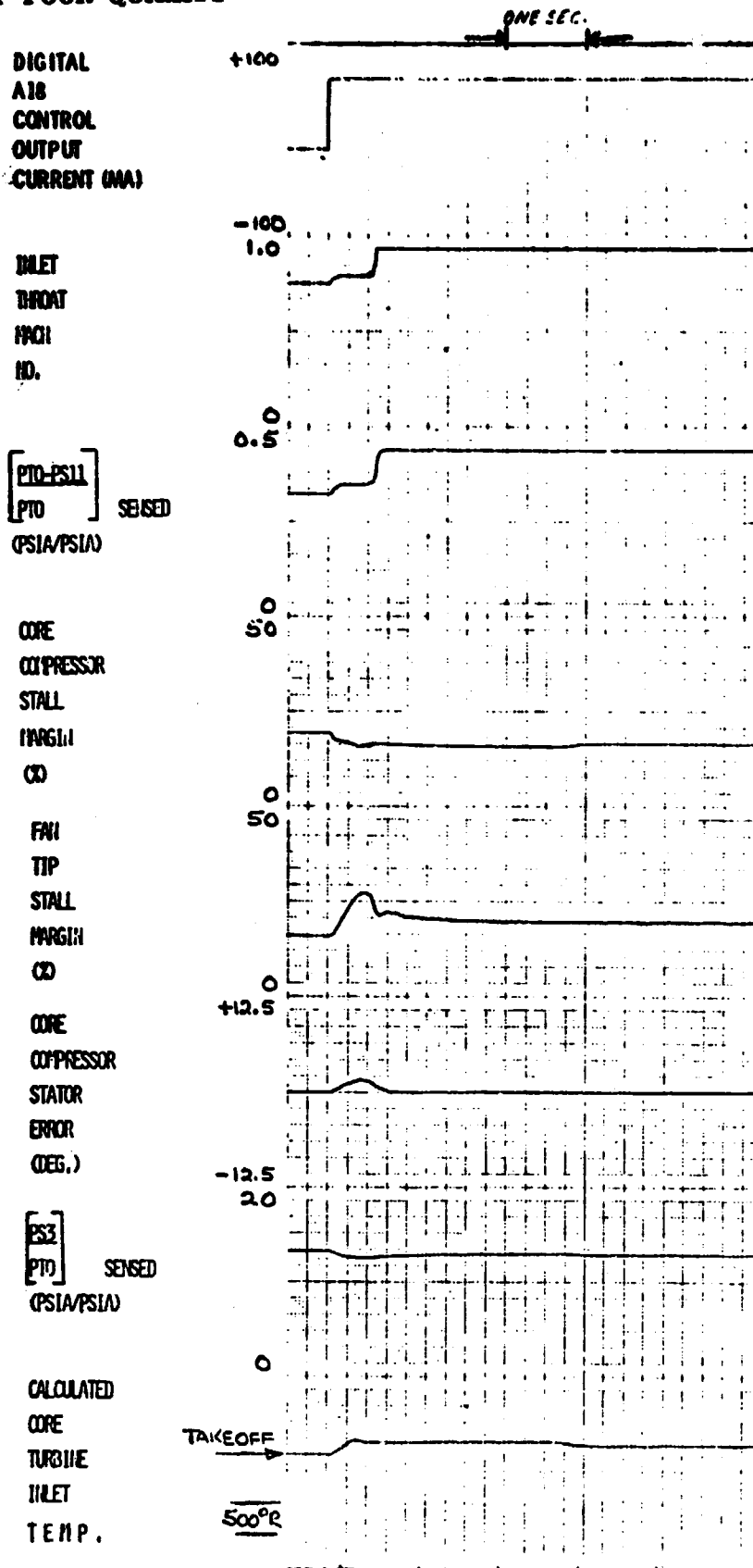


Figure 98. UTW Experimental Engine Transient When Digital Control A18 Output Circuit Fails to Maximum Open (Takeoff, SLS, Std. Day) (Concluded).

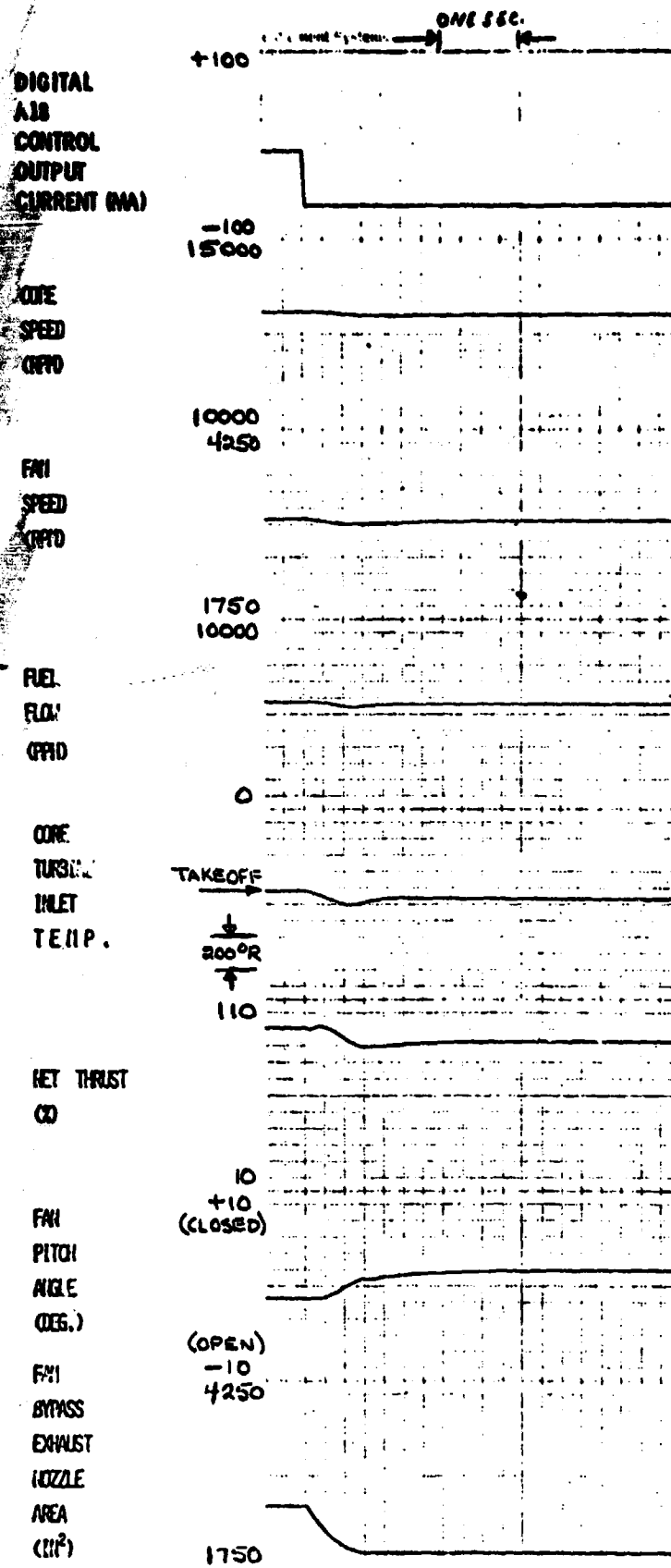


Figure 99. UTW Experimental Engine Transient When Digital Control A18 Output Circuit Fails to Maximum Closed (Takeoff, SLS, Std. Day).

ORIGINAL PAGE IS
OF POOR QUALITY

DIGITAL
A18
CONTROL
OUTPUT
CURRENT (MA)

INLET
THROAT
PACI
NO.

PTD-PS11
PTD SENSED
(PSIA/PSIA)

CORE
COMPRESSOR
STALL
MARGIN
(%)

FAI
TIP
STALL
MARGIN
(%)

CORE
COMPRESSOR
STATOR
ERROR
(DEG.)

PS3
PTD SENSED
(PSIA/PSIA)

CALCULATED
CORE
TURBINE
INLET
TEMP.

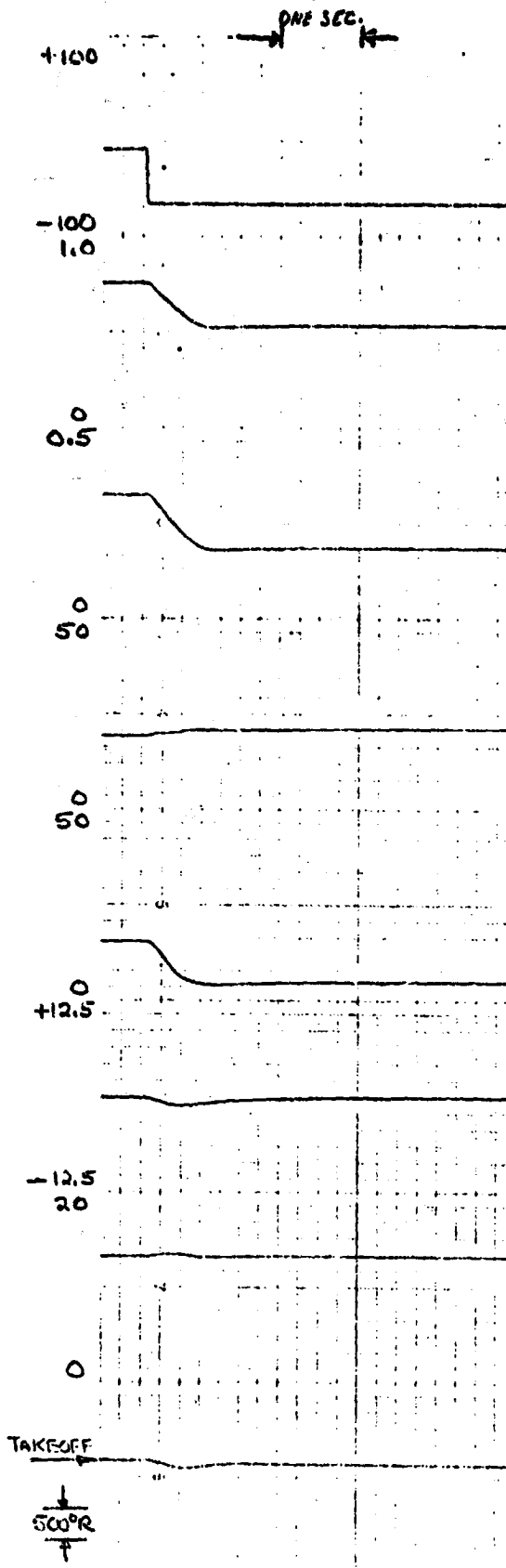


Figure 99. UTW Experimental Engine Transient When Digital Control A18 Output Circuit Fails to Maximum Closed (Takeoff, SLS, Std. Day) (Concluded).

APPENDIX D

DIGITAL CONTROL PROCESSOR
INSTRUCTION SET AND PROGRAM

APPENDIX D

DIGITAL CONTROL PROCESSOR INSTRUCTION SET AND PROGRAM

1. Instruction Repertoire

<u>Mnemonic</u>	<u>Execution Time (Microseconds)</u>	<u>Operation</u>
OUT 0	1	No - operation
OUT 1	1	Load DA converter
OUT 2	1	Sample Output Sample & Hold No. 1
OUT 3	1	Sample Output Sample & Hold No. 2
OUT 4	1	Sample Output Sample & Hold No. 3
OUT 5	1	Sample Output Sample & Hold No. 4
OUT 6	1	Sample Output Sample & Hold No. 5
OUT 13	1	Transmit accumulator off-engine equipment.
OUT 14	1	Initiate AD conversion
OUT 15	1	Reset program counter input counter
LDA XXX	1	Load accumulator with contents of scratch pad memory address XXX (XXX is 0 to 255).
LAI XXXX	12	Load accumulator with the number XXXX (0 to 4095).
LMI XXXX	12	Load MQ register with the number XXXX (0 to 4095).
ADD XXX	1	Add contents of scratch pad memory address: XXX (0 to 255) to contents of accumulator.
ADD C XXX	1	Add, with carry, contents of memory address XXX (0 to 255) to contents of accumulator.
SUB XXX	1	Subtract contents of scratch pad memory address XXX (0 to 255) from contents of accumulator.
SUBC XXX	1	Subtract, with borrow, contents of scratch pad memory address XXX (0 to 255) from contents of accumulator.
STO XXX	1	Store contents of accumulator in scratch pad memory address XXX (0 to 255).
BRMA XXXX	1	Branch on negative result of last subtraction to program memory address XXXX (0 to 4095).
BRMR XXXX	1	Branch on negative result of last subtraction to program memory address which is present address plus XXXX (XXXX must result in an address within the memory range-branch relative).

<u>Mnemonic</u>	<u>Execution Time (Microseconds)</u>	<u>Operation</u>
INP Ø	12	
INP 1	12	Transfer AD register to accumulator. Transfer command link register to accumulator.
MPYM XXX	12	Multiply scratch pad memory address XXX (0 to 255) by contents of MQ register. Result is double preci- sion with the most significant por- tion in accumulator and least signi- ficant portion in MQ register. Re- sult is unsigned, and multiplication is fractional.
MPY XXX	12	Same as MPYM except multiplication in memory is signed as is result (two's complement).
RSH XXXX	1	Shift accumulator and MQ registers arithmetically right one place.
RSHM XXX	1	Shift accumulator and MQ registers right logically one place.
LSH XXX	1	Left shift accumulator and MQ regis- ters left one place.
ROT XXX	12	Interchange the contents of the accu- mulator and the MQ registers.
DIV XXX	12	Divide the contents of the combined accumulator and MQ registers by the signed divisor in scratch pad memory address XXX (0 to 255). Quotient is in MQ register and is signed. (one's complement). Division is not frac- tional.
JUPA	1	Same as BRMA except transfer is un- conditional.
JMPR	1	Same as BRMR except transfer is un- conditional.

2. PROGRAM LISTING

Strobes Off-Engine Input
and Stores Selected
Numbers for Future Use

Performs Test on AD and DA Converter, Command Link Test Word, and General Operation of Central Processor. Continues Program if Checks O.K. Causes Outputs to Go to Fail-Safe Condition if Test Fails.

Transfer
Command Link
Store Re-
mote Mode
Word

Store PLA
Demand

Continue at 55

56	BRMR	
57	LDA	
58	JMPR	
59	LDA	
60	STO	
61	ADD	6
62	RSHM	2
63	STO	60
64	LDA	5
65	STO	64
66	LDA	0
67	SUB	60
68	LAI	512
69	BRMR	2
70	LDA	0
71	ADD	63
72	STO	63
73	LDA	235
74	SUB	0
75	BRMR	2
76	JMPR	2
77	LDA	231
78	STO	235
79	OUT	5
80	LAI	0
81	LSH	2
82	STO	20
83	LDA	0
84	LSH	2
85	STO	21
86	LDA	0
87	LSH	2
88	STO	22
89	LDA	0
90	LSH	2
91	STO	23
92	LDA	0
93	LSH	2
94	STO	24
95	LDA	0
96	LSH	2
97	STO	25
98	LDA	0
99	LSH	2
100	STO	26
101	LDA	0
102	LSH	2
103	STO	167
104	LDA	0
105	LSH	2
106	STO	30
107	LDA	0
108	LSH	2
109	STO	31

Self-Check Routine
Continued

Decodes and Stores
Input Command on
Mode Word (Remote,
Manual, Auto Fwd, -
Local, Etc.)

Local
Mode
Word

Remote Mode

Manual
Arde

Auto Fwd
Mode

Auto
Rev.

Manual A18

Manual 6F

Manual
A18, 8F

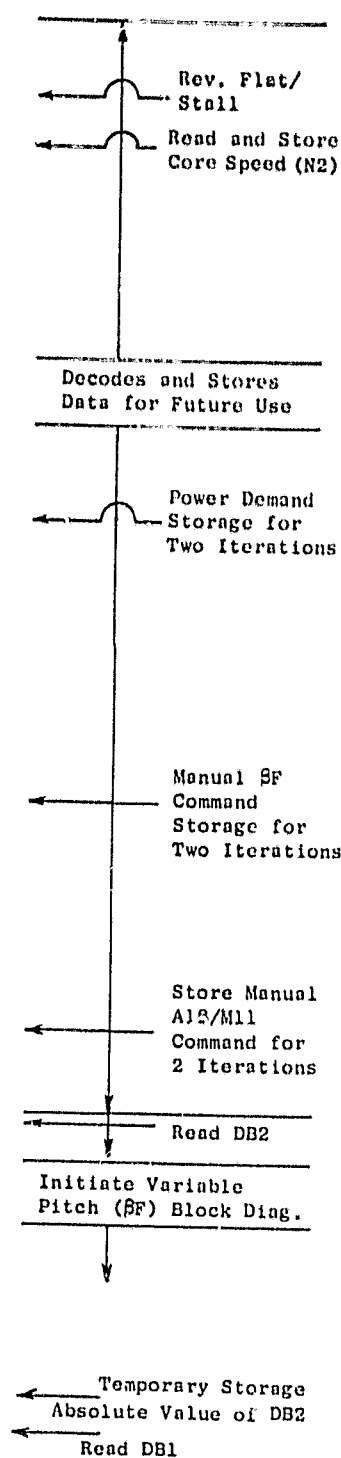
VSV T.M.
Sig.

WF Direct

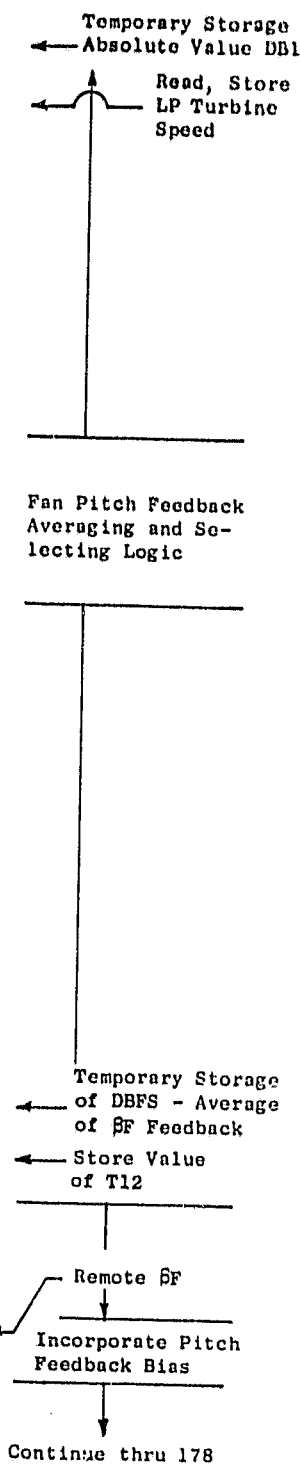
Continues at 110

FICA On/Off

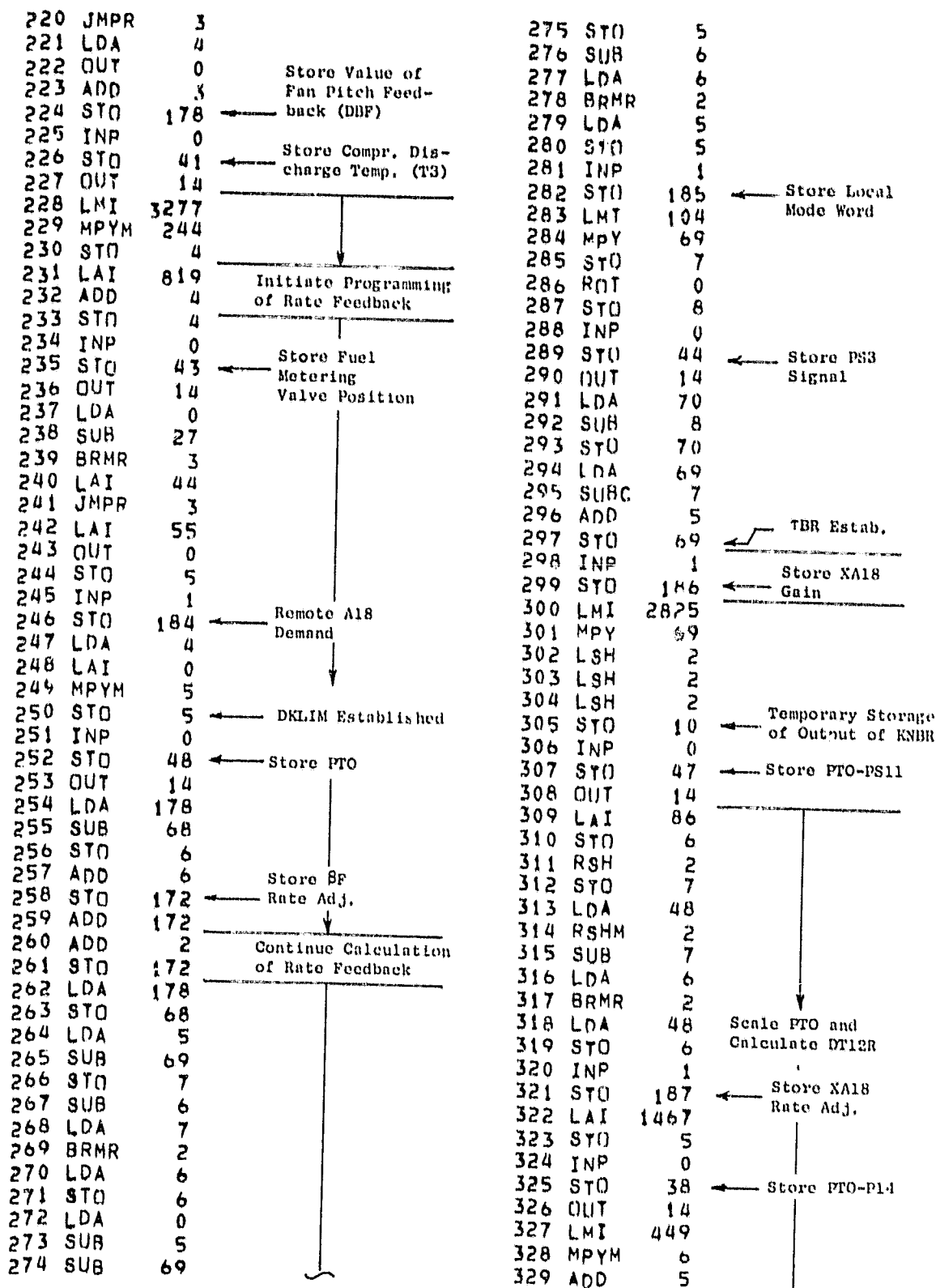
110	LDA	0
111	LSH	2
112	STO	27
113	INP	0
114	STU	42
115	OUT	14
116	LDA	0
117	SUB	61
118	LDA	1
119	BRMR	2
120	STU	31
121	LDA	21
122	SUB	20
123	LDA	252
124	BRMR	2
125	JMPR	2
126	LDA	232
127	STO	252
128	LDA	22
129	ADD	23
130	STU	17
131	ADD	24
132	SUB	20
133	LDA	254
134	BRMR	2
135	JMPR	2
136	LDA	233
137	STO	254
138	LDA	17
139	ADD	25
140	SUB	20
141	LDA	253
142	BRMR	2
143	JMPR	2
144	LDA	234
145	STO	253
146	INP	1
147	STO	182
148	LDA	29
149	RSHM	2
150	STO	3
151	SUB	66
152	STO	5
153	BRMR	3
154	OUT	0
155	JMPR	3
156	LDA	0
157	SUB	5
158	STO	5
159	LDA	28
160	RSHM	2
161	STO	6
162	SUB	66
163	STO	7
164	BRMR	3



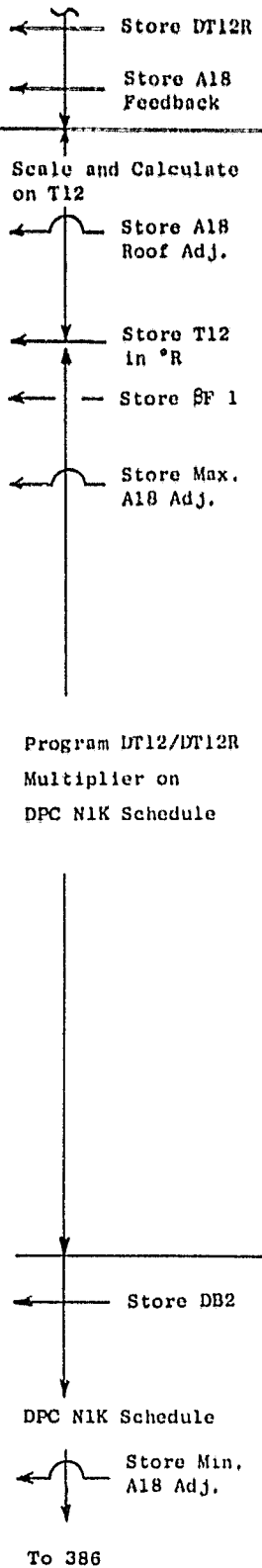
165	OUT	0
166	JMPR	3
167	LDA	0
168	SUB	7
169	SUB	5
170	STU	4
171	INP	0
172	STU	45
173	OUT	14
174	LAI	40
175	STU	5
176	SUB	4
177	BRMR	16
178	LDA	0
179	SUB	5
180	SUB	4
181	LDA	3
182	BRMR	2
183	JMPR	16
184	RSHM	2
185	STU	3
186	LDA	0
187	RSHM	2
188	ADD	3
189	OUT	0
190	OUT	0
191	OUT	0
192	JMPR	15
193	LDA	0
194	OUT	0
195	OUT	0
196	OUT	0
197	OUT	0
198	OUT	0
199	STU	3
200	LDA	1
201	ADD	1
202	ADD	1
203	ADD	1
204	ADD	63
205	STU	63
206	LDA	3
207	STU	3
208	INP	0
209	STU	46
210	OUT	14
211	LMI	33
212	MPYM	248
213	STU	4
214	INP	1
215	STU	183
216	LDA	0
217	SUB	27
218	BRMR	3
219	SUB	4



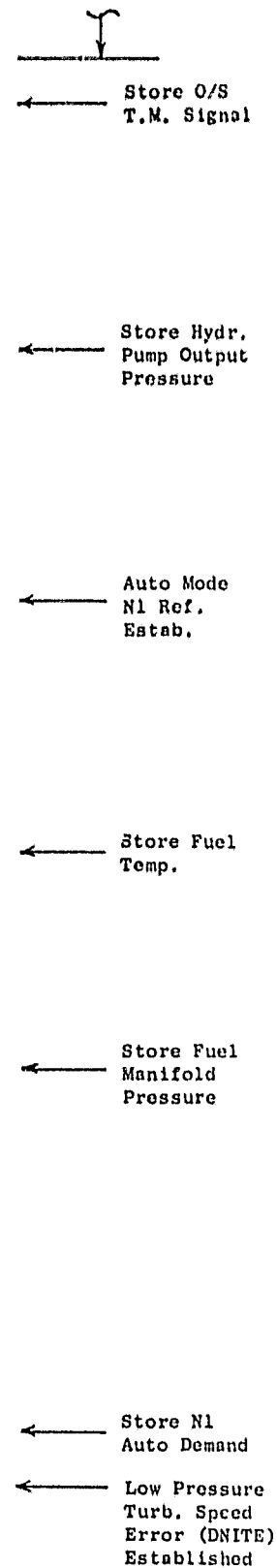
ORIGINAL PAGE IS
OF POOR QUALITY



330 STI 179
 331 INP 0
 332 STO 49
 333 OUT 14
 334 LAI 1387
 335 STI 7
 336 INP 1
 337 STO 188
 338 LMI 661
 339 MPYM 46
 340 ADD 7
 341 STI 177
 342 INP 0
 343 STO 28
 344 OUT 14
 345 INP 1
 346 STI 189
 347 LDA 177
 348 SUH 179
 349 BRMR 18
 350 LMI 1308
 351 MPY 177
 352 DIV 179
 353 ROT 0
 354 STI 5
 355 LAI 1990
 356 SUB 5
 357 STI 5
 358 ADD 5
 359 STI 5
 360 ADD 5
 361 ADD 5
 362 OUT 0
 363 OUT 0
 364 OUT 0
 365 OUT 0
 366 JMPR 7
 367 ROT 0
 368 ROT 0
 369 ROT 0
 370 ROT 0
 371 ROT 0
 372 LAI 4095
 373 STI 5
 374 INP 0
 375 STI 29
 376 OUT 14
 377 LMI 601
 378 MPYM 6
 379 STI 8
 380 INP 1
 381 STI 190
 382 LAI 2060
 383 SUB 8
 384 LAI 0



385 MPYM 5
 386 STI 5
 387 INP 0
 388 STI 37
 389 OUT 14
 390 LAI 171
 391 STI 6
 392 LMI 343
 393 MPYM 254
 394 SUB 6
 395 STI 6
 396 INP 0
 397 STI 101
 398 OUT 14
 399 LDA 5
 400 SUB 6
 401 BRMR 3
 402 OUT 0
 403 JMPR 3
 404 LDA 2
 405 SUB 1
 406 STI 5
 407 LDA 45
 408 RSHM 2
 409 STI 8
 410 LMI 2956
 411 MPYM 177
 412 RSHM 2
 413 STI 6
 414 INP 0
 415 STI 103
 416 OUT 14
 417 LAI 3693
 418 SUB 6
 419 LAI 0
 420 MPYM 177
 421 STI 6
 422 INP 0
 423 STI 104
 424 OUT 14
 425 LAI 763
 426 ADD 6
 427 LAI 0
 428 MPYM 5
 429 LSH 2
 430 STI 6
 431 SUH 0
 432 LDA 95
 433 RSHM 2
 434 BRMR 2
 435 LDA 6
 436 STI 169
 437 SUB 8
 438 STI 180
 439 INP 0



ORIGINAL PAGE IS
OF POOR QUALITY

440 STO	105	← Store T5L Signal	495 STI	6	
441 OUT	14		496 RSH	2	
442 LAI	66		497 STI	4	
443 STO	6		498 LDA	5	
444 INP	1		499 RSH	2	
445 STO	191	← Store WF Auto Gain	500 SUB	4	
446 LAI	79		501 LDA	5	
447 STO	7		502 BRMR	2	
448 LAI	430		503 LDA	6	
449 STO	8		504 STI	5	
450 INP	0		505 INP	0	
451 STO	106	← Store Fuel Flow	506 STI	108	← Store Lube and Scav. Pressure
452 OUT	14		507 OUT	14	
453 LDA	252	← Load Power Demand (DPS)	508 LDA	0	
454 RSHM	2		509 SUB	6	
455 STO	9		510 STI	6	
456 LAI	1945		511 RSH	2	
457 SUB	9		512 STI	4	
458 BRMR	7		513 LDA	5	
459 LAI	0		514 RSH	2	
460 STO	115		515 SUB	4	
461 OUT	0		516 LDA	6	
462 OUT	0		517 BRMR	2	
463 OUT	0		518 LDA	5	
464 JMPR	20	Logic Calculation on SF Transient Reset	519 STI	5	
465 LDA	180		520 ADD	5	
466 SUB	0		521 ADD	5	
467 BRMR	2		522 STI	6	
468 JMPR	2		523 LMI	2396	
469 LDA	0		524 MPY	5	
470 STO	11		525 ADD	6	
471 SUB	8		526 SUB	71	
472 LDA	0		527 STI	5	
473 BRMR	2		528 INP	0	
474 JMPR	2		529 STI	109	← Store Lube Inlet Temp.
475 LDA	6		530 OUT	14	
476 STO	65	← Transient Reset of SF Floor Schedule Estab. (DBTRST)	531 LMT	623	
477 STO	115		532 MPY	5	
478 LDA	7		533 STI	5	
479 SUB	11	← Partial DBTRST for A18 Loop	534 ROT	0	
480 LDA	0		535 ADD	72	
481 BRMR	2		536 STI	72	
482 JMPR	2		537 INP	0	
483 LDA	65		538 STI	110	← Scav. Oil Discharge Temp.
484 STI	65		539 OUT	14	
485 LDA	4		540 LDA	5	
486 LAI	0		541 ADDC	71	
487 MPY	180	← DNITE	542 STI	71	
488 STO	5		543 STI	5	
489 INP	0		544 JMPR	3010	
490 STI	107	← Store Engine Oil Inlet Pressure	545 LDA	5	
491 OUT	14		546 STI	7	
492 INP	1		547 INP	0	
493 STI	192	← Store WF Rate Feedback Adj.	548 STI	111	
494 LAI	570		549 OUT	14	← Store T25 Signal

550	LDA	95
551	SUB	245
552	STO	8
553	INP	1
554	STO	193
555	LMI	1821
556	MPYM	8
557	STO	8
558	LDA	0
559	SUB	8
560	STO	9
561	INP	0
562	STO	112
563	OUT	14
564	LDA	0
565	SUB	27
566	LDA	66
567	BRMR	25
568	SUB	178
569	BRMR	12
570	LAI	1020
571	STO	11
572	LAI	321
573	SUB	178
574	BRMR	3
575	LAI	3974
576	JMPR	3
577	LAI	2276
578	OUT	0
579	STO	12
580	JMPR	36
581	LAI	2276
582	STO	12
583	LAI	1614
584	SUB	178
585	BRMR	3
586	LAI	1820
587	JMPR	3
588	LAI	100
589	OUT	0
590	STO	11
591	JMPR	25
592	SUB	178
593	BRMR	12
594	LAI	1820
595	STO	11
596	LAI	183
597	SUB	178
598	BRMR	3
599	LAI	3989
600	JMPR	3
601	LAI	2276
602	OUT	0
603	STO	12
604	JMPR	12

Max. EPR Stored

Store P5 Signal

DBF

Logic and Calculations Associated with β F Rate Limits DBMPR and DBMNR

605	LAI	2276
606	STU	12
607	LAI	1868
608	SUB	178
609	BRMR	3
610	LAI	1820
611	JMPR	3
612	LAI	127
613	OUT	0
614	STU	11
615	OUT	0
616	LDA	11
617	SUB	8
618	LDA	11
619	BRMR	2
620	LDA	8
621	STU	11
622	INP	0
623	STU	113
624	OUT	14
625	LDA	4
626	SUB	12
627	LDA	12
628	BRMR	2
629	LDA	4
630	STU	12
631	LDA	0
632	SUB	23
633	LDA	0
634	BRMR	7
635	SUB	27
636	BRMR	3
637	LAI	76
638	JMPR	4
639	LAI	95
640	JMPR	7
641	SUB	27
642	BRMR	3
643	LAI	65
644	JMPR	3
645	LAI	81
646	OUT	0
647	STU	13
648	LDA	178
649	SUB	73
650	STU	6
651	LDA	178
652	STU	73
653	INP	0
654	STU	175
655	OUT	14
656	LDA	13
657	SUB	74
658	STU	6
659	SUB	6

DBMPR Established

Calculate Rate Limit DLMBR

DBMNR Established

Store Gearbox Brg. Temp. Signal

DBF

Store Horiz. Vib. Signal

Continues to 692

ORIGINAL PAGE IS
OF POOR QUALITY

660	LDA	8
661	BRMR	2
662	LDA	6
663	STO	6
664	LDA	0
665	SUB	13
666	SUB	74
667	STO	13
668	SUB	6
669	LDA	6
670	BRMR	2
671	LDA	13
672	STO	13
673	INP	1
674	STO	194
675	LMT	104
676	MPY	74
677	STO	8
678	ROT	0
679	STO	9
680	LDA	75
681	SUB	9
682	STO	75
683	LDA	74
684	SUBC	8
685	ADD	13
686	STO	74
687	INP	0
688	STO	173
689	OUT	14
690	LMI	3736
691	MPY	74
692	LSH	2
693	STO	10
694	INP	1
695	STO	195
696	LAI	1638
697	STO	6
698	LDA	0
699	SUB	252
700	BRMR	3
701	LDA	6
702	JMPR	3
703	LDA	252
704	OUT	0
705	STO	9
706	INP	0
707	STO	102
708	OUT	14
709	LAI	1175
710	STO	8
711	SUB	9
712	LDA	9
713	BRMR	2
714	LDA	8

Calculation of
DDR-KBR Output

SF Auto
Gain Stored

Store Vert.
VB Signal

Max. SF
Rate Stored

Store VSV
Position
Signal

715	STO	9
716	SUB	6
717	LDA	9
718	BRMR	2
719	LDA	6
720	STO	6
721	LMI	867
722	MPY	6
723	STO	6
724	INP	0
725	STO	114
726	INP	1
727	STO	196
728	LAI	2067
729	SUB	6
730	SUB	65
731	STO	6
732	LAI	2925
733	STO	8
734	LDA	0
735	SUB	27
736	LDA	0
737	BRMR	2
738	LDA	8
739	ADD	6
740	STO	6
741	LMI	1843
742	MPYM	247
743	STO	8
744	INP	1
745	STO	197
746	LMI	3337
747	MPYM	8
748	STO	9
749	LAI	1717
750	SUB	9
751	STO	9
752	LAI	1944
753	SUB	8
754	STO	8
755	LDA	0
756	SUB	27
757	LDA	8
758	BRMR	2
759	LDA	9
760	STO	8
761	LDA	8
762	SUB	6
763	LDA	6
764	BRMR	2
765	LDA	8
766	SUB	178
767	STO	5
768	RSH	2
769	STO	6

Calculated SF
Floor
Sched. DBFS

Store Clock Fail
Indicator Signal

Store SF Roof

DBTRST

SF Floor
Stored

Calculation of
DBFS Channel with
DBFLOR, DBF, DBMPR
Limits, to Min.
Selection in Main
Channel. Con-
tinues to 861.

DBFLOR

DBF

770 INP	1	
771 STO	198	← SF Feedback Bias Stored
772 LAI	1470	
773 STO	36	
774 RSH	2	
775 SUB	6	
776 LDA	36	
777 BRMR	2	
778 LDA	5	
779 SIO	5	
780 LDA	0	
781 SUB	36	
782 STO	9	
783 RSH	2	
784 SUB	6	
785 LDA	5	
786 BRMR	2	
787 LDA	9	
788 STO	5	
789 LMI	1607	
790 MPY	5	
791 ADD	5	
792 STO	5	
793 SUB	0	
794 BRMR	5	
795 SUB	11	
796 BRMR	4	
797 LDA	11	
798 JMPR	4	
799 JMPR	3	
800 LDA	5	
801 OUT	0	
802 STO	5	
803 INP	1	
804 STO	199	← Idle N2 Stored
805 LAI	676	
806 STO	35	
807 LDA	0	
808 SUB	35	
809 STO	13	
810 LDA	5	
811 SUB	76	← TB Floor
812 STO	6	
813 LMT	311	
814 MPY	6	
815 STO	6	
816 ROT	0	
817 ADD	77	
818 STO	77	
819 LDA	76	
820 ADDC	6	
821 STO	76	
822 STO	5	
823 JMPP	3010	
824 LDA	5	

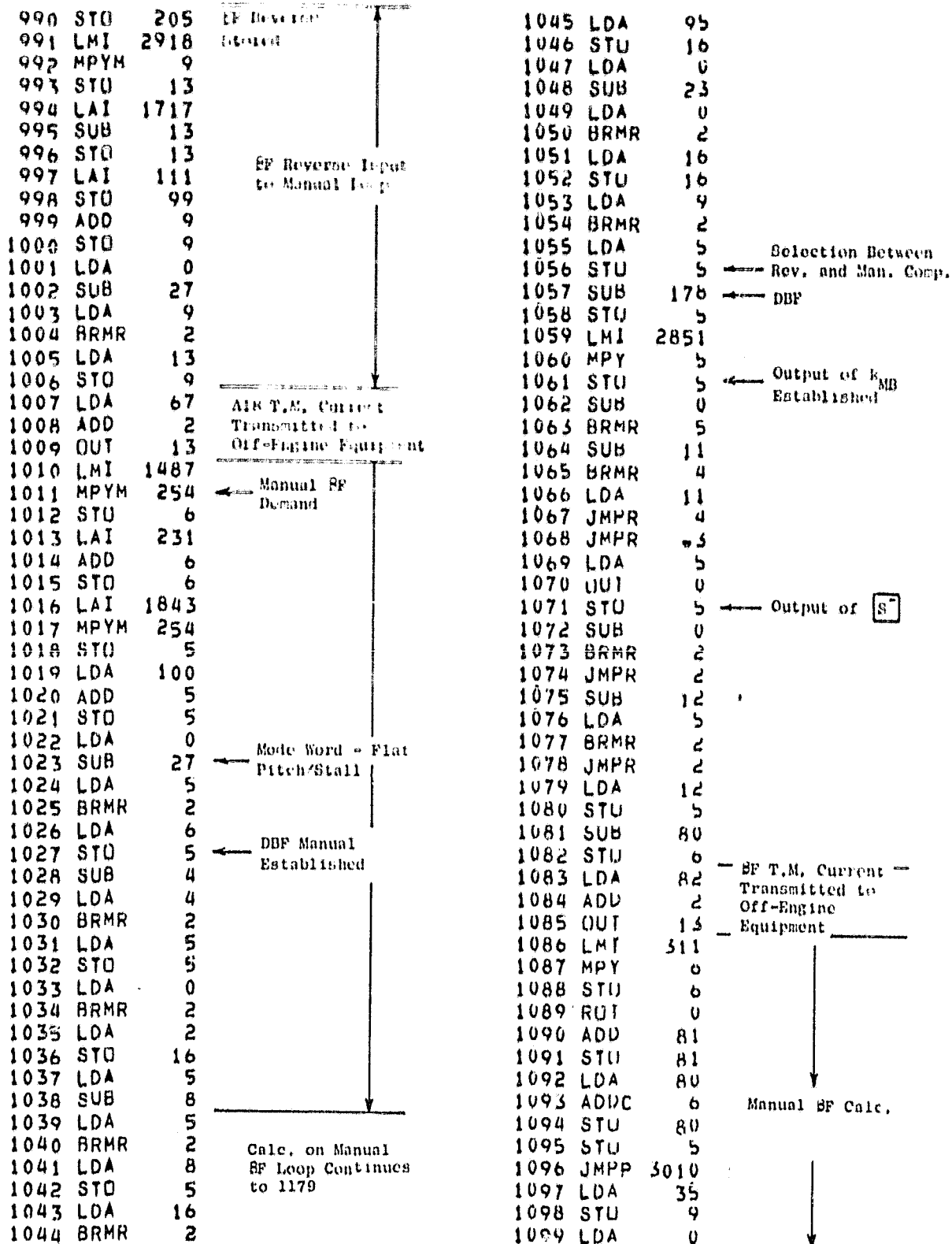
825 SUB	0	
826 BRMR	5	
827 SUB	35	
828 BRMR	4	
829 LDA	35	
830 JMPR	4	
831 JMPR	3	
832 LDA	5	
833 OUT	0	
834 STO	5	
835 SUB	0	
836 BRMR	2	
837 JMPR	2	
838 SUB	13	
839 BRMR	3	
840 LDA	5	
841 JMPR	3	
842 LDA	13	
843 OUT	0	
844 STO	5	
845 INP	1	
846 STU	200	Rev. Interlock Stored
847 LMI	3096	
848 MPY	5	
849 LSH	2	
850 LSH	2	
851 STO	5	
852 LDA	5	
853 RSH	2	
854 STU	6	
855 LDA	7	
856 RSH	2	
857 SUB	6	
858 LDA	7	
859 BRMR	2	
860 LDA	5	
861 STU	7	
862 LDA	0	
863 BRMR	2	
864 LDA	95	
865 STU	83	← SF MCI Word
866 LMI	1843	
867 MPYM	246	← SF Roof Z ⁻²
868 STU	9	
869 INP	1	
870 STU	201	
871 LMI	3337	Max. T41C Ref. Stored
872 MPYM	9	
873 STU	4	
874 LAI	231	SF Roof Channel thru [S+] in Main Channel.
875 ADD	4	
876 STU	4	
877 LAI	102	
878 STU	100	
879 ADD	9	

Continues to 981

ORIGINAL PAGE IS
OF POOR QUALITY

880	STO	9	
881	LDA	0	
882	SUB	27	
883	LDA	9	
884	BRMR	2	
885	LDA	4	
886	STO	4	DB Roof Estno.
887	SUR	178	DBF
888	STO	5	
889	RSH	2	
890	STO	6	
891	LDA	36	
892	STO	9	
893	RSH	2	
894	SUB	6	
895	LDA	5	
896	BRMR	2	
897	LDA	5	
898	SIO	5	
899	LDA	0	
900	SUB	9	
901	STO	9	
902	RSH	2	
903	SUB	6	
904	LDA	5	
905	BRMR	2	
906	LDA	9	
907	STO	5	
908	INP	1	
909	STO	202	Power Demand Stored
910	LMI	1607	
911	MPY	5	
912	ADD	5	
913	STO	5	
914	SUB	0	
915	BRMR	2	
916	JMPR	2	
917	SUB	12	
918	BRMR	3	
919	LDA	5	
920	JMPR	3	
921	LDA	12	
922	OUT	0	
923	STO	5	
924	LDA	35	
925	SIO	9	
926	LDA	0	
927	SUB	9	
928	STO	13	
929	LDA	5	
930	SUB	78	
931	STO	6	
932	INP	1	
933	STO	203	Manual A18/Auto XM11 Stored
934	LMT	311	

935	MPY	6	
936	STO	6	
937	RSH	0	
938	AND	79	TD Roof - LSB
939	STO	79	
940	LDA	78	TD Roof - MSB
941	ADDC	6	
942	STO	78	
943	STO	5	
944	JMPP	3010	
945	LDA	5	
946	SUB	0	
947	BRMR	5	
948	SUB	9	
949	BRMR	4	
950	LDA	9	
951	JMPR	4	
952	JMPR	3	
953	LDA	5	
954	OUT	0	
955	STO	5	
956	SUB	0	
957	BRMR	2	
958	JMPR	2	
959	SUB	13	
960	BRMR	3	
961	LDA	5	
962	JMPR	3	
963	LDA	13	
964	OUT	0	
965	STO	5	
966	INP	1	
967	STO	204	Manual SF Demand, Auto N1 Sched. Stored
968	LMI	3098	
969	MPY	5	
970	LSH	2	
971	LSH	2	
972	STO	5	
973	RSH	2	
974	STO	9	
975	LDA	7	
976	RSH	2	
977	SUB	9	
978	LDA	5	
979	BRMR	2	
980	LDA	7	
981	STO	7	
982	LDA	2	
983	BRMR	2	
984	LDA	83	
985	STO	83	BF MCI
986	LMI	551	
987	MPYM	255	BF Rev. Input
988	STO	9	
989	INP	1	



ORIGINAL PAGE IS
OF POOR QUALITY

1100	SUB	9
1101	STO	13
1102	LDA	5
1103	SUB	0
1104	BRMR	5
1105	SUB	9
1106	BRMR	4
1107	LDA	9
1108	JMPR	4
1109	JMPR	-3
1110	LDA	5
1111	OUT	0
1112	STO	5
1113	SUB	0
1114	BRMR	2
1115	JMPR	2
1116	SUB	13
1117	LDA	5
1118	BRMR	2
1119	JMPR	2
1120	LDA	13
1121	STO	5
1122	LDA	96
1123	ADD	2
1124	OUT	13
1125	LMI	3098
1126	MPY	5
1127	LSH	2
1128	LSH	2
1129	STO	5
1130	LDA	0
1131	SUB	21
1132	SUB	25
1133	SUB	23
1134	SUB	26
1135	LDA	5
1136	BRMR	2
1137	LDA	7
1138	STO	7
1139	LDA	16
1140	BRMR	2
1141	LDA	83
1142	STO	83
1143	LDA	106
1144	OUT	13
1145	LAI	1367
1146	STO	9
1147	LDA	1
1148	SUB	9
1149	STO	13
1150	LDA	7
1151	SUB	0
1152	BRMR	5
1153	SUB	9
1154	BRMR	4

Manual BF Calc.
Cont. thru
Inst. 1179

WF T.M. Current
Transmitted to
Off-Engine Equip.

Fuel Flow Trans-
mitted to Off-
Engine Equip.

1155	LDA	9
1156	JMPR	4
1157	JMPR	-3
1158	LDA	7
1159	OUT	0
1160	STO	7
1161	SUB	0
1162	BRMR	2
1163	JMPR	2
1164	SUB	13
1165	LDA	7
1166	BRMR	2
1167	JMPR	2
1168	LDA	13
1169	STO	7
1170	LAI	5
1171	STO	5
1172	LDA	49
1173	OUT	13
1174	LMI	3061
1175	MPY	7
1176	LSH	2
1177	SUB	5
1178	STO	82
1179	OUT	1
1180	LAI	1212
1181	STO	3
1182	LDA	178
1183	ADD	178
1184	OUT	13
1185	LMI	2884
1186	MPYM	252
1187	ADD	3
1188	STO	3
1189	LDA	60
1190	ADD	31
1191	SUB	1
1192	SUB	1
1193	BRMR	2
1194	JMPR	2
1195	OUT	4
1196	LAI	1940
1197	STO	6
1198	RSH	2
1199	STO	7
1200	LDA	104
1201	OUT	13
1202	LDA	48
1203	RSHM	2
1204	SUB	7
1205	LDA	6
1206	BRMR	2
1207	LDA	48
1208	STO	6
1209	LDA	177

Manual BF
Calculated

A18 Feedback Signal
Transmitted to
Off-Engine Equip.

End of BF Blk
Diag. Calc.

Begin WF Control
Calc. - Call DMPLT

DBF Transmitted to
Off-Engine Equip.

Calculate DPC EPR

BF Sample and
Hold Output

Fuel Manifold
Pressure Trans-
mitted to Off-
Engine Equipment

Continued

1210	SUB	179	
1211	BRMR	18	
1212	LMI	1391	
1213	MPY	177	
1214	DIV	179	
1215	ROT	0	
1216	STO	5	
1217	LAI	2414	
1218	SUB	5	
1219	STO	5	
1220	OUT	0	
1221	ADD	5	
1222	ADD	5	
1223	ADD	5	
1224	OUT	0	
1225	OUT	0	
1226	OUT	0	
1227	OUT	0	
1228	JMPR	7	
1229	ROT	0	
1230	ROT	0	
1231	ROT	0	
1232	ROT	0	
1233	ROT	0	
1234	LAI	4095	
1235	STO	5	
1236	LDA	171	
1237	OUT	13	
1238	LMI	381	
1239	MPYM	6	
1240	STU	8	
1241	LAI	400	
1242	STC	6	
1243	LAI	1630	
1244	SUB	8	
1245	LAI	1	
1246	MPYM	5	
1247	SUB	6	
1248	STO	5	
1249	LDA	170	
1250	OUT	13	
1251	LMI	801	
1252	MPYM	243	
1253	ADD	5	
1254	LAI	0	
1255	MPYM	3	
1256	STO	5	
1257	LDA	48	
1258	RSHM	2	
1259	STO	3	
1260	LDA	176	
1261	OUT	13	
1262	LAI	232	
1263	STO	176	
1264	SUB	3	

Continue DPCEPR Calculation

T41C Transmitted to Off-Engine Equipment

XM11 Transmitted to Off-Engine Equipment

PS3/PTO Transmitted to Off-Engine Equipment

1265	LDA	176	
1266	BRMR	2	
1267	JMPR	2	
1268	LDA	3	
1269	STU	3	
1270	LMI	161	
1271	MPYM	44	
1272	DIV	3	
1273	ROT	0	
1274	STO	176	
1275	LAI	417	
1276	STO	4	
1277	SUB	176	
1278	LDA	176	
1279	BRMR	2	
1280	JMPR	2	
1281	LDA	4	
1282	STU	176	
1283	LMI	2510	
1284	MPYM	176	
1285	LSH	2	
1286	LSH	2	
1287	LSH	2	
1288	STU	176	
1289	LDA	5	
1290	SUB	176	
1291	STU	5	
1292	LDA	1	
1293	SUB	21	
1294	SUB	20	
1295	LDA	252	
1296	BRMR	2	
1297	JMPR	2	
1298	ADD	2	
1299	OUT	13	
1300	LAI	192	
1301	STU	6	
1302	LDA	0	
1303	SUB	6	
1304	STU	7	
1305	LMI	3413	
1306	MPYM	241	
1307	ADD	32	
1308	STU	4	
1309	LAI	0	
1310	MPY	5	
1311	STU	5	
1312	SUB	0	
1313	BRMR	5	
1314	SUB	6	
1315	BRMR	4	
1316	LDA	6	
1317	JMPR	4	
1318	JMPR	3	
1319	LDA	5	

Calculate PS3/PTO

DPCEPR - PS3/PTO

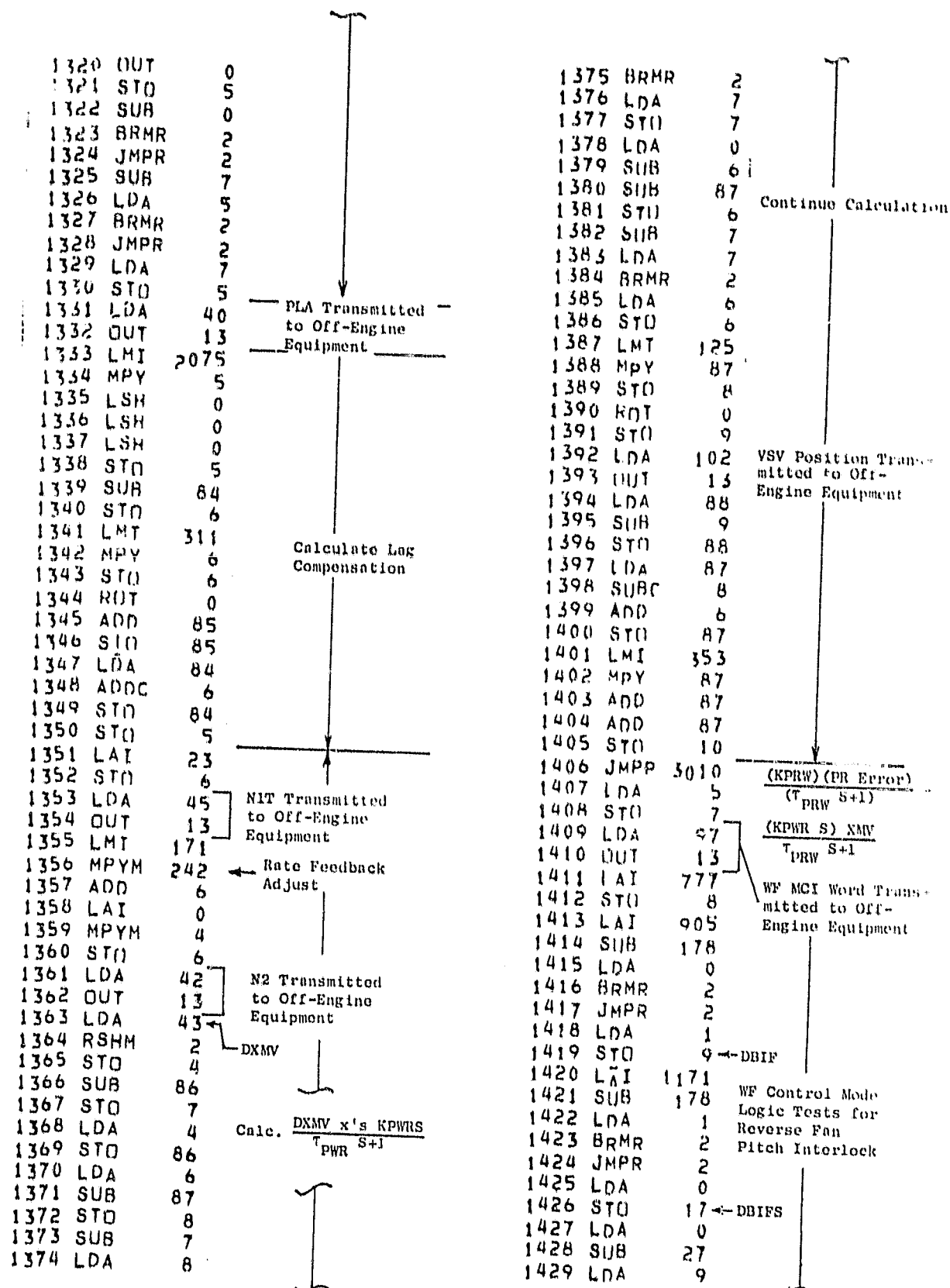
Identify Mode Control and Transmit to Off-Engine Equipment

Calculate Gain and Multiply by PR Error

k_{PRW} Gain Adjust Valve

Apply Limits

ORIGINAL PAGE IS
OF POOR QUALITY



1430	BRMR	2	
1431	JMPR	2	
1432	LDA	17	
1433	STO	9	DBIF
1434	LAI	231	
1435	STO	12	
1436	LDA	95	
1437	SUB	250	Reverse Inter- lock Adjust.
1438	STO	11	
1439	LDA	83	
1440	OUT	13	BF MCI Word Trans- mitted to Off- Engine Equipment
1441	LMI	1487	
1442	MPYM	11	
1443	ADD	12	
1444	STO	11	DBRIFP
1445	LDA	99	
1446	STO	13	
1447	LMI	1825	
1448	MPYM	250	Control Mode Logic Tests Continued
1449	ADD	13	
1450	SUB	178	
1451	LDA	0	
1452	BRMR	2	
1453	JMPR	2	
1454	LDA	1	
1455	STO	12	DBIRS
1456	LDA	11	
1457	SUB	178	
1458	LDA	1	
1459	BRMR	2	
1460	JMPR	2	
1461	LDA	0	DBIRF
1462	STO	11	
1463	LDA	62	A18 MCI Word Trans- mitted to Off- Engine Equipment
1464	OUT	13	
1465	LDA	0	
1466	SUB	27	
1467	LDA	12	
1468	BRMR	2	
1469	LDA	11	
1470	STO	11	DBIR
1471	LDA	0	
1472	SUB	23	
1473	LDA	11	
1474	BRMR	2	
1475	LDA	1	
1476	STO	11	DBIR
1477	LAI	1182	
1478	STO	6	
1479	LDA	252	Power Demand
1480	SUB	0	
1481	BRMR	2	
1482	JMPR	2	
1483	LDA	6	Generate N2 Sched.
1484	STO	5	

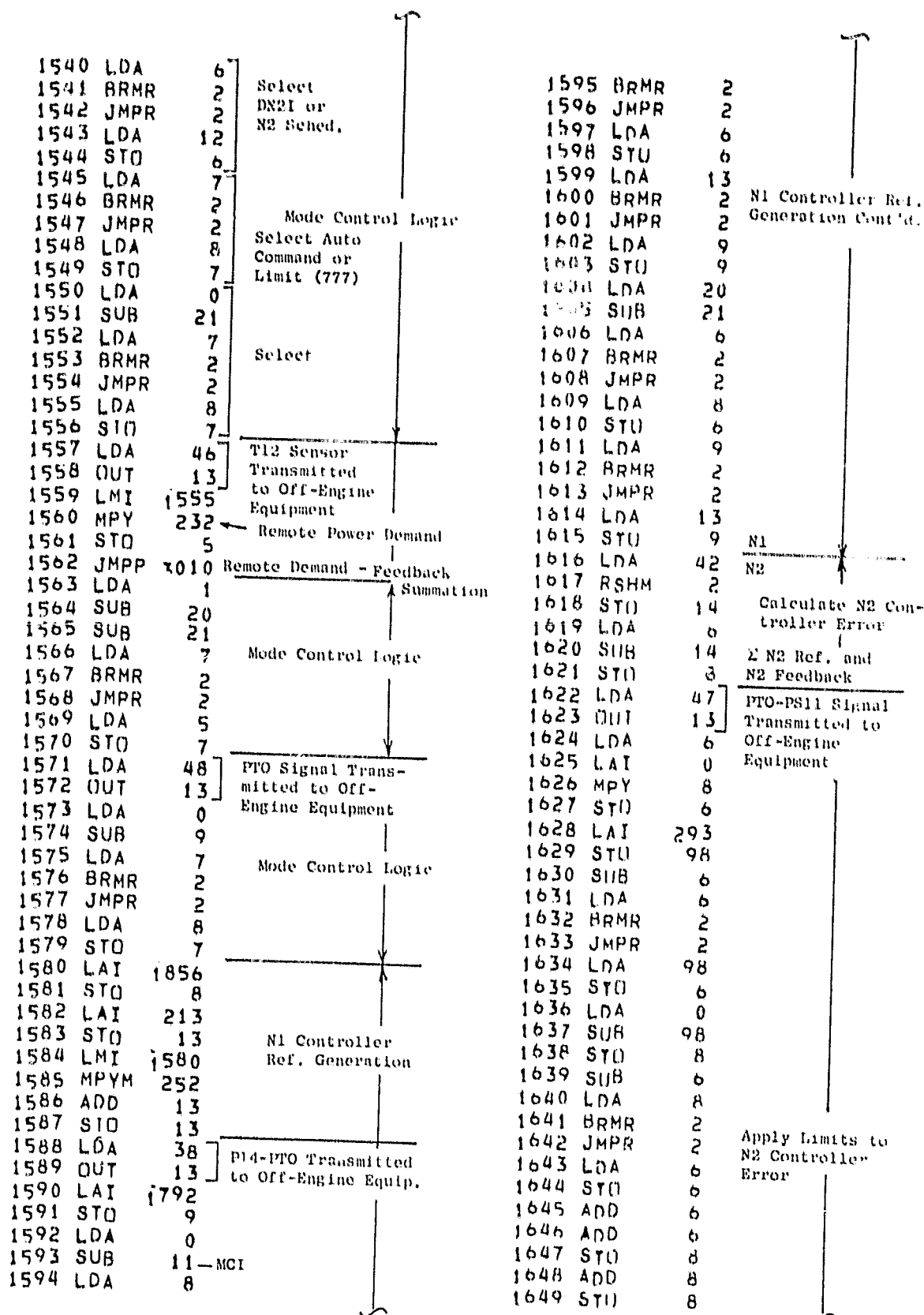
1485	SUB	6	
1486	LDA	6	
1487	BRMR	2	
1488	JMPR	2	
1489	LDA	5	
1490	STO	5	
1491	LAI	614	
1492	SUB	5	
1493	BRMR	7	
1494	LAI	856	
1495	STO	6	
1496	LMI	3986	
1497	MPYM	5	
1498	ADD	6	
1499	JMPR	7	
1500	LAI	1018	
1501	STO	6	
1502	LMI	2900	
1503	MPYM	5	
1504	ADD	6	
1505	OUT	0	
1506	STO	6	N2 Schedule
1507	LDA	20	
1508	SUB	21	
1509	LDA	0	
1510	BRMR	5	
1511	SUB	23	
1512	BRMR	5	Mode Control Logic
1513	LDA	4	
1514	JMPR	5	
1515	OUT	0	
1516	OUT	0	
1517	OUT	0	
1518	LDA	1	
1519	STO	4	DBIF
1520	LDA	2	
1521	RSHM	2	
1522	RSH	2	
1523	SUB	114	
1524	LDA	0	
1525	BRMR	2	
1526	JMPR	2	
1527	LDA	1	
1528	ADD	63	
1529	OUT	13	
1530	LDA	0	
1531	STO	63	
1532	LAI	855	
1533	STO	12	
1534	LMI	794	
1535	MPYM	249	
1536	ADD	12	
1537	STO	12	
1538	LDA	0	
1539	SUB	9	DBIR

Clock Failure
Test

Fault Word Trans-
mitted to Off-
Engine Equipment

Establish Range
for DN2I

ORIGINAL PAGE IS
OF POOR QUALITY



1650 LDA	44	PS3 Sensor Transmitted to Off-Engine Equipment
1651 OUT	13	
1652 LMI	662	
1653 MPY	8	
1654 ADD	8	Calculate DXMV Rate
1655 STO	5	
1656 LDA	4	
1657 SUB	89	
1658 STO	6	DXMV Transmitted to Off-Engine Equipment
1659 LDA	4	
1660 STO	89	
1661 LAI	109	
1662 STO	8	
1663 SUB	90	
1664 STO	10	
1665 SUB	6	
1666 LDA	10	
1667 BRMR	2	
1668 LDA	6	
1669 STU	6	
1670 LDA	0	
1671 SUB	90	
1672 SUB	8	
1673 STO	8	
1674 SUB	6	
1675 LDA	6	
1676 BRMR	2	
1677 LDA	8	
1678 STO	8	
1679 LDA	43	
1680 OUT	13	
1681 LMT	62	
1682 MPY	90	
1683 STO	10	
1684 ROT	0	
1685 STO	11	
1686 LDA	91	
1687 SUB	11	
1688 STO	91	
1689 LDA	90	
1690 SUBC	10	
1691 ADD	8	
1692 STO	90	
1693 LDA	28	
1694 OUT	13	
1695 LMI	3925	
1696 MPY	90	
1697 LSH	2	
1698 STO	10	
1699 JMP	3010	
1700 LDA	5	
1701 RSH	2	
1702 STO	6	
1703 LDA	7	
1704 RSH	2	

DB1 BF 1 Feedback Transmitted to Off-Engine Equipment

DNWR

E N2 Controller Error with XMV Rate Feedback

Mode Control Logic

1705 SUB	6
1706 LDA	5
1707 BRMR	2
1708 JMPR	2
1709 LDA	7
1710 STU	7
1711 LDA	29
1712 OUT	13
1713 LAI	3072
1714 STU	33
1715 BRMR	2
1716 JMPR	2
1717 LDA	0
1718 STU	97
1719 LAI	251
1720 STU	5
1721 LMI	717
1722 MPYM	41
1723 ADD	5
1724 STU	5
1725 LDA	169
1726 ADD	169
1727 OUT	13
1728 LAI	262
1729 STU	18
1730 LAI	760
1731 STU	11
1732 LDA	4
1733 SUB	16
1734 LDA	4
1735 BRMR	2
1736 JMPR	2
1737 LDA	18
1738 STU	6
1739 LAI	37
1740 STU	18
1741 LMI	3908
1742 MPYM	6
1743 STU	17
1744 LAI	360
1745 ADD	17
1746 LAI	0
1747 MPYM	6
1748 SUB	18
1749 LAI	0
1750 MPYM	11
1751 ROT	11
1752 STU	17
1753 ROT	31
1754 STU	6
1755 LSH	2
1756 STU	11
1757 LDA	168
1758 ADD	2
1759 OUT	13

DB2 BF2 Feedback Transmitted to Off-Engine Equipment

WF MCI

T3 Gain and Ranging Calculation

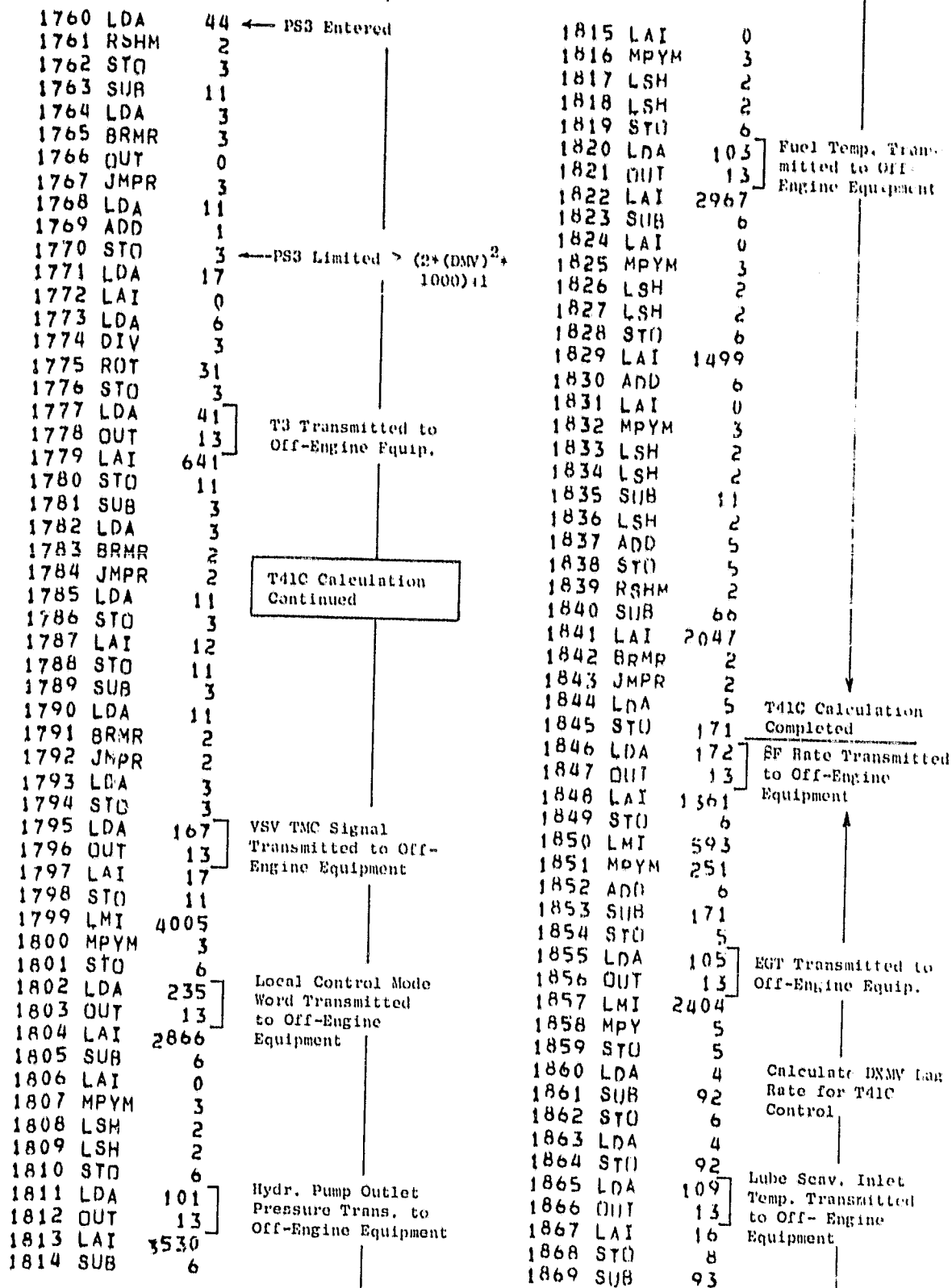
T3

N3 Auto Demand Transmitted to Off-Engine Equip.

DXMV

T41C Calculation Continued

ORIGINAL PAGE IS
OF POOR QUALITY



Address	Operation	Value	Comment
1870	STO	11	
1871	SUB	6	
1872	LDA	11	
1873	BRMR	2	
1874	LDA	6	
1875	STO	6	
1876	LDA	0	
1877	SUB	8	
1878	SUB	93	
1879	STO	8	
1880	SUB	6	
1881	LDA	6	
1882	BRMR	2	
1883	LDA	8	
1884	STO	8	
1885	LMT	311	
1886	MPY	93	
1887	STO	11	
1888	ROT	0	
1889	STO	13	
1890	LDA	94	
1891	SUB	13	
1892	STO	94	
1893	LDA	93	
1894	SUBC	11	
1895	ADD	8	
1896	STO	93	
1897	LMI	3924	
1898	MPY	93	
1899	LSH	0	
1900	STO	10	DTWR
1901	JMPP	3010	DT41C and DTWR
1902	LDA	5	
1903	RSH	2	
1904	STO	6	
1905	LDA	7	
1906	RSH	2	
1907	SUB	6	
1908	LDA	5	
1909	BRMR	2	
1910	JMPR	2	
1911	LDA	7	
1912	STO	7	
1913	LDA	2	
1914	BRMR	2	
1915	JMPR	2	
1916	LDA	97	
1917	STO	97	WF MCI
1918	LDA	110	Scav. Oil Discharge
1919	OUT	13	Temp. Trans. to Off-
1920	LAI	505	Engine Equip.
1921	STO	11	
1922	LDA	45	NIT
1923	RSHM	2	
1924	STO	5	
1925	LDA	9	N1 Ref. (DNITR)
1926	SUB	5	
1927	STU	5	DNITR-DNIT
1928	LAI	1364	Limits
1929	STU	13	
1930	LMI	3413	
1931	MPYM	241	WF Auto Gain Adj.
1932	ADD	32	683
1933	LAI	0	
1934	MPY	5	
1935	STU	6	
1936	SUB	0	
1937	BRMR	5	
1938	SUB	13	
1939	BRMR	4	
1940	LDA	13	
1941	JMPR	4	
1942	JMPR	-3	
1943	LDA	6	
1944	OUT	0	
1945	STU	6	
1946	LDA	107	
1947	OUT	13	Engine Oil Inlet
1948	LDA	0	Press. Trans. to
1949	SUB	13	Off-Engine Equip.
1950	STU	13	
1951	LDA	6	
1952	SUB	0	
1953	BRMR	2	
1954	JMPR	2	
1955	SUB	13	
1956	LDA	6	
1957	BRMR	2	
1958	JMPR	2	
1959	LDA	13	
1960	STU	6	
1961	RSH	2	
1962	ADD	6	
1963	STU	6	(DNITE Error)
1964	LDA	0	(D Gain W)
1965	SUB	21	Manual Mode
1966	LDA	5	
1967	BRMR	2	
1968	JMPR	2	
1969	LDA	6	
1970	STU	5	
1971	SUB	0	
1972	BRMR	5	
1973	SUB	11	
1974	BRMR	4	
1975	LDA	11	
1976	JMPR	4	
1977	JMPR	-3	
1978	LDA	5	
1979	OUT	0	

ORIGINAL PAGE IS
OF POOR QUALITY

1980	STO	5
1981	LDA	0
1982	SUB	11
1983	STO	11
1984	LDA	5
1985	SUB	0
1986	BRMR	2
1987	JMPR	2
1988	SUB	11
1989	LDA	5
1990	BRMR	2
1991	JMPR	2
1992	LDA	11
1993	STO	5
1994	ADD	5
1995	STO	11
1996	ADD	11
1997	STO	11
1998	LDA	108
1999	OUT	13
2000	LMI	207
2001	MPY	5
2002	ADD	11
2003	STO	5
2004	LMI	3925
2005	MPY	90
2006	LSH	0
2007	STO	10
2008	JHPP	3010
2009	LAI	1638
2010	STO	6
2011	LDA	31
2012	SUB	1
2013	BRMR	27
2014	LDA	175
2015	RSHM	2
2016	SUB	6
2017	OUT	0
2018	BRMR	13
2019	LDA	173
2020	RSHM	2
2021	SUB	6
2022	BRMR	13
2023	LDA	174
2024	SUB	1
2025	STO	174
2026	BRMR	18
2027	LAI	0
2028	OUT	0
2029	OUT	0
2030	JMPR	19
2031	OUT	0
2032	OUT	0
2033	OUT	0
2034	OUT	0

N1 Controller
Calculations Cont'd.

Gearbox Brg. Temp.
Trans. to Off-Eng.
Equipment

High Vibs
Shutdown
Calculation

← FICA on

← Horiz. Vib.

← Vert. Vib.

2035	LAI	9
2036	STO	174
2037	LDA	0
2038	OUT	0
2039	JMPR	-11
2040	OUT	0
2041	OUT	0
2042	OUT	0
2043	JMPR	-12
2044	LDA	95
2045	STO	97
2046	STO	174
2047	LAI	2048
2048	STO	7
2049	ADD	63
2050	STO	63
2051	LDA	45
2052	RSHM	2
2053	STO	6
2054	LDA	31
2055	SUB	1
2056	BRMR	7
2057	LAI	860
2058	SUB	14
2059	BRMR	7
2060	RNT	0
2061	OUT	0
2062	JMPR	15
2063	RNT	0
2064	OUT	0
2065	JMPR	-5
2066	LAI	256
2067	SUB	6
2068	BRMR	9
2069	LDA	95
2070	STO	97
2071	LDA	2
2072	STO	7
2073	RSHM	2
2074	RSH	2
2075	RSH	2
2076	JMPR	9
2077	LDA	0
2078	OUT	0
2079	OUT	0
2080	OUT	0
2081	OUT	0
2082	OUT	0
2083	OUT	0
2084	OUT	0
2085	ADD	63
2086	STO	63
2087	LDA	5
2088	RSH	2
2089	STO	6

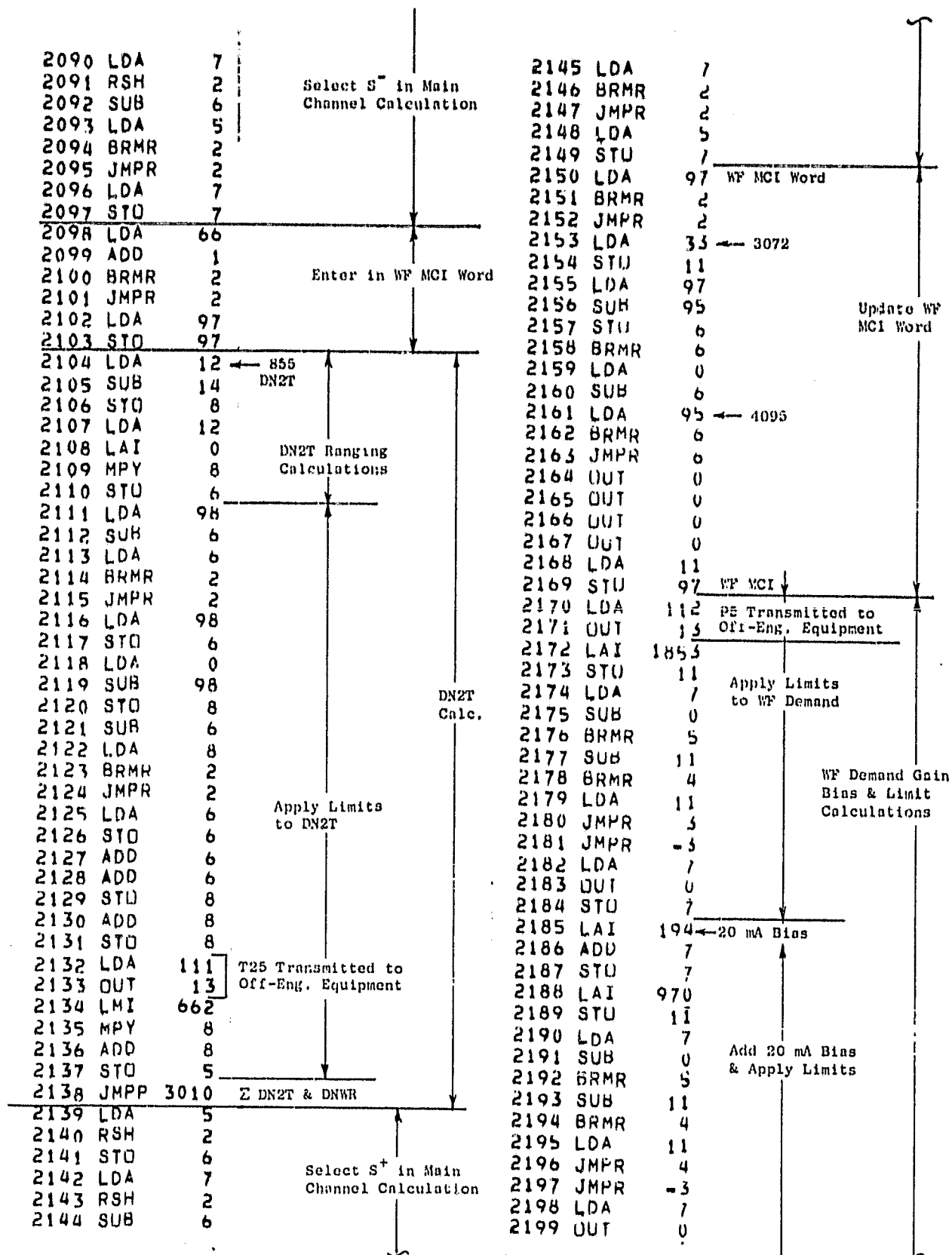
9 ← N1

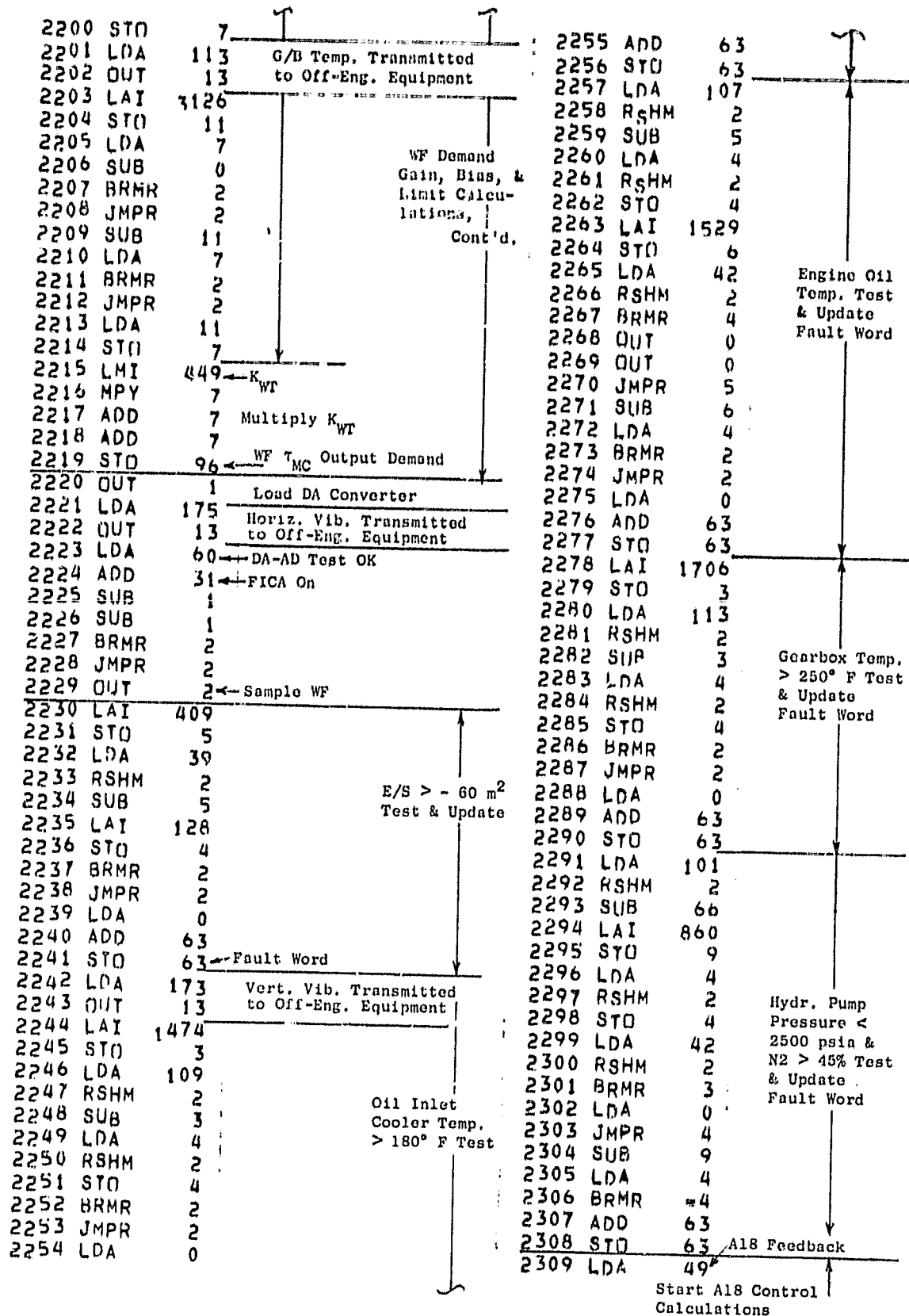
← Fault Word

← NIT

NIT Sensor
Signal Logs
Shutdown Calc.

← Fault Word



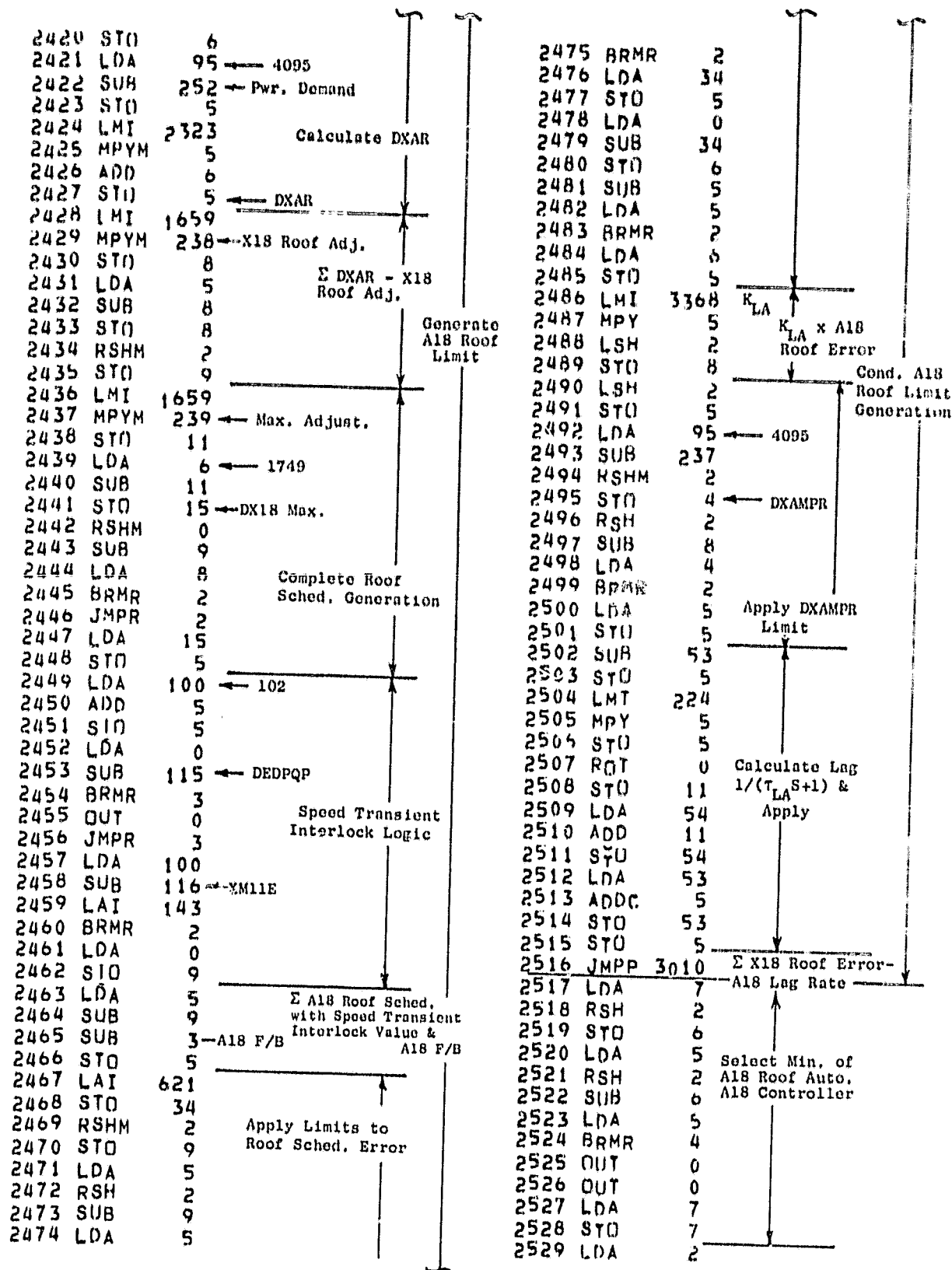


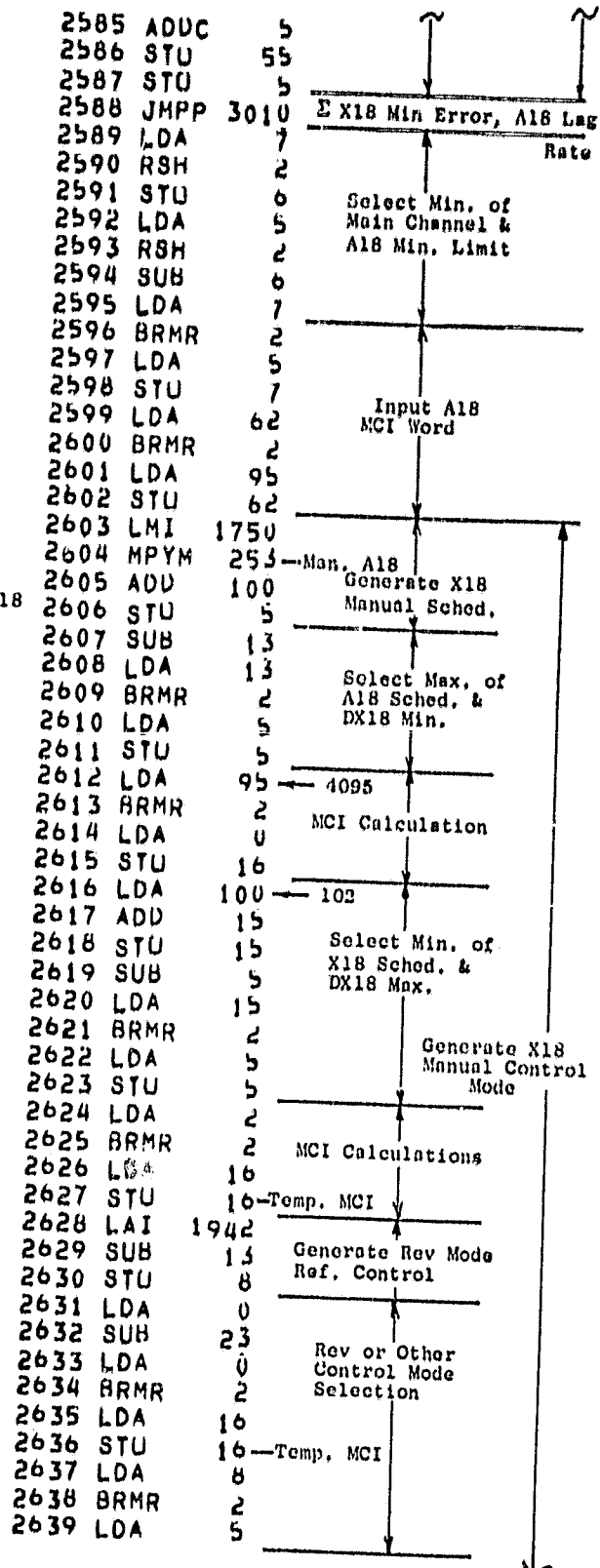
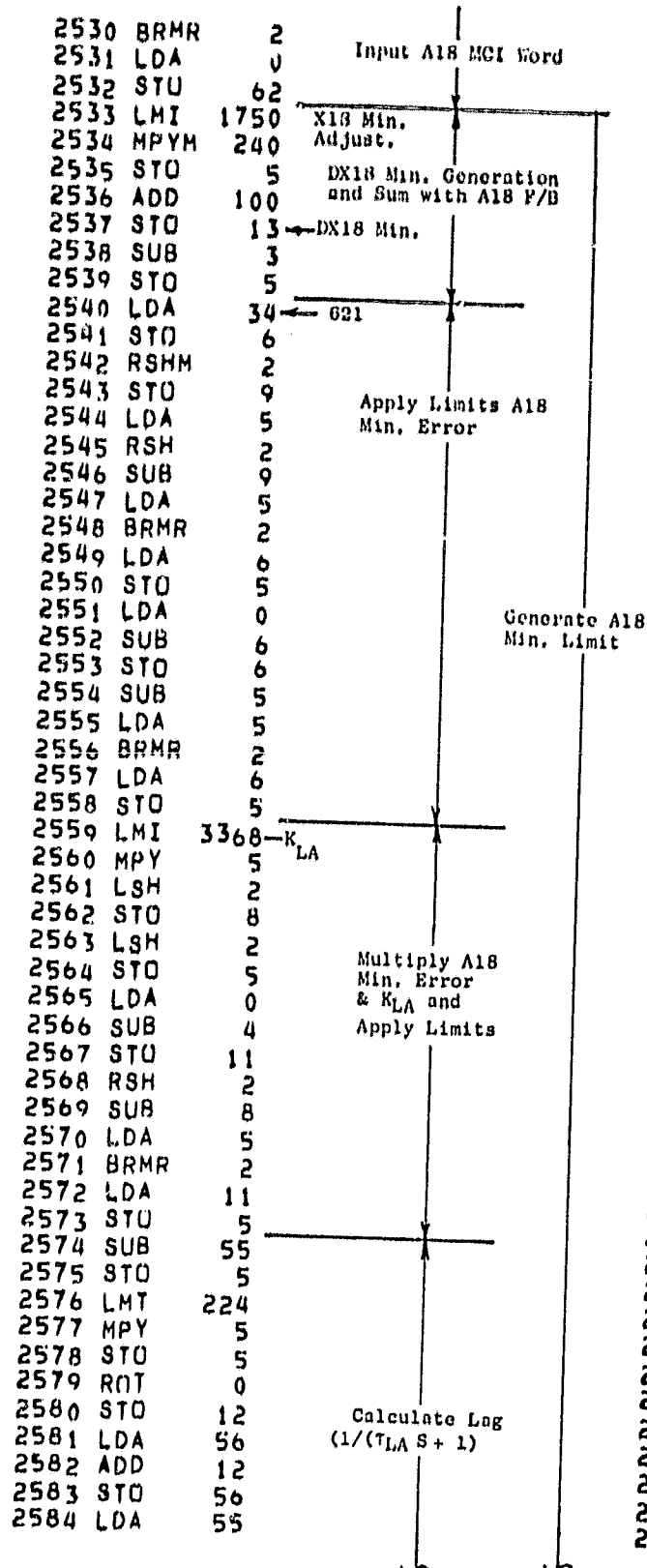
2310	RSHM	2
2311	STO	3
2312	SUB	50
2313	STO	5
2314	LDA	3
2315	STO	50
2316	LDA	0
2317	SUB	22
2318	SUB	25
2319	BRMR	3
2320	LAI	77
2321	JMPR	3
2322	LAI	26
2323	OUT	0
2324	STO	7
2325	LMT	224
2326	MPY	51
2327	STO	8
2328	ROT	0
2329	STO	9
2330	SUB	52
2331	LDA	8
2332	SUBC	51
2333	ADD	7
2334	STO	10
2335	SUB	5
2336	LDA	10
2337	BRMR	2
2338	LDA	5
2339	STO	5
2340	LDA	10
2341	SUB	7
2342	SUB	7
2343	STO	7
2344	SUB	5
2345	LDA	5
2346	BRMR	2
2347	LDA	7
2348	STO	5
2349	LDA	52
2350	SUB	9
2351	STO	52
2352	LDA	51
2353	SUBC	8
2354	ADD	5
2355	STO	51
2356	LDA	52
2357	ROT	0
2358	LDA	51
2359	LSH	2
2360	LSH	2
2361	LSH	2
2362	STO	5
2363	LMI	3409 ← KLA ²
2364	MPY	5

A18 F/B Lag Rate
Gain and Limiting
Calculations

2365	STU	10	← DARE
2366	LMI	718	
2367	MPYM	253	← M11 Adj.
2368	STU	6	
2369	LAI	881	Auto. Mode Ref. Generation
2370	SUB	6	
2371	STU	6	
2372	LDA	48	← PTO
2373	RSHM	2	
2374	STU	7	XM11 Calculation
2375	LMI	647	
2376	MPYM	47	← PTO-PS11
2377	DIV	7	
2378	ROT	0	
2379	STU	7	
2380	STU	170	
2381	LDA	0	
2382	SUB	7	XM11 Ref. - XM11
2383	STU	116	← XM11E
2384	LMI	3901	
2385	MPYM	236	← X18 Gain Adj.
2386	STU	8	
2387	LAI	195	
2388	ADD	8	XM11E x Gain Adj.
2389	LAI	0	
2390	MPY	116	
2391	STU	7	
2392	LAI	3887	Generate Auto Mode Control Ref.
2393	STU	8	
2394	LDA	7	
2395	SUB	8	
2396	LDA	8	
2397	BRMR	2	
2398	LDA	7	
2399	STU	7	Apply Limits to XM11E
2400	LDA	0	
2401	SUB	8	
2402	STU	8	
2403	SUB	7	
2404	LDA	8	
2405	BRMR	2	
2406	LDA	7	
2407	STU	7	
2408	LMI	2496	
2409	MPY	7	
2410	LSH	2	Multiply by KPA
2411	LSH	2	
2412	LSH	2	
2413	LSH	2	
2414	STU	5	
2415	STU	168	
2416	JMPP	3010	Σ A18 Mode Ref & DARE
2417	LDA	5	
2418	STU	7	← Min. Error Select Store
2419	LAI	1749	

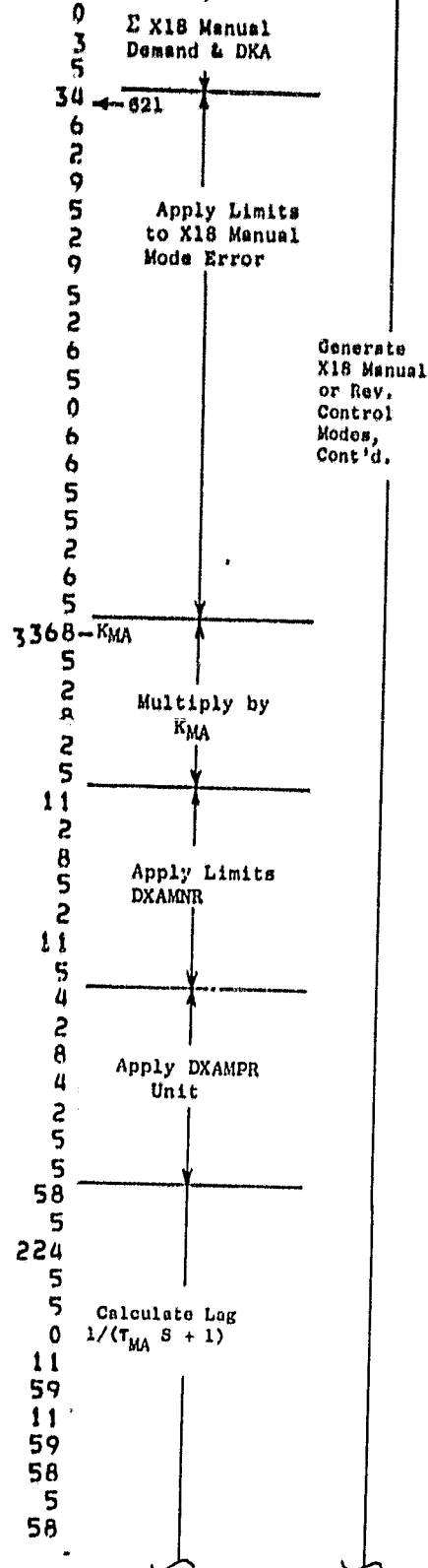
ORIGINAL PAGE IS
OF POOR QUALITY



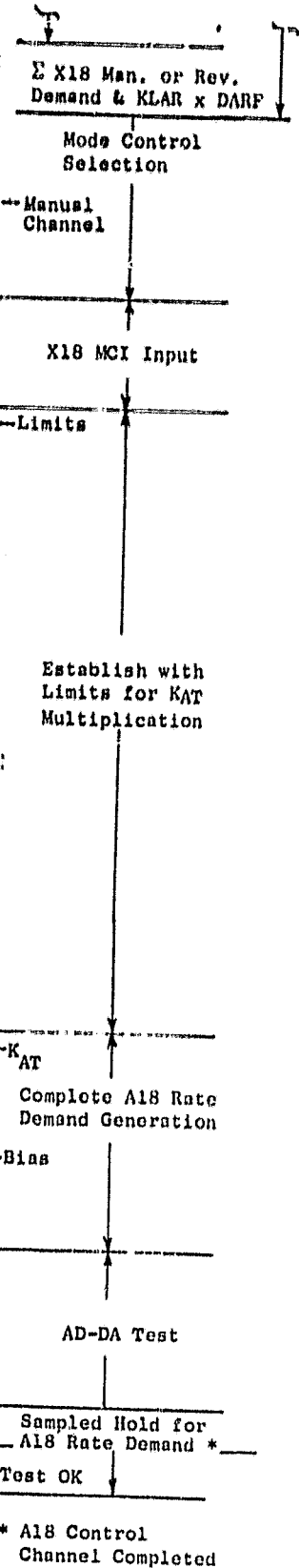


ORIGINAL PAGE IS
OF POOR QUALITY

2640 OUT 0
2641 SUB 3
2642 STO 5
2643 LDA 34
2644 STO 6
2645 RSHM 2
2646 STO 9
2647 LDA 5
2648 RSH 2
2649 SUB 9
2650 LDA 5
2651 BRMR 2
2652 LDA 6
2653 STO 5
2654 LDA 0
2655 SUB 6
2656 STO 6
2657 SUB 5
2658 LDA 5
2659 BRMR 2
2660 LDA 6
2661 STO 5
2662 LMI 3368
2663 MPY 5
2664 LSH 2
2665 STO 2
2666 LSH 2
2667 STO 5
2668 LDA 11
2669 RSH 2
2670 SUB 8
2671 LDA 5
2672 BRMR 2
2673 LDA 11
2674 STO 5
2675 LDA 4
2676 RSH 2
2677 SUB 8
2678 LDA 4
2679 BRMR 2
2680 LDA 5
2681 STO 5
2682 SUB 58
2683 STO 5
2684 LMT 224
2685 MPY 5
2686 STO 5
2687 ROT 0
2688 STO 11
2689 LDA 59
2690 ADD 11
2691 STO 59
2692 LDA 58
2693 ADDC 5
2694 STO 58



2695 STO 5
2696 JMPP 3010
2697 LDA 0
2698 SUB 22
2699 SUB 25
2700 LDA 7
2701 BRMR 2
2702 LDA 5
2703 STO 7
2704 LDA 62
2705 BRMR 2
2706 LDA 16
2707 STO 62
2708 LAI 1834
2709 STO 9
2710 RSH 2
2711 STO 8
2712 LDA 7
2713 RSH 2
2714 SUB 8
2715 LDA 7
2716 BRMR 2
2717 LDA 9
2718 STO 7
2719 LDA 0
2720 SUB 9
2721 STO 9
2722 RSH 2
2723 STO 8
2724 LDA 7
2725 RSH 2
2726 SUB 8
2727 LDA 9
2728 BRMR 2
2729 LDA 7
2730 STO 7
2731 LMI 463
2732 MPY 7
2733 ADD 7
2734 STO 7
2735 LAI 4091
2736 ADD 7
2737 OUT 1
2738 STO 67
2739 LDA 60
2740 ADD 31
2741 SUB 1
2742 SUB 1
2743 BRMR 2
2744 JMPP 2
2745 OUT 3
2746 LDA 0
2747 SUB 61
2748 BRMR 13
2749 ROT 0



2750	ROT	0
2751	ROT	0
2752	ROT	0
2753	ROT	0
2754	ROT	0
2755	ROT	0
2756	ROT	0
2757	OUT	0
2758	OUT	0
2759	OUT	0
2760	JMPR	101 Failure of AD-DA Test
2761	LDA	206
2762	STO	231
2763	LDA	207
2764	STO	232
2765	LDA	208
2766	STO	233
2767	LDA	209
2768	STO	234
2769	LDA	210
2770	STO	235
2771	LDA	211
2772	STO	236
2773	LDA	212
2774	STO	237
2775	LDA	213
2776	STO	238
2777	LDA	214
2778	STO	239
2779	LDA	215
2780	STO	240
2781	LDA	216
2782	STO	241
2783	LDA	217
2784	STO	242
2785	LDA	218
2786	STO	243
2787	LDA	219
2788	STO	244
2789	LDA	220
2790	STO	245
2791	LDA	221
2792	STO	246
2793	LDA	222
2794	STO	247
2795	LDA	223
2796	STO	248
2797	LDA	224
2798	STO	249
2799	LDA	225
2800	STO	250
2801	LDA	226
2802	STO	251
2803	LDA	227
2804	STO	252

Refresh Input Data
from Off-Engine
Equipment

2805	LDA	228
2806	STU	253
2807	LDA	229
2808	STU	254
2809	LDA	230
2810	STU	255
2811	LDA	181
2812	STU	206
2813	LDA	182
2814	STU	207
2815	LDA	183
2816	STU	208
2817	LDA	184
2818	STU	209
2819	LDA	185
2820	STU	210
2821	LDA	186
2822	STU	211
2823	LDA	187
2824	STU	212
2825	LDA	188
2826	STU	213
2827	LDA	189
2828	STU	214
2829	LDA	190
2830	STU	215
2831	LDA	191
2832	STU	216
2833	LDA	192
2834	STU	217
2835	LDA	193
2836	STU	218
2837	LDA	194
2838	STU	219
2839	LDA	195
2840	STU	220
2841	LDA	196
2842	STU	221
2843	LDA	197
2844	STU	222
2845	LDA	198
2846	STU	223
2847	LDA	199
2848	STU	224
2849	LDA	200
2850	STU	225
2851	LDA	201
2852	STU	226
2853	LDA	202
2854	STU	227
2855	LDA	203
2856	STU	228
2857	LDA	204
2858	STU	229
2859	LDA	205

Continued

ORIGINAL PAGE IS
OF POOR QUALITY

2860 STO	230		2915 OUT	0
2861 OUT	15	Iteration Complete	2916 OUT	0
2862 OUT	0		2917 OUT	0
2863 OUT	0		2918 OUT	0
2864 OUT	0		2919 OUT	0
2865 OUT	0		2920 OUT	0
2866 OUT	0		2921 OUT	0
2867 OUT	0		2922 OUT	0
2868 OUT	0		2923 OUT	0
2869 OUT	0		2924 OUT	0
2870 OUT	0		2925 OUT	0
2871 OUT	0		2926 OUT	0
2872 OUT	0		2927 OUT	0
2873 OUT	0		2928 OUT	0
2874 OUT	0		2929 OUT	0
2875 OUT	0		2930 OUT	0
2876 OUT	0		2931 OUT	0
2877 OUT	0		2932 OUT	0
2878 OUT	0		2933 OUT	0
2879 OUT	0		2934 OUT	0
2880 OUT	0		2935 OUT	0
2881 OUT	0		2936 OUT	0
2882 OUT	0		2937 OUT	0
2883 OUT	0		2938 OUT	0
2884 OUT	0		2939 OUT	0
2885 OUT	0		2940 OUT	0
2886 OUT	0		2941 OUT	0
2887 OUT	0		2942 OUT	0
2888 OUT	0		2943 OUT	0
2889 OUT	0		2944 OUT	0
2890 OUT	0		2945 OUT	0
2891 OUT	0		2946 OUT	0
2892 OUT	0		2947 OUT	0
2893 OUT	0		2948 OUT	0
2894 OUT	0		2949 OUT	0
2895 OUT	0		2950 OUT	0
2896 OUT	0		2951 OUT	0
2897 OUT	0		2952 OUT	0
2898 OUT	0		2953 OUT	0
2899 OUT	0		2954 OUT	0
2900 OUT	0		2955 OUT	0
2901 OUT	0		2956 OUT	0
2902 OUT	0		2957 OUT	0
2903 OUT	0		2958 OUT	0
2904 OUT	0		2959 OUT	0
2905 OUT	0		2960 OUT	0
2906 OUT	0		2961 OUT	0
2907 OUT	0		2962 OUT	0
2908 OUT	0		2963 OUT	0
2909 OUT	0		2964 OUT	0
2910 OUT	0		2965 OUT	0
2911 OUT	0		2966 OUT	0
2912 OUT	0		2967 OUT	0
2913 OUT	0		2968 OUT	0
2914 OUT	0		2969 OUT	0

2970	OUT	0
2971	OUT	0
2972	OUT	0
2973	OUT	0
2974	OUT	0
2975	OUT	0
2976	OUT	0
2977	OUT	0
2978	OUT	0
2979	OUT	0
2980	OUT	0
2981	OUT	0
2982	OUT	0
2983	OUT	0
2984	OUT	0
2985	OUT	0
2986	OUT	0
2987	OUT	0
2988	OUT	0
2989	OUT	0
2990	OUT	0
2991	OUT	0
2992	OUT	0
2993	OUT	0
2994	OUT	0
2995	OUT	0
2996	OUT	0
2997	OUT	0
2998	OUT	0
2999	OUT	0
3000	OUT	0
3001	OUT	0
3002	OUT	0
3003	OUT	0
3004	OUT	0
3005	OUT	0
3006	OUT	0
3007	OUT	0
3008	OUT	0
3009	OUT	0
3010	LAI	1
3011	STO	1
3012	ADD	57
3013	STO	57
3014	LDA	5
3015	SUB	0
3016	BRMR	17
3017	LDA	10
3018	SUB	0
3019	BRMR	7
3020	LDA	5
3021	SUB	10
3022	OUT	0
3023	OUT	0
3024	OUT	0

Subroutine,
Cont'd.

Subroutine for
Signed Summation
with Overflow Limits

3025	JMPR	17
3026	LDA	5
3027	SUB	10
3028	BRMR	2
3029	JMPR	-5
3030	LDA	2
3031	SUB	1
3032	JMPR	10
3033	LDA	10
3034	SUB	0
3035	BRMR	-15
3036	LDA	5
3037	SUB	10
3038	BRMR	-15
3039	LDA	2
3040	OUT	0
3041	OUT	0
3042	STO	5
3043	LDA	57
3044	SUB	1
3045	BRMP	545
3046	SUB	1
3047	BRMP	824
3048	SUB	1
3049	BRMP	945
3050	SUB	1
3051	BRMP	1097
3052	SUB	1
3053	BRMP	1407
3054	SUB	1
3055	BRMP	1563
3056	SUB	1
3057	BRMP	1700
3058	SUB	1
3059	BRMP	1902
3060	SUB	1
3061	BRMP	2009
3062	SUB	1
3063	BRMP	2139
3064	SUB	1
3065	BRMP	2417
3066	SUB	1
3067	BRMP	2517
3068	SUB	1
3069	BRMP	2589
3070	SUB	1
3071	BRMP	2697

Tests
for
Return
to
Program

REFERENCES

1. Kuo, Benjamin C., Automatic Control Systems, Prentice-Hall, Inc.;
C 1962; pp. 419-422.
2. The General Electric Company; "Quiet Clean Short-Haul Experimental
Engine (QCSEE) Under-the-Wing Engine Simulation Report," NASA
CR-134914, July 1977.